

**PREDICTION & MITIGATION OF AC INDUCED
PIPELINE CORROSION UNDER CATHODIC PROTECTION**

A thesis submitted to the
University of Petroleum and Energy Studies

For the award of
Doctor of Philosophy
in
Oil and Gas

BY
Ajit Kumar Thakur

April 2023

SUPERVISOR (s)
Dr. Adarsh Kumar Arya
Associate Professor & Associate Dean (Incubation)

Dr. Pushpa Sharma
Distinguished Professor



Department of Chemical Engineering
(School of Engineering)
University of Petroleum and Energy Studies
Dehradun - 248007: Uttarakhand

**PREDICTION & MITIGATION OF AC INDUCED
PIPELINE CORROSION UNDER CATHODIC PROTECTION**

A thesis submitted to the
University of Petroleum and Energy Studies

For the award of
Doctor of Philosophy
in
Oil and Gas

BY
Ajit Kumar Thakur
(SAP ID 500056543)

April 2023

Supervisor (s)

Dr. Adarsh Kumar Arya

Department of Chemical Engineering

Associate Professor & Associate Dean (Incubation)

Harcourt Butler Technical University, Kanpur

Dr. Pushpa Sharma

Distinguished Professor

Department of Petroleum Engineering and Earth Sciences

Energy Cluster, SOE

University of Petroleum and Energy Studies, Dehradun



Department of Chemical Engineering
(School of Engineering)

University of Petroleum and Energy Studies

Dehradun - 248007: Uttarakhand

**I dedicate this thesis to my family members and
colleagues whose belief in me gave me the courage
to undertake this work**

APRIL 2023
DECLARATION

I declare that the thesis entitled" *Prediction & Mitigation of AC Induced Pipeline Corrosion under Cathodic Protection*" has been prepared by me under the guidance of Dr. Adarsh Kumar Arya, Associate Professor & Associate Dean (Incubation), Harcourt Butler Technical University, Kanpur, and Dr. Pushpa Sharma, Distinguished Professor of the Department of Petroleum Engineering and Earth Sciences, University of Petroleum and Energy Studies, Dehradun. No part of this thesis has formed the basis for the award of any degree or fellowship previously.



Ajit Kumar Thakur

School of Engineering

University of Petroleum and Energy Studies

Dehradun

DATE: 03.04.2023



हरकोर्ट बटलर प्राविधिक विश्वविद्यालय

नवाबगंज, कानपुर - 208002, उ.प्र., भारत

HARCOURT BUTLER TECHNICAL UNIVERSITY

NAWABGANJ, KANPUR - 208002, U.P., INDIA

(Formerly Harcourt Butler Technological Institute, Kanpur)

Phone : +91-0512-2534001-5, 2533812, website : <http://www.hbtu.ac.in>, Email : vc@hbtu.ac.in

100 YEARS
1921 - 2021

THESIS COMPLETION CERTIFICATE

This is to certify that the thesis entitled" *Prediction & Mitigation of AC Induced Pipeline Corrosion under Cathodic Protection*" by Ajit Kumar Thakur, in partial completion of the requirements of the award of Degree of Philosophy (Engineering), is an original work carried by him under my supervision and guidance.

It is certified that work has not been submitted anywhere else for the award of any other diploma or degree of this or any other University

Supervisor

Dr. Adarsh Kumar Arya

(Formerly with UPES – Dehradun)

Associate Professor & Associate Dean (Incubation)

Harcourt Butler Technical University

Kanpur- 208002

17-04

-2023

THESIS COMPLETION CERTIFICATE

This is to certify that the thesis entitled “**Prediction & Mitigation of AC Induced Pipeline Corrosion under Cathodic Protection**” by Ajit Kumar Thakur, in partial completion of the requirements of the award of Degree of Philosophy (Engineering), is an original work carried by him under my supervision and guidance.

It is certified that the work has not been submitted anywhere else for the award of any other diploma or degree of this or any other University.

Supervisor



Dr. Pushpa Sharma

Distinguished Professor
Department of Petroleum Engineering and Earth Sciences
Energy Cluster, SOE
University of Petroleum and Energy Studies
Dehradun

Date : 17/04/2023

EXECUTIVE SUMMARY

The ever-increasing energy demands encourage efficient means of energy transport. While pipelines transport gas and oil in bulk quantities, transmission lines enable bulk transportation of electrical energy. Both transportation systems are vital to meet energy demands.

The pipelines and transmission lines transport energy from supply points to demand centers. Pipelines and Transmission lines need to be installed linearly. The number of pipelines crossing or running parallel to one another at multiple locations is increasing daily. Energy corridors are increasing where pipelines and transmission lines are laid in proximity. Electric flow in transmission lines results in AC interference on nearby pipelines. Such pipelines are usually underground, provided with suitable corrosion-resistant coatings, and supplemented with cathodic protection systems.

The AC corrosion due to nearby transmission lines remains complex and continues to surprise the pipeline Industry with continued deterioration. Several studies have been undertaken to establish and understand various factors affecting AC corrosion. While these studies contribute to a better understanding and guide the industry to look for specific aspects, the Industry problem of AC corrosion continues to grow. It is time to look for practical elements the industry can adopt to control the vital components responsible for AC corrosion.

This study attempts to solve the industry problem by addressing the vital components of AC density, protection potential, and coating stress voltage. The study considers a unique in-house experimental setup to compare various pipe grades in similar test conditions. The comparison proves that no pipe grade can sustain high AC corrosion, and the performance of some pipe grades is relatively

better at low AC interference levels. This aspect can help the selection of pipe grades at the design time, especially where AC corrosion is not likely due to the absence of transmission lines in remote areas.

Further research also summarizes that the Zinc and Magnesium Anodes fail to provide requisite protection to pipelines under high AC interference. Previous studies for specific pipe grades validate weight loss test results.

The application of modeling through a state-of-the-art software tool demonstrates the viable solution for predicting AC interference based on several parameters, including transmission line data, pipeline characteristics, soil resistivity, and soil pH. The validation of the modeled parameters with the actual parameters collected in the field enables cross-checking the solution, thereby taking corrective actions to reduce/account for the variations.

Mitigation measures to control AC interference are modeled, and their effect is predicted before costly mitigation measures are implemented. The addition/deletion of mitigation measures becomes handy through the modeling solution.

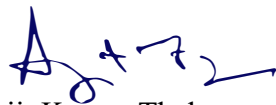
Summarizing the unique experimental and modeling work enables the identification of the Risk Matrix to prioritize depending on the likely severity of AC corrosion, and the industry can deploy the corresponding corrosion model for effective AC corrosion management.

PREFACE

The primary motivation for this research began with daily concerns faced by the pipeline industry concerning the safety of the pipeline systems. Pipeline engineers' primary objective is to ensure pipeline integrity, and they look for a maintenance methodology that will assist them in reducing the chances of pipeline failure at an optimized cost. The AC corrosion threat to the pipelines is increasing daily, and Industry is struggling to change/modify its maintenance practices to minimize the danger. In India, little work exists on this aspect of AC corrosion, and a practical solution for reducing AC corrosion needs immediate attention.

The author is well aware of the pipeline integrity threat, given India's increasing network of transmission lines. Interestingly, due to improved and better pipeline coatings with few defects, the AC corrosion threat has become more pronounced as the AC density at the defect points can be enormously high, leading to the quick failure of pipelines.

Besides, AC corrosion is now known to cause a pipeline rupture; thus, the quantity of leakage of highly volatile hydrocarbons (vapor or liquid) may be enormous as to other modes of pipeline damage, and the quantum of environmental and public safety risk is much higher. Considering the above, the present research is pertinent and needs the pipeline industry's hours.



Ajit Kumar Thakur

Guwahati, Assam, India

April 2023

ACKNOWLEDGEMENT

The author expresses gratitude to the UPES (University of Petroleum and Energy Studies) for permission to conduct this research. The author is grateful to the administration and setup of the University for their support and encouragement.

Thanks to the Faculty Research Committee (FRC) for guidance, researching the topic of interest, and providing continual support with valuable inputs to improve the thesis.

The author expresses tremendous gratitude to the esteemed guide, Dr. Adarsh Kumar Arya, and co-guide, Dr. Pushpa Sharma, for their proactive help, guidance, and trust during the work.

The author acknowledges the support extended by renowned industry expert Mr. K B Singh for his help with pertinent and accurate information on the subject.

Last, the author acknowledges the invaluable support extended by his wife Sumedha and sons Aprajit and Shaurya, who supported them wholeheartedly, sacrificing their comfort and adjusting to the author's frequent absence on multiple family requirements.



Ajit Kumar Thakur

Dehradun, 2023

TABLE OF CONTENTS

DECLARATION	iii
THESIS COMPLETION CERTIFICATE.....	iv-v
EXECUTIVE SUMMARY	vi-vii
PREFACE.....	viii
ACKNOWLEDGEMENT	ix
TABLE OF CONTENTS.....	x-xii
LIST OF ABBREVIATIONS.....	xiii
LIST OF FIGURES	xiv-xv
LIST OF TABLES.....	xvi-xvii
CHAPTER 1: INTRODUCTION.....	1-8
1.1 BACKGROUND.....	1-2
1.2 THEOR.....	3-4
1.3 PROBLEM STATEMENT	5
1.4 NEED AND MOTIVATION	5-7
1.5 OBJECTIVES	7-8
1.6 RESEARCH METHODOLOGY.....	8
CHAPTER 2: REVIEW OF LITERATURE.....	9-31
2.1 RESEARCH METHODOLOGY.....	9-10
2.2 PIPELINE FAILURE AND CORROSION.....	10-11
2.3 ALTERNATING CURRENT INTERFERENCE ON PIPELINES .	11-13
2.4 COLLOCATED TRANSMISSION LINES AND PIPELINES	13-16
2.5 AC INTERFERENCE SOURCES.....	16-17
2.6 INVESTIGATIONS OF AC CORROSION OF PIPELINES	17-21
2.7 AC CORROSION	21-31
CHAPTER 3: EXPERIMENTAL WORK	32-42
3.1 POTENTIOSTATIC AND GALVANOSTATIC TESTS.....	32

3.2	ELECTRICAL CIRCUIT	32-36
3.3	TEST CONDITIONS.....	36-38
3.4	EXPERIMENTAL ARRANGEMENTS	39-40
3.5	DATA COLLECTION.....	40-42
CHAPTER 4: MODELING WORK.....		43-62
4.1	MODELING METHOD AND SOFTWARE	43-44
4.2	MODELLING CONDITIONS.....	44
4.3	MODELLING ACTIVITIES	44-49
4.4	INDUCTIVE AC INTERFERENCE COMPUTATION.....	49-51
4.5	TOTAL INTERFERENCE COMPUTATION – STEADY STATE	51-53
4.6	MODELLING PROCEDURE FOR FAULT CONDITION.....	53-54
4.7	SOIL RESISTIVITY AND pH STUDY	55-56
4.8	FAULT CURRENT USED IN MODELLING	56-57
4.9	FAULT CURRENT SIMULATION	57-62
CHAPTER 5: EXPERIMENTAL RESULTS AND DISCUSSIONS.....		63-78
5.1	BACKGROUND.....	63
5.2	PROTECTION POTENTIAL WITHOUT AC APPLICATION.....	63-65
5.3	PROTECTION POTENTIAL UNDER AC INTERFERENCE	66-71
5.4	PROTECTION DENSITY UNDER AC INTERFERENCE	71-76
5.5	WEIGHT LOSS TESTS.....	77-78
CHAPTER 6: MODELING RESULTS AND DISCUSSIONS		79-97
6.1	BACKGROUND.....	79
6.2	SOIL RESISTIVITY AND pH	79
6.3	TOUCH VOLTAGES AT A STEADY STATE.....	80-84
6.4	PRE-MITIGATION LEAKAGE CURRENT DENSITY.....	84-86
6.5	MITIGATION MEASURES.....	86-89
6.6	POST-MITIGATION LEAKAGE CURRENT DENSITY	89-90
6.7	POST-MITIGATION TOUCH VOLTAGE	90-92
6.8	SUMMARY RESULTS PRE- AND POST-MITIGATION	93-95
6.9	TOTAL INTERFERENCE UNDER FAULT CONDITIONS	95-97
CHAPTER 7: CONCLUSIONS AND WAY FORWARD		98-102
7.1	CONCLUSION.....	98
7.2	RISK ASSESSMENT AND AC CORROSION MODEL.....	98-100

7.3	IMPLEMENT / REMOVE MITIGATION MEASURES	100-101
7.4	ACHIEVEMENT OF OBJECTIVES	101-102
7.5	FUTURE WORKS.....	102
REFERENCES		103-131
APPENDIX A: LIST OF PUBLICATIONS.....		132

LIST OF ABBREVIATIONS

AC: Alternating Current

ANSI: American National Standards Institute

API: American Petroleum Institute

ckm: Circuit kilometer

CDEGS: Current Distribution, Electromagnetic Interference, Grounding, and Soil Structure Analysis

DC: Direct Current

DFBE: Double fusion bonded epoxy

3LPE: Three-layer polyethylene

HT: High tension

ILI: In-line inspection

kV: Kilovolt

mA: Milli Ampere

mV: Milli Volt

NACE: National Association of Corrosion Engineers

PSP: Pipe to soil potential

PD: Protection density

LIST OF FIGURES

Figure 1.1: Inductive coupling with the underground pipeline.....	3
Figure 1.2: Electrostatic coupling with the above-ground pipeline.....	4
Figure 1.3: 400 kV Transmission line crossing two pipelines at five locations	6
Figure 1.4: AC corrosion damage in District Jamnagar, Gujarat, India	7
Figure 2.1: Inductive coupling schematic	23
Figure 2.2: Resistive coupling schematic	24
Figure 3.1: Electric Circuit - DC and AC coupled.....	33
Figure 3.2 : Steel specimen Arrangement.....	35
Figure 3.3: Protection potential and AC density measurement setup.....	39
Figure 3.4: Set up for weight loss on AC interference	40
Figure 4.1: Polyline route of the pipeline and HT line (208.58 km)	45
Figure 4.2: Energisation of terminal	46
Figure 4.3: Soil definition for derivation of Soil model	47
Figure 4.4: Generating Regions	48
Figure 4.5: Regions and Terminals.....	49
Figure 4.6: Portion of the created circuit	50
Figure 4.7: Scheme modelled in CDEGS	50
Figure 4.8: Pipeline earth impedance at 104.95 km.....	51
Figure 4.9: Substation ground impedance	52
Figure 4.10: Pipeline earthing modelled.....	52
Figure 4.11: Pipeline earth defined.....	53
Figure 4.12: Pipeline and Transmission lines on Google Earth.....	58
Figure 4.13: Pipeline and HT line for fault analysis on Google Earth	60

Figure 4.14: Faulted Tower locations	60
Figure 4.15: Modeled scheme in CDEGS.....	61
Figure 4.16: Reference circuit model.....	62
Figure 5.1: Protection Density at PD 0.3 A/m ²	69
Figure 5.2: Protection current density – X46.....	72
Figure 5.3: Change in protection density – X46.....	73
Figure 5.4: Protection density at protection potential -1150 mV.....	74
Figure 5.5: Protection density – X52	75
Figure 5.6: Protection Density – X80	76
Figure 6.1: Touch voltage Pre-mitigation (104.95 to 208.58 km).....	81
Figure 6.2: Touch voltage pre-mitigation (at 208.58 km)	82
Figure 6.3: Touch voltage Pre-mitigation (208.58 to 284.32 km).....	82
Figure 6.4: Touch voltage Pre-mitigation (at 284.32 km).....	83
Figure 6.5: Touch voltage field validation (104.95 to 208.58 km).....	83
Figure 6.6: Touch voltage field validation (208.58 to 284.32 km).....	84
Figure 6.7: Leakage density pre-mitigation (104.95 to 208.58 km).....	85
Figure 6.8: Leakage density pre-mitigation at chainage 208.58 km.....	86
Figure 6.9: Leakage density pre-mitigation (208.58 to 284.32 km).....	87
Figure 6.10: Leakage density pre-mitigation at 284.32 km.....	87
Figure 6.11: Leakage density post mitigation (Chainage 104.95 to 208.58 km)..	89
Figure 6.12: Leakage density post mitigation (Chainage 208.58 to 284.32 km)..	90
Figure 6.13: Touch voltage Post-mitigation (Chainage 104.95 to 208.58 km)	91
Figure 6.14: Pipeline Touch voltage post-mitigation (Zoom view at 208.58 km) 91	
Figure 6.15: Touch voltage Post-mitigation (Chainage 208.58 to 284.32 km)	92
Figure 6.16: Total interference-Faulted phase Mermundal to Vedanta 400 kV ...	95
Figure 6.17: Total interference-Faulted phase Mermundal to Mendhasal 400 kV96	
Figure 6.18: Coating stress voltage-Angul to Sundargarh 765 kV Ckt 1&2	97
Figure 6.19: Coating stress voltage-Mendhasal to Pandiabali 400 kV	97
Figure 7.1: AC Corrosion Model.....	100

LIST OF TABLES

Table 1.1: Global Transmission line network.....	1
Table 2.1: Review publications on AC Induced corrosion.....	22
Table 2.2: Techniques for AC Corrosion.....	30
Table 3.1: Test conditions for Galvanostatic measurements	37
Table 3.2: Test conditions for Potentiostatic measurements	38
Table 3.3: Test conditions for measurement of weight loss	38
Table 4.1: Pipeline cross-section defined for burial depth	46
Table 4.2: Pipeline cross-section Existing Pipeline Earthing Locations	54
Table 4.3: Soil resistivity measurements at 115.4 and 117.72 km.....	55
Table 4.4: Soil resistivity and pH measurement locations in the field	56
Table 4.5: Details of Transmission Lines nearby/crossing Pipeline system.....	57
Table 4.6: Total Interference Levels.....	62
Table 5.1: Polarised Potential	64
Table 5.2: Protection potential at $PD = 0.1 \text{ A/m}^2$	64
Table 5.3: Summary of Protection Potential without AC	65
Table 5.4: Protection potential for X46 pipe under AC ($PD=0.1 \text{ A/m}^2$)	66
Table 5.5: Protection potential for X52 pipe under AC ($PD=0.1 \text{ A/m}^2$)	67
Table 5.6: Anodic shift at $PD = 0.1 \text{ A/m}^2$	67
Table 5.7: Protection potential X46 at $PD=0.3 \text{ A/m}^2$	68
Table 5.8: Potential shift at $PD 0.3 \text{ A/m}^2$	69
Table 5.9: Protection Potential X46 at $PD= 0.5 \text{ A/m}^2$	70
Table 5.10: Protection potential shift at $PD=0.5 \text{ A/m}^2$	70
Table 5.11: Protection potential shift at $PD = 1 \text{ A/m}^2$	71
Table 5.12: Protection potential $PD 2.0$ and 10.0 A/m^2	71

Table 5.13: Protection of Current Density Shift with polarisation potential	76
Table 5.14: Weight loss X46 at AC Density 200 A/m ²	77
Table 5.15: Weight loss X65 at AC Density 200 A/m ²	77
Table 5.16: Weight loss X80 at AC Density 200 A/m ²	78
Table 6.1: Soil Model for two locations	79
Table 6.2: pH measurement in the field	80
Table 6.3: Mitigation measures (104.95 to 208.58 km).....	88
Table 6.4: Comparison of pre and post-mitigation (Ch. 104.95 to 208.58 km)....	92
Table 6.5: Comparison of pre and post-mitigation (Ch. 208.58 to 284.32 km)....	93
Table 6.6: Comparison of pre and post-mitigation (Ch. 284.32 to 389.88 km)....	94
Table 7.1: Risk Assessment Matrix	99

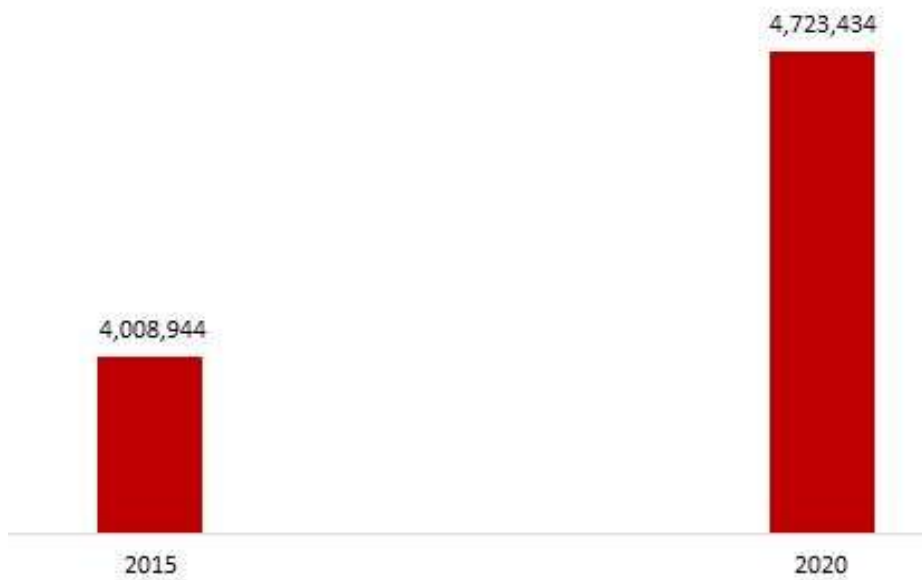
CHAPTER I

INTRODUCTION

1.1 BACKGROUND

Increasing energy demand has necessitated the use of more efficient modes of transportation. Two primary modes of energy transfer include pipelines and transmission lines. Pipelines ensure the bulk transport of gas and oil, and transmission lines ensure the transfer of electrical energy. Eleven thousand six hundred sixty-four circuit km (ckm) of transmission lines were laid in India alone in 2019-20 to ensure continuous power supply to consumers. As of August 2020, India's total length of transmission lines (220 kV and above) is 4,28,582 circuit km (Global transmission Report). Global Transmission line lengths have increased from 40,08,944 km in 2015 to 47,23,434 Km in 2020 (Table 1.1).

Table 1.1: Global Transmission line network



Source Open Global Transmission report – Data and Statistics

On the other hand, the most economical and safe oil and gas transportation can be done through pipelines. As of 31.3.2021, more than a 60,000 Km pipeline network is operational in India. Globally as of 31.12.2020, 1.89 million km of Pipelines enable the smooth transfer of Bulk oil and gas from one location to another.

Transmission lines and pipelines both facilitate the connection of supply and demand centers. Transmission lines and pipelines are linear systems that frequently run parallel or intersect at various locations. Due to land availability constraints, more and more pipelines and transmission lines are laid in the same corridors. Pipelines near transmission lines are susceptible to accelerated corrosion due to alternating current voltage from high voltage alternating current power lines [1]-[3].

Underground pipelines/structures are typically coated to arrest corrosion from outside. Cathodic protection system [4]-[6] as secondary protection, supplement coatings to prevent decay.

The following section emphasizes the widely prevalent criteria [7]-[9] for corrosion prevention of pipelines under cathodic protection:

1. Cathodic protection polarizes pipeline steel near -850 mV. A reference electrode saturated with copper sulfate electrolyte helps determine the polarized potential. Positive side polarization greater than -850 mV shall be insufficient to protect against corrosion. Polarization more negative than -1200 mV is known to cause coating disbandment.
2. In acidic environments, -950 mV polarization is considered, in the presence of dissimilar metals, in the presence of sulfides, and in anaerobic bacteria, among other conditions.
3. The current output from sources providing cathodic protection affecting that pipe section is interrupted simultaneously to measure polarization potential between the pipe and the earth for a coated pipeline. Compliance with the above, under cathodic protection, protects the Pipelines adequately.

However, coated pipelines, even under cathodic protection, deteriorate over time at several locations [10]-[12]. With transmission lines parallel to gas and oil pipelines, AC escaping the steel pipe leads to corrosion. This work highlights the AC-induced corrosion mechanisms and then details the work done to predict and mitigate corrosion induced due to AC interference on pipelines.

1.2 THEORY BEHIND

AC interference on pipelines located near the overhead AC transmission lines under steady-state conditions is as follows:

AC interference by induction

AC flow in the conductors of the transmission line generates an electromagnetic field around the conductor. The resultant electric field induces an AC in the underground metallic pipeline (Figure 1.1).

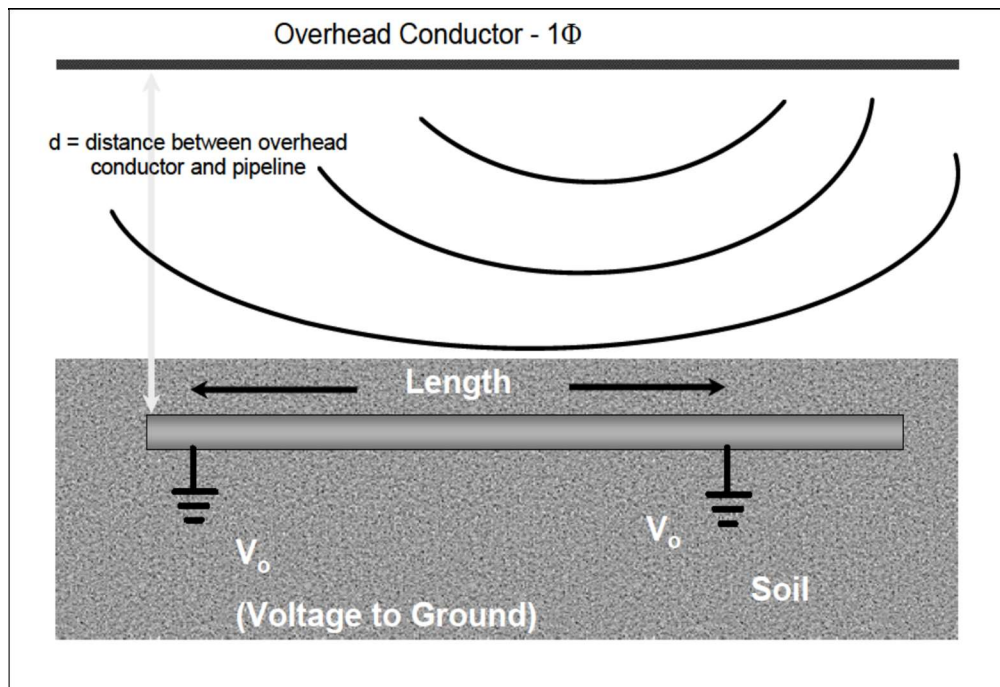


Figure 1.1 Inductive coupling with the underground pipeline (Source Open)

AC interference on account of the capacitive effect

Alternating current flow in the conductor generates an electric field around the conductor. The resultant electric field, in turn, results in a capacitive potential on aboveground metallic pipelines concerning the ground. Such capacitive coupling may be of significant concern when the pipeline is stored on the supports aboveground for activities such as welding, joint coating, and testing prior to actual laying underground (Figure 1.2). For a pipeline laid underground, capacitive coupling gets discharged to ground through tiny coating defects.

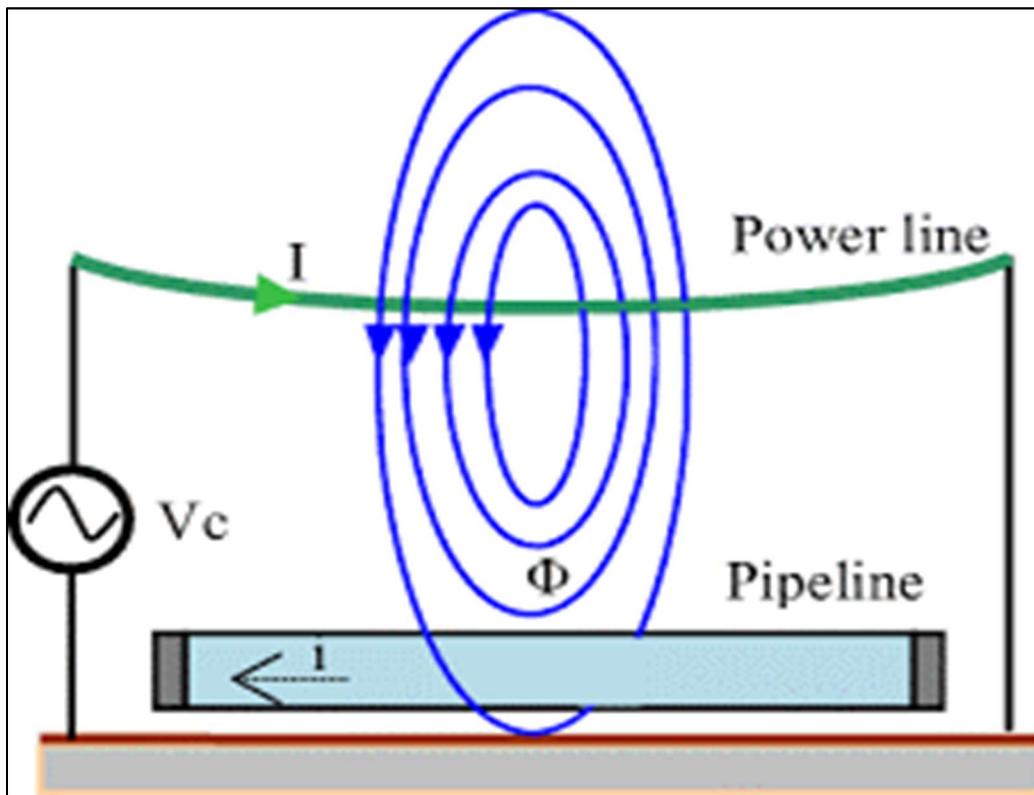


Figure 1.2: Electrostatic coupling with the above-ground pipeline (Source Open)

Numerous experimental studies [13]-[30] in AC interference under Cathodic Protection focus on several elements of AC interference like AC frequency, AC Voltage, AC to DC ratio, type of coating, size, and shape of coating defects, and transmission line orientation concerning pipeline. These features impact the severity and magnitude of AC corrosion on the pipeline, depending upon the soil resistivity and the surroundings.

Very few studies [31]-[35] evaluating the impact of AC corrosion on various pipe materials under cathodic protection establish the relative performance of pipe grades concerning AC-induced corrosion. Limited studies [36]-[40] attempt to simulate or predict AC-induced corrosion of pipelines under CP (cathodic protection). Modeling works [41]-[45] can help implement effective mitigation measures.

1.3 PROBLEM STATEMENT

During design, pipe material selection considers characteristics of the fluid, design pressure, maximum allowable operating pressure requirement as per ANSI B31.4, and various elements (like allowable stress, shut down head, specified minimum allowable stress, and common weld factor).

Designers also consider reasonable safety margins to decide on pipe thickness. Usually, no corrosion allowance is considered because of the plan to provide CP as a supplement to coating. Practically instances of enhanced corrosion of pipelines, even under cathodic protection, may occur over time [46]-[50], which may result in sudden early failure of the pipelines. Under cathodic protection (CP), pipelines fail due to AC-induced corrosion. Accordingly, it becomes essential to evaluate the feasibility of selecting pipes [51]-[52] less prone to AC-induced corrosion, especially under CP for multiple soil surroundings.

Conventionally, providing a Zinc grounding or SSDD (Solid State Decoupling device) [53]-[55] enables effective discharge of AC into the ground, thereby maintaining the PSP (pipe to soil potential) with appropriate protection. Few publications [56] evaluate corrosion prevention measures.

Modeling and simulation studies [57]-[60] can predict and mitigate AC interference parameters. Modeling works enable the design of mitigation measures and evaluation strategies for mitigation.

1.4 NEED AND MOTIVATION

In India, cross-country pipeline networks of over 41,000 km transport gas and oil round the clock. Overhead transmission lines also expand fast and run parallel to or cross the pipelines at several places.

AC interference on pipelines due to transmission lines seriously affects the integrity of the pipeline network. Enhanced corrosion on account of AC interference results in faster deterioration of the pipelines with the risk of leakage, rupture, and consequent damage to the environment and potential fire hazards. Any pipeline failure may also adversely affect the reputation and brand of the pipeline operator.

A 400 kV transmission line system was operationalized in 2016 in the Jamnagar district of Gujarat. This transmission line system crosses two operating pipelines at five places and runs parallel, as shown in Figure 1.3.

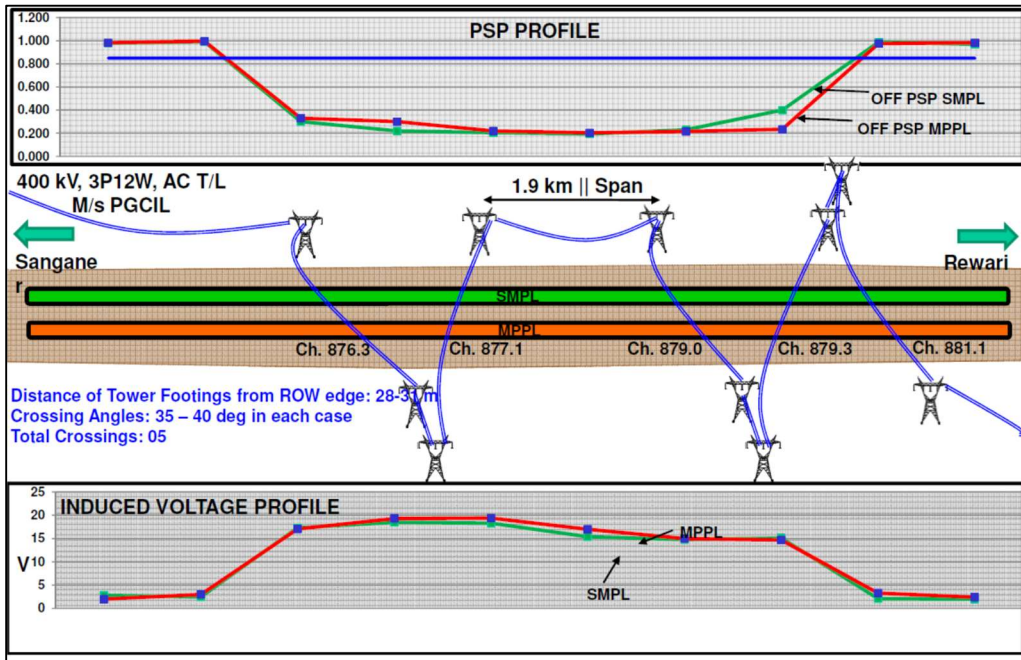


Figure 1.3: 400 kV Transmission line crossing two pipelines at five locations (In District Jamnagar, Gujarat, India, Source Open)

In June 2017, almost four months after the date of operation of the transmission line system, one of the pipelines ruptured with crude oil leakage of more than 2000 kls (Figure 1.4). The pipeline operations remained suspended for many days, and a considerable cost was incurred to salvage the crude oil, clean the area and repair the pipeline system.

Experts evaluated the reason for the burst of the pipeline system and concluded that AC corrosion resulted in pipeline failure. Such a pattern of pipeline failure was later observed at other locations also. A closer analysis of cathodic performance at several locations revealed the pipeline operator's difficulty in maintaining the PSP within the range for adequate protection, primarily due to adjacent transmission power lines.

The selection of pipe material depends primarily upon the requisite mechanical properties of service. Recent studies have revealed that maintaining adequate protection levels under AC interference ensures the pipeline's integrity.

PSP more positive than -850 mV may lead to pipeline corrosion because of inadequate cathodic protection levels. However, PSP more negative than -850 mV may be adequate to prevent general corrosion but may fail to protect the pipeline in the presence of AC interference. Also, the pipe grades may exhibit corrosion-resistant differential performance under AC interference. The influence of AC interference on pipelines under varying soil conditions also needs to be examined.



Figure 1.4: AC corrosion damage in District Jamnagar, Gujarat, India
(In 2017, burst in 128 days of pipeline commissioning, Source Open)

Standard AC mitigation measures include grounding pipelines using Zinc ribbons/anodes. Structured guidelines in this regard are required. Existing works refer to modeling for specific measures. Such modeling solutions must be developed and implemented for practical applications of long pipeline systems.

1.5 OBJECTIVES

The goals and objectives of this research are to:

1. Evaluate pipeline steel grade more resistant to AC Corrosion by observing the effect on protection density and protection potential on account of AC interference under cathodic protection.
2. Study AC interference impact on the Zinc and Magnesium anodes under cathodic protection.
3. Develop a Risk Assessment Matrix considering cathodic protection Potential, Pipe Grades, AC density, AC voltage, and pipe material.
4. Based upon the matrix, propose an AC corrosion model and optimize the proposed model using CDEGS/Python/Matlab.

1.6 RESEARCH METHODOLOGY

The present research work is a unique combination of experimental work and modelling application, which addresses the critical pipeline industry issue of maintaining the integrity of cathodically protected cross-country pipelines from external corrosion under AC interference. Empirical studies provide laboratory data on the AC corrosion behaviour of the various pipe grades under cathodic protection. Experimental studies comparing five pipe grades simultaneously in similar conditions help identify the ones more suitable for AC interference applications. Modelling analysis using state-of-the-art software (CDEGS) helps compare the pre- and post-mitigation measures. The mitigation measures are iteratively optimized for implementing the most economical mitigation measures. Field verification on the pipeline concerning modelled values help iteratively optimize the mitigation measures.

The research study develops a comprehensive corrosion model which the pipeline industry can utilize to address the issue of AC corrosion under cathodic protection and avoid pipeline failures due to AC corrosion.

CHAPTER 2

REVIEW OF LITERATURE

2.1 PIPELINES – THE LIFELINES

The crude oil must be transported from exploration wells, generally located in remote areas, to Refineries. While various means of transport, such as ships, roads, and trains, are also used, inland transportation is done chiefly through pipelines. A network of pipelines ensures uninterrupted and most economical transportation on a round-the-clock basis. The finished products such as Gasoline, High-speed diesel, and other fluids are also transported inland to consumption centers, mainly through pipelines. Similarly, the natural gas from wells is transported inland to the consumption centers through an elaborate network of pipelines. Accordingly, the pipelines are energy lifelines enabling bulk transport [61]-[62] of oil and gas most economically and reliably. In addition, pipeline transportation [63]-[64] is much safer when compared to other means of transportation.

However, any pipeline incident attracts widespread attention from the public, media, and regulators [65] due to its severe consequences on the environment and the public. The safety of pipeline transportation systems is vital for Nation and the Environment.

A failure in the pipeline system may cause havoc not only for the industry but for the public at large. A pipeline failure with an explosion in 2013 in China [66] resulted in the death of 62 people, many injured, and property damages worth millions.

The Operators thus accord safe operation and maintenance of the pipeline systems a top priority. The integrity management of pipelines [67]-[72] continually assesses, mitigates, and prevents risks for reliable, secure, and environmentally friendly service. Through systematic data collection and analysis, the risk

mitigation measures [73]-[99] are identified, planned, designed, implemented, and monitored to control and prevent pipeline failures.

2.2 PIPELINE FAILURE AND CORROSION

Humankind has known corrosion from times immemorial. While general corrosion remains challenging, people try to combat consequent deterioration by painting, coating, and cathodic protection methods.

Corrosion affects the underground pipelines due to the decline due to environmental factors adjacent to the pipelines. The pipelines are laid in various types of soil conditions and are affected by multiple types of corrosion, which include:

- General Corrosion, primarily chemical
- Galvanic corrosion due to differences in metals
- Electrochemical corrosion due to differences in electrolyte
- Stray current corrosion due to electrical interferences

The leading reasons for pipeline failures include metal loss due to corrosion, construction defects, and cracking. Corrosion remains the primary cause of failure in Pipelines [100]-[106]. Corrosion in pipelines occurs internally as well as externally. Quality of fluids flowing in the pipelines and regular cleaning by pigging minimizes Internal corrosion threat. Also, chemical treatment by adding biocides and inhibitors helps mitigate internal corrosion.

Mitigation of external corrosion primarily works by providing coatings as primary protection and cathodic protection systems as a secondary defence [107]-[113]. The coatings protect the pipelines from environmental attack and hinder the flow of corrosion current, thereby reducing the corrosion on the pipelines. The coatings' quality and application method become vital for the long-term performance of the coatings. The coatings' performance may be affected due to improper handling, storage, aging, or operational errors.

Cathodic Protection systems supplement the coatings to provide requisite polarisation to prevent the flow of corrosion currents. However, cathodic protection systems are prone to shielding and losing protective ability due to several factors.

The coatings contain holes too small for the naked eye, which can allow ingress of water or other corrosive liquids that can corrode the pipeline below the defects.

Corrosion products at such defects prevent the CP current from reaching the pipe. Thus, the cathodic currents reach the mouth of the Fault, and the line below remains unprotected due to shielding [114]-[117]. The coating disbondment at the coating defect surface also prevents the cathodic protection currents from reaching the pipe surface due to crevices formation.

Stray corrosion on pipelines occurs when the pipeline becomes the anode and corrodes due to the current flow between the pipeline and the electrolyte/soil. Stray corrosion may occur due to the flow of Direct current (DC), Alternate current (AC), or a combination of both. Stray corrosion is highly severe [118]-[120] and can emerge under various humidity, pH, and temperature conditions.

Stray corrosion [121]-[122] on account of DC results in metal loss directly proportional to DC density. However, due to periodic corrosion mechanisms, stray deterioration due to AC remains complex [123]-[130] and challenging to analyze.

2.3 ALTERNATING CURRENT INTERFERENCE ON PIPELINES

High-voltage AC transmission lines cater to the increasing need for the transportation of electrical energy from production centers to consumption centers. Simultaneously an extensive network of pipelines caters to the growing demand for energy by transporting fluids from one place to another. The instances of transmission lines being laid near the pipelines thus become unavoidable. The transmission lines and the pipelines are being laid in common corridors [131]-[150] in many places, mainly due to land use restrictions, better transportation efficiency, lower construction cost, and minimal environmental impacts. Land use restrictions become necessary when the new facilities are set up in heavy population areas, where securing independent utility corridors may become challenging and require sharing the existing corridors.

The proximity to transmission lines is challenging for pipeline operators concerning the integrity of the pipeline systems. Reports of pipeline failures on account of AC interference are on the rise.

Initially, the stray AC corrosion remained underestimated, considered less dangerous and negligible than DC corrosion [151]-[155]. Using Faraday's Law, Gellings explained the polarization in metals due to the passage of periodic signals [155] and linked the magnitude of the AC signal to the metal weight loss.

Investigations demonstrated the flow of minimal AC, causing charge transfer through polarization resistance for corrosion to occur [156]. The simplified analysis used voltage and current equations to control electrode potential rather than AC superimposition.

Measurements in different soils [157] indicated dense iron oxide membrane formation between anode and cathode and linear relation between anode weight loss and soil corrosiveness. Corrosion investigations on buried ferrous metals in various soils related [158] soil resistivity to corrosion current, maximum pit depth, corrosion current, and CP current. Soil conductivity calculations using the moisture retention function enabled [159] a single measurement of hydraulic conductivity.

AV modulation method evaluates [160]-[162], wherein alternating voltage shifts the corrosion potential negatively in the active region, resulting in enhanced current dissolution and destroying the mild steel passivity. Using the charge transfer model and numerical simulation, the polarization curves showed key characteristics in agreement with the experimental results.

While evaluating AC corrosion of copper, aluminum, lead alloy, and steel [165]-[166], several corroded pits on pipeline surfaces are observed at high AC magnitudes. AC was found to increase the corrosion current, shift corrosion potential negatively, and destroy the mild steel passivity.

Thevenin equivalent circuits used to predict induced voltages on buried pipelines [163]-[164]. Proposed methodologies to determine Thevenin circuits and pipeline characteristics can serve as ready reckoners for the Industry.

Various available mitigation [167]-[168] methods are evaluated. The study considers operational compatibility and personnel safety with induced current and voltage analysis in a study in the energy corridor.

Linear potentiodynamic anodic polarizations of stainless steel [169] observed that AC de-passivated the in-active region of the polarization curve, enhancing AC density magnitude and decreasing frequency. They utilized a crystal-based piezoelectric technique for the resolution on a real-time basis of the cell currents between competing reactions. Mass flux experiments on piezoelectric electrodes attempted to resolve the formation of the passive film.

Defects were observed on a CP-protected pipeline section due to AC corrosion [170], with local metal loss as high as 40%. A gas leakage on a cathodically protected pipeline from a pinhole occurred in 2002. The investigations revealed exposure to high induced AC voltages due to collocated transmission lines on the pipeline, which failed with pitting corrosion [171]-[173].

Pipelines experience accelerated corrosion in AC interference [174]-[175]. AC interference also results in coating disbondment, enhancing the corrosive environment below the coatings [176]-[177]. AC interference also adversely impacts the CP effectiveness by shifting potential away from the design.

AC interference also increases the risk of shock to the person touching or standing near the AC voltage gradient, which may endanger lives during fault conditions.

2.4 COLLOCATED TRANSMISSION LINES AND PIPELINES

Many experiments/investigations on alternating current corrosion of various metals suggest that AC corrosion results from complex mechanism characteristics, which requires reliable and sound methods for determining the extent of the corrosion. In practical situations, it is impossible to avoid laying pipelines adjacent to or near the transmission lines because of the non-availability of adequate lands or the linear requirement to cross each other.

Because of such constraints, more pipelines are installed near the transmission lines. The availability of nearby transmission lines, whether running parallel or crossing pipelines, increases the risk of AC corrosion on pipelines and calls for effective mitigation methods to mitigate corrosion due to AC interference.

Union Gas, Chatham, Ontario, installed a pipeline coated with Coal tar in 1972. Induced AC on this pipeline was observed at around 33 volts, and installed mitigation measures to reduce AC interference in 1994 [173], [178]-[180]. During internal ILI inspection, irregular corrosion defects were observed in the section near transmission lines. The flaws have an average depth of up to 40% of wall thickness, with maximum penetration of up to 80%. Bell hole inspections revealed that the disbanded coating covered the defect with a hard tubercle of a height of 50 mm. The soil resistivity near the Fault was 2000 Ohm-m and pH greater than 8.5. PSP

at the site was -1560 mV. The flaws were attributed to AC's corrosion upon investigation.

In the first reported case in Germany, two corrosion perforations on a gas pipeline near rail transit systems [173] were observed in 1986. In Europe, a gas pipeline installed in 1992 was reported to be corrosion in 1993 [181]. The pipeline ran parallel to the 400 kV transmission line for 3 km. AC voltage on the pipeline was 13 V. Corrosion depths up to 0.8 mm observed with disbonded coating and a pH of 13 near the iron oxide corrosion product.

A PE-coated natural gas pipeline [64], [182], [183] detected corrosion failure under CP, with a protective density of less than five mA/m². The pipeline ran parallel to the traction system. AC voltage on pipeline up to 60 V observed near corrosion sections. The presence of Cations, and anions in corrosion products, indicated the occurrence of anodic and cathodic reactions.

A 3LPE-coated gas pipeline in China, protected by Magnesium Anodes, was reportedly running at high risk of AC interference [94] with AC voltage over 10 V, with a maximum AC density of 101.7 A/m². The pipeline was running parallel to 22 kV and 110 kV transmission pipelines. A pipeline in Hebei, China, developed several pits of 10 mm in diameter, with an average depth of 3mm, due to an attack by AC from a nearby electric railway.

In India, a crude oil 3LPE coated pipeline reported 78% metal loss [184] during ILI in 1997. The PSP survey did not reveal any abnormality. The operator excavated the site, adjoining a 66 kV power line, to verify the ILI report physically. Pinhole damage was observed on the coating upon excavation, and the balance coating was in good condition. Coating removal indicated a deep pit formed due to high current discharge.

Furthermore, the presence of AC causes a change in PSP and reduces the CP's effectiveness in protecting the pipelines [185], [186].

Underground pipeline subjected to stray interference fails early, resulting in conditions that may be hazardous for the public. It is challenging to provide adequate protection to pipelines against stray corrosion influenced by many complex factors [187]-[192]. Several parameters, such as humidity, porosity, salinity, pH, soil resistivity, and temperature, influence corrosion severity, and extent.

Stray AC Interference has resulted in severe pipeline system failures because the HVAC transmission line passes nearby. Accelerated AC corrosion observed in the pipeline before commissioning the pipeline [136] in a short span of five months after laying in the HVAC utility corridor.

Anodic dissolution and cathodic reduction decreased the cathodic Tafel slope [19]-[196], resulting in a higher corrosion current for a constant anodic Tafel slope. Research expressed corrosion potential as a function of the anodic-to-cathodic Tafel slope ratio. A subsequent model for the corrosion under AC voltages [197]-[198] suggested faradaic processes and explained charging current in terms of two-layer impedance and capacitance. Root mean square values are a better indicator of the corrosion process occurrence than the absolute ratio of the anodic to cathodic Tafel slope.

A study of corrosion caused by 60 Hz AC voltage in steel [195] through immersion tests indicated an enormous increase in corrosion rate. The study also evaluated the pH of the soil-simulating medium for any influence on AC corrosion.

The potential cycling impact on the development of oxide layers on the steel surface [199] indicated the occurrence of diffusion-controlled redox reactions in the oxide layers. Mechanism of OH^- transport limited corrosion growth, concluding that AC passage flowing through structures accelerates the corrosion rate. A corrosion anomaly study [68] discusses steps for AC corrosion identification on pipelines and ways to minimize AC corrosion risk.

The numerical model coupled finite element and boundary element methods for a cathodically protected [200] underground pipeline system and considered the drop in voltages upon simulation. The calculated stray currents on CP-protected underground pipelines [201] established the simulation deployment for multiple pipelines under CP systems.

A study of corrosion systems due to AC [202] under activation control suggested simple functions for the AC voltage concerning the corrosion potential and corrosion rate, considering both cathodic and anodic reactions. The research mentions numerical analysis as essential for determining cathodic responses under mixed control and anodic reactions under activation control. The study also identifies that induced AC voltages strongly impact corrosion behavior depending on the Tafel parameters.

The field and circuit approaches enable the study of electromagnetic interference [203]-[215] mechanism on a pipeline. A study comparing both and using field and circuit approaches on a pipeline enabled the comparison of results. A network model computed results (less than a 15% difference between the two approaches) to determine the capacitive, inductive, and conductive interference effects.

A literature review revealed the influence of AC interference of extra high voltage transmission lines [180] on pipelines considering various parameters, including polarisation level, AC density, cathode surface area, and soil composition.

A simulation model optimizes a pipeline system's touch potentials in various mitigation problems. The study validates the design of mitigation measures by comparing simulation results with field measurements.

2.5 AC INTERFERENCE SOURCES

Sources that cause AC interference on pipelines include:

2.5.1 Transmission lines

Transmission lines transmit power from one central station to another and may include power lines with one or double circuits. As the three phases carry sinusoidal AC at 120 Degrees apart, the sum of the three phases is zero for balance loading in all three phases. Accordingly, the vector addition of the magnetic field for a balanced three-phase system is zero. However, some amount of phase imbalance [216], [217] remains, resulting in AC interference on pipelines.

2.5.2 Traction Systems

Many traction systems, including AC or DC traction systems, are prevalent. DC systems dominate for shorter lines, whereas 25 kV AC traction systems are commonly used globally. AC traction system interference on pipelines may cause shock and corrosion in steady-state and Fault conditions [218]-[221].

2.5.3 Other Sources

Low-frequency communication systems and geomagnetically induced currents are other sources that may cause AC interference on pipelines. Equipment or vehicles nearby pipelines may also generate AC voltages. High AC voltage may also occur on pipelines during construction while being above ground due to any source.

2.6 INVESTIGATIONS OF AC CORROSION OF PIPELINES

In the early 1900s, researchers investigated AC frequency's effect on corrosion [222]. Studies to understand whether AC flowing between the metal and soil would result in decay [151], [223]-[235] primarily considered AC corrosion an unimportant issue until the 1980s. The results obtained at that time indicated that the rate of AC corrosion [236]-[237] was just 1% of the similar corrosion caused by DC AC Corrosion of steels at 60 Hz, found lesser than 1% of the corrosion induced by equivalent DC [153].

An investigation of the wall thickness loss of a high-pressure extended pipeline network attributed the loss to AC induced interference [170]. The investigation indicates likely causes of AC corrosion, including prediction and mitigation. Under AC interference, the author studied parameters such as AC density, voltage, soil resistivity, and frequency [238]-[243] and recommended independent protection criteria under AC interference. A study [8] explained Fe₂ oxidization in the rusted layer and analyzed experimental results. A study presents [183] measurements of Off potential and its interpretations concerning soil type and composition. Data analysis of measurements collected over six months through continuous data acquisition concludes that AC corrosion risk is affected by climatic conditions and soil composition.

A study was presented on the performance and design of the devices [244] to minimize AC corrosion without compromising the CP system performance. The study enhanced the CP system performance by significantly reducing AC voltage, total CP current, and PSP fluctuations. The resultant parameters indicate reliable measurements of CP parameters and the general reduction in corrosion risk.

While dealing with the aboveground transmission line design with single/double circuit configurations [92], a study presents mitigation of AC voltage on the pipeline at some distance from the transmission line.

Experimental studies [245] on AC-induced interference on steel specimen concludes that the oxygen reduction process occurs at the cathode when AC flows at high current densities. The studies recommend further investigations to determine the AC density threshold and further understand AC corrosion.

AC interference tests [246] in water, soil, and concrete solutions revealed local corrosion, which corroborated with the published literature. However, study results in sodium chloride solution are at variance with the available models. A study presents a mathematical model for assessing the capacitive effect [131] due to extra high voltage aboveground transmission lines on pipelines. Multiple factors affect AC-induced voltages on pipelines [247], [248].

A study presents an assessment of the corrosion of pipelines [114] using assessment methods, theoretical analysis, and experimental tests. The study compares various techniques and identifies the best available technique. Another study presents the CP analysis using equations for the dual boundary element method [256] and conducts experiments to validate simulations. Stray corrosion simulation and analysis using boundary elements [118], [119] find corrosion rate directly proportional to current density. Numerical studies investigate the cathodic and anodic interferences and determine that anodic interference is less severe than cathodic interference. The study finds software (BEASY) convenient for analyzing stray interference on an adjacent, non-protected structure.

A methodology of corrosion for inverse problems [249] considers genetic algorithms and boundary elements to optimize based upon boundary elements considering evolutionary principles.

A mechanism [250] indicates corrosion occurring with a minimal discharge of AC. AC corrosion happens based on AC flow through an electrochemical interface in the ohmic portion of the parallel RC. AC corrosion involves the sudden development of the diffusion process in soils. The total impedance reduces with an increase in AC under the diffusion-control mechanism.

A study presented the AC effect on galvanic corrosion [251] and conducted weight loss tests to estimate AC corrosion threshold parameters. He evaluated the AC effect of AC on the corrosion mechanism and compared mathematical models with experimental data to conclude the AC density threshold, mechanism of AC-induced corrosion, corrosion morphology in the presence of AC, AC-induced corrosion of

carbon steel in alkaline solution (concrete), and cathodic protection monitoring.

The studies evaluated the capability and performance [137], [252], [253] of various software tools to determine and predict AC induced voltage on pipelines. The studies considered steady state and fault interference analysis of the pipeline in the utility corridor. Assessment of the installed mitigation systems duly earthed with insulating joints shows that the mitigation system is adequate to limit coating stress voltage on a pipeline. While multiple mitigation measures are compared concerning the cost of installation and performance, the mitigation of AC-induced interference using the gradient control wire method is preferable.

Electrochemical studies [254] conducted on steel in marine environments revealed that AC density influences the benign steel specimens' surface morphology, experimental solution pH, and steel corrosion rate. Beyond a threshold limit, an increase in AC density results in an enhanced corrosion rate.

A study evaluates the corrosion effect of stray interference on steel in concrete on the corrosion behavior of steel in concrete [245]. Due to anodic density, the presence of chlorides in the concrete, and interruptions in current, corrosion initiates after some time in concrete. The study also suggests that AC corrosion in concrete may be less severe than DC corrosion, though AC influences steel corrosion in concrete.

A model mentions negative polarization during the negative half cycle with a positive polarization at the time of the positive half cycle considering the traditional evaluation of the corrosion process [257] under AC interference. The current exhibited a much more significant change than during the cathodic (negative) semi-cycle. During the anodic semi-cycle, the reduction current decreased, but to a lesser degree as it increased during the cathodic semi-cycle. Therefore, the complete AC cycle resulted in a net increase in the reduction current.

Modeling considering boundary and finite element methods to estimate the DC interference [59], [255] exhibited the stray current interference from the DC traction system on the underground geometry of sheet steel walls.

A corrosion model [258] showing the effect of AC on nanostructured surface films under CP validated through experiments relating corrosion to nanostructured surfaces and showed that the mechanism of the electrode process could be studied using AC Voltammetry. They identified the characterization of the crystalline metal structure as future works.

Studied presented the anodic and cathodic reactions and subsequent effects of corrosion product deposit for X series steels [259]-[263]. They used localized electrochemical impedance spectroscopy, scanning vibrating micro-electrode, macroscopic EIS measurements, and surface analysis. They found that the deposited layer formed on the steel surface is porous and non-compact. The presence of a corrosion product layer enhanced adsorption & inhibit the permeation of hydrogen atoms into steel. The corrosion product deposit layer on the electrode surface enhanced the anodic dissolution of the steel.

A model [264] for current and steady-state corrosion potential considered double-layer capacitance, solution, and polarization resistance. Using the Perturbation method, a non-linear model for the corrosion of metals subjected to alternating voltage-induced corrosion [265] included polarization resistance, double-layer capacitance, and the development of solution resistance. They presented corrosion under AC conditions in terms of peak potential and increase in the ratio of the anodic-to-cathodic Tafel slope. They concluded that the AC-induced corrosion rate decreased with the applied signal's frequency and increased the DC corrosion potential. They also showed that the AC-induced corrosion rate was independent of the DC corrosion rate and increased with the peak potentials of the AV signal.

Detected AC corrosion using coulometric oxidation by Fe(II) oxidizing the rust layer and analyzed experimental results to determine the effect of the CP level on corrosion rate [8].

A boundary element method to simulate the sacrificial anode CP problem of the steel storage tank [266] optimized the location of the anode and studied the influence of anode length and paint defect on the level of protection provided. The study concluded that the boundary element method was beneficial in modeling and analyzing CP systems. They found consistency in calculations with expectations from basic corrosion concepts.

Various studies [267]-[277] on the AC-induced corrosion of coated pipeline steel in a solution simulating used potentiodynamic polarization measurements, immersion tests, and surface characterization techniques and found that an AC application resulted in a negative shift of corrosion potential of the steel, caused an oscillation of anodic current density, and degraded the steel passivity developed in the solution. An increase in AC density increased the corrosion rate. Uniform corrosion occurred at a low AC density, while pitting corrosion occurred

extensively on the steel electrode surface at a high AC density.

Investigations [278]-[279] of the AC interference corrosion problems in Pipelines under Cathodic Protection through weight loss tests done in soil-simulating conditions at various AC densities up to 900 A/m^2 . They also presented polarisation test results and concluded that AC enhanced localized corrosion and that the corrosion rate was not acceptable at AC densities higher than 30 A/m^2 . The influence of induced AC interference [280], [281] on the localized corrosion resistance of passive metals included potentiodynamic tests to analyze the effects of AC stationary interference on passivity. They identified critical AC density, corrosion morphology, and time to corrosion as essential considerations for investigating AC interference on passivity.

Several works have indicated/documentated the harmful effects of AC [282]-[300] on pipeline safety because of enhanced pipeline corrosion. Garcia A. et al. [301] used Monte Carlo Simulations to present an innovative and practical solution for determining AC Interference by changing lateral distance (between pipeline and transmission line), coating conductance, and pipeline diameter. The index matrix (based on first, second, and total order effect values of all inputs) shows individual and interactive effects on induced voltage.

Other works [3], [111], [112] involving DC Potential measurements and weight loss tests for pipeline specimens concluded that CP potential applied on steels for corrosion protection could not be relied upon in the presence of AC Interference. Accordingly, the available CP standards shall continue to review, update and consider AC interference for adequate corrosion protection.

2.7 AC CORROSION

2.7.1 AC CORROSION EVOLVING

Even though the experiments for understanding AC corrosion commenced in 1891 or earlier, the investigations of more practical importance started in 1905, which inferred that the corrosion loss due to alternating currents is negligible. By 1916, researchers described the experimental work done to determine the effect of AC on corrosion and inferred that corrosion reduces with an increase in AC frequency [222].

However, AC corrosion has been investigated actively since observing the first AC corrosion damages [183] on cathodically protected pipelines around 1988. Even after numerous investigations & experiments, the mechanism of AC corrosion is still to be understood fully, and effective measures to mitigate AC corrosion risk are still evolving. Some review publications on induced AC corrosion are indicated in Table 2.1.

Table 2.1: Review publications on AC Induced corrosion

Year	Review Publications	Author
2001	Risk evaluation of AC corrosion. Parameters influencing AC corrosion risk for further mitigation.	Collet, Erwan, Bernard Delores, Michel Gabillard, and Isabelle Ragault
2012	The science of pipe corrosion: A literature review on the corrosion of ferrous metals in soils	Cole, Ivan S., and D. J. C. S. Marney
2016	A review of quantitative risk assessment of onshore pipelines	Da Cunha, SB
2017	Review of Recent Developments in Induced AC Corrosion Mitigation Design, Materials, Installation, and Monitoring Technologies	Sirola, T
2018	Mitigation of corrosion problems in API 5L steel pipeline-a review	Kolawole, F.O., Kolawole, S.K., Agunsoye, J.O., Adebisi, J.A., Bello, S.A. and Hassan, S.B
2020	A comprehensive review: Evaluation of AC Induced Voltage on Buried Pipeline Near Overhead Transmission Lines and Mitigation Techniques	Mahmoudian, A., Niasati, M. and Karam, F
2020	The science of alternating current-induced corrosion: a literature review on pipeline corrosion-induced due to high-voltage alternating current transmission pipelines	Thakur, Ajit Kumar, Adarsh Kumar Arya, and Pushpa Sharma

2.7.2 AC INTERFERENCE FORMS

Stray AC interference may occur on underground pipelines [302] due to nearby AC Transmission lines through Inductive, Conductive, and Capacitive coupling.

Inductive Coupling

Inductive coupling (Figure 2.1) may occur because of the transmission line and underground pipeline's electromagnetic coupling in both steady state and fault conditions. The currents discharged by the transmission line into the ground form the potential [241]-[243] gradient in the ground. If the pipeline is in such a potential gradient, there arises the risk of personal hazard (increase in touch potential) or pipeline corrosion (during high transient induced AC voltage).

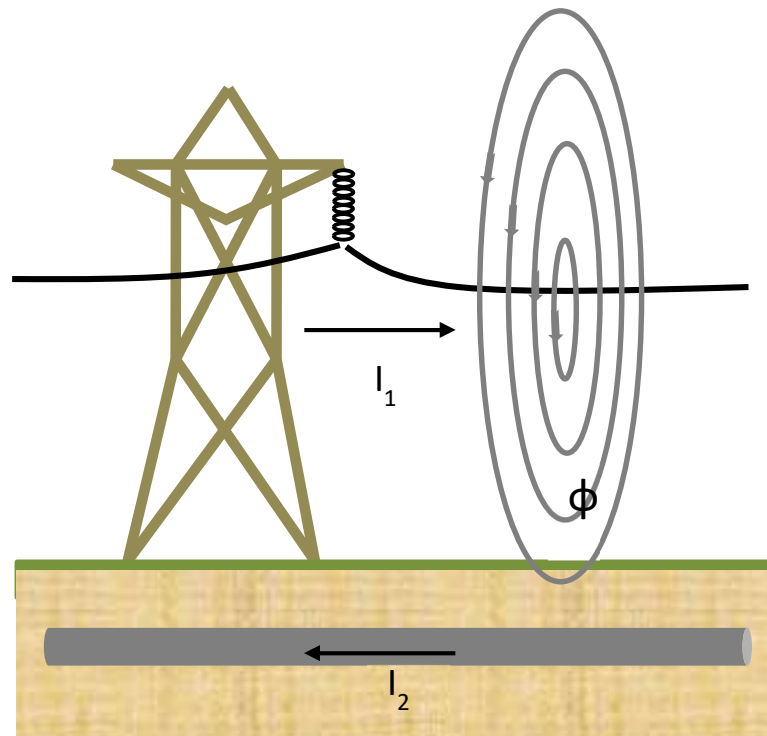


Figure 2.1: Inductive coupling schematic

When the pipeline is sufficiently close and parallel to the transmission line, the magnetic field will cross the pipeline, resulting in induced alternating voltage. The flow of resultant-induced AC through coating defects may cause AC Corrosion. Induced voltage magnitude depends upon several factors [22], [246], such as the

type of conductor used in a power line, length of exposure, current extent, existing grounding system, separation distance (between buried pipeline and power line), and soil resistivity.

Conductive or Resistive coupling

Conductive coupling is attributable to the influence of two or more circuits on each other due to conduction between the circuits (Figure 2.2). During line faults or lightning surge current discharge, electric arc formation may result in coating failure and damage to the pipeline.

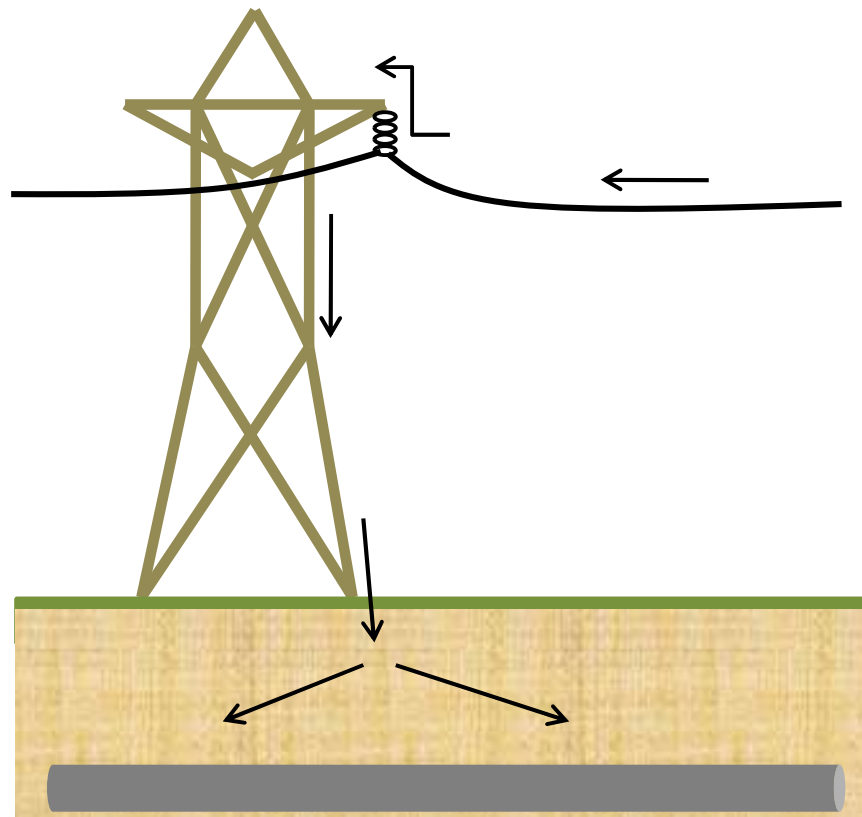


Figure 2.2: Resistive coupling schematic

The pipeline's peak coating voltage stress (Eqn. 2.1) depends upon [303] lightning current, the separation distance (between the pipeline and the tower structure), and soil resistivity. The equivalent pipeline model is as below:

$$U_{max} = \frac{(Ad+B)\rho I_0}{100(d+C)} \quad (2.1)$$

Where U_{\max} - Maximum coating voltage, kV

I_o - Stray current at tower grounding structure, kA

ρ - Soil Resistivity, Ωm

d - Distance between pipeline and tower edge

A, B, C - Constant Coefficients

Accordingly, the lightning electrical strength of the pipeline coating can determine the safe distance between the structure edge and the pipeline. During faults in the transmission system, a large current is discharged into the earth by the faulted structure, which raises the soil potential. The resultant difference in potential results in conductive interference [304]-[310] as a function of potential ground rise, separation distance, size of structure grounding system & soil characteristics.

Capacitive Coupling

The above transmission line may induce AC voltage through capacitive coupling when the coated pipeline is above ground during installation. Regular earthing of the pipeline effectively grounds the induced AC voltage. The capacitive coupling [204] effect is minimal for a buried pipeline, almost negligible.

2.7.3 PARAMETERS AFFECTING AC CORROSION

The main parameters related to AC Corrosion [30], [127] are AC Density, AC Voltage, Cathodic Polarization, Coating defect surface area, Electrolyte composition, and Soil Resistivity. Alternating Frequency and AC to DC intensity ratio influence AC Corrosion. It is evident from various publications that the generally agreed-upon mechanism of AC Corrosion in soils is missing, and there seems to be a difference concerning threshold values of multiple parameters affecting alternating current corrosion.

Alternating Current (AC) Density

Laboratory experiments involving measurements [9] of weight loss on CP-protected pipeline samples under the influence of AC with current densities (10 to 500 A/m²) indicated that the -850 mV CSE criterion may not always be safe in the presence of AC interference and overprotection is the most severe and dangerous under AC interference.

Studies have indicated that AC corrosion occurs at an AC density of 100 A/m² [171]-[173]. Laboratory tests determined AC corrosion occurs in applied cathodic protection beyond a threshold AC density of 30 A/m² [245] because of the oxygen reduction cathodic process.

Further studies have also indicated that cathodic protection may be ineffective in protecting the pipeline from corrosion [111]-[112] in the presence of a small AC density of 10 A/m².

Field experiences indicate that AC corrosion may not occur up to 20 A/m² AC density. Between AC densities from 20-100 A/m², AC corrosion may occur. However, AC corrosion is inevitable for AC densities [311] more significantly than 100 A/m². The evolution of hydrogen [127], [245] on the surface of the specimen is observed at high AC densities (> 100 A/m²).

Laboratory studies have further concluded that a higher corrosion rate is unacceptable [30], [251] at AC densities of 30 A/m² or more. Such accelerated AC corrosion is due to the irreversible process during an anodic half-cycle, which fails to reverse fully during the cathodic half-cycle.

The corrosion rates at 10 A/m² of AC density were almost twice the corrosion without AC interference, establishing that the AC interference of 10 A/m² may also be harmful. Additionally, AC corrosion results in localized pitting at high AC density. Corrosion pattern changes from uniform to pitting corrosion at alternating current densities above 100 A/m². [94], [312], [313].

AC Voltage

Experimental studies [161], [162] indicated that the AC Voltage shifts the corrosion potential toward the active region, resulting in an increase in current density and thereby affecting the passivity of the mild steel. AC Voltage is a critical factor in evaluating AC corrosion and is measured directly on the structure. AC voltage on pipelines should not exceed 10 V for high soil resistivity (above 25 Ω-m) and 4 V where low soil resistivity (below 25 Ω-m) at any time.

The relation between AC corrosion rate and AC voltage [193] using anodic and cathodic reactions is depicted as per Tafel Equations (2.2) and (2.3).

$$E_a = m_a \times \ln i_a + c_a \quad (2.2)$$

$$E_c = m_c \times \ln i_c + c_c \quad (2.3)$$

where, E_a & V_c are anode & cathode potential, m_a & m_c are Tafel slopes for anode & cathode, i_a & i_b are anode & cathode currents & c_a & c_c are open circuit anode & cathode potential.

The corrosion potential ($E_{\text{corr, DC}}$), the steady-state DC potential when anode and cathode currents are equal, is given by Eqn. (2.4)

$$E_{\text{corr, DC}} = \frac{m_a c_c - m_c c_a}{m_a - m_c} \quad (2.4)$$

Corrosion current ($I_{\text{corr, DC}}$) thus is given by Eqn. (2.5)

$$\begin{aligned} I_{\text{corr, DC}} &= \exp \left[\frac{E_{\text{corr, DC}} - c_a}{m_a} \right] \\ &= \exp \left[\frac{E_{\text{corr, DC}} - c_c}{m_c} \right] \end{aligned} \quad (2.5)$$

The steady-state potential when time-averaged anodic and cathodic currents are equal, Corrosion potential, $V_{\text{corr, AV}}$, can be obtained from Eqn. (2.6).

$$V_{\text{corr, AV}} = V_{\text{corr, DC}} - \alpha \quad (2.6)$$

Where:

$$\alpha = \left(\frac{m_a c_c}{m_a - m_c} \right) \ln \left[\frac{\sum_{K=1}^{\infty} \frac{1}{m_a - (K!)^2} \left(\frac{E p}{2 m_c} \right)^{2K} + 1}{\sum_{K=1}^{\infty} \frac{1}{m_a - (K!)^2} \left(\frac{E p}{2 m_a} \right)^{2K} + 1} \right] \quad (2.7)$$

NACE recommends estimating AC corrosion risk using the formula as per Eqn. (2.8).

$$I = \frac{8 V_{\text{ac}}}{\pi \rho d} \quad (2.8)$$

Where I – AC density

V_{ac} – AC voltage to remote earth

ρ – Soil resistivity

d – Diameter of the circular holiday equal to the area of an actual holiday

However, predicting induced AC corrosion rate based on AC voltage magnitude is challenging, as enhanced corrosion may not occur at the maximum induced alternating voltage. Assessment of AC Corrosion based on AC Voltage can be confusing, and AC mitigation addresses safety considerations by restricting the AC voltage below 15 V. Numerical analysis and modelling [202] based upon Tafel parameters can evaluate the AC voltage effect on corrosion behaviour.

AC frequency

AC frequency affects the pit density, passive current density, and morphology [314]-[317]. The corrosion rate reduces with an increase in AC frequency, and the magnitude of potential shift also decreases with frequency [153], [222], [224].

AC to DC density

The AC to DC density of ten or more indicates a specific corrosion risk [180]. The risk of corrosion is appreciable when AC to DC density is more than three. AC to DC density of lesser than two may indicate lower risk; however, it does not indicate a complete absence of risk. The AC to DC density is higher at corrosion sites compared with other areas where the ratio is small.

Type of coating and defects

Pipeline coatings improved significantly [318] over the last three decades. First-generation coatings (Coal Tar, Asphalt, single-layer polyethylene) have been replaced by second Generation coatings (liquid coatings or one-layer FBE). Third Generation coatings follow them (three layers of polyethylene, three-layer polypropylene. & Double layers Fusion bonded epoxy). High-quality coating materials are available today, providing high dielectric and mechanical characteristics and high coating resistance. The coating quality improvement has resulted in fewer coating damages and increased susceptibility of pipelines in areas of AC corrosion.

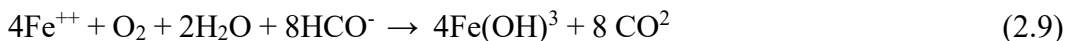
The coating defect shape and size influence AC corrosion. The defect area is reciprocal to electrical resistance; accordingly, the protection current finds it more difficult to reach a defect smaller than a more significant fault.

Transmission lines orientation to Pipelines

Distributed source analysis of the inductive coupling may predict induced voltage on the pipeline in common right of way with transmission lines [319], [320]. Pipeline orientation to Transmission lines influences the magnitude and distribution of induced AC voltage. The complex characteristics like electrical discontinuity of power line, a change of pipeline path, shield wires, and multiple conductors' analysis include mutual impedance, unknown currents program, pipeline characteristics, and Thevenin circuit Programs.

Numerical models [321] simulate the induction due to the pipeline and transmission line proximity at various angles. AC transmission line induces minimal AC on the pipeline when it crosses it at nearly ninety degrees. However, an AC transmission line running parallel to the pipeline may induce significant AC on the pipeline. Field investigations have indicated that corrosion occurs [186] mainly at defects with areas up to 1 cm². Different holiday areas experience different corrosion rates, and various-sized defects [322] accelerate corrosion under AC. The corrosion behaviour of pipeline steel [187], [188] using the EIS test, Polarisation curve, immersion test & Mott-Schottky curve has indicated that the reduction in AC frequency shifts the corrosion potential more negatively and enhances the steel corrosion rate, resulting in increased occurrence of corrosion pits.

Observations and measurements [158] exist in the early nineteens evaluating steel corrosion under cathodic protection in various soils and outline basic theory. The electrochemical theory of underground corrosion explains the concentration of hydroxide ions at the cathode, ferrous ions at the anode, and increased circuit resistance due to the oxidation of ferrous ions in the presence of bicarbonate to ferric hydroxide:



The study by Denison involved corrosion for a short exposure period of up to two weeks and described the formation of membrane between anode and cathode. The position of the membrane concerning the anode is attributable to factors such as

soil permeability, soil reaction, and concentration of soluble salts. Empirical equations have been derived and found to remarkably agree [159] with experimental results for the pitting corrosion in well-aerated soils, well-aerated soils, and poor-aerated and very poor-aerated soils.

The effects of stray alternating currents on pipeline steel have been investigated through multiple laboratory tests, such as Immersion tests, Electrochemical tests, and explained with the help of a mathematical model of AC interference. Corrosion morphology changes from generally uniform to predominantly pitting [245] in the presence of AC interference. Various tests undertaken to study the AC-induced interference effect on passive metals have shown that AC's presence reduces steel's resistance to corrosion, resulting in the enhanced deterioration with decreased critical chloride threshold. Table 2.2 represents some techniques used to evaluate AC Corrosion.

Table 2.2: Techniques for AC Corrosion

Study	Objective	Technique used
I A Dgnison et al., 1939	Steel Corrosion under cathodic protection in different soils	Corrosion cell observation in different soils
M. Frazier et al., 1986	AC interference Study of a common utility corridor	Software development for steady-state analysis to determine pipeline voltages and currents
Sara Goldanich, 2005	Effect of AC on corrosion of metals	AC density threshold determination, Corrosion rate, and study corrosion kinetics
Sara Goidanich et al., 2010	Investigate Ac interference corrosion problems causing pipeline failures	Weight loss tests performed at different AC densities in soil simulating solutions on a carbon steel specimen
Dan D. Micu et al., 2012	Study of EM interference between transmission lines and pipelines	Loop Current technique based on a hybrid model to solve equivalent electric circuit
A Q Fu et al., 2013	Effect of AC on CP performance	Electrochemical, weight loss, and surface characterization

M Buchler et al., 2013	Potential measurement under AC corrosion	Continuous data acquisition
Zitao Jiang et al., 2014	Simulate coating holidays under AC on buried pipeline	Laboratory experiments conducted
Huiru Wang et al., 2017	AC effect on cathodic protection	Voltammetry method, Potential monitoring, and surface characterization
Thakur, Ajit Kumar et al., 2022	Prediction and Mitigation of AC interference	Experimental studies coupled with modeling using CDEGS

The above techniques are deployed to determine and understand the AC corrosion mechanism under cathodic protection. Few authors have conducted experimental studies involving weight loss measurements, voltammetry, and other tests on steel specimens under cathodic protection, to evaluate the influence of alternating current interference. Studies have revealed that corrosion has occurred in the presence of CP. The -850 mV CSE criterion is not always safe, and over-protection is the most dangerous condition in the presence of AC.

Further simulation /modeling studies duly validated with field measurements involving prediction and mitigation of AC interference for extensive pipeline networks are unavailable. Pipeline design engineers use this study to select the appropriate pipe steel for applications subjected to AC interference.

The prediction and consequent mitigation of pipeline AC corrosion under cathodic protection through a mix of experiments and validation through simulation studies help develop a robust corrosion model, which is helpful to the pipeline industry to mitigate AC corrosion effectively.

CHAPTER 3

EXPERIMENTAL WORK

3.1 POTENTIOSTATIC AND GALVANOSTATIC TESTS

The experimental studies below are conducted under cathodic protection to determine the Alternating Current Interference effect under simulated soil conditions as below:

- 3.1.1 Determine the effect on protection potential through Galvanostatic measurements across API pipe grades X46, X52, X60, X65, and X80.
- 3.1.2 Determine the effect on protection current density through Potentiostatic measurements across API pipe grades X46, X52, X60, X65, and X80.

The Galvanostatic and Potentiostatic measurements enabled us to compare the relative performance of respective API pipe grades regarding resistance to AC corrosion under the influence of AC interference under cathodic protection.

3.2 ELECTRICAL CIRCUIT

The electrical circuit (Figure 3.1) controlled, separated, and measured the DC and AC. The basic properties of Inductors and Capacitors enabled the coupling of an AC circuit with a DC circuit without interference. The Inductor blocks AC circulation in the DC circuit, and the capacitor prevents DC flow in the AC Circuit, enabling taking unaffected and reliable measurements under cathodic protection.

The electrical circuit combines two circuits, one DC and another AC circuit.

3.2.1 DC CIRCUIT

DC circuit consists of the following:

- The shunt, R2 (10 Ohms, 200 W), for DC measurement.

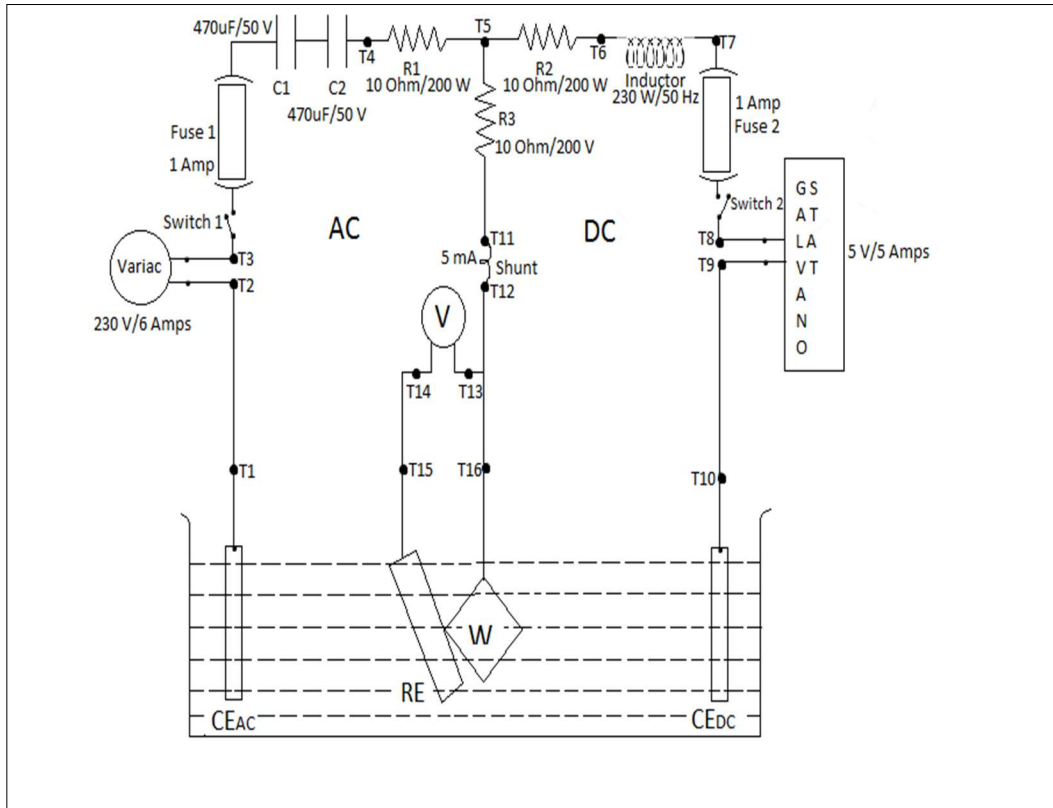


Figure 3.1: Electric Circuit - DC and AC coupled (Thakur et al. 2020)

- A Galvanostat provides a DC supply between the working specimen (W) and counter electrode (CE_{DC}).
- An inductor (20 H, 230 V) blocks the flow of AC in the circuit while permitting DC flow. Reactance (X_L) of the Inductor (L) at frequency f is represented by:

$$X_L = 2\pi fL \quad (3.1)$$

3.2.2 AC CIRCUIT

AC circuit consists of the following:

- The shunt, R1 (10 Ohms, 200 W) for AC measurement.
- A Variable Transformer (Variac) provides an AC supply, which flows between the working specimen (W) and counter electrode (CE_{AC}).
- A pair of capacitors ($500 \mu\text{F}$, 230 V) blocks the flow of DC in the circuit while

permitting AC flow. Reactance (XC) of the capacitors (C) at frequency f is represented by:

$$XC = \frac{1}{2\pi fC} \quad (3.2)$$

- The Variac provided the requisite AC through the pipeline specimen, and Galvanostat ensured the requisite DC through the pipeline specimen. While the flow of DC provided cathodic protection to the pipeline specimen, AC provided the necessary current for AC interference.

3.2.3 CONSOLIDATED AC AND DC CIRCUIT

For the study of AC interference under cathodic protection conditions, primary capacitor, and inductor circuits are as below:

- AC circuit consisting of Variac with autotransformer facilitated the flow of AC between the specimens and counter electrode (CE_{AC}).
- DC is supplied through Galvanostat to facilitate the flow of DC between the specimen and counter electrode (CE_{DC}).
- Capacitors (C1 and C2) inhibit DC flow in an AC circuit. A capacitor with capacitance C offers impedance (X_c) which is inversely proportional to the frequency (f) of the electrical signal.

$$X_c = 1/2\pi fC$$

- Inhibited AC flow in the DC circuit by the presence of an Inductor (L) as impedance (X_L) of an inductor is directly proportional to the frequency (f) of the electrical signal.

$$X_L = 2\pi fL$$

- The protection potential of the specimen (W) is measured accurately to the Cu-CuSo4 Reference cell.
- A voltage across the fixed resistance Shunt S determines the current passing through the specimen.
- Derived protection density, considering the current passing through a fixed specimen area (1 sq. cm).
- Influence on protection potential and protection current density at various AC

and DC currents are measured suitably to analyze CP performance's effect and determine which pipe grade is least affected.

- Observed the effect of AC on protection potential at various protection potentials to determine the most stable protection potential in the presence of AC.
- Counter electrodes complete requisite circuits, and current flow is measured using a shunt. A Cu-CuSo₄ reference electrode (RE) helped measure the specimen's DC potential.

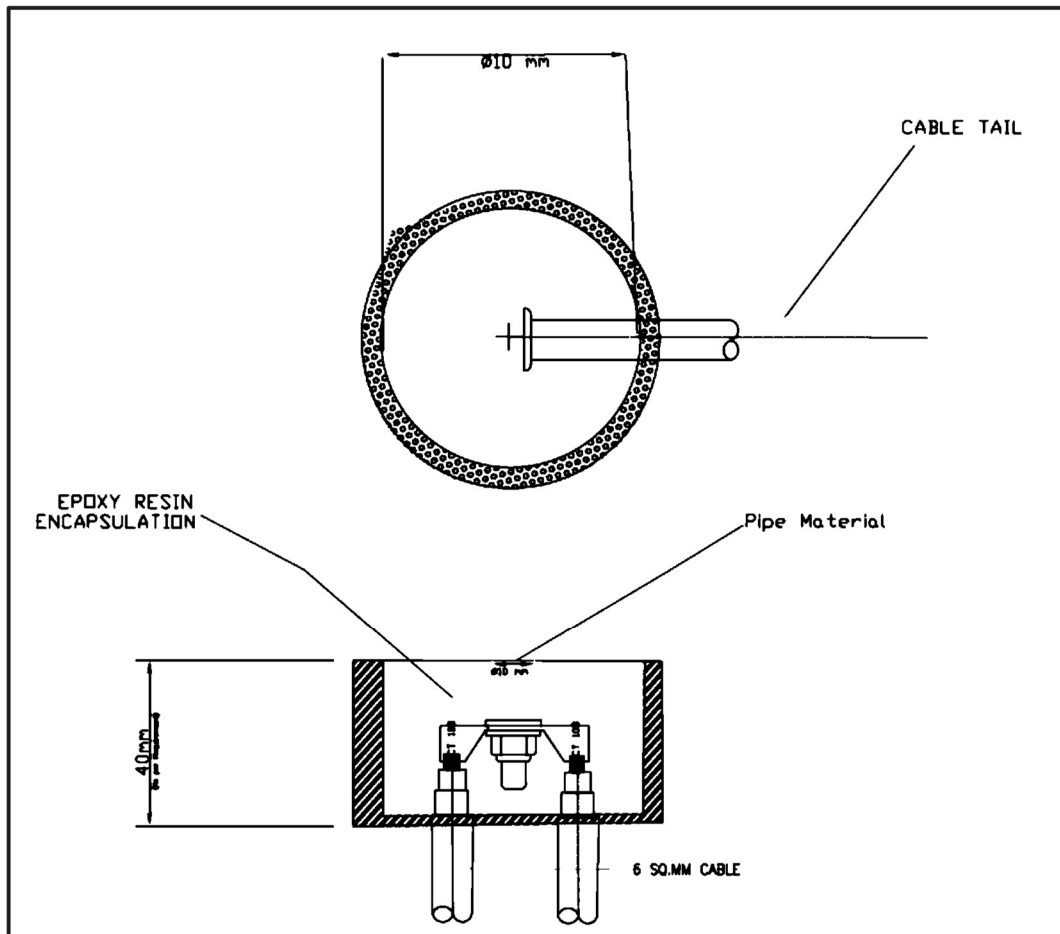


Figure 3.2: Steel specimen Arrangement (Source Open)

3.2.4 WEIGHT LOSS TESTS

Weight loss tests on API pipe grades X46, X52, X60, X65, and X80, included Zinc and Magnesium anodes. The weight loss tests enabled us to compare the relative

performance of the API pipe grades under similar conditions. Further, the weight loss tests also helped reach in performance of Zinc and Magnesium anodes.

3.2.5 STEEL SPECIMEN

Prepared steel specimens, each measuring 100 mm diameter and 6 mm thickness, using API pipes. Each sample was thoroughly cleaned using demineralized water and placed in a PVC cylindrical tube of 40 mm length and 10 mm internal diameter. A weld attachment on one side of the specimen secured a six mm² copper cable for an electrical connection. We kept a bare surface of 10 mm diameter on the other side of the sample to enable the current flow. We filled the cylindrical tube with epoxy for an airtight arrangement (Figure 3.2).

3.2.6 SOLUTION SIMULATING SOIL

Used a new solution simulating soil for dipping each specimen. Each liter of the solution consisted of a mixture of Sulphate ions (500 mg), Chloride ions (200 mg), and silica sand. The soil simulating solution's pH (about 6.4) and electrical resistivity (about 5 Ohm-m) are measured. After each test, discard the existing mixture and clean the container for subsequent measurements.

3.3 TEST CONDITIONS

3.3.1 PROTECTION POTENTIAL MEASUREMENTS

Galvanostatic tests on pipeline specimens at various AC densities included studying the effects of Alternating current on protection potential. Each prepared sample in a cylindrical tube is cleaned and immersed in the soil-simulating solution. Each set of tests used a fresh ground-simulating solution.

Applied various alternating current densities in steps as interference with the applied protection densities, and the resultant protection potential was measured (Table 3.1).

Table 3.1: Test conditions for Galvanostatic measurements

Protection Density (A/m ²)	AC Density (A/m ²)
0.1	10, 30, 50, 100, 200
0.3	10, 30, 50, 100, 200
0.5	10, 30, 50, 100, 200
1.0	10, 30, 50, 100, 200
2.0	10, 30, 50, 100, 200
10.0	10, 30, 50, 100, 200

Initially, the protection current was applied at 0.01 A/m² for 24 hours without AC. After measuring protection potential, the protection current was increased to 0.1 A/m² and applied 10 A/m² AC for 30 minutes. For 30 minutes, measure the protection potential every five minutes. The applied AC was then reduced to zero and left for stabilization for five minutes at the applied protection current.

The measurements were repeated by applying AC for 30, 50, 100, and 200 A/m² at the applied protection density.

Subsequently, the protection current was increased to 0.3 A/m², and the measurements were repeated at the different AC densities. The process was continued for various protection currents (0.5, 1.0, 2.0, and 10.0 A/m²).

3.3.2 PROTECTION DENSITY MEASUREMENTS

Potentiostatic tests included studying the effect of Alternating current on protection density. During tests, various current densities applied to the applied protection potential, and the resultant current density was measured (Table 3.2).

Potentiostatic tests, applied in steps, included studying the effect of Alternating current on protection current density at various alternating current densities.

Initially, protection potential was applied at -0.8 V for 24 hours without AC. After measuring protection density, protection potential was increased to -0.85 V and applied 10 A/m² AC for 30 minutes. During the period, the protection density measured every five minutes. The applied AC was then reduced to zero and left for stabilization for five minutes at the applied protection potential.

Table 3.2: Test conditions for Potentiostatic measurements

Protection Potential (-V)	AC Density (A/m²)
0.85	10, 30, 50, 100, 200
0.95	10, 30, 50, 100, 200
1.05	10, 30, 50, 100, 200
1.15	10, 30, 50, 100, 200
1.25	10, 30, 50, 100, 200
1.35	10, 30, 50, 100, 200

The measurements were repeated by applying AC for 30, 50, 100, and 200 A/m² at the applied protection potential.

Subsequently, the protection potential was increased to -0.95 V, and the measurements were repeated at the different AC densities. The process was continued for various protection potentials (-1.05, -1.15, -1.25, and -1.35 V).

3.3.3 WEIGHT LOSS TESTS

Performed weight loss tests under alternating current on pipe samples for different periods (Table 3.3) as below:

Table 3.3: Test conditions for measurement of weight loss

AC density (A/m²)	Time (Months)
200	0, 1, 2, 3, 4

Initially, all the pipe samples were thoroughly cleaned and dried. The initial weight of each sample and the corresponding anode were measured. The samples with anodes were divided into five sets and kept in the soil in pots. One collection of pieces was not subjected to AC. The balance four groups were subjected to fixed AC of 200 A/m². A requisite set of samples was retrieved monthly, cleaned, and weighed. Loss of weight is attributable to AC corrosion due to the flow of AC.

3.4 EXPERIMENTAL ARRANGEMENTS

The following were the experimental arrangement(s) for conducting tests:

3.4.1 GALVANOSTATIC AND POTENTIOSTATIC MEASUREMENTS

The in-house experimental arrangement (Figure 3.3) consisted of the following:

- A Galvanostat feeds DC through the prepared sample (immersed in soil simulating solution) to provide requisite cathodic protection.
- An autotransformer provided the requisite variable AC to enable AC flow through the prepared sample.
- Shunts and multimeters enabled measuring AC/DC voltage and current.
- Capacitors enabled the flow of AC in the AC circuit and simultaneously blocked the flow of DC in the respective circuit.
- Inductors enabled the flow of DC in the DC circuit and simultaneously blocked the flow of AC in the respective circuit.
- Counter electrodes immersed in the soil-simulating solutions provided the requisite stability to the respective circuits.

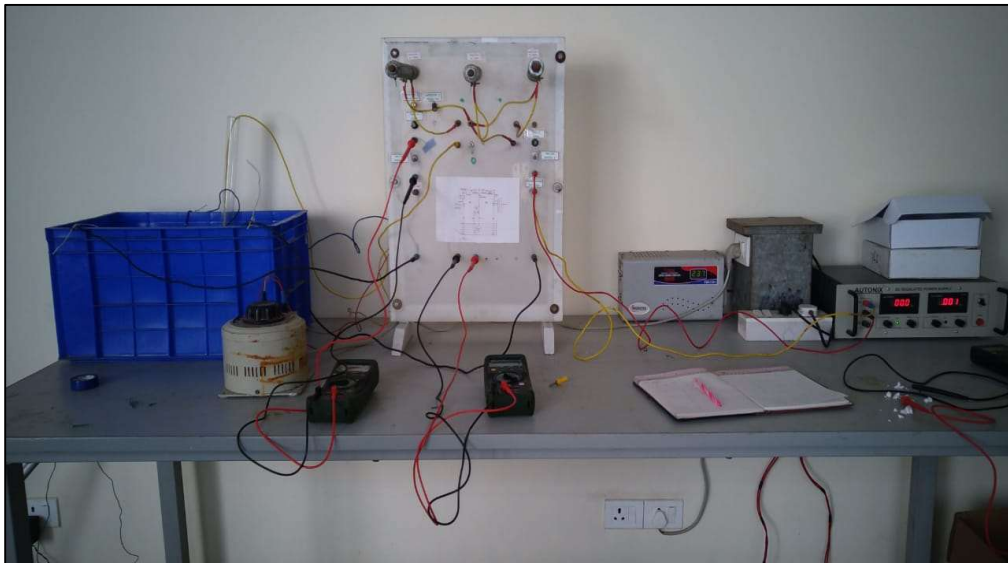


Figure 3.3: Protection potential and AC density measurement setup

- The sample immersed in a soil simulating circuit was subjected to a flow of AC in the presence of DC. The protection potential of the sample was measured along with the AC current flowing.

3.4.2 WEIGHT LOSS MEASUREMENT

A separate in-house circuit (Figure 3.4) enabled weight loss measurement due to AC. The weight loss tests were conducted for four months by exposing the pipe samples of different grades to AC interference. Galvanic anodes protect from corrosion by injecting DC current. One set of each pipe grade was retrieved after one month, and actual weight loss was measured. Similarly, each group was retrieved at the end of the second, third, and four months, and the weight loss was measured after cleaning.

The pipe samples not exposed to AC interference were also retrieved monthly to determine the weight loss.

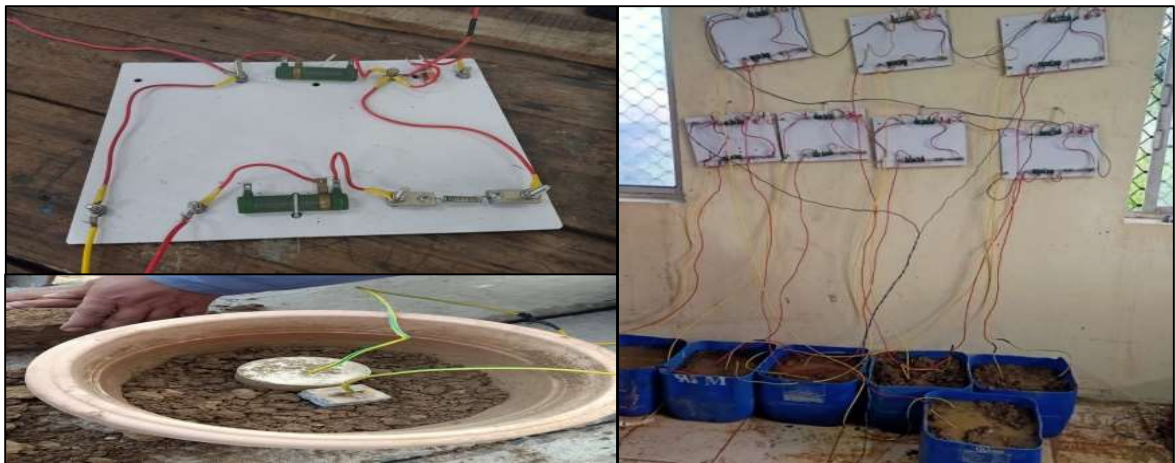


Figure 3.4: Set up for weight loss on AC interference (Thakur et al 2022)

3.4.3 SOIL RESISTIVITY AND pH MEASUREMENTS

The soil resistivity and pH were measured for the soil-simulating solution used for protection potential and AC density measurements.

3.5 DATA COLLECTION

Collected data through experimentation as below:

- 3.5.1 Measure protection potential (upon 24 hours polarization) of pipe samples (X46, X52, X60, X65, and X80).

- 3.5.2 Soil resistivity for each new solution for experimental testing.
- 3.5.3 pH for each new solution for experimental testing.
- 3.5.4 Protection potential variation at various AC densities in 30-minute steps (measurement every five minutes) for X46, X52, X60, X65, and X80 pipe samples:
- At a protection density of 0.1 A/m²
 - At a protection density of 0.3 A/m²
 - At a protection density of 0.5 A/m²
 - At a protection density of 1.0 A/m²
 - At a protection density of 2.0 A/m²
 - At a protection density of 10.0 A/m²
- 3.5.5 Protection density variation at various AC densities in 30-minute steps (measurement every five minutes) for X46, X52, X60, X65, and X80 pipe samples:
- At a protection potential of -0.85 V
 - At a protection potential of -0.95 V
 - At a protection potential of -1.05 V
 - At a protection potential of -1.15 V
 - At a protection potential of -1.25 V
 - At a protection potential of -1.35 V
- 3.5.6 Weight loss measurements at the AC density of 200 A/m² for X46, X52, X60, X65, and X80 pipe samples:
- After one month
 - After two months
 - After three months
 - After four months
- 3.5.7 Weight loss measurements at the AC density of 200 A/m² for Magnesium and Zinc anodes:
- After one month
 - After two months
 - After three months
 - After four months

The data collected is analyzed statistically in Graphs to determine the pipe grade that is least affected due to AC interference in the presence of Cathodic Protection.

Completed results validation through extended weight loss tests on pipe samples of different grades in soil simulating solution.

Weight loss tests were also analyzed to determine the performance of Magnesium and Zinc anodes under AC interference.

CHAPTER 4

MODELING WORK

4.1 MODELING METHOD AND SOFTWARE

The AC modelling study used CDEGS (Current Distribution Electromagnetic, Grounding, and Soil Structure Analysis) software to profile HVAC power lines with a zone of interference coinciding with the pipeline route, including collecting power line data, measuring soil resistivity data, and conducting a simulation study. CDEGS (Current Distribution Electromagnetic Interference Grounding and Soil Structure Analysis) by Safe Engineering Services, Canada, is an automated software tool that enables complex modeling and simulation of overhead transmission lines on pipelines.

Right-of-Way (ROW) package of CDEGS is an automated AC Interference analysis software specifically designed for AC interference studies. Right-of-Way Pro software includes the TRALIN (Transmission line parameters), SPLITS (Simulation of Power Lines, Interconnections, and Terminal Stations), RESAP (Soil Resistivity Analysis), and MALZ (Low and high-frequency grounding) engineering modules and several other related tools and components.

The specially designed Right-of-Way package of CDEGS deployed to complete AC interference studies under fault conditions, including inductive, conductive, and capacitive couplings. Using the TRALIN and SPLITS engineering software modules, it is possible to rapidly model a corridor in which multiple energized and de-energized power line circuits and other utilities run simultaneously at varying separation distances. The MALZ module of the ROW software package supports the combined conductive and inductive interference effects through the EMF energization feature taken directly from Right-of-way.

The circuit approach and finite element analysis allow the analysis of complex domains involving several conductors and multilayered soils.

The modeling of the pipeline system based on the circuit theory approach consists of three steps:

- Circuit Model Setup
- Line parameter calculations
- Circuit Analysis

4.2 MODELLING CONDITIONS

4.2.1 FAULT CONDITION

Conductive coupling occurs when a fault exists in the tower or along the transmission line. If a fault condition occurs on a high voltage transmission line, all the electricity in the line gets dumped into the earth. The pipeline in the earth is then subjected to a discharge of current due to failure of the high voltage transmission line. It can cause current arcing through the soil, which under extreme conditions, can burn a hole in the pipeline leading to catastrophic failure. The damage done to the pipeline depends upon the intensity of the voltage.

4.2.2 STEADY-STATE CONDITION

Electromagnetic induction can occur in a parallel pipeline to the power transmission line. If the pipeline is close enough to fall within the electromagnetic field, then some form of current induces the pipeline in the opposite direction. This induced current picked up by the pipeline can result in high voltages along long pipeline sections due to the Longitudinal electromagnetic field (LEF). There are very few places for this current to exit for well-coated pipelines. Failure of the current to exit the pipeline. This current exits through defects in the pipeline, such as holidays, leading to AC-induced pipeline corrosion.

4.3 MODELLING ACTIVITIES

The Right of Way software of CDEGS software with circuit theory approach consists of three steps

- Circuit model setup
- Line parameter calculations
- Circuit analysis
- Total Interference

The circuit model setup uses the ROWCAD module, Line parameter calculations done using the TRALIN module, and the circuit analysis performed using the SPLITS module for Inductive and MALZ module for total interference.

The sequence of steps involved in developing the complete network using ROWCAD are

- Import Polylines, describing the routes of pipelines, transmission lines, and railways, from Google Earth (Figure 4.1).

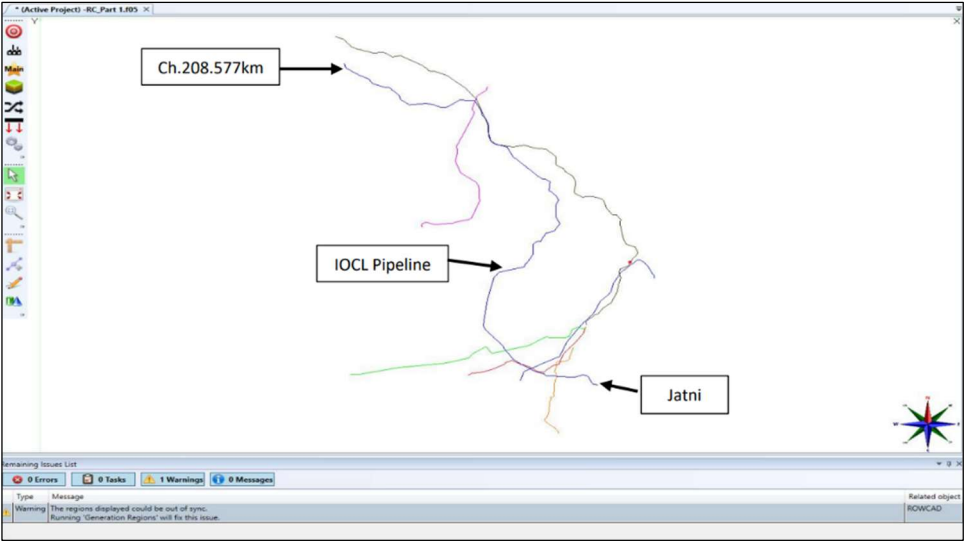


Figure 4.1: Polyline route of the pipeline and HT line (208.58 km)

- Each route of the pipeline has different cross-sections. Under the Cross-Section tab, the electrical characteristics of a pipeline, transmission line phase conductors & shield wires, and traction line defined. In addition, physical features like the buried depth of a pipeline (Table 4.1), phase-to-phase clearance, phase-to-shield wire distances, height from the FGL, and geometrical position of the Traction line also defined.
- Pipeline characteristics defined for their dimension and electrical and magnetic properties are:

Conductor characteristics

Inner radius	0.22225 m
Outer radius	0.2286 m
Thickness	0.00635 m

Relative resistivity	10.35
Relative permeability	300

Coating characteristics

Outer radius	0.2292 m
Thickness	0.0006 m
Area Resistance	23000 Ω m ²
Relative permittivity	23
Relative permeability	1

Table 4.1: Pipeline cross-section defined for burial depth

Location	Name	Z(m)	Associated phase
1	Pipeline	-1.7292	1-pipeline

Depth from GL to pipeline center.

- 400kV transmission line – Centre line symmetry**

Each conductor in the Transmission line (Phase wires & shield wires) is represented as Phases. The transmission lines with two shield wires, as the two shield wires are tied at every tower, share the same potential along the line. So based on the circuit model approach, the two shield wires are bundled as single-phase self and mutual impedance, which is enough to represent the two shield wire conductors.

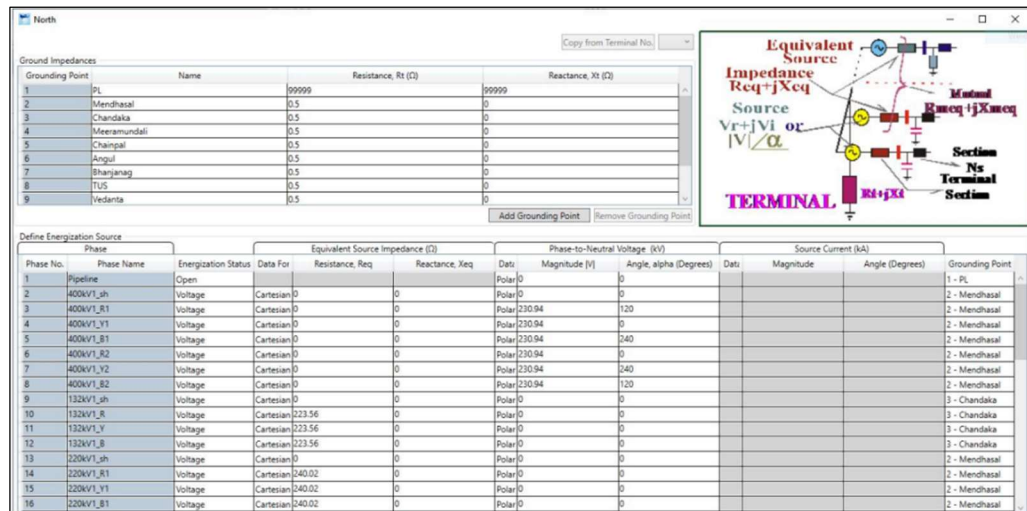


Figure 4.2: Energisation of terminal

A total of 7 phases represent one transmission line of 400 kV with a single shield wire. The geometrical distances, heights, and electrical characteristics are defined. The conductor characteristics for phase conductors and shield wire are selected from the SES Library and assigned to related phases. Shield wire configuration (Steel with a resistance of 2.5 ohm/km) and phase conductor's configuration (twin moose conductor with a spacing of 450mm) are defined in this stage.

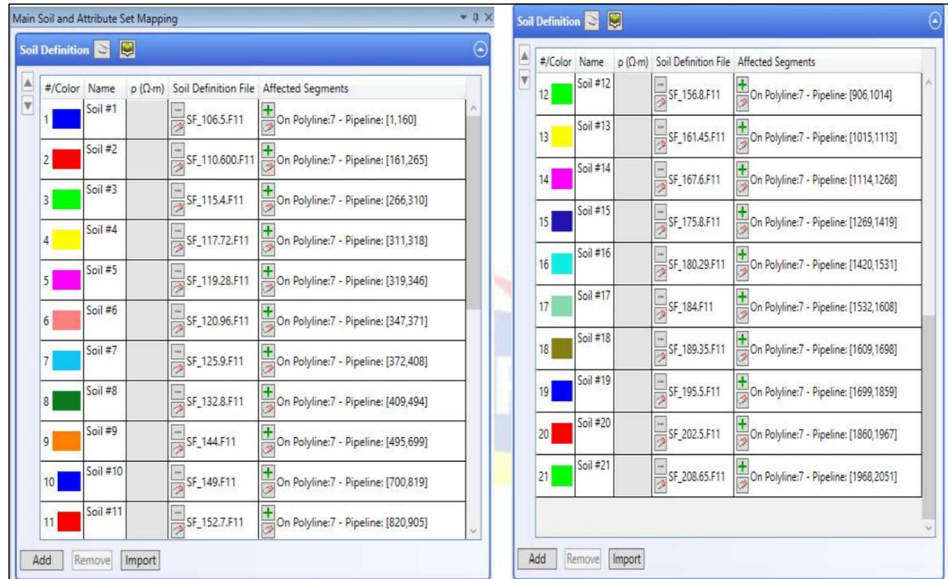


Figure 4.3: Soil definition for the derivation of the Soil model

- **Phase leakage**

Transmission lines' neutral or shield wire conductor is usually connected to towers with known footing impedance. The " Ω /Tower" option is used to define the tower ground impedance.

- **Energization**

The Energization for each terminal is defined by system voltage, load impedances & terminal ground impedances (Figure 4.2).

- **Soil model**

A multi-layered soil model was derived (Figure 4.3) based on site measurements at 21 locations along ROU for this pipeline section 103.624 km.

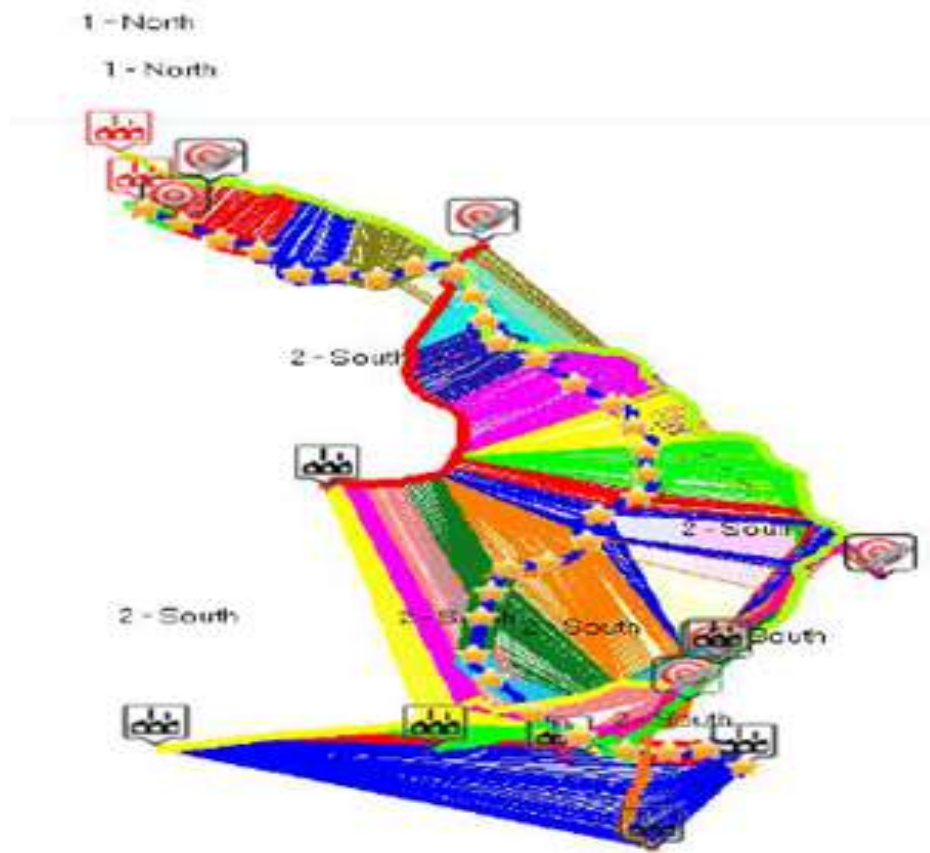


Figure 4.4: Generating Regions

- **Generating regions**

After all, specifications are defined, use RowCAD to subdivide the system into regions that form the base unit for representing the system in circuit form.

One hundred two regions in terminal 1 and 2335 regions in terminal 2 generated, as shown in Figure 4.4.

- **Starting Right-of-way**

The ROWCAD network is imported by clicking Import from the Build System Configuration tab. After successfully importing the network, regions, and terminals are defined (Figure 4.5).

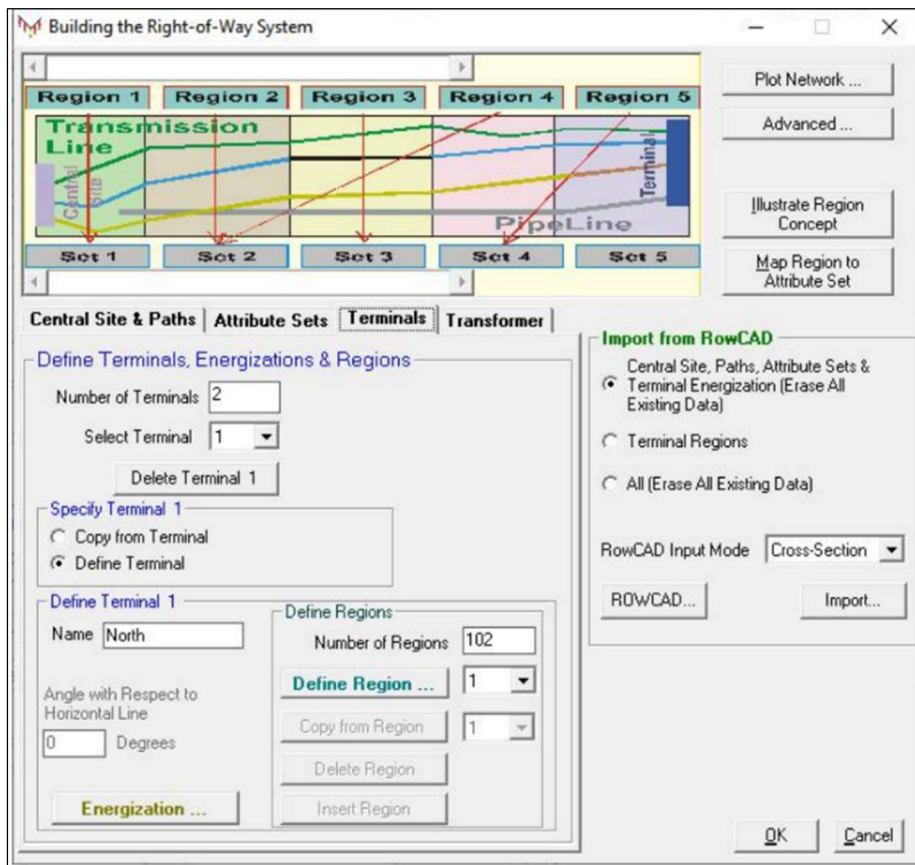


Figure 4.5: Regions and Terminals

4.4 INDUCTIVE AC INTERFERENCE COMPUTATION

- The inductive AC interference starts by selecting the CREATE circuit button (Figure 4.6).

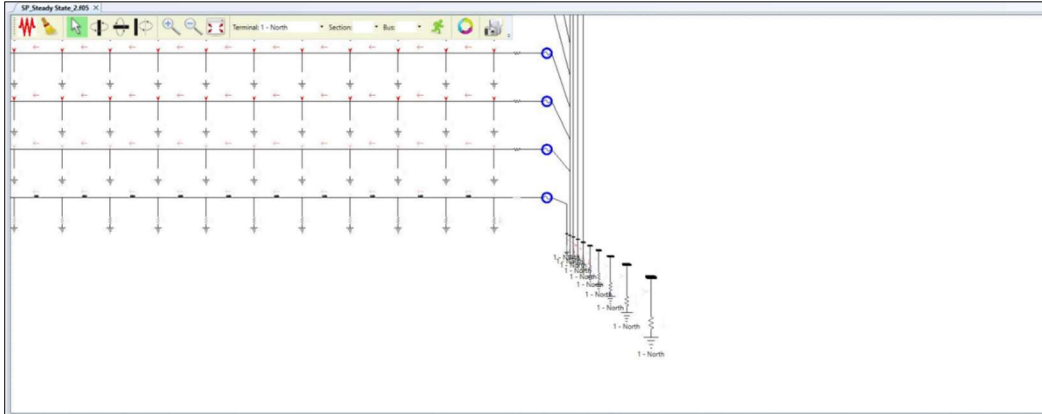


Figure 4.6: Portion of the created circuit

- The Inductive AC interference computation initiates the circuit above by selecting the PROCESS button. The modeled scheme in CDEGS is as per Figure 4.7 with existing pipeline ground locations.

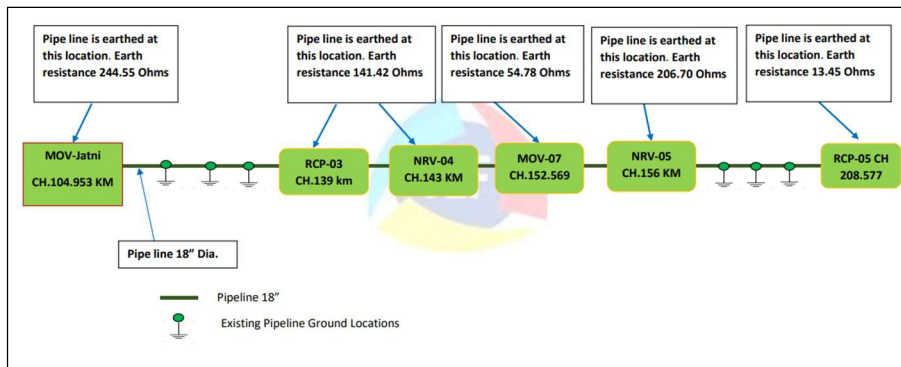


Figure 4.7: Scheme modelled in CDEGS

- The pipeline earthing impedance is defined in Right-of-Way software. Figure 4.8 shows pipeline earth impedance for one location (Ch. 104.953 km). It is defined for all locations similarly.

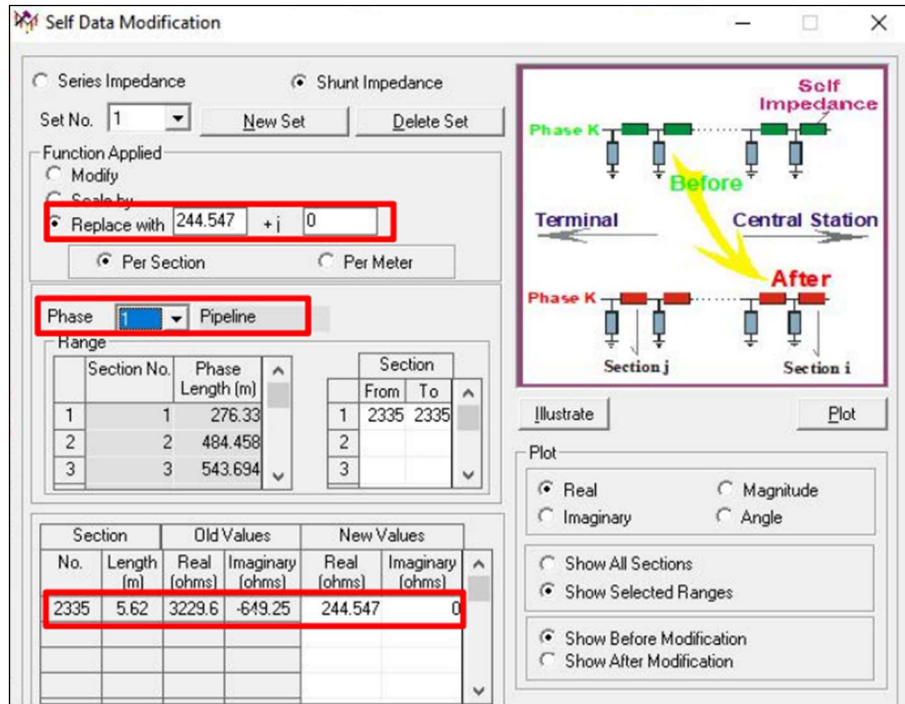


Figure 4.8: Pipeline earth impedance at 104.95 km

4.5 TOTAL INTERFERENCE COMPUTATION – STEADY STATE

This module creates various conductive MALZ files for each soil zone. The MALZ model is based on the ROW system defined in ROWCAD and the options and definitions specified in this module. It also includes EMF terms computed from previous SPLIT (inductive) steady-state computations. Consequently, the MALZ model computation gives the total interference level (conductive and inductive components).

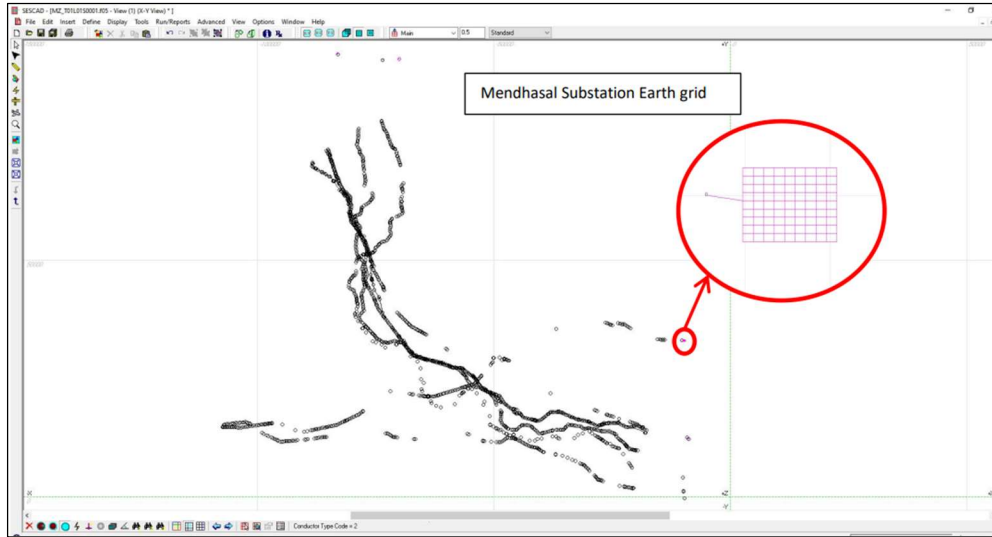


Figure 4.9: Substation ground impedance

The total interference module is re-simulated with the newly created MALZ file incorporated with the new entries/operations, and finally, the results are examined.

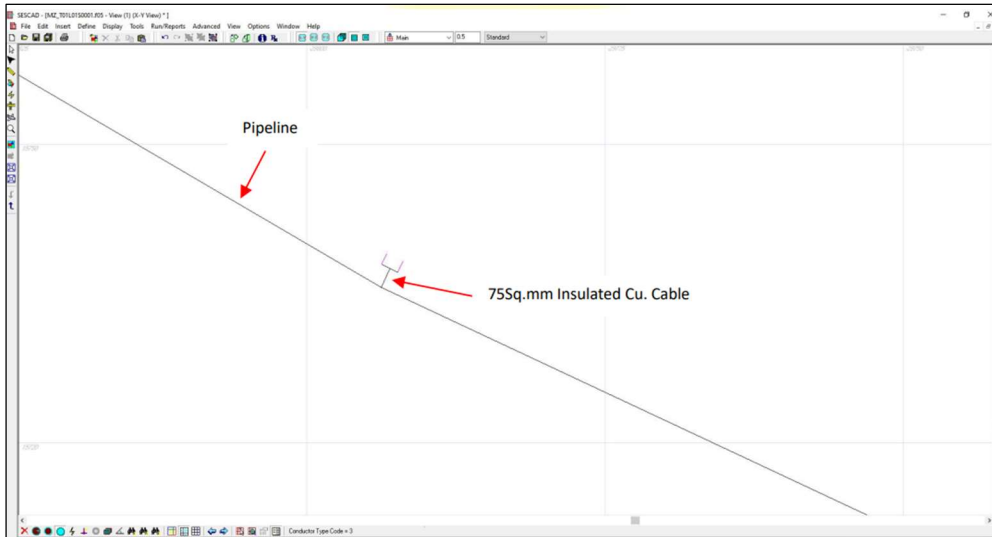


Figure 4.10: Pipeline earthing modelled

The steps involved include:

- Selecting "Total Interference" on the main screen of ROW allows access to Creating the Total Interference Model. All towers of 220kV & 110kV transmission lines set and exported to the MALZ file.
- Substation ground impedance (Figure 4.9) is achieved by modeling the appropriate earthing grids & placed them at corresponding locations.
- Pipeline earthing is modeled as per Figure 4.10. and defined as per Figure 4.11.

- The total interference is computed by incorporating the above details and processed by clicking the "Create and Process" option.

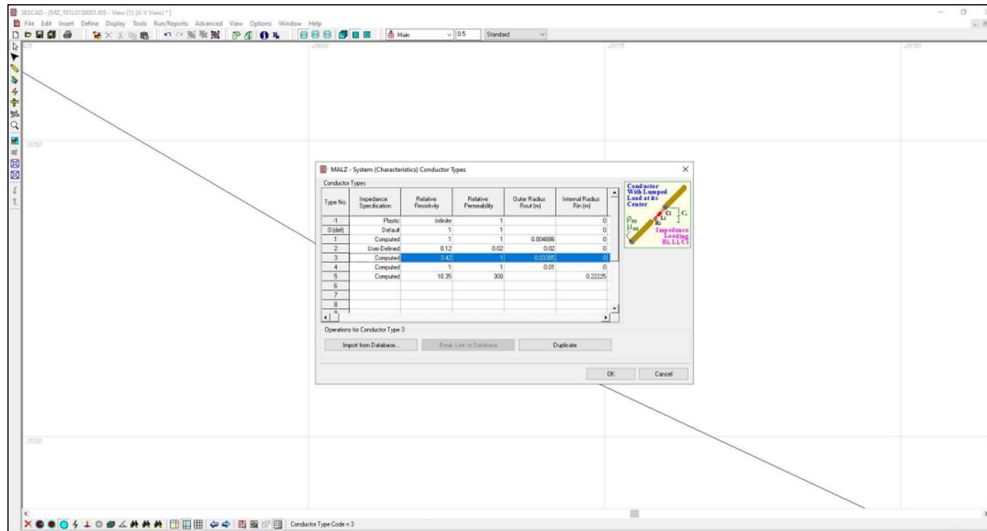


Figure 4.11: Pipeline earth defined

4.6 MODELLING PROCEDURE FOR FAULT CONDITION

Conductive and inductive interference levels are combined during fault conditions to compute pipeline potentials, stress voltages, and touch & step voltages. Faults should be simulated at representative intervals throughout the usage corridor at the transmission line structure, and currents injected into the earth by transmission line structures during conductive coupling should be considered appropriately.

When there is a powerline fault at a tower, there is a potential ground rise (GPR), which raises the earth's potential in contact with the pipeline. If the pipeline runs parallel to the transmission line, there can also be induced voltage on the pipeline, which adds vectorially to the potential ground rise. Any voltage transferred to the pipeline would reduce the voltage across the coating, which can lead to dielectric breakdown of the pipeline coating, depending on the magnitude and duration of the applied voltage.

Table 4.2: Existing Pipeline Earthing Locations

Chainage (km)	Type	Chainage (km)	Type	Chainage (km)	Type	Chainage (km)	Type
105	DMV	235.3	DAC	271.3	DAC	307.8	DAC
112.8	DAC	238.6	DAC	274.7	DAC	309.6	DMV
119.5	DAC	239.5	DMV	275.1	DAC	310	DAC
119.5	DAC	240.5	DAC	276.1	DAC	310.4	DAC
123	DMV	244.5	DAC	277.6	DAC	317.9	DAC
152.2	DMV	248.6	DAC	277.9	DAC	319	DMV
172.9	DMV	251.3	DAC	279	DMV	322	DAC
175.1	DAC	253	DAC	279.6	DAC	325	DAC
177.2	DAC	254	DAC	280	DMV	329	DAC
180	DAC	255	DAC	289	DAC	330	DAC
181.5	DAC	256.5	DAC	290	DAC	334	DAC
184.5	DAC	257.5	DAC	291	DAC	337	DAC
207.4	DAC	259	DAC	296	DAC	339	DAC
209.8	DMV	261	DAC	298	DAC	351	DAC
220.7	DAC	263	DAC	299	DAC	354.6	DAC
225.7	DAC	265	DAC	305	DAC	372	DAC
227.6	DAC	270.3	DAC	305.6	DAC	375	DAC
231.1	DAC	265	DAC	307.1	DAC		

Type DMV for Valve locations and Type DAC for Transmission lines

Modelling under fault conditions has been carried out for a total pipeline length of 285 km, starting from Jatni at a chainage of 104.953 KM to Sambalpur at a chainage of 389.884 KM. The pipeline network has an outer diameter (OD) of 45.72 mm (18 inches), a wall thickness of 6.35 mm, the material of construction steel grade API 5LX70, and a coating leakage resistance of 23000 ohm-m². The pipeline system has DFBE Coating, with a minimum coating thickness of 0.6 mm, buried at 1.5 m from finished ground level (FGL).

The pipeline system is earthed at several locations near transmission lines through DAC type TLP and at block valve locations through DMV TLP, as shown in Table 4.2.

4.7 SOIL RESISTIVITY AND pH STUDY

The electrical soil resistivity measurement is crucial for AC interference modeling and implementation of mitigation measures as required. Soil resistivity is the function of soil properties such as particle size distribution, pore size, connectivity, water content, temperature, and medium. At various electrode spacings, soil resistivity was recorded at 59 locations along the pipeline route. Table 4.3 indicates the soil resistivity measurements at Chainage 115.4 and 117.72 km. Soil resistivity measurements are then resolved into multilayered soil structures using the RESAP module.

Chainage	115.4 km			117.72 km		
	Resistivity (Ohm-m)		Average Soil Resistivity (Ohm-m)	Resistivity (Ohm-m)		Average Soil Resistivity (Ohm-m)
	X	Y		X	Y	
0.5	2.21	6.94	5.83	63	197.95	178.47
1	0.75	4.71	5.84	33	207.37	194.80
2	0.31	3.90	4.59	14.53	182.61	230.18
3	0.23	4.34	4.71	13	245.08	245.17
5	0.24	7.54	6.76	7	219.94	184.44
10	0.17	10.68	11.00	2	125.68	83.58
20	0.14	17.60	15.08	1	125.68	109.97
30	0.16	30.16	30.16	0.5	94.26	61.27
50	0.11	34.56	34.56	0.19	59.70	59.70

Table 4.3: Soil resistivity measurements at 115.4 and 117.72 km

pH values measured at 63 locations along the pipeline route. Table 4.4 indicates the locations of Soil resistivity and pH measurements.

4.8 FAULT CURRENT USED IN MODELLING

During a single-phase-to-ground fault, the current on the faulted phase is much larger than the current on the non-faulted phase. Hence only faulted phase is modelled with fault current as three times the current flowing through transmission lines. Transmission lines are considered a two-terminal network that acts as sources for the given fault current. The fault current will flow from both terminals to the faulted tower. The fault current for the simulation has been calculated based on the distance and impedance of the faulted phase conductor.

Table 4.4: Soil resistivity and pH measurement locations in the field

Measurement locations Chainage (km)							
Soil Resistivity				pH			
106.50	184.00	270.00	345.80	106.22	231.30	280.02	325.50
110.60	189.35	274.20	355.49	113.45	234.30	283.30	328.00
111.40	195.50	280.00	359.50	115.99	237.35	291.40	331.00
117.72	202.50	285.50	362.50	116.92	238.96	292.40	337.30
119.28	208.65	291.90	364.80	117.09	245.50	295.07	341.30
120.96	213.40	295.09	371.60	119.28	247.98	297.60	345.30
125.90	217.10	299.40	372.40	120.19	248.44	299.60	362.42
132.80	225.50	305.70	376.30	123.76	249.56	301.50	364.42
144.00	234.10	310.40	383.70	173.36	257.82	305.45	367.40
149.00	238.80	311.10	387.56	180.29	260.20	307.32	371.40
152.70	241.70	317.65	391.50	184.00	261.30	310.42	372.40

Measurement locations Chainage (km)						
Soil Resistivity			pH			
156.80	245.70	323.20	185.45	270.37	311.55	375.39
161.45	247.10	328.80	219.60	274.10	314.10	376.00
167.60	249.00	330.15	225.80	275.70	317.50	380.00
175.80	254.20	331.45	228.75	276.10	321.20	389.00
180.29	264.40	337.90	230.30	277.10	323.20	

4.9 FAULT CURRENT SIMULATION

4.9.1 TRANSMISSION LINES

Using 3D imagery, we observed that 18 transmission lines of different voltages ranging from 132 kV to 765 kV parallel the above pipeline (Table 4.5).

Table 4.5: Details of Transmission Lines nearby/crossing Pipeline system

Name of Transmission line	Utility Owner	Transmission Voltage (kV)	Number of circuits	Design Load (Amps)	Phase Arrangement
Mendhasal-Pandabili	PGCIL	400	Four	335/335/410/130	-
Mermundal-Mendhasal	OPTCL	400	Double	380/350	Centre Line
Narendrapur-Mendhasal	OPTCL	220	Single	270	Centre Line
Nayagarh-Chandaka	OPTCL	220	Double	260/230	Centre Line
Khurda-Mendhasal	OPTCL	132	Single	100	-
Nuapatna LILO	OPTCL	132	Double	110/105	Centre Line
Angul-Sundargarh Ckt 1-2	PGCIL	765	Double	250/240	Centre Point
Angul-Sundargarh Ckt 3-4	PGCIL	765	Double	270/260	Centre Point

Name of Transmission line	Utility Owner	Transmission Voltage (kV)	Number of circuits	Design Load (Amps)	Phase Arrangement
Angul-Meramundhali TUS	PGCIL	400	Single	105	-
Meramundhali-Vedanta	Vedanta	400	Double	410/390	Centre Point
Angul-JPTIL	JPTIL	400	Double	410/405	Centre Line
Meramundhali-Mendhasal	OPTCL	400	Double	380/350	Centre Line
Angul-Kaniha PP	OMR	400	Double	525/390	Centre Line
Angul-Meramundhali	PGCIL	400	Double	525/390	Centre Line
Meramundhali-JSPL PP	JSPL	400	Double	405/405	Centre Line
Bhnajanagar-Meramundhali	OPTCL	220	Double	260/230	Centre Line
Angul-Boinda	OPTCL	132	Single	80	-
Boinda-Sambalpur	OPTCL	132	Single	90	-

Based on satellite imagery, Google Earth renders a three-dimensional (3D) representation of the earth. This program maps the earth onto a 3D globe by superimposing satellite images, aerial photography, and GIS data, giving users a multi-angular view of cities and landscapes. Google Earth representation for pipeline and transmission lines is as per Figure 4.12.

The following transmission lines have been identified for fault current simulation based on the magnitude of fault current and the proximity of their tower locations to the pipeline

1. TL 400KV Meramundhali to Vedanta.
2. TL 400KV Meramundhali to Mendhasal
3. TL 765KV Angul to Sundargarh Ckt 1&2
4. TL 400KV Mendhasal to Pandiabili

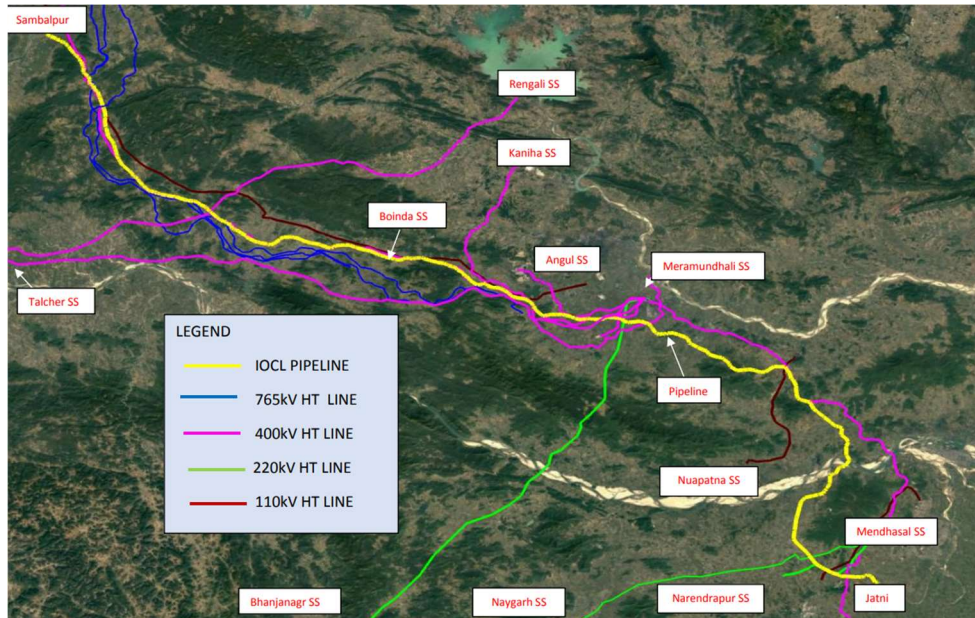


Figure 4.12: Pipeline and Transmission lines on Google Earth

4.9.2 FAULT TOWER IDENTIFICATION

The towers are identified based on the separation distance from the pipeline. The conductor close to the pipeline faulted to the ground and simulated with fault current.

- The identified transmission line 400kV Meramundhali to Vedanta runs parallel to the pipeline for about 165 KM at chainage 220 km to 385 km and crosses the pipeline at 36 locations. A single line to a ground fault simulated at Ten (10) towers along the route.
- Transmission line 400kV, Meramundhali to Mendhasal, runs parallel to a pipeline for about 55 km and crosses the pipeline at two locations. A single line-to-ground fault simulated at Nine (9) towers along the route
- Transmission line 765kV, Angul to Sundargard Ckt 1&2, runs parallel to a pipeline for about 115 KM and crosses the pipeline at one location. A single line to a ground fault simulated at Eight (8) towers along the route.
- Transmission line 400KV, Mendhasal to Pandiabali, crosses the pipeline at one location. A single line to a ground fault is simulated at Four (4) towers along the route.

4.9.3 FAULT CONDITION MERAMUNDHALI TO VEDANTA 400 kV

The pipeline and HT line (Mermundhali to Vedanta, 400 kV) indicated on Google Earth as per Figure 4.13 are faulted towers, as represented in Figure 4.14.



Figure 4.13: Pipeline and HT line for fault analysis on Google Earth

The plan view of the scheme modeled for simulation is as per Figure 4.15. The simulation is carried out with mitigation grounds recommended for normal load operation in a plan.

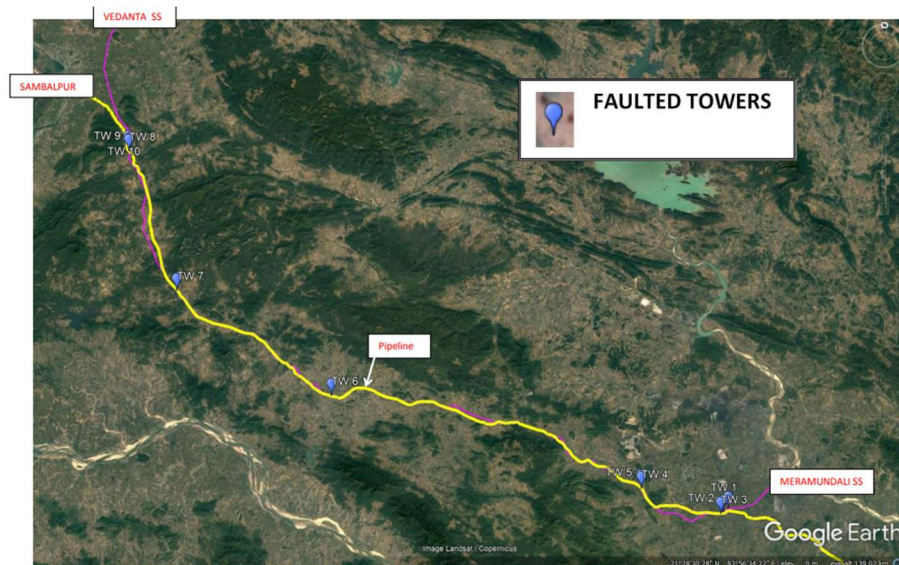


Figure 4.14: Faulted Tower locations

- Defined the Fault between the 'R' phase of circuit 2 and the Shield wire of

Mermundal to Vedanta 400kV line at ten towers.

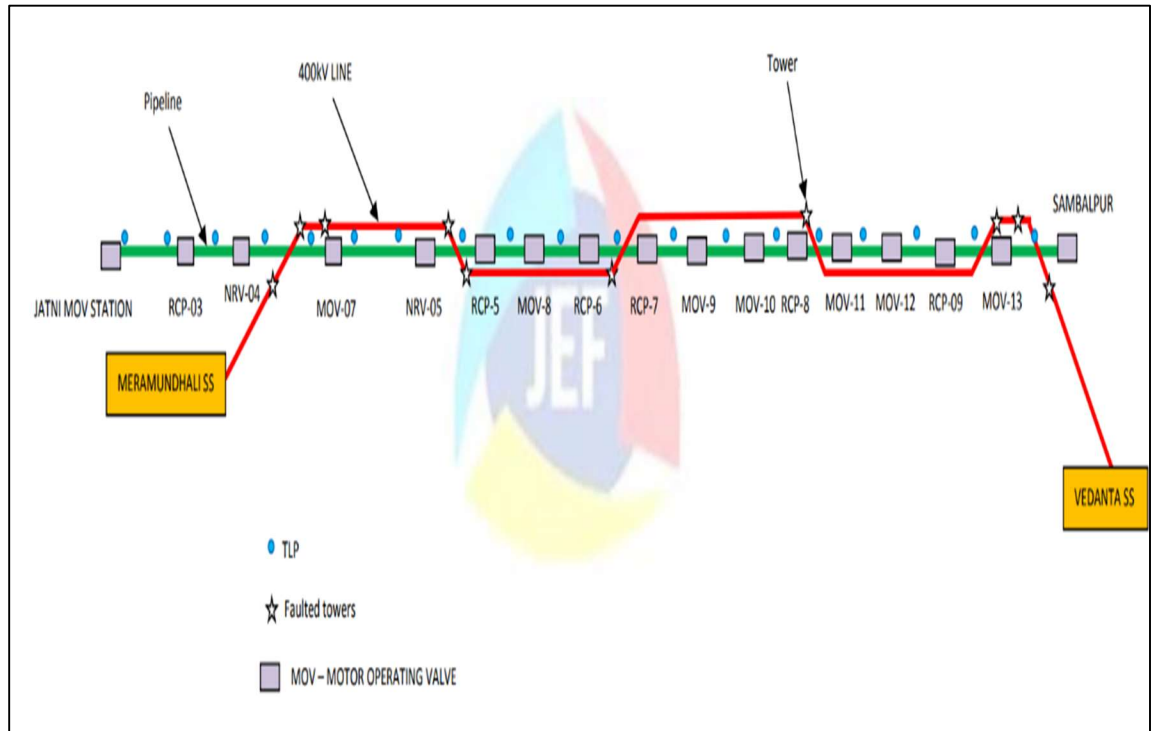


Figure 4.15: Modelled Scheme in CDEGS

Parameters used

Reference phases	2
Faulted phases	3
Type of source	Source Current
Interpolation method	Linear interpolation
Terminal No	1(South)/2(North)
Fault Connection Impedance	0.0001 ohms

- Defined current source in both ends at terminals Mermundal and Vedanta.
- Total Interference levels are determined as per Table 4.6.

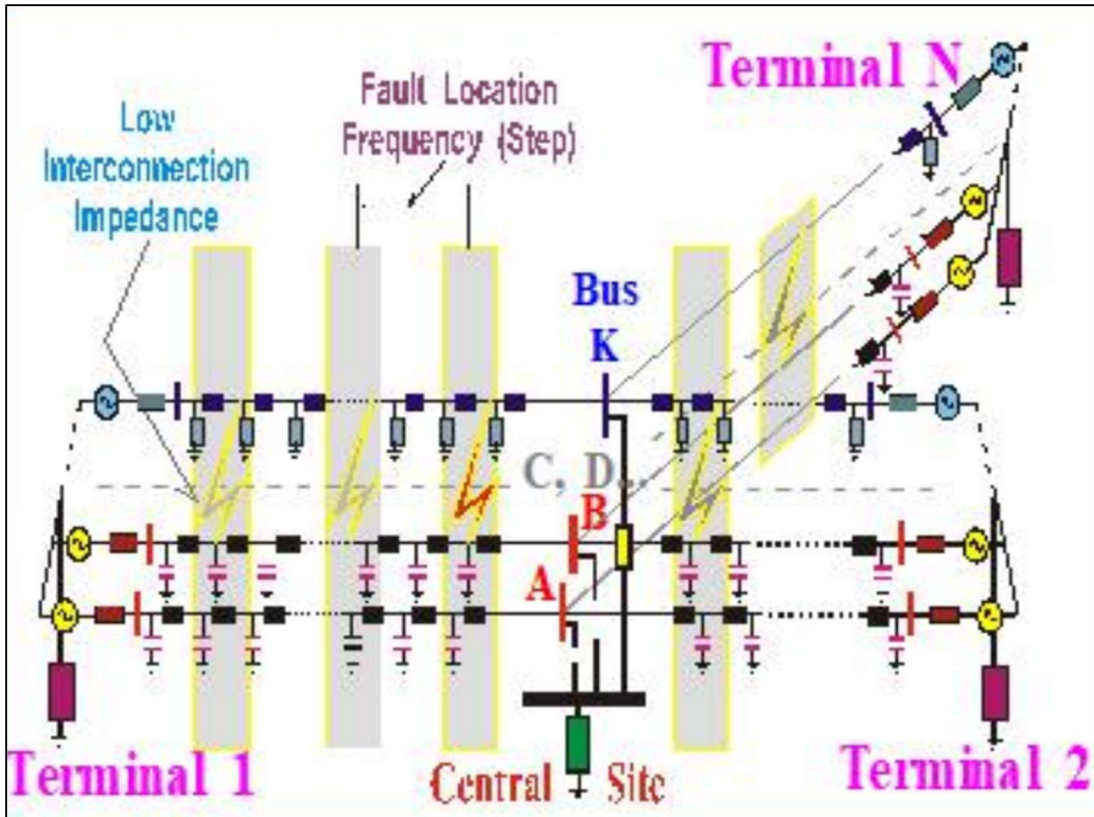


Figure 4.16: Reference Circuit Model

Parameters used

- Interpolation phases 3
 - Reference terminal 1
 - End terminal 2
 - Interpolation method based on faulted phase.
- } → Refer Figure 4.16

Table 4.6: Total Interference Levels

Fault Location (Km)	Magnitude (Amp) from reference terminal 1	Angle from ref. Terminal 1 (degrees)	Magnitude from end terminal 2 (Amp)	Angle from end terminal 2 (degrees)
9.9	36828	-88	1991	-76
93.4	3918	-86	3646	-81
157.2	2328	-85	9999	-82

CHAPTER 5

EXPERIMENTAL RESULTS AND DISCUSSIONS

5.1 BACKGROUND

The in-house experimental arrangement enabled potentiostatic, and galvanostatic tests required on pipe samples of five API grades (X46, X52, X60, X65, and X80) in the soil-simulating solution with/without AC interference.

While Galvanostatic tests determined the effect of alternating current on protection potential at specific protection densities, the potentiostatic tests determined the effect of alternating current on the protection density at specific protection potentials. Subsequently, weight loss tests determined the extent of actual weight loss in four months at an AC density of 200 A/m². Weight loss test results validated by published studies.

Modeling and optimization studies on the existing pipe network in Odisha, India, enabled the prediction and mitigation of AC interference. The physical parameters of the transmission lines, pipeline network, soil, and pH are collected. Field validations enabled the optimization of the mitigation measures.

The results of the experimental research work are as below:

5.2 PROTECTION POTENTIAL WITHOUT AC APPLICATION

5.2.1 INITIAL PROTECTION DENSITY AND POLARISATION PERIOD

The pipe-grade samples are polarized for 24 hours before subjecting to AC interference. The stable protection potential after polarization ensures adequate protection at 0.01 A/m² without AC interference.

DC protection density polarises all the samples for 24 hours before subjecting them to galvanostatic or potentiostatic tests. Without AC interference, a DC protection

density (PD) of 0.01 A/m² polarises the pipe samples. Table 5.1 illustrates the variation in protection potential after 24 hours:

Table 5.1: Polarised Potential

Pipe Grade	Protection potential (mV)		
	At Start	After 24 Hours period	Variation
X46	-1051	-1052	-1
X52	-1042	-1043	-1
X60	-1035	-1035	0
X65	-1043	-1044	-1
X80	-1057	-1058	-1

The potential between -1035 and -1058 mV indicates satisfactory polarisation at the applied protection density.

5.2.2 PROTECTION DENSITY (PD) OF 0.1 A/m²

A protection density of 0.1 A/m² supplies protection current to protect pipe samples without AC interference.

Table 5.2 indicates protection potential in steps of 5 min each at the protection density of 0.1 A/m².

Table 5.2: Protection potential at PD = 0.1 A/m²

Pipe Grade	Protection potential (mV)						
	TS	TS+5 min	TS+10 min	TS+15 min	TS+20 min	TS+25 min	TS+30 min
X46	-1067	-1068	-1067	-1066	-1067	-1069	-1069
X52	-1051	-1050	-1051	-1051	-1050	-1050	-1050
X60	-1040	-1040	-1039	-1039	-1039	-1039	-1039
X65	-1052	-1051	-1051	-1052	-1052	-1051	-1050
X80	-1064	-1064	-1063	-1064	-1065	-1065	-1066

The variation in protection potential in the observation period for the X46 sample is 0.2%. The similar variation for X52, X60, X65 and X80 grade samples is - 0.1%, - 0.1%, - 0.2% and 0.2% respectively. The variation is small enough to be ignored, considering the level of measurements.

At the protection density of 0.1 A/m², the minimal variation in protection potential without AC interference indicates similar corrosion behavior. Indicated protection density protects all pipe grades at this point.

5.2.3 Protection density (PD) of 0.3 A/m² to 10 A/m²

As the protection density increases, the protection potential increases in the negative direction for all pipe grades. Table 5.3 summarizes the protection potentials at various protection densities without AC.

For the X52 pipe, samples are protected with -1065 mV potential at a DC density of 0.1 A/m² with no AC interference. With the change in DC density (from 0.1 A/m² to 10 A/m²), the protection potential turned more negative (from -1065 to -1387 mV), indicating improved corrosion protection. The protection potential exceeds -1200 mV with an increase in DC density beyond 0.5 A/m², which may result in coating damage in some time.

For a protection density of 1 A/m², the protection potential is beyond -1200 mV. Further increase in protection density leads to overprotection [226]. In practice, overprotection leads to coating disbondment over a long period. Coating disbandment renders CP ineffective [111], [322] due to separating cathodic and anodic reactions with depletion of dissolved oxygen.

Table 5.3: Summary of Protection Potential without AC

Pipe Grade	Protection potential (mV) at Protection density (PD in A/m ²)				
	PD=0.3	PD=0.5	PD=1	PD=2	PD=10
X46	-1151	-1201	-1250	-1280	-1401
X52	-1065	-1196	-1241	-1278	-1387
X60	-1060	-1187	-1227	-1278	-1387
X65	-1061	-1240	-1225	-1279	-1409
X80	-1135	-1181	-1215	-1256	-1383

5.3 PROTECTION POTENTIAL UNDER AC INTERFERENCE

5.3.1 PROTECTION DENSITY (0.1 A/m²)

Grade X46

For API X46 Grade Pipe samples, the protection potential became more positive from -1070 mV to -865 mV with an increase in AC density from 0 to 200 A/m². Table 5.4 indicates the Protection potential at a DC density of 0.1 A/m² under AC for the X46 pipe.

Table 5.4: Protection potential for X46 pipe under AC (PD=0.1 A/m²)

AC Density (A/m ²)	Protection Potential (mV)						
	TS	TS+5 min	TS+1 0 min	TS+1 5 min	TS+2 0 min	TS+2 5 min	TS+3 0 min
10	-1068	-1063	-1057	-1055	-1053	-1051	-1050
30	-1052	-1042	-1030	-1021	-1010	-1006	-998
50	-996	-992	-987	-980	-978	-976	-976
100	-974	-968	-969	-960	-953	-946	-941
200	-940	-928	-910	-887	-870	-858	-844

The protection potential shift for X46 pipe is -1.7% at 10 A/m² and -5.5% at 30 A/m². At 50 A/m², the protection potential shift is -2.1%, and at 100 A/m², it is -2.5%. A high protection potential shift of -8.8% was observed at an AC density of 200 A/m².

With increased AC density, protection potential is shifting positively at the fixed value of protection density (PD=0.1 A/m²) using a Galvanostat. In the worst condition of AC density of 200 A/m², the protection potential is -844 mV, indicating an anodic shift of 225 mV concerning the condition of no AC interference. However, at 30 A/m², the anodic change concerning the non-interference state is 71 mV.

Grade X52

The protection potential shift for the X52 pipe (Table 5.5) is -0.3% at 10 A/m² and -5.6% at 30 A/m². At 50 A/m², the protection potential shift is -1.0%, and at 100 A/m², it is -2.4 %. A high protection potential shift of -7.2% is observed at an AC density of 200 A/m².

Table 5.5: Protection potential for X52 pipe under AC (PD=0.1 A/m²)

AC Density (A/m ²)	Protection Potential (mV)						
	TS	TS+5 min	TS+1 0 min	TS+1 5 min	TS+2 0 min	TS+2 5 min	TS+3 0 min
10	-1050	-1050	-1049	-1049	-1048	-1047	-1047
30	-1046	-1041	-1031	-1019	-1001	-991	-987
50	-983	-981	-980	-979	-975	-973	-973
100	-971	-963	-959	-952	-950	-948	-948
200	-939	-931	-919	-899	-877	-870	-871

At an AC density of 200 A/m², the protection potential is -871 mV, indicating an anodic shift of 179 mV concerning no AC interference. However, at 30 A/m², the anodic change concerning the non-interference state is 63 mV.

The anodic shift at 30 A/m² for both X46 and X52 grade pipes is very close due to the similarity in microcrystalline [276] structure and established manufacturing processes. Both grades follow an identical pattern under AC interference at the indicated protection density.

Grade X60, X65 and X80

The anodic shift (Table 5.6) in protection potential concerning the non-interference state at a current protection density of 0.1 A/m² for X60, X65, and X80 is high beyond 30 A/m². The grades may experience high corrosion at high AC densities.

Table 5.6: Anodic shift at PD = 0.1 A/m²

AC Density (A/m ²)	Anodic Shift (mV)		
	X60	X65	X80
10	4	13	10
30	48	53	68
50	68	75	90
100	96	103	125
200	167	175	222

The protection potential positively shifted for all pipe grades with AC density change from 0 A/m² to 200 A/m². The anodic shift is higher for all pipes at an AC density of 200 A/m² due to enhanced corrosion.

5.3.2 PROTECTION DENSITY (0.3 A/m²)

Protection potential shift (Table 5.7) for the X46 pipe is -0.8% at 10 A/m² and -5.1% at 30 A/m². At 50 A/m², the protection potential shift is -2%, and at 100 A/m² it is -3.4 %. A high protection potential shift of -10.2% at an AC density of 200 A/m² indicates enhanced corrosion.

Table 5.7: Protection potential X46 at PD=0.3 A/m²

AC Density (A/m ²)	Protection Potential (mV)						
	TS	TS+5 min	TS+1 0 min	TS+1 5 min	TS+2 0 min	TS+2 5 min	TS+3 0 min
10	-1150	-1145	-1141	-1134	-1130	-1125	-1122
30	-1121	-1115	-1110	-1104	-1078	-1056	-1046
50	-1041	-1038	-1031	-1029	-1027	-1025	-1022
100	-1022	-1022	-1021	-1020	-1020	-1019	-1019
200	-1015	-1011	-1002	-991	-984	-977	-970

While Figure 5.1 presents the protection potential, Table 5.8 shows the protection potential shift for X52, X60, X65, and X80 pipes.

Both protection potential and protection potential shifts indicate adequate protection up to 30 A/m² AC density and higher corrosion probability at higher AC densities. Passive film breakdown is likely at AC densities from 30 A/m² to 50 A/m².

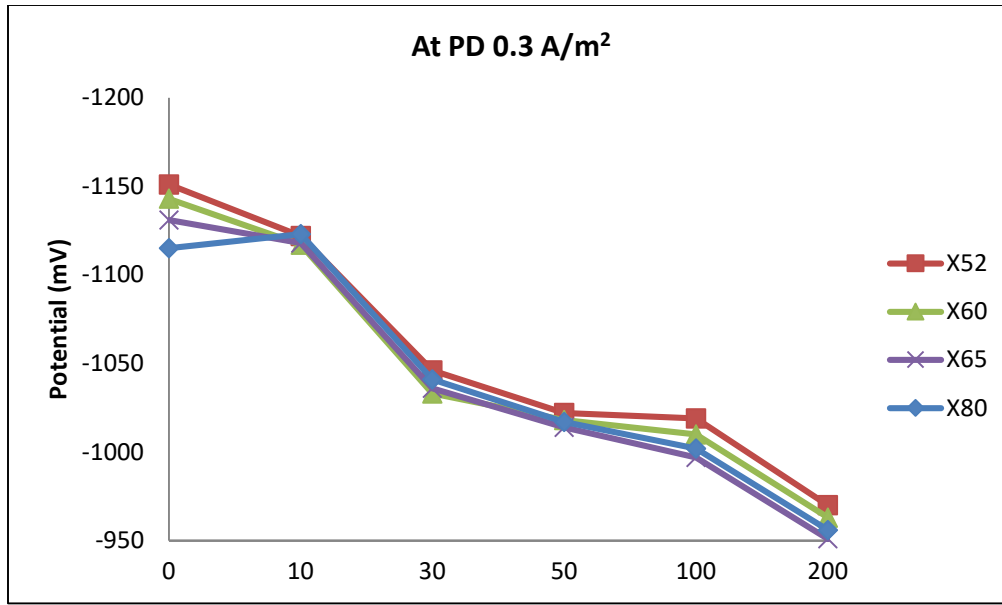


Figure 5.1: Protection potential at PD 0.3 A/m²

The protection potential of X52 Grade pipe samples increased from -1143 mV to -963 mV, at a current protection density of 0.3 A/m², with a variation of AC density from 0 to 200 A/m². The passive film is significantly damaged at current densities of 50-200 A/m², enhancing corrosion. X52 exhibits comparable corrosion resistance up to an AC density of 10 A/m². At higher AC densities, the passive film quickly deteriorates, allowing the protection potential to shift positively.

At a current protection density of 0.3 A/m², the protection potential of X65 Grade Pipe samples increased from -1131 mV to -951 mV with a change in AC density from 0 to 200 A/m². The protection potential of the X80 pipe changed from -1135 mV to -956 mV. Similar AC corrosion occurs in the X70 and X80 samples at smaller AC densities with positive protection potential change. The passive film ruptures at higher AC densities, increasing corrosion.

Table 5.8: Potential shift at PD 0.3 A/m²

AC Density (A/m ²)	Protection Potential Shift (%)			
	X52	X60	X65	X80
10	-1.6	-1.2	-1.4	1.0
30	-5.0	-4.6	-4.4	-6.2
50	-1.0	-1.6	-1.5	-2.2
100	-2.7	-2.9	-2.9	-1.4
200	-7.1	-7.1	-6.4	-4.5

The protection potential for the X65 pipe shifted from -1061 mV to -839 mV and the X80 Grade pipe from -1066 mV to -844 mV in response to the change in AC densities. X65 and X80 pipes fail to meet the -850 mV protection criteria with PD of 0.1 A/m² and an AC density of 200 A/m², resulting in enhanced corrosion.

Protection potential shift in 30 minutes for X46 pipe is -2.8% at 10 A/m² and -4.7% at an AC density of 200 A/m². Positive anodic change at all AC densities indicates the effect of AC interference. Higher anodic shift at 200 A/m² results in enhanced corrosion.

5.3.3 PROTECTION DENSITY (0.5 A/m²)

Table 5.9 represents the protection potential of the X46 sample at a DC density of 0.5 A/m².

Table 5.9: Protection Potential X46 at PD= 0.5 A/m²

AC Density (A/m ²)	Protection Potential (mV)						
	TS	TS+5 min	TS+10 min	TS+15 min	TS+20 min	TS+25 min	TS+30 min
10	-1195	-1189	-1179	-1171	-1167	-1164	-1162
30	-1159	-1143	-1137	-1121	-1109	-1097	-1080
50	-1079	-1071	-1065	-1061	-1059	-1057	-1055
100	-1051	-1049	-1047	-1044	-1043	-1042	-1040
200	-1038	-1031	-1021	-1009	-1003	-995	-989

For other pipe grades, Table 5.10 summarises potential protection shifts.

Table 5.10: Protection potential shift at PD=0.5 A/m²

AC Density (A/m ²)	Protection Potential Shift (%)				
	X46	X52	X60	X65	X80
10	- 2.8	- 3.7	- 3.2	- 4.9	- 1.8
30	- 6.8	- 6.4	- 5.1	- 5.7	- 5.8
50	- 2.2	- 2.1	- 3.8	- 2.9	- 3.8
100	- 1.0	- 1.0	- 3.9	- 3.6	- 2.0
200	- 4.7	- 5.3	- 1.5	- 1.8	- 5.3

5.3.4 PROTECTION DENSITY (1.0 A/m²)

The protection potential shift (Table 5.11) for the X46 pipe is -4.0% at 100 A/m² and -3.5% at an AC density of 200 A/m².

Table 5.11: Protection potential shift at PD = 1 A/m²

AC Density (A/m ²)	Protection Potential Shift (%)				
	X46	X52	X60	X65	X80
10	-1.5	-3.0	-2.4	-1.4	1.4
30	-2.2	-1.1	-1.1	-1.2	-2.7
50	-2.3	-2.1	-1.6	-1.2	-3.6
100	-4.0	-5.1	-5.2	-4.6	-6.3
200	-3.5	-3.2	-3.1	-1.9	-2.6

5.3.5 PROTECTION DENSITY (2.0 AND 10.0 A/m²)

At DC density of 2.0 & 10.0 A/m², the percentage change in protection potential for the X46 sample is as per Table 5.12.

Protection potential shift and significant anodic change for all grades at higher protection densities of 2.0 A/m² and 10.0 A/m² are attributable to higher corrosion occurring under over-protection conditions under AC interference.

Table 5.12: Protection potential PD 2.0 and 10.0 A/m²

AC Density (A/m ²)	Protection Potential (mV)					
	PD = 2 A/m ²			PD = 10 A/m ²		
	TS	TS+30 min	% Potential shift	TS	TS+30 min	% Potential shift
10	-1277	-1263	-1.1%	-1399	-1389	-0.7%
30	-1255	-1231	-1.9%	-1387	-1355	-2.3%
50	-1229	-1202	-2.2%	-1355	-1335	-1.5%
100	-1200	-1169	-2.6%	-1330	-1295	-2.6%
200	-1158	-1113	-3.9%	-1280	-1201	-6.2%

5.4 PROTECTION DENSITY UNDER AC INTERFERENCE

Protection current density (Figure 5.2) for X46 Grade changed from 0.01 to 1.29 A/m² with a variation in protection potential from -850 mV to -1350 mV.

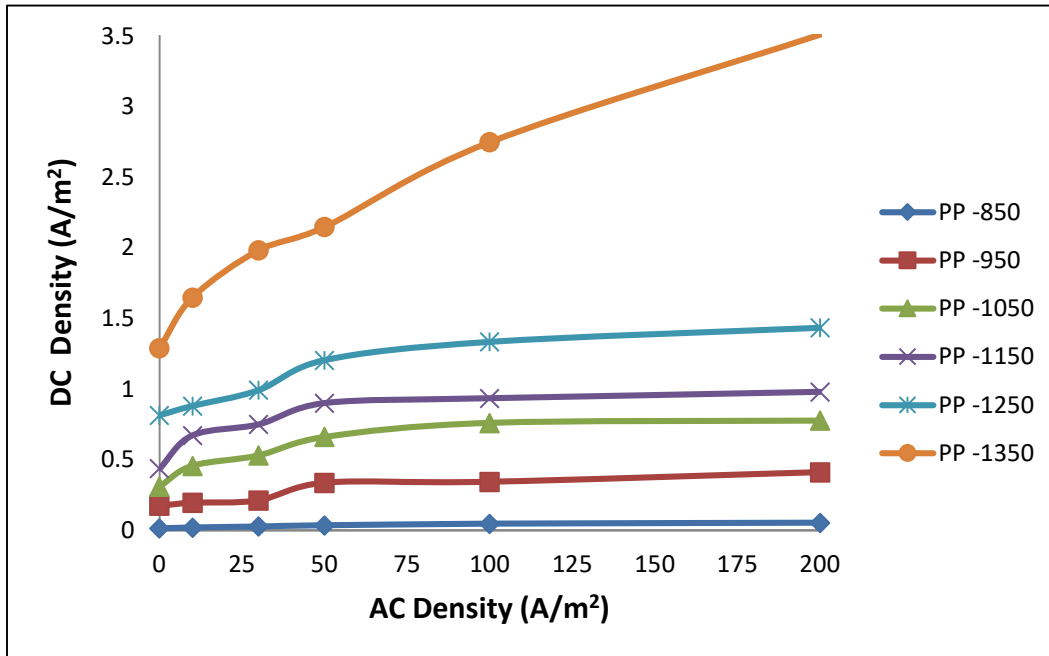


Figure 5.2: Protection current density - X46

Under AC interference of 30 A/m², the current protection density increased from 0.03 to 2.0 A/m². However, for higher AC densities, the protection current density requirement is very high, indicating accelerated corrosion. Protection density more negative than -1200 mV for an extended period disbands coating, enhancing the corrosion processes.

Up to 30 A/m² AC density and for protection potential from -950 mV to -1150 mV, protection density for X46 samples remains reasonably low to avoid over-protection. Accordingly, X46 grade shall remain protected in an AC density of 30 A/m². A cathodic protection system cannot protect the sample from general corrosion for a protection potential more positive than -850 mV.

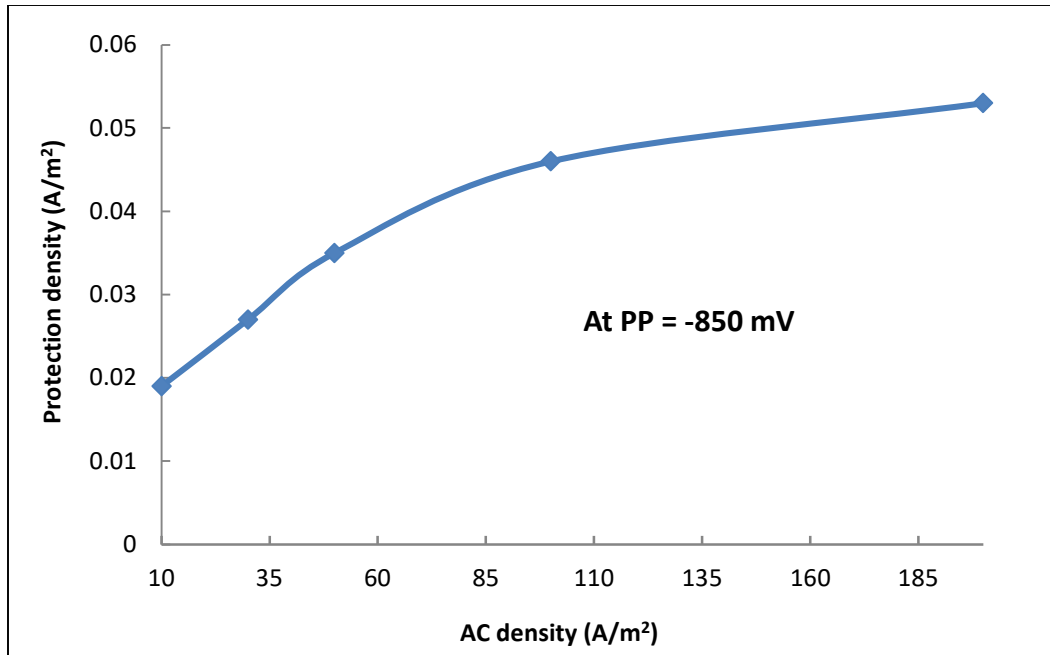


Figure 5.3: Change in Protection Density – X46

The protection density increased from 0.019 to 0.05 A/m², at a protection potential of -850 mV, with a change in AC density from 10 to 200 A/m², indicating a 179% increase in protection current density (Figure 5.3).

The protection density increased from 0.2 to 0.41 A/m², at a protection potential of -950 mV, with a change in AC density from 10 to 200 A/m², indicating a 111% change in protection density.

Protection density is almost constant for X46 pipe at the protection potential of -1150 mV, from 50-100 A/m², indicating the superior performance of X46 steel to other grades (Figure 5.4).

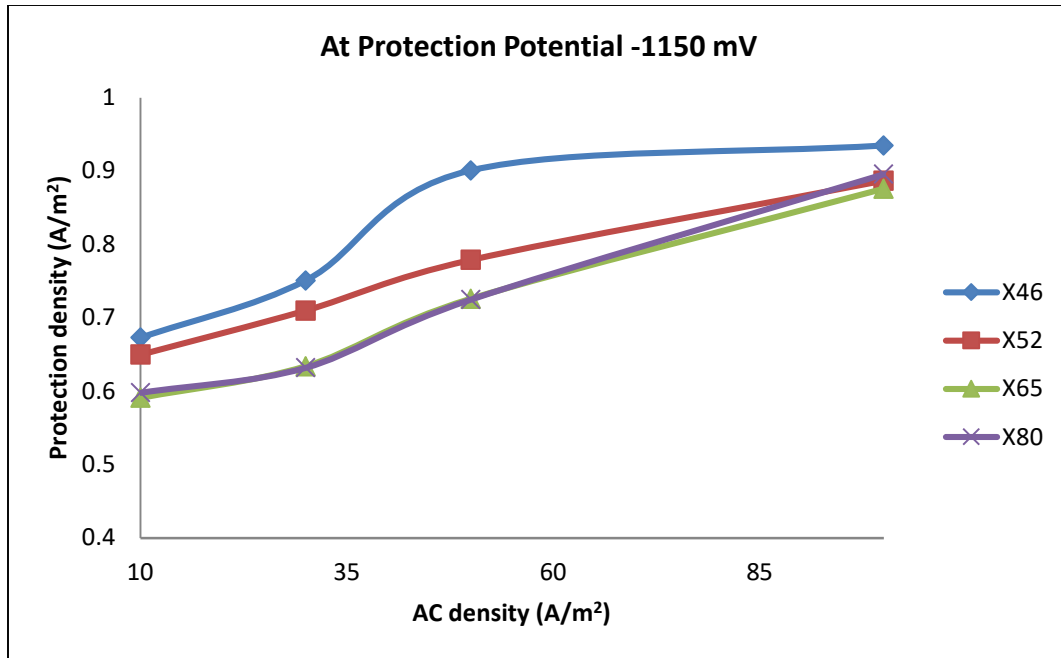


Figure 5.4: Protection density at protection potential -1150 mV

The percentage change in current protection density is low when the protection potential ranges from -1050 to -1250 mV. At lower protection potential, the high percentage increase in protection density indicates the tendency of the CP system to provide requisite cathodic protection. However, overprotection may result in coating failure over the long run at a protection potential more cathodic than -1200 mV.

The X46 pipe samples achieved protection with a potential of -1069 mV and a DC density of 0.1 A/m² without AC interference. With the rise in DC density (from 0.1 A/m² to 10 A/m²), the protection potential became more cathodic, indicating improved corrosion protection due to forming a passive film on the pipe sample's surface. However, the protection potential exceeds -1200 mV when the DC density exceeds 1 A/m², resulting in coating damage over time.

The protection potential of X46 Grade Pipe samples increased from -1151 mV to -970 mV at a current protection density of 0.3 A/m² as the AC density increased from 0 to 200 A/m². The passive film is significantly damaged at current densities of 50-200 A/m², enhancing corrosion.

For X52 pipes (Figure 5.5) without AC interference, with a change in protection potential from -850 mV to -1350 mV, the current densities increased from 0.02 to

1.33 A/m². X52 samples shall also remain protected at an AC density of 30 A/m² and a protection potential of up to -1200 mV.

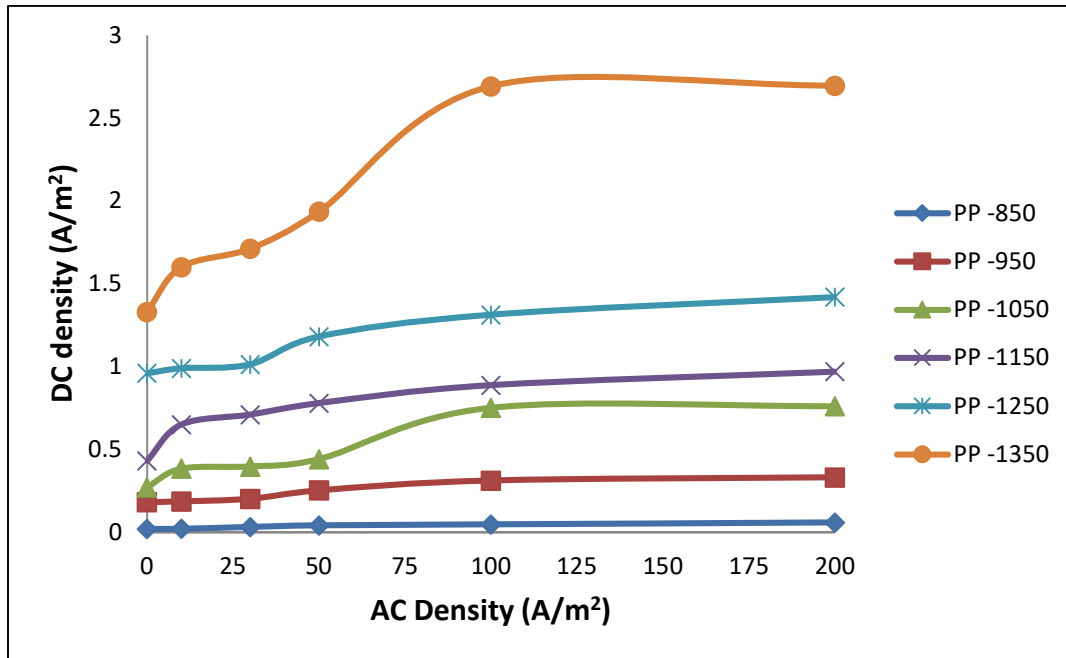


Figure 5.5: Protection density – X52

For the X52 pipe, the protection density shifts from 0.021 to 0.059 A/m² (at a protection potential of - 850 mV), with AC density changing from 10 to 200 A/m², indicating a 181% increase in protection density.

Also, under AC interference of 30 A/m², with protection potential shift from -850 mV to -1350 mV, the protection density increased from 0.03 to 1.79 A/m² for X60 grade pipes and from 0.19 to 1.67 A/m² for X65 grade pipes.

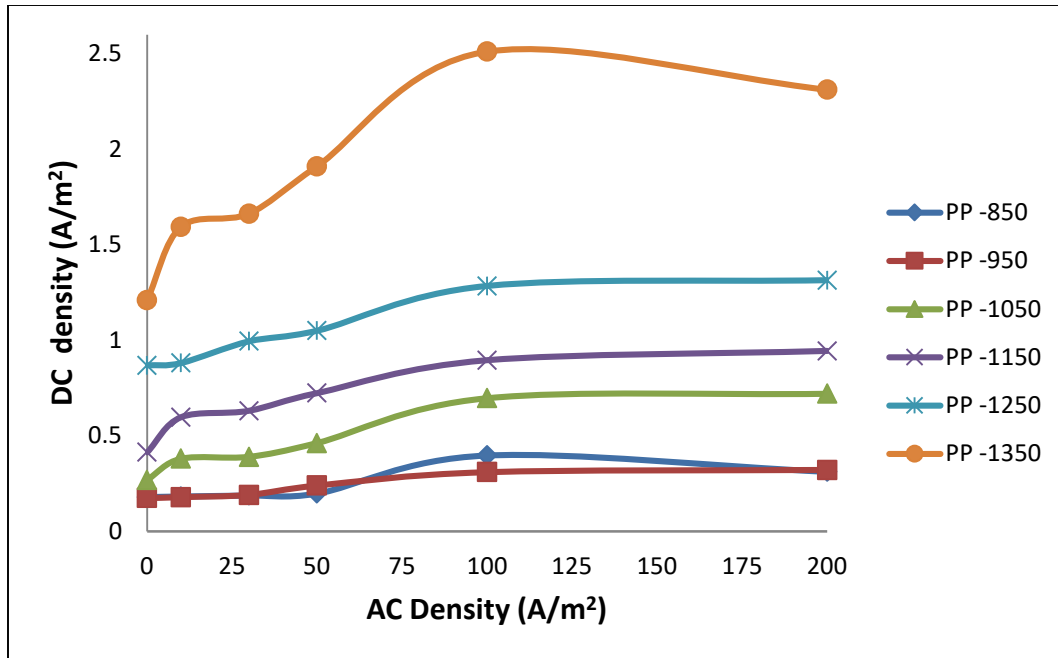


Figure 5.6: Protection density - X80

However, at a protection potential of -1350 mV, the maximum protection current density of 3.5 A/m^2 is required at an AC density of 200 A/m^2 . For X60, X65, and X80 grade pipes (Figure 5.6), at the protection potential of -1350 mV, the maximum protection density is 100 A/m^2 .

Table 5.13: Protection of Current Density Shift with polarisation potential

AC Current Density (A/m²)	Change in protection density (A/m²)		
	X46	X52	X80
0	1.47	1.13	1.03
30	1.96	1.76	1.47

The rate of change of protection density for X80 grade pipes (Table 5.13) under AC interference is lesser than X46 or X52 grade pipes, indicating a lesser tendency for corrosion protection under AC interference.

For X60, X65, and X80 grade pipes, the percentage increase in protection density is 167%, 105%, and 70%, respectively. The varying percentages are due to specific microcrystalline structures of the pipe grades.

5.5 WEIGHT LOSS TESTS

We performed Weight loss tests for four months at the AC density of 200 A/m². All samples are cleaned and weighed before weight loss tests. Samples are retrieved every month, cleaned, and weight measured. One piece for each grade is not exposed to AC to determine the weight loss occurring without AC. Zinc and Magnesium anodes provide the requisite cathodic protection.

X46 samples exhibit weight loss (Table 5.14) without AC at 4.9% after one month and 12.2% after four months. However, under AC interference, the weight loss percentage increases to 6.2% with magnesium anode after one month and increases to 19.1% in four months. Further weight loss supplements 7.3% with zinc anode after one month and increases to 20.3% in four months.

Table 5.14: Weight loss X46 at AC Density 200 A/m²

Duration in Months	Weight loss (%)		
	Without AC	With AC & Zinc Anode	With AC & Magnesium Anode
1	4.9	7.3	6.2
2	6.3	10.8	10.0
3	6.7	12.5	11.9
4	12.2	20.3	20.1

Weight loss occurs for pipe grade without AC due to general corrosion. However, weight loss in the presence of AC is enhanced substantially. Accelerated corrosion happens on account of AC interference. Magnesium or Zinc anodes fail to protect the pipe sample in the presence of large AC.

Table 5.15: Weight loss X65 at AC Density 200 A/m²

Duration in Months	Weight loss (%)		
	Without AC	With AC & Zinc Anode	With AC & Magnesium Anode
1	4.5	6.9	6.7
2	5.8	11.2	10.5
3	7.1	17.9	17.7
4	11.8	24.8	25.1

Similarly, the weight loss percentage in four months under AC interference is more than 20% with any anode. Weight loss on X65 (Table 5.15) and X80 (Table 5.16) samples has been much higher than on the X46 pipe, even at the end of one month. While X46 and X52 pipes have weight loss of 20% in four months, the weight loss for X60, X65, and X80 pipes has been 25% in four months.

Table 5.16: Weight loss X80 at AC Density 200 A/m²

Duration Months	in	Weight loss (%)		
		Without AC	With AC & Zinc Anode	With AC & Magnesium Anode
1		5.3	15.9	16.3
2		6.2	19.5	20.3
3		7.3	22.8	21.9
4		13.1	25.8	25.7

All pipe grades sustain considerable corrosion on AC over the test period. The weight loss tests validated by other published papers [323]-[328] regarding the severity of AC corrosion on X80 and different pipe grades.

The mechanism of AC corrosion remains complex and must be predicted and mitigated. The parameters such as leakage current density and AC voltage are vital, along with soil resistivity and pH monitoring. Under fault conditions, the stress voltage on the coating also needs to be predicted for any damage to the coating. The prolonged overprotection of the pipeline system results in coating disbondment, accelerating AC corrosion [329]-[330]. Zinc and Magnesium anodes cannot provide requisite corrosion protection in the presence of AC [331].

CHAPTER 6

MODELING RESULTS AND DISCUSSIONS

6.1 BACKGROUND

Computer modeling applications for AC interference have been attempted in previous works [332]-[338]. The focus primarily remained on determining AC voltage using one software or another. Some recent studies [339]-[346] show renewed interest and need for determining various parameters critical for AC corrosion through numerical studies, finite element methods, or other modeling tools. Some studies consider steady-state conditions, and few have attempted to address fault conditions.

Table 6.1: Three Layer Soil Model for two locations

Chainage (Km)	115.4		117.72	
Layer	Resistivity (Ohm-m)	Thickness (m)	Resistivity (Ohm-m)	Thickness (m)
Top	6	10.6	166.8	0.5
2	4	5.1	251	4.1
Bottom	80	Infinite	61	Infinite
RMS Error (%)	10.9		7.00	

The modeling and optimization study on the pipeline network using CDEGS software considered both steady state and fault conditions. The physical parameters of the pipeline, transmission lines, soil resistivity, and pH are considered [347]-[354].

6.2 SOIL RESISTIVITY AND pH

6.2.1 SOIL RESISTIVITY MEASUREMENTS

Soil resistivity was measured at 59 locations along the pipeline route and resolved in a three-layer soil model for all locations. Table 6.1 represents the three-layer soil model derived from soil resistivity measurements at two chainages.

6.2.2 PH MEASUREMENTS ALONG THE PIPELINE ROUTE

pH values at 63 locations along the pipeline route (Table 6.2) indicate average pH of 6.4, with a maximum of 7.2 and a minimum of 5.8. The pH values are resolved in the software.

6.3 TOUCH VOLTAGES AT A STEADY STATE

Before examining the touch voltage on the pipeline, the currents in all transmission lines are plotted to ensure the correct energization. The current flow is the most critical parameter for the touch voltage.

Table 6.2: pH measurement in the field

Chainage (Km)	pH	Chainage (Km)	pH	Chainage (Km)	pH	Chainage (Km)	pH
106.22	6.6	231.30	6.4	280.02	6.4	325.50	6.8
113.45	6.3	234.30	6.2	283.30	6.4	328.00	5.9
115.99	6.5	237.35	5.8	291.40	6.2	331.00	6.5
116.92	6.4	238.96	6.4	292.40	6.5	337.30	6.7
117.09	6.8	245.50	6.4	295.07	6.3	341.30	6.7
119.28	6.6	247.98	6.8	297.60	6.8	345.30	6.8
120.19	6.1	248.44	6.7	299.60	6	362.42	6.5
123.76	6.5	249.56	6.6	301.50	6.4	364.42	6.3
173.36	6.6	257.82	6.4	305.45	6.3	367.40	6.2
180.29	6.4	260.20	6.3	307.32	6.7	371.40	6.3
184.00	6.4	261.30	6.3	310.42	7.2	372.40	6.3
185.45	6.3	270.37	6.5	311.55	5.9	375.39	6.8
219.60	6.4	274.10	6.6	314.10	6.2	376.00	6.7
225.80	6.4	275.70	6.2	317.50	6.8	380.00	6.6
228.75	6.7	276.10	6.4	321.20	6.5	389.00	6.4
230.30	6.3	277.10	6.5	323.20	6.3		

6.3.1 PRE-MITIGATION MODELING

Chainage 104.95 to 208.58 km

Figure 6.1 and Figure 6.2 indicate the pipeline voltage for the section chainage 104.95 to 208.58 km without any mitigation measures. The touch voltage peak is observed at chainage 173.34 km.

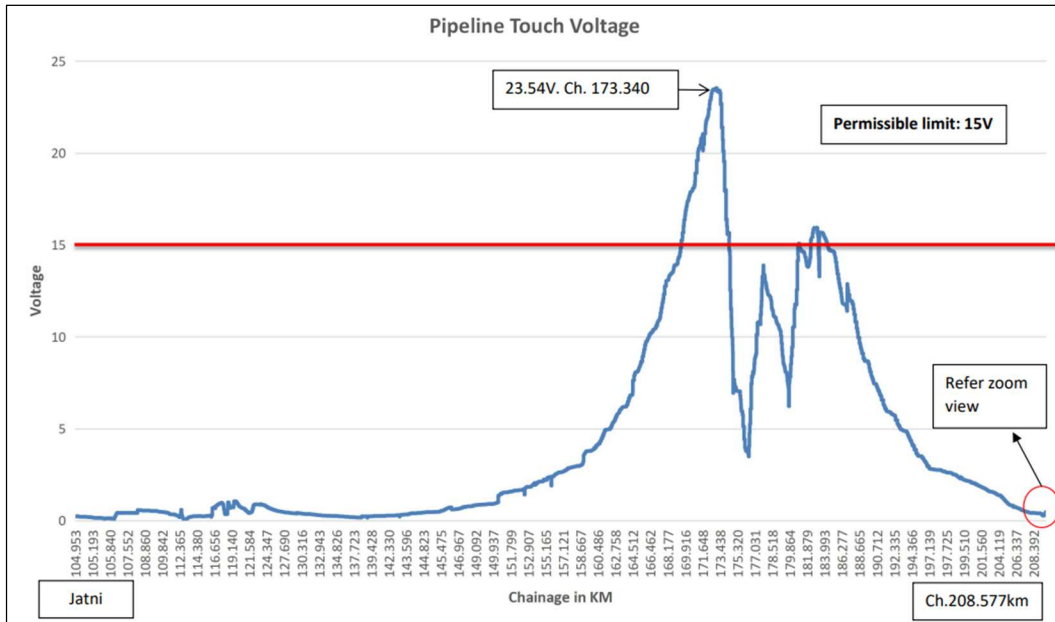


Figure 6.1: Touch voltage Pre-mitigation (104.95 to 208.58 km)

The touch voltage stays within the permissible limit of 15 V within most of the length of the section. The touch voltage on the pipeline exceeds the prescribed safe limit of 15 V between chainage 169.098 and 174.387 with a maximum of 23.54 V, where the soil resistivity is high at 600 Ohm-M. The touch voltage exceeds the permissible value of 15 V for a distance of about 5.289 km.

Chainage 208.58 to 284.32 km

Figure 6.3 and Figure 6.4 indicate the pipeline voltage for the section chainage 208.58 to 284.32 km without any mitigation measures. The touch voltage peak is observed at chainage 242.71 km.

The touch voltage stays within the permissible limit of 15 V within most of the length of the section. The touch voltage exceeds the allowable value of 15 V for a distance of about 3.234 km.

Zoom view near Chainage 208.577KM (Ch 208.264 to 208.577km).

Normal load with existing pipeline ground points

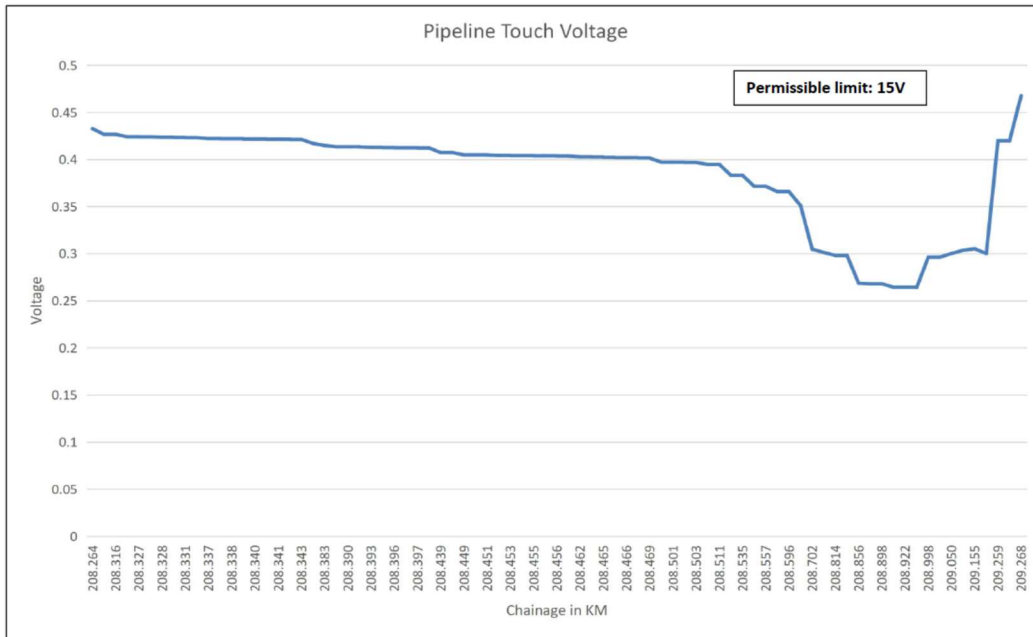


Figure 6.2: Touch voltage pre-mitigation (at 208.58 km)

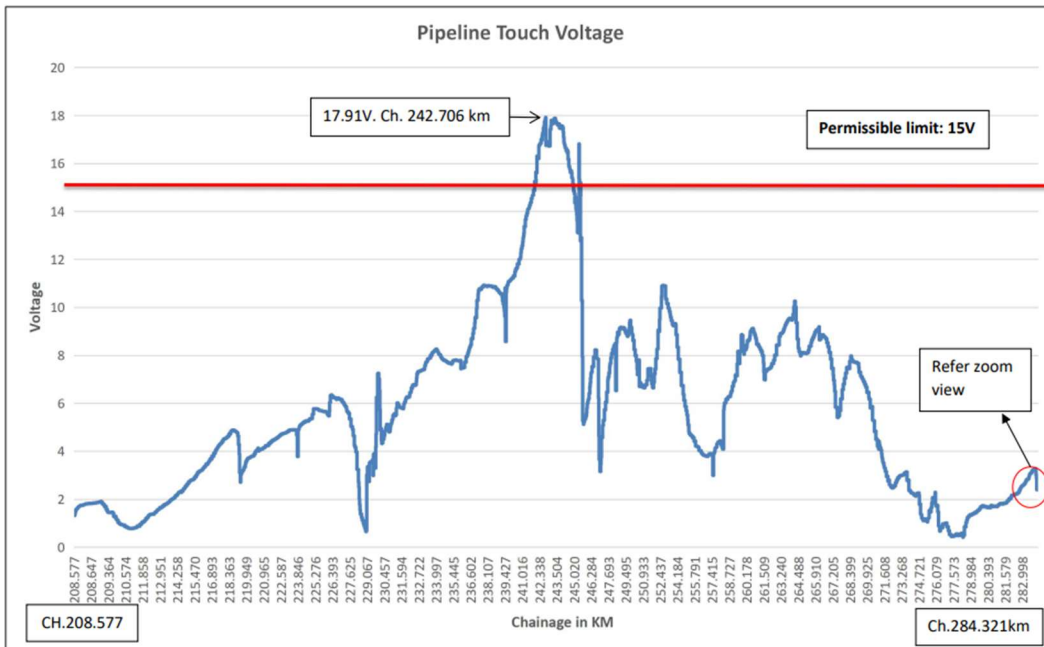


Figure 6.3: Touch voltage Pre-mitigation (208.58 to 284.32 km)

Zoom view near Chainage 284.321KM (Ch 283.165 to 284.321 km).

Normal load with existing pipeline ground points

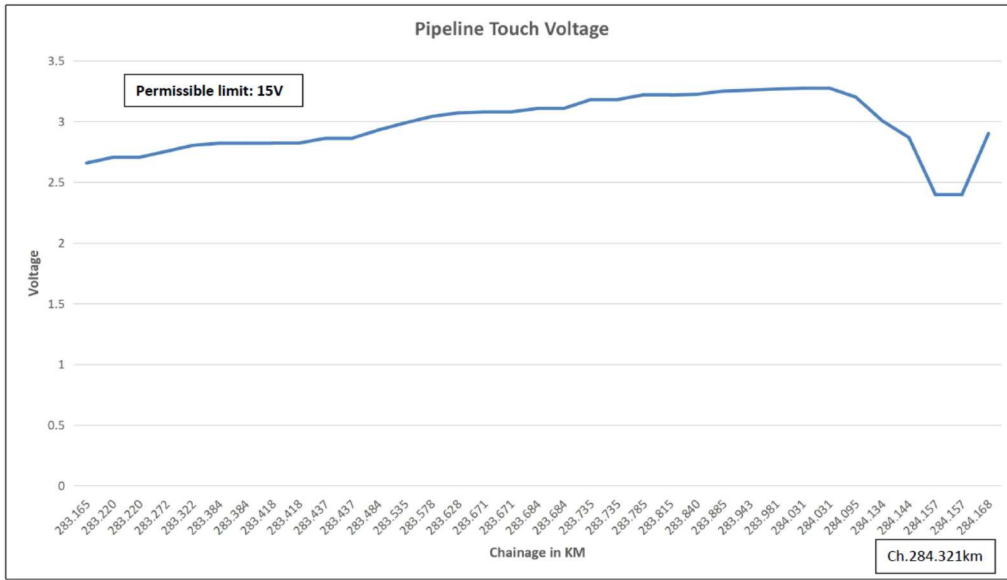


Figure 6.4: Touch voltage Pre-mitigation (at 284.32 km)

6.3.2 PRE-MITIGATION FIELD VALIDATION

Chainage 104.95 to 208.58 km

The touch voltage on the pipe was compared and validated (Figure 6.5) with Base Line Interference Voltage (PSP) Data Collection using 24-hour data loggers.

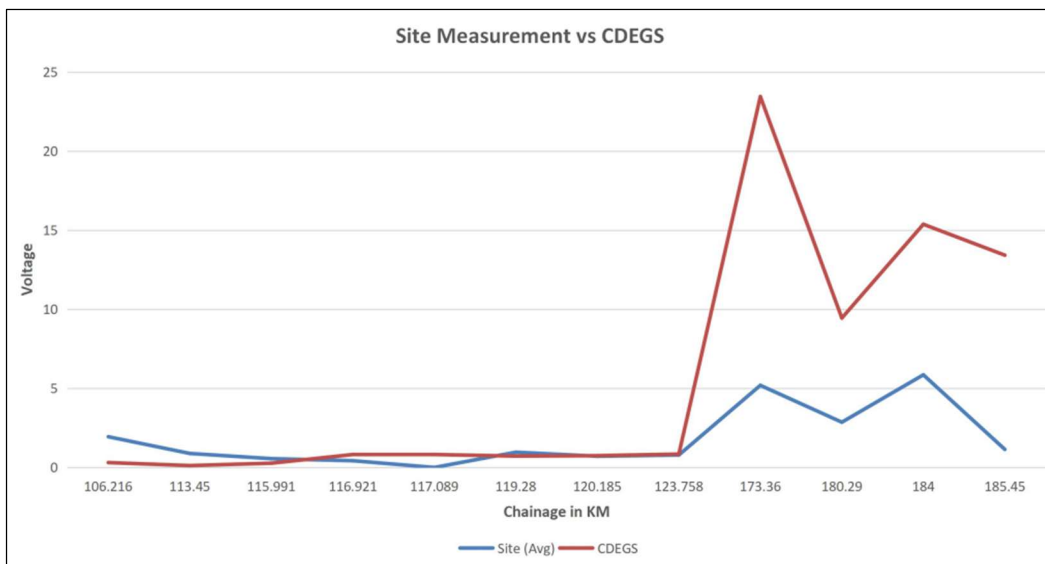


Figure 6.5: Touch voltage field validation (104.95 to 208.58 km)

The field measurements average is in close agreement with the touch voltage of the pipeline from CDEGS till chainage 123.758 km. After chainage of 123.758 km, the pipeline's touch voltage from CDEGS shows a higher trend than site measurements.

Chainage 208.58 km to 284.32 km

The field measurements average is low concerning the touch voltage from CDEGS (Figure 6.6). The peak voltage at the field is around 8 V, compared to the peak of 17.91 V observed in CDEGS.

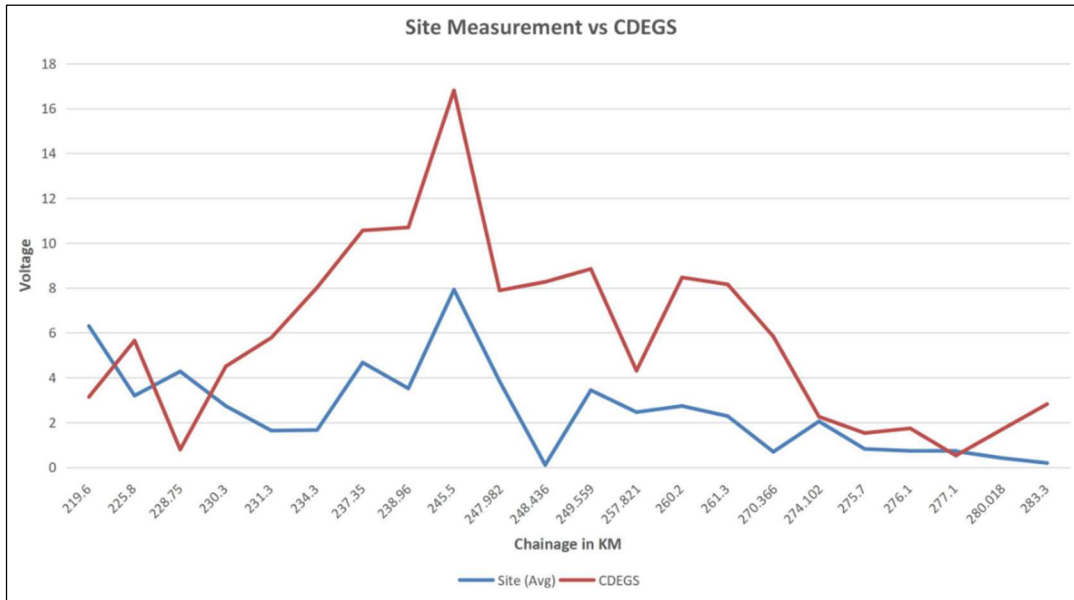


Figure 6.6: Touch voltage field validation (208.58 to 284.32 km)

Further, the location of peaks of touch voltage observed in the field agrees with the peaks projected by CDEGS, which validates the modelling because the magnitude of peaks depends upon the difference in design loading and actual loading of the transmission lines. The model considers the design load of the transmission lines, whereas the actual loading may be small compared to the design load.

6.4 PRE-MITIGATION LEAKAGE CURRENT DENSITY

Chainage 104.95 to 208.58 km

The leakage current density pre-mitigation is indicated in Figure 6.7 and Figure 6.8. It reaches its peak value at 171.648 km. The leakage current density remains within the permissible value for most of the length of the pipeline except few locations. High leakage current density values occur between chainage 164.410 km and

171.648 km and between chainage 177.890 km and 186.559 km. In these areas, transmission line 400KV Mermundal to Mendhasal running parallel close to the pipeline crosses and deviates from the pipeline. Further, the low resistivity soil ($14 \Omega\text{-m}$) in this region at pipeline depth contributes to higher leakage current density. The leakage current density exceeds 30 A/m^2 for about 21.086 km.

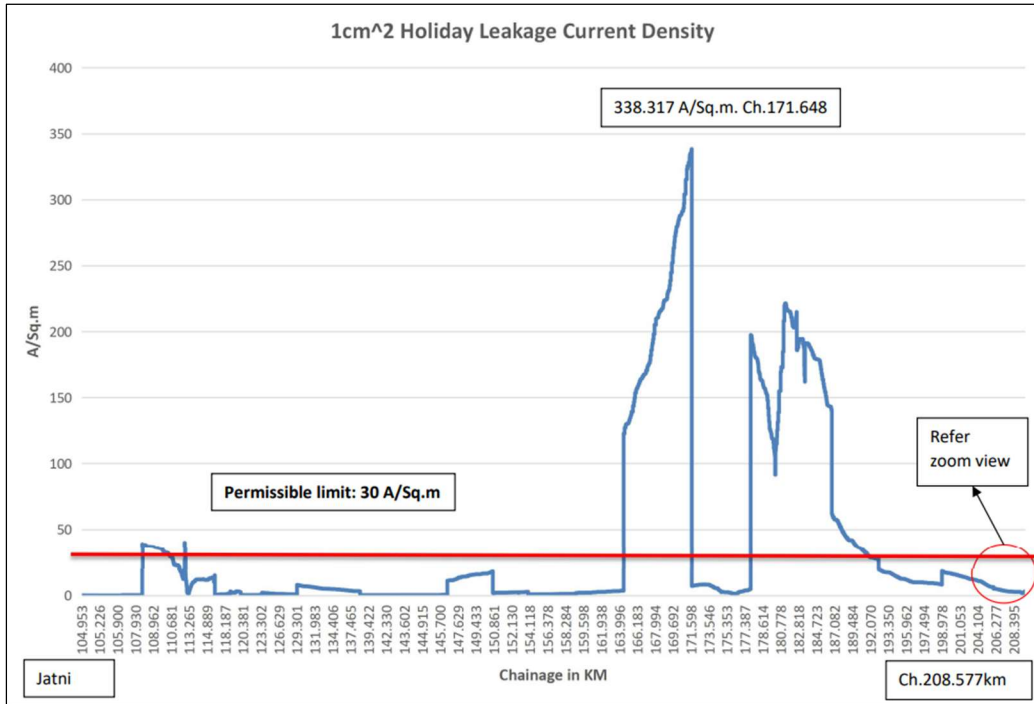


Figure 6.7: Leakage density pre-mitigation (104.95 to 208.58 km)

Chainage 208.58 to 284.32 km

The leakage current density pre-mitigation is indicated in Figure 6.9 and Figure 6.10. It reaches its peak value of 1788.80 A/m^2 at 245.52 km. The leakage current density remains within the permissible value for most of the length of the pipeline except few locations. High leakage current density values occur between chainage 242.664 km and 276.1 km. In this area, transmission line 400KV Mermundal to Vedant runs parallel to the pipeline crosses and deviates after the pipeline crossing. Further, the low resistivity soil ($2.12 \Omega\text{-m}$) in this region at pipeline depth contributes to higher leakage current density. The leakage current density exceeds 30 A/m^2 for about 47.802 km.

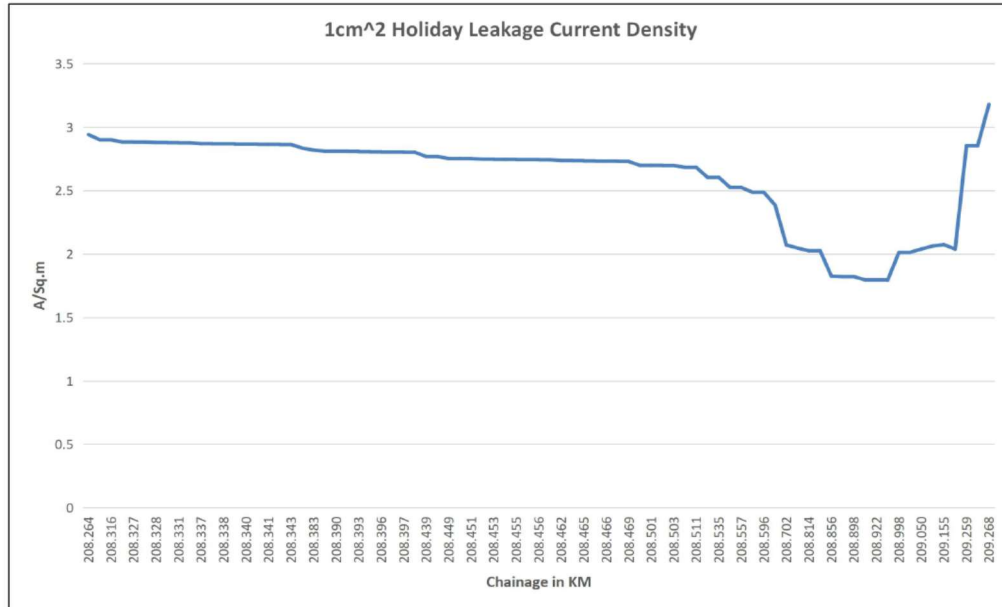


Figure 6.8: Leakage density pre-mitigation at chainage 208.58 km

6.5 MITIGATION MEASURES

The result plots with normal load and existing pipeline ground points indicate that the leakage current density values exceed the design objective and require implementing the mitigation system.

As the first step towards applying mitigation, the section of the pipeline with a leakage current density value above 30 A/m^2 was identified.

The location of available TLPs at these pipeline sections (where the leakage current density exceeds 30 A/m^2) identified to enable and suggest mitigation grounding. The mitigation measures depend on the type of soil structure at the location and length of the pipeline section with leakage current density value exceeding 30 A/m^2 .

As a proposed measure, mitigation grounding shall be a Zinc ribbon installed at or near the surface of pipe depth.

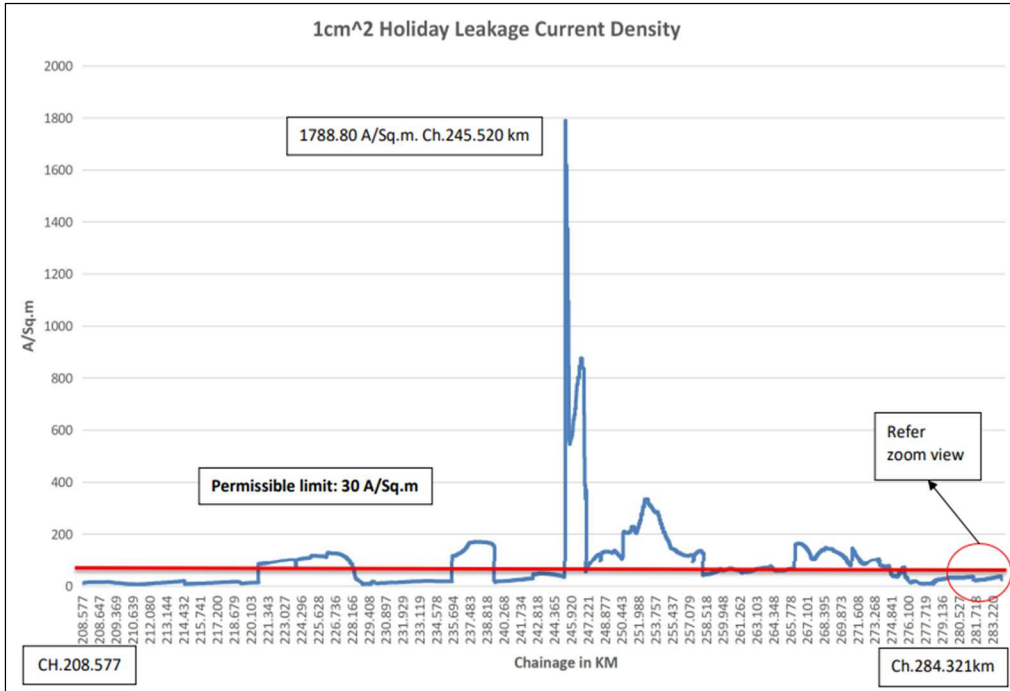


Figure 6.9: Leakage density pre-mitigation (208.58 to 284.32 km)¹⁰

Zoom view near Chainage 284.321KM (Ch 283.165 to 284.321 km).

Normal load with existing pipeline ground points

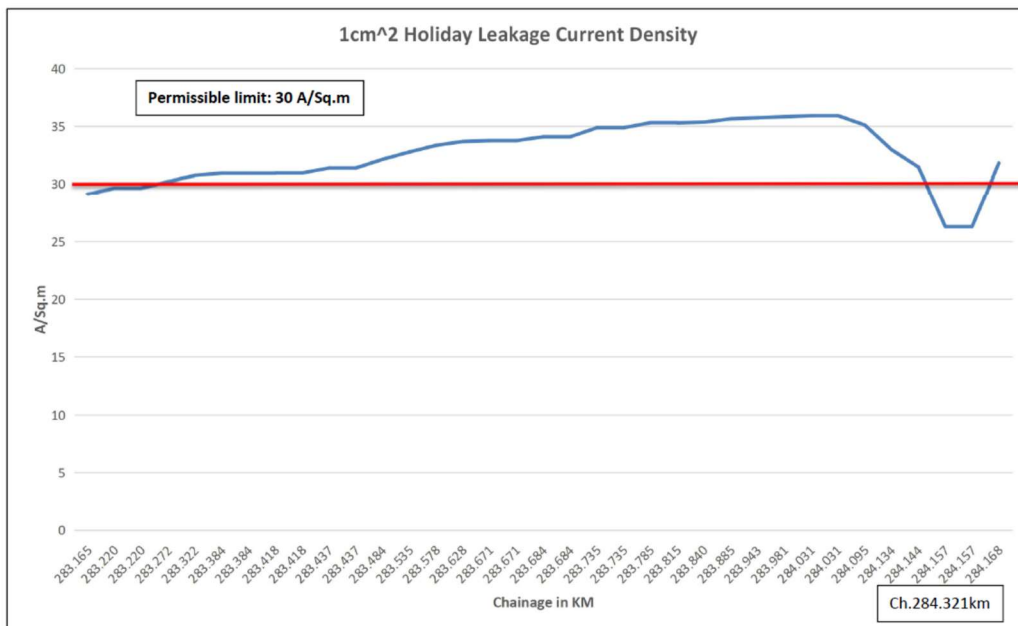


Figure 6.10: Leakage density pre-mitigation at 284.32 km

Table 6.3 shows the details of the chainages for proposed mitigation groundings for the pipeline section from 104.95 to 208.58 km.

Table 6.3: Mitigation measures (104.95 to 208.58 km)

Touch Voltage Reduction			Leakage density Reduction		
Chainage (km)	Mitigation type	Impedance to Earth (Ω)	Chainage (km)	Mitigation type	Impedance to Earth (Ω)
172.156	Zinc Ribbon 328 feet	10.1636	170.541	Zinc Ribbon 500 feet	0.3004
172.464	Zinc Ribbon 328 feet	10.1636	171.494	Zinc Ribbon 500 feet	0.3004
172.898	Zinc Ribbon 328 feet	10.1636	177.397	Zinc Ribbon 500 feet	0.1953
173.129	Zinc Ribbon 328 feet	10.1636	178.213	Zinc Ribbon 500 feet	0.3655
173.332	Zinc Ribbon 328 feet	10.1636	178.848	Zinc Ribbon 500 feet	0.1953
173.546	Zinc Ribbon 328 feet	10.1636	180.019	Zinc Ribbon 500 feet	0.1953
173.961	Zinc Ribbon 328 feet	10.1636	181.161	Zinc Ribbon 500 feet	0.1953
177.205	Zinc Ribbon 328 feet	10.1636	182.096	Zinc Ribbon 500 feet	0.1953
177.576	Zinc Ribbon 328 feet	10.1636	182.505	Zinc Ribbon 500 feet	0.3655
177.843	Zinc Ribbon 328 feet	10.1636	182.664	Zinc Ribbon 500 feet	0.1986
			183.576	Zinc Ribbon 500 feet	0.1986

The mitigation measures include deploying zinc ribbons (328 ft) at 10 locations with impedances around 10Ω for a reduction in touch voltage and deploying zinc ribbons (500 ft) at 11 sites with impedances around 0.19 to 0.36Ω for a decrease in leakage current density.

For the pipeline section from 208.58 to 284.32 km, mitigation measures include the deployment of zinc ribbons (10 ft) at 17 locations (impedances 34 to 61Ω) for a reduction in touch voltage and deployment of zinc ribbons (500/250 ft) at 17 sites (impedances from 0.08 to 1.44Ω). The same is modelled for simulation and evaluation of the results.

6.6 POST-MITIGATION LEAKAGE CURRENT DENSITY

Chainage 104.95 to 208.58 km

After applying mitigation measures, the leakage current density determined as per Figure 6.11. After using measures, the leakage current density reduces by a significant amount when compared with values without mitigation. The peak value of leakage current density is 39.68 A/m^2 , which occurs at chainage 111.44 km. Leakage current density for about 98% of the pipeline section is under 30 A/m^2 .

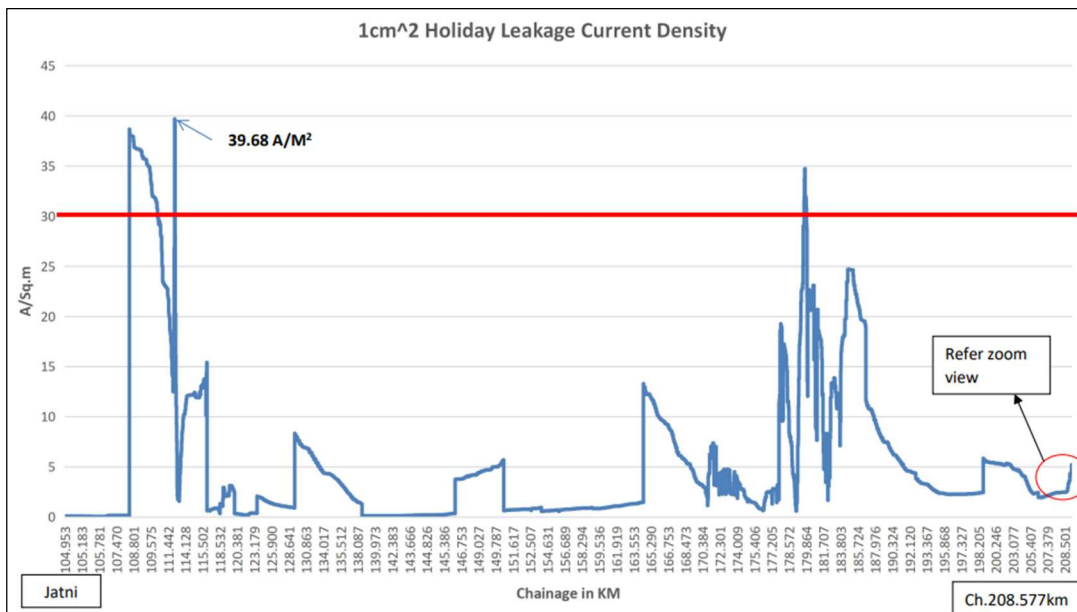


Figure 6.11: Leakage density post mitigation (Chainage 104.95 to 208.58 km)

Chainage 208.58 to 284.32 km

After applying mitigation measures, the leakage current density determined as per Figure 6.12. After using measures, the leakage current density reduces from 1788.80 A/m² to 311 A/m². Leakage current density for about 98% of the pipeline section is under 30A/m². Further reduction in leakage current density requires elaborate mitigation measures along the significant length of the pipeline.

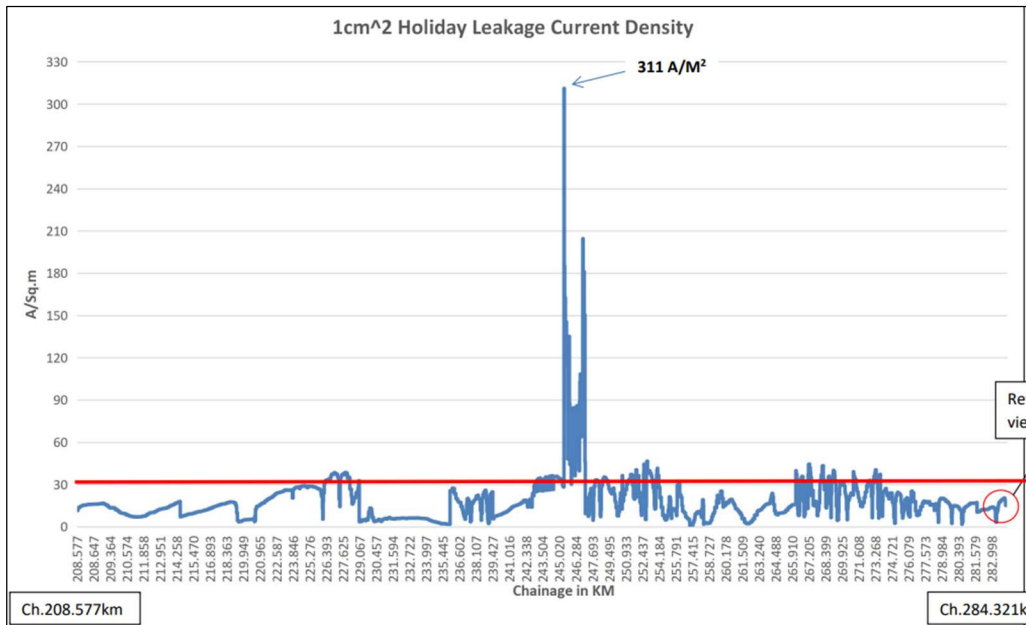


Figure 6.12: Leakage density post mitigation (Chainage 208.58 to 284.32 km)

6.7 POST-MITIGATION TOUCH VOLTAGE

Chainage 104.95 to 208.58 km

After applying mitigation measures, pipeline touch voltage (Figure 6.13 and Figure 6.14) is reduced considerably compared to previous results. The peak value is 13.42 V. The pipeline-induced voltage for touch voltage hazards has decreased to less than 15 V per requirement.

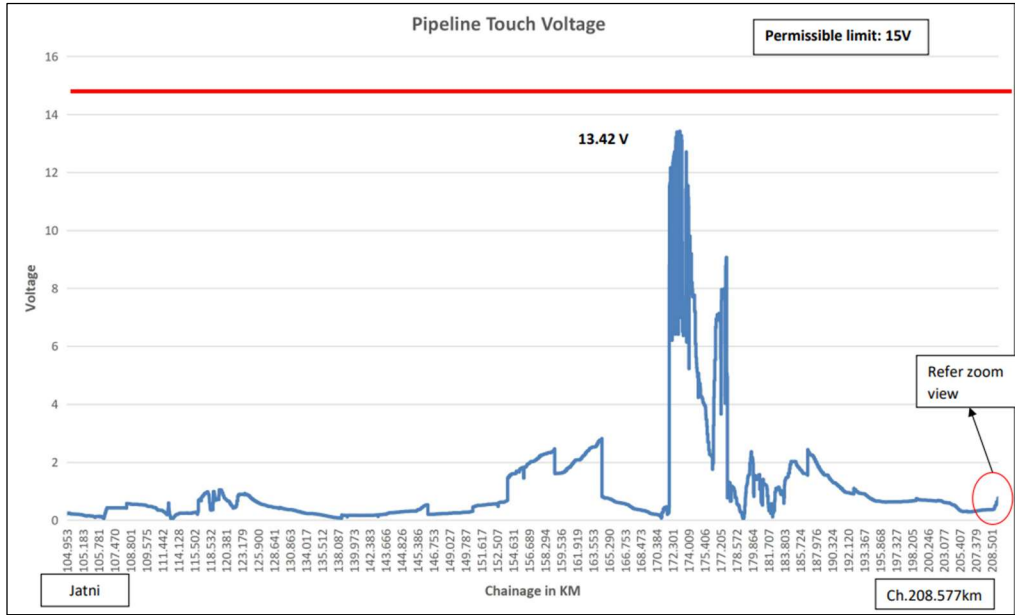


Figure 6.13: Touch voltage Post-mitigation (Chainage 104.95 to 208.58 km)

Zoom view near 208.577KM (Ch 208.264 to 208.577km).

Mitigation for Normal load.

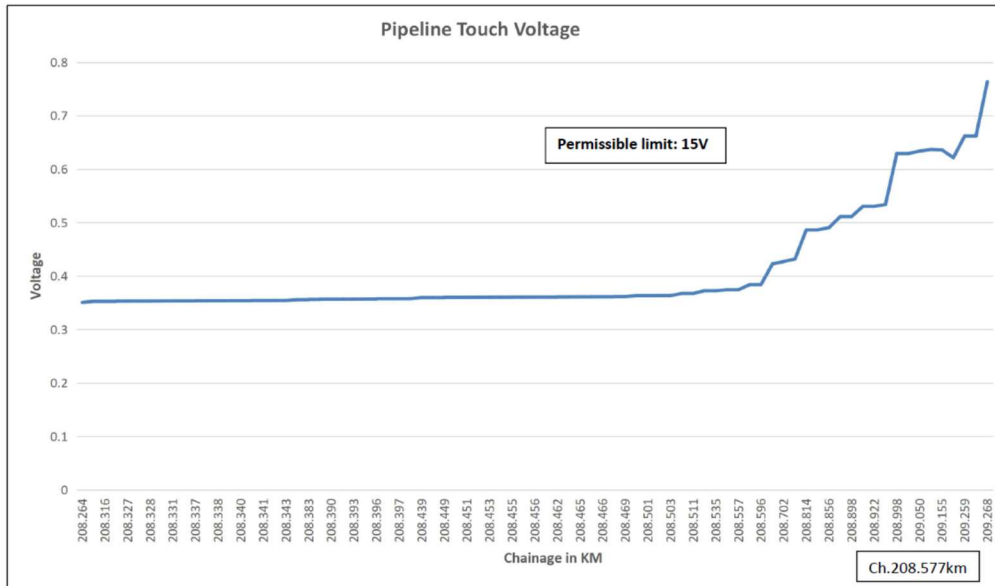


Figure 6.14: Pipeline Touch voltage post-mitigation (Zoom view at 208.58 km)

Chainage 208.58 to 284.32 km

After applying mitigation measures, pipeline touch voltage (Figure 6.15) is reduced considerably compared to previous results. The peak value is 13.78 V. The pipeline-induced voltage for touch voltage hazards has decreased to less than 15 V per requirement.

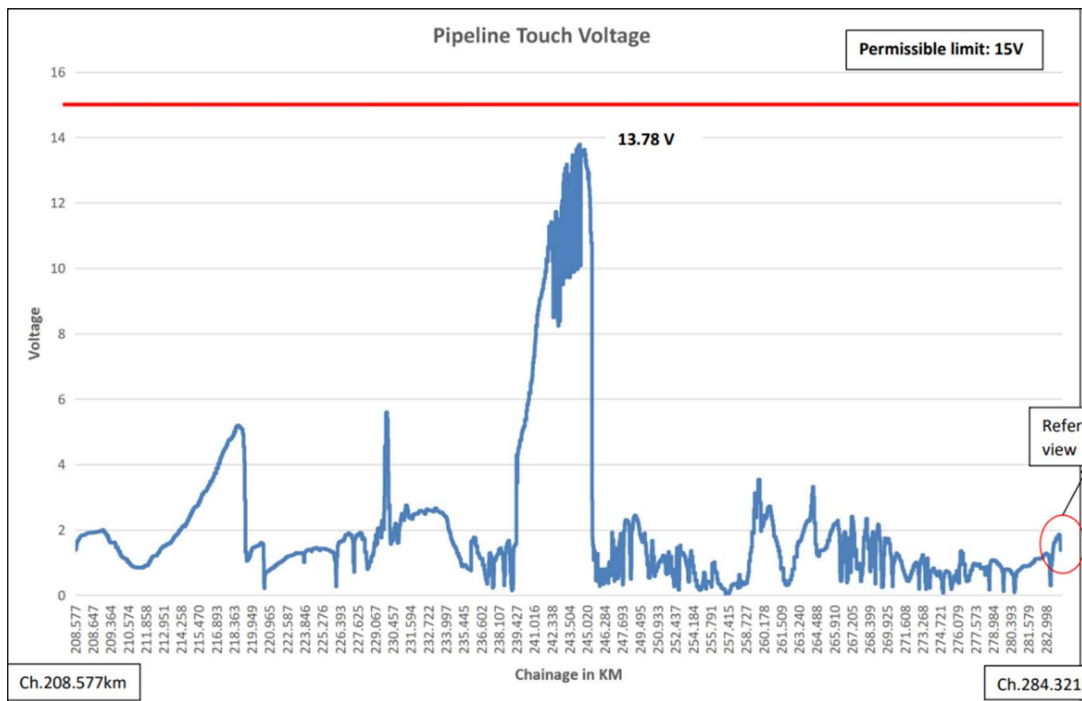


Figure 6.15: Touch voltage Post-mitigation (Chainage 208.58 to 284.32 km)

Table 6.4: Comparison of pre-and post-mitigation (Ch. 104.95 to 208.58 km)

Parameters	Limits	Without Mitigation	With Mitigation
Length of Pipeline (km)	-	103.624	103.624
Touch Voltage (maximum)	AC 15 V	23.54 V	13.42 V
Holiday Leakage Current Density (maximum)		338.32 A/m ²	39.68 A/m ²
Length of Pipeline exceeding the prescribed limit of touch voltage	15 V	5.289 km	-
Leakage current density (A/m ²) for the pipe section	Less than 30	80.953 km	101.643 km
	30 to 75	6.764 km	1.981 km
	75 to 100	-	-
	Above 100	15.907 km	-

6.8 SUMMARY RESULTS PRE- AND POST-MITIGATION

Table 6.4 provides pre- and post-mitigation status for the pipeline section from Ch. 104.85 to 208.58 km. The touch voltage reduces from 23.54 V to 13.42 V after applying mitigation. After mitigation, all pipeline lengths are exposed to touch voltage less than the permissible value of 15 V.

Similarly, the maximum leakage current density reduces sharply from 338.32 A/m² to 39.68 A/m². No portion of the pipeline experiences a current density higher than 75 A/m². Further mitigation measures may also reduce the leakage current density further down. However, designers must balance the need to reduce leakage current density to safe limits vs. the cost of additional mitigation measures.

Table 6.5: Comparison of pre-and post-mitigation (Ch. 208.58 to 284.32 km)

Parameters	Limits	Without Mitigation	With Mitigation
Length of Pipeline (km)	-	72.744	72.744
Touch Voltage (maximum)	AC 15 V	17.91 V	13.78 V
Holiday Leakage Current Density (maximum)		1788.88 A/m ²	311 A/m ²
Length of Pipeline exceeding the prescribed limit of touch voltage	15 V	3.254 km	-
Leakage current density (A/m ²) for the pipe section	Less than 30	27.734 km	63.663 km
	30 to 75	15.856 km	10.532 km
	75 to 100	7.118 km	0.777 km
	Above 100	25.036 km	0.77km

Table 6.5 provides pre- and post-mitigation status for the pipeline section from Ch. 208.58 to 284.32 km. The touch voltage reduces from 17.91 V to 13.78 V after applying mitigation. After mitigation, all pipeline lengths are exposed to touch voltage less than the permissible value of 15 V.

Similarly, the maximum leakage current density reduces sharply from 1788.88 A/m² to 311 A/m². Some portions of the pipeline still experience a current density higher than 75 A/m². Further mitigation measures may be prohibitively costly and ineffective in reducing the leakage current density below 30 A/m². However, designers must balance the need to reduce leakage current density to safe limits vs. the cost of additional mitigation measures. Also, high leakage current density values may be complicated to bring down and require several other criteria for avoiding AC corrosion.

Table 6.6 provides pre- and post-mitigation status for the pipeline section from Ch. 284.32 to 389.88 km. The touch voltage reduces from 32.52 V to 14.14 V after applying mitigation. After mitigation, all pipeline lengths are exposed to touch voltage less than the permissible value of 15 V.

Table 6.6: Comparison of pre-and post-mitigation (Ch. 284.32 to 389.88 km)

Parameters	Limits	Without Mitigation	With Mitigation
Length of Pipeline (km)	-	105.563	105.563
Touch Voltage (maximum)	AC 15 V	32.52 V	14.14 V
Holiday Leakage Current Density (maximum)		504.68 A/m ²	50 A/m ²
Length of Pipeline exceeding the prescribed limit of touch voltage	15 V	38.875 km	-
Leakage current density (A/m ²) for the pipe section	Less than 30	40.161 km	94.229 km
	30 to 75	23.102 km	11.328 km
	75 to 100	10.221 km	-
	Above 100	32.079 km	-

Similarly, the maximum leakage current density reduces sharply from 504.68 A/m² to 50 A/m². The pipeline experiences a current density less than or equal to 50 A/m². Further mitigation measures may be prohibitively costly to reduce the leakage current density below 30 A/m². However, designers must balance the need to reduce leakage current density to safe limits vs. the cost of additional mitigation measures. Also, high

leakage current density values may be challenging to bring down and require several other criteria for avoiding AC corrosion.

6.9 TOTAL INTERFERENCE UNDER FAULT CONDITIONS

Transmission line Mermundal substation to Vedanta substation

Total interference evaluated under fault conditions for 400 kV transmission line from Mermundal substation to Vedanta substation using CDEGS. Figure 6.16 indicates the section current in phase wire, section current in shield wire, shunt current in tower earthing, and coating stress voltage on pipelines under fault conditions.

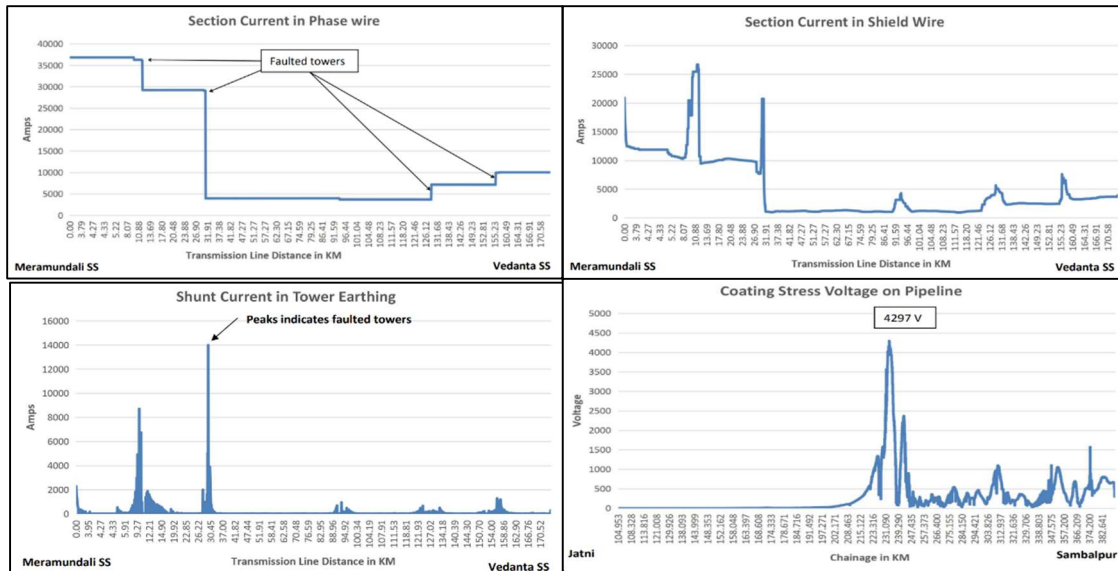


Figure 6.16: Total interference -Faulted phase Mermundal to Vedanta 400 kV

The coating stress voltage in fault conditions is 4.3 kV, less than the specified value of 5kV for DFBE coating on the pipeline.

Transmission line Mermundal substation to Mendhasal substation

Total interference evaluated under fault conditions for 400 kV transmission line from Mermundal substation to Mendhasal substation using CDEGS. Figure 6.17 indicates the section current in phase wire, section current in shield wire, shunt current in tower earthing, and coating stress voltage on pipelines under fault conditions.

In this case, the coating stress voltage in fault condition is 0.7 kV, which is less than the specified value of 5kV for DFBE coating on the pipeline.

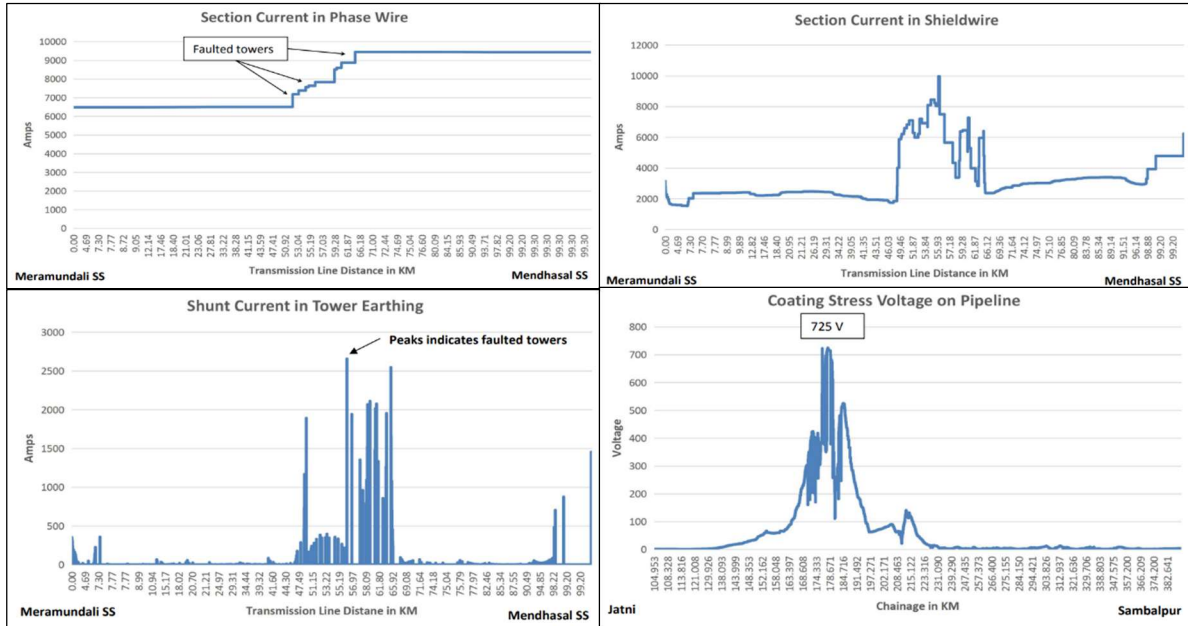


Figure 6.17: Total interference -Faulted phase Mermundal to Mendhasal 400 kV

Transmission line Angul to Sundargarh Ckt 1 & 2

Total interference was evaluated under fault conditions for the 765 kV transmission line from the Angul substation to Sundargarh substation Ckt 1 & 2 using CDEGS. Figure 6.18 indicates coating stress voltage on pipelines under fault conditions.

In this case, the coating stress voltage in fault condition is 2.3 kV, which is less than the specified value of 5kV for DFBE coating on the pipeline.

Transmission line Mendhasal to Pandibali 400 kV

Total interference was evaluated under fault conditions for a 400 kV transmission line (from Mendhasal to Pandibali) using CDEGS. Figure 6.19 indicates coating stress voltage on pipelines under fault conditions.

In this case, the coating stress voltage in fault condition is 3.4 kV, which is less than the specified value of 5kV for DFBE coating on the pipeline.

Total interference evaluation using CDEGS enables predicting coating stress voltage under fault conditions. In the instant case, the expected stress voltage for all four transmission lines is less than the limit of 5 kV for DFBE coating, and no separate mitigation measures are required.

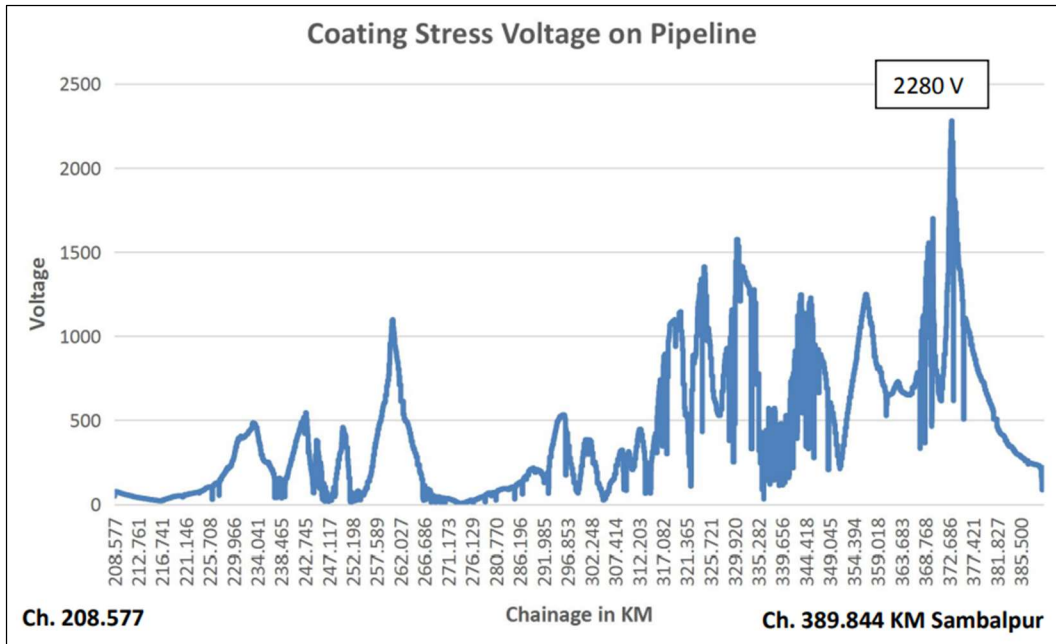


Figure 6.18: Coating stress voltage - Angul to Sundargarh 765 kV Ckt 1&2

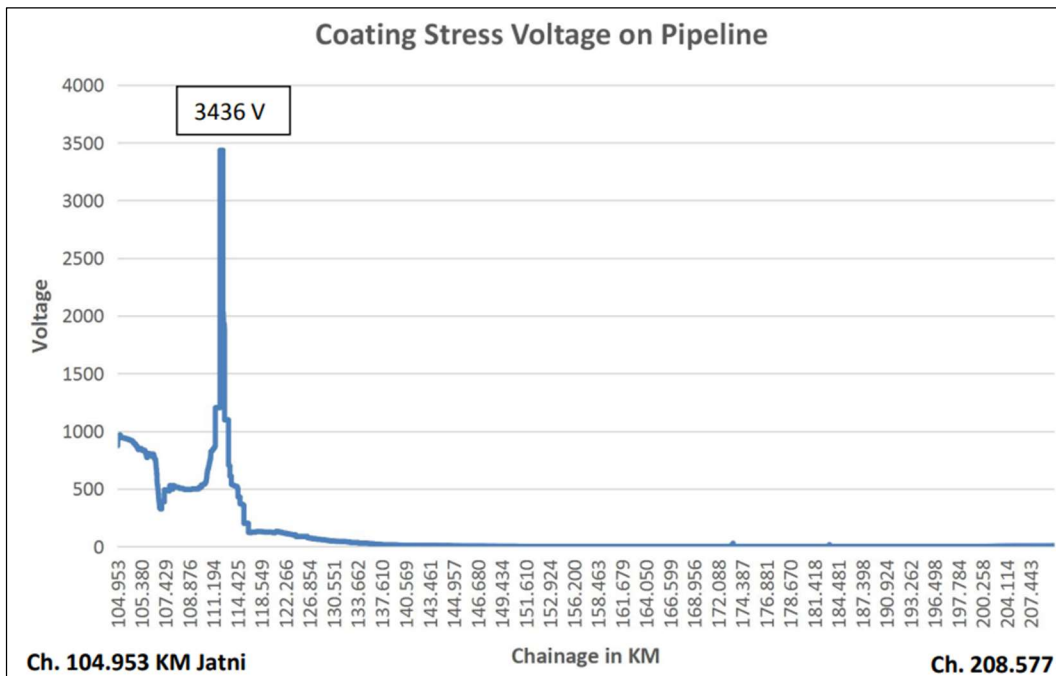


Figure 6.19: Coating stress voltage – Mendhasal to Pandibali 400 kV

If required, mitigation measures under fault conditions are modelled similarly to Steady-state conditions to determine post-mitigation coating stress voltage.

CHAPTER 7

CONCLUSIONS AND WAY FORWARD

7.1 CONCLUSION

This unique research considers inputs from the data collected at the experimental stage and the soil resistivity and pH measurements to determine a risk assessment matrix and a corrosion model. The modeling using CDEGS enabled the prediction and mitigation of critical parameters such as touch voltage, leakage current density, and coating stress voltage.

The predicted outputs are validated with field measurements, and variance is analyzed to optimize the mitigation measures.

Five pipe grades were analysed for corrosion performance in alternating current under cathodic protection. All the pipe grades exhibit good corrosion performance in terms of protection potential, protection density, and anodic shift at the protection density up to 30 A/m² AC density. The pipe samples at 0.3 A/m² of protection density remain below over-protection even without AC.

7.2 RISK ASSESSMENT AND AC CORROSION MODEL

AC corrosion mechanism is complex and is affected by several parameters. Some parameters that affect the corrosion performance include the level of protection, the current density of AC interference, the level of DC protection, current density, soil resistivity and pH, and exposure time.

Accordingly, a risk assessment matrix (Table 7.1) shall be a ready reckoner for the pipeline industry.

7.2.1 PIPE GRADE AND APPLICATION

The in-house experimental arrangement enabled conducting of potentiostatic and galvanostatic tests to determine AC interference on pipe samples of different grades. Better corrosion performance of X46 and X52 samples in test conditions

provides insight into the need to be aware of the grade of pipes in terms of AC corrosion performance at the time of design of the pipeline system. The selection of pipe grade shall also consider the AC corrosion likelihood, and suitable corrosion allowances may be assessed accordingly [355]-[357]. Awareness of the application/route of the pipeline system, especially concerning transmission line systems, shall be helpful.

Table 7.1: Risk Assessment Matrix

Factor	Risk Severity			
	Urgent	Major	Minor	Negligible
Protection Potential (mV)	More negative than -1200	Between -850 and -1200	More positive than -850	More positive than -850
AC voltage (V)	>10	5 to 10	<5	0
AC Density (A/m ²)	>30	10 to 30	<10	0

7.2.2 FIELD MEASUREMENTS AND RISK ASSESSMENT

Field measurements involving soil data such as pH and resistivity must be undertaken for practical risk assessment. The transmission line systems' knowledge and operating parameters are required for the risk assessment of the pipeline system [358]- [360].

Weight loss tests at an AC density of 200 A/m² have revealed that none of the pipe grades can sustain high AC interference, and the integrity of the pipeline system might be affected in a matter of days.

The anode systems are also ineffective in AC interference and must be monitored closely.

7.2.3 PREDICTION USING CDEGS/MODELLING SOFTWARE

The research has demonstrated that modeling software such as CDEGS can predict and help mitigate AC interference using field measurements. The modeling accounts for the steady state as well as fault conditions. However, modeling

requires careful data input, such as transmission lines, pipe grades, soil resistivity, and pH. Modeling predicts the coating stress voltage as well as touch voltage.

Undertaking/modeling mitigation measures help reduce the leakage current density, coating stress, and touch voltage.

7.2.4 FIELD VALIDATION

Field validation of the predicted touch voltages helps to check the model's efficacy and validate the assumptions. Field validation helps in the economical selection of mitigation measures by avoiding over-mitigation.

7.3 IMPLEMENT / REMOVE MITIGATION MEASURES

Assess risk severity regularly using the model to contain the same to "Minor" or "Negligible." Initiate actions for mitigations for "Urgent" or "Major."

The research proposes the AC Corrosion Model (Figure 7.1) depending on the risk matrix. The AC corrosion model considers the importance of carefully selecting the pipe grades at design/construction. The field measurements and validation form an integral part of the model, which enables the assessment of AC corrosion risk based on the risk assessment matrix.

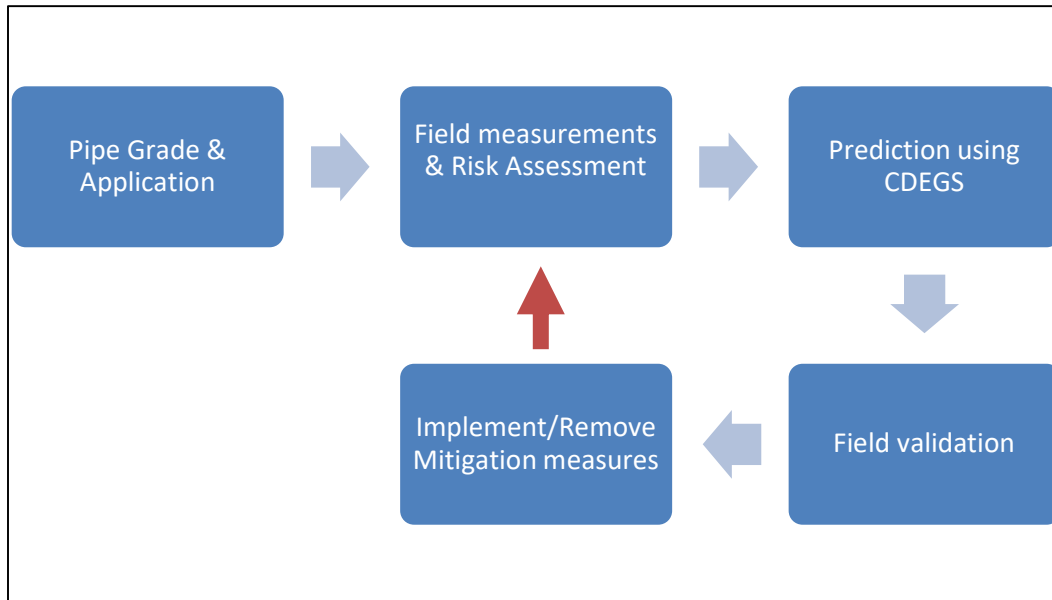


Figure 7.1: AC Corrosion Model

Software modeling using the established tools enables the prediction of the critical AC interference parameters. Field validation of the parameters enables correlation with the assumptions. Finally, the modeling allows for the implementation/deletion of mitigation measures, which is essential to achieve techno-commercially viable solutions for AC interference mitigation.

Feedback on the mitigation measures is critical for continual risk assessment through field measurements. Timely actions for mitigations are crucial and essential to ensure the integrity of the pipeline systems against the ever-increasing threat of AC corrosion.

7.4 ACHIEVEMENT OF OBJECTIVES

The research has achieved all the objectives below:

Determine pipeline steel grade more resistant to AC corrosion by observing variations in protection potential and current density due to AC interference under cathodic protection.

Five pipe grades were subjected to potentiostatic and galvanostatic testing to observe their performance against AC corrosion under cathodic protection. The unique experimental setup enabled conducting of relevant tests in soil-simulating solutions. The weight loss tests through a separate experimental setup for up to 4 months evaluated the performance of pipe grades at the AC density of 200 A/m².

The AC corrosion resistance performance is better for X46 and X52 grades at lower AC densities. Better performance is attributable to the microcrystalline structure of X46 and X52 grade pipes manufactured using conventional time-tested manufacturing processes. The higher grades require stringent temperature/process control, which may not be suitable for AC corrosion performance.

However, no pipe grade can sustain higher AC densities. Accordingly, there is a need to implement mitigation measures to bring down the AC interference magnitude.

Study AC interference effect on the performance of Galvanic and Zinc Anodes under cathodic protection.

Weight loss tests have studied the AC interference effect on Zinc and Magnesium anodes along with pipe grades. Zinc and Magnesium anodes cannot protect at AC densities of 200 A/m².

Develop an AC corrosion model through a Risk Assessment matrix, considering pipe grades, cathodic protection potential, AC interference voltage, and AC density.

The Risk Assessment Matrix and the AC Corrosion model have been developed above. The pipeline integrity against AC corrosion requires integrated efforts during the life cycle of pipelines. The field measurements of critical parameters at regular intervals and knowledge of the transmission line parameters are also vital.

Simulate and optimize the proposed corrosion model using CDEGS (Current Distribution, Electromagnetic fields, Grounding & Soil Structure Analysis) software.

CDEGS software has been successfully modelled and integrated with the corrosion model. The model permitted the addition/deletion of mitigation measures for optimizing the mitigation measures in steady state and fault conditions.

With the above, all objectives of the research work have been achieved.

7.5 FUTURE WORKS

Research work shall find applications in Pipeline Industry for developing robust systems to maintain pipeline integrity concerning AC interference. Future research may include considering other parameters like stray DC interference, evaluating High Silicon Anodes' performance evaluation of the polarisation layer, and integrating the same in the corrosion model.

This research work is done on a single pipeline system. However, future research may consider the presence of more than one pipeline system in the immediate vicinity.

REFERENCES

- 1) Ghanbari, E., Iannuzzi, M., & Lillard, R. S. (2016). The mechanism of alternating current corrosion of API grade X65 pipeline steel. *Corrosion*, 72(9), 1196-1210.
- 2) Kuang, D. (2016). *Pipeline corrosion and coating failure under alternating current interference*.
- 3) Ibrahim, I., Tribollet, B., Takenouti, H. and Meyer, M. (2015). AC-induced corrosion of underground steel pipelines. Faradaic rectification under cathodic protection: Theoretical approach with negligible electrolyte resistance. *Journal of the Brazilian Chemical Society*.
- 4) Thakur, Ajit Kumar. (2017). *Corrosion Control for Above Ground Crude Oil Storage Tanks*. NACE International Corrosion Conference Proceedings.
- 5) Thakur, A. K., Arya, A. K., & Sharma, P. (2022). Prediction and mitigation of AC interference on the pipeline system. *Corrosion Reviews*, 40(2), 149-157.
- 6) Guo, Y., Meng, T., Wang, D., Tan, H., & He, R. (2017). Experimental research on the corrosion of X series pipeline steels under alternating current interference. *Engineering Failure Analysis*, 78, 87-98.
- 7) Büchler, M. (2020). On the mechanism of cathodic protection and its implications on criteria including AC and DC interference conditions. *Corrosion*, 76(5), 451-463.
- 8) Buchler, M., & Schoneich, H. G. (2009). Investigation of alternating current corrosion of cathodically protected pipelines: Development of a detection method, mitigation measures, and a model for the mechanism. *Corrosion*, 65(9), 578-586.
- 9) Brenna, A. (2012). A proposal of AC corrosion mechanism of carbon steel in cathodic protection condition. *Corrosion*.
- 10) Brenna, A., Lazzari, L., Pedferri, M., & Ormellese, M. (2014). Cathodic protection condition in the presence of AC interference. *La Metallurgia Italiana*, 6, 29-34.
- 11) Helm G., Helm T., Heinzen H., Schwenk W. (1993). Investigation of corrosion of cathodically protected pipeline steel subjected to alternating currents. *Corrosion Science*, 5, 246.
- 12) Dabkowski, J. and Taflove, A. (1979). Mitigation of Buried Pipeline Voltages Due to 60 Hz AC Inductive Coupling Part II--Pipeline Grounding

- Methods. *IEEE Transactions on Power Apparatus and Systems*, (5), 1814-1823.
- 13) Al-Badi, A. (2004). Analysis of factors affecting the level of electromagnetic interference on pipelines close to power lines. *WSEAS Transactions on Circuits and Systems*, 3(9), 1977-1982.
 - 14) Al-Badi, A. H., & Salam, M. A. (2006). *Computation of the capacitive coupling in conductors installed nearby AC power lines*. IEEE/PES Transmission & Distribution Conference and Exposition.
 - 15) Anqing, F. U., Naixin, L., Zhenquan, B., Chengxian, Y. I. N., Yaorong, F. E. N. G., & Chunyong, H. U. O. (2014). Impacts of AC stray current on the corrosion behaviour of pipe steel for long-distance pipeline. *Oil & Gas Storage & Transportation*, 33(7), 748-756.
 - 16) Al-Gabalawy, M., Mostafa, M. A., & Hamza, A. S. (2021). Mitigation of AC induced voltage on the metallic pipeline based-on the optimal design of KOH-Polarization cells. *Electric Power Systems Research*, 194, 107081.
 - 17) Adedeji, K. B., Ponnle, A. A., Abe, B. T., Jimoh, A. A., Abu-Mahfouz, A. M., & Hamam, Y. (2018). AC induced corrosion assessment of buried pipelines near HVTLs: A case study of South Africa. *Progress In Electromagnetics Research B*.
 - 18) Adedeji, K.B., Ponnle, A.A., Abe, B.T. and Jimoh, A.A. (2015). *Effect of increasing energy demand on the corrosion rate of buried pipelines in the vicinity of high voltage overhead transmission lines*. Intl Symposium on Advanced Electromechanical Motion Systems, 299-303.
 - 19) AlShahri, A. S., Dinh, M. T. N., & Nair, N. K. C. (2014). *Induced voltage on pipeline located close to high voltage lines due to electromagnetic induction*. Australasian Universities Power Engineering Conference.
 - 20) Abdel-Gawad, N. M., El Dein, A. Z., & Magdy, M. (2015). Mitigation of induced voltages and AC corrosion effects on buried gas pipeline near to OHTL under normal and fault conditions. *Electric Power Systems Research*, 127, 297-306.
 - 21) Adedeji, K. B., Abe, B. T., Hamam, Y., Abu-Mahfouz, A. M., Shabangu, T. H., & Jimoh, A. A. (2017). *Pipeline grounding condition: A control of pipe-to-soil potential for AC interference induced corrosion reduction*. The 25th Southern African Universities Power Engineering Conference.
 - 22) Brenna, A., Beretta, S., & Ormellese, M. (2020). AC Corrosion of Carbon Steel under Cathodic Protection Condition: Assessment, Criteria and Mechanism. A Review. *Materials*, 13(9), 2158.

- 23) Chapman, C. (2021). AC Power Interactions with Pipelines–The Usual Suspect, The Ugly Geology, and, Finally, The Weird: Faulty AC Power Conditioning Capacitors Interacting with Well-Coated Pipeline. *Corrosion*.
- 24) Bolzoni, F., Goidanich, S., Lazzari, L., Ormellese, M., & Pedferri, M. (2004). Laboratory testing on the influence of alternated current on steel corrosion. *Corrosion*.
- 25) Chen, L., Du, Y., Liang, Y., & Li, J. (2021). Research on corrosion behaviour of X65 pipeline steel under dynamic AC interference. *Corrosion Engineering, Science and Technology*, 56(3), 219-229.
- 26) Lu, M. X., Tang, D. Z., Du, Y. X., & Zhang, L. (2015). Investigation on corrosion of zinc ribbon under alternating current. *Corrosion Engineering, Science and Technology*, 50(3), 256-263.
- 27) Ding, Q., Li, Z., & Hao, H. (2013). Effects of AC interference on the optimum cathodic protection potential of X70 steel in soil solution. *Anti-Corrosion Methods and Materials*.
- 28) Fu, A. Q., & Cheng, Y. F. (2012). Effect of alternating current on corrosion and effectiveness of cathodic protection of pipelines. *Canadian Metallurgical Quarterly*, 51(1), 81-90.
- 29) Guo, Y. B., Liu, C., Wang, D. G., & Liu, S. H. (2015). Effects of alternating current interference on corrosion of X60 pipeline steel. *Petroleum Science*, 12(2), 316-324.
- 30) Goidanich, S., Lazzari, L., & Ormellese, M. (2010). AC corrosion. Part 2: Parameters influencing corrosion rate. *Corrosion Science*, 52(3), 916-922.
- 31) Guo, Y., Tan, H., Meng, T., Wang, D., & Liu, S. (2016). Effects of alternating current interference on the cathodic protection for API 5L X60 pipeline steel. *Natural Gas Science and Engineering*, 36, 414-423.
- 32) Liu, Q., Wu, W., Pan, Y., Liu, Z. Y., Zhou, X. C., & Li, X. G. (2018). Electrochemical mechanism of stress corrosion cracking of API X70 pipeline steel under different AC frequencies. *Construction and Building Materials*, 171, 622-633.
- 33) Thakur, A. K., Arya, A. K., & Sharma, P. (2020). The science of alternating current-induced corrosion: a review of literature on pipeline corrosion induced due to high-voltage alternating current transmission pipelines. *Corrosion Reviews*, 38(6), 463-472.
- 34) Tang, D. Z., Du, Y. X., Lu, M. X., Jiang, Z. T., Dong, L., & Wang, J. J. (2015). Effect of AC current on corrosion behaviour of cathodically protected Q235 steel. *Materials and Corrosion*, 66(3), 278-285.

- 35) Zhu, M., Du, C. W., Li, X. G., & Liu, Z. Y. (2014). Stress corrosion cracking of X80 pipeline steel under various alternating current frequencies in high-pH carbonate/bicarbonate solution. *Corrosion*, 70(12), 1181-1188.
- 36) Dabkowski, J. (2017). The Evolution of AC Predictive and Mitigation Software. *Corrosion*.
- 37) Al-Alawi, S., Al-Badi, A. and Ellithy, K. (2005). An artificial neural network model for predicting gas pipeline induced voltage caused by power lines under fault conditions. *COMPEL-The international journal for computation and mathematics in electrical and electronic engineering*.
- 38) Bortels, L., Baeté, C., & Dewilde, J. M. (2012). Accurate modelling and troubleshooting of ac interference problems on pipelines. *Corrosion*.
- 39) Bortels, L., Deconinck, J., Munteanu, C., & Topa, V. (2005). A general applicable model for AC predictive and mitigation techniques for pipeline networks influenced by HV power lines. *IEEE transactions on power delivery*, 21(1), 210-217.
- 40) Bortels, L., Deconinck, J., Munteanu, C. and Topa, V. (2003). A User-Friendly Simulation Software for AC Predictive and Mitigation Techniques. *Corrosion*.
- 41) Al Shahri, A. S., & Nair, N. K. C. (2016). Mitigation system for protecting buried pipeline located close to HV OHTL/power cable. *IEEE International Conference on Power System Technology*.
- 42) Al-Badi, A. H., & Ellithy, K. A. (2003). Designing mitigation system of AC induced voltages occurred on gas pipelines using CDEGS-practical case study. *International Conference on Modelling, Simulation and Optimization*, 125-130.
- 43) Babaghayou, F., Zegnini, B. and Seghier, T. (2018). Numerical Study and Remediation of Ac Interference Corrosion on Neighbouring Pipelines. *Engineering Science and Technology*, 13(7): 2047-2064.
- 44) Cristofolini, A., Popoli, A., & Sandrolini, L. (2018). *Numerical modelling of interference from ac power lines on buried metallic pipelines in presence of mitigation wires*. In International Conference on Environment and Electrical Engineering.
- 45) Dabkowski, J. (1996). A Statistical Approach to Designing Mitigation for Induced AC Voltages. *Corrosion*.
- 46) Eden, D. A. (2006). AC interference and accelerated pipeline corrosion in utility corridors—an alternative perspective to the root causes. *Corrosion*.
- 47) Baeté, C., Van Den Bossche, B., & Bortels, L. (2013). Simulation of AC corrosion on pipelines under AC and DC interference. *CeoCor*.

- 48) Brelsford, C. (2015). Mitigating AC Corrosion on Cathodically Protected Pipelines. *Pipeline & Gas Journal*.
- 49) Di Biase, L., Cigna, R., & Fumei, O. (2010). AC corrosion and cathodic protection of buried pipelines. *Corrosion*.
- 50) Du, Y., Tang, D., Lu, M., & Chen, S. (2017). Researches on the effects of AC interference on CP parameters and AC corrosion risk assessment for cathodic protected carbon steel. *Corrosion*.
- 51) Ghanbari, E., Lillard, S., & Carpenter, C. (2017). The Influence of Scale Formation on the AC Corrosion of API Grade X65 Pipeline Steel Under Cathodic Protection. *Corrosion*.
- 52) Ghanbari, E., Lillard, S., Iannuzzi, M., & Ortiz, M. R. (2015). Corrosion behaviour of buried pipeline in presence of AC stray current in controlled environment. *Corrosion*.
- 53) Kemp, D., Finneran, S. and Arellano, D. (2015). Examination of Grounding Methodologies for HVAC Induction on Buried Pipelines. *Corrosion*.
- 54) Finneran, S., Evans, K., & Gossard, J. (2018). Comparison of AC Mitigation Grounding Materials Through Electrochemical Analysis. *Corrosion*.
- 55) Evans, K., & Gossard, J. (2018). Comparison of AC Mitigation Grounding Materials Through Electrochemical Analysis. *Corrosion*.
- 56) Tachick, M. H. (2003). Common Misconceptions Regarding Decoupled Grounding Systems When Mitigating Induced AC Voltages on Pipelines. *Corrosion*.
- 57) Arya, A. K., & Honwad, S. (2016). Modelling, simulation, and optimization of a high-pressure cross-country natural gas pipeline: application of an ant colony optimization technique. *Pipeline Systems Engineering and Practice*.
- 58) Arya, A. K., & Honwad, S. (2018). Optimal operation of a multi-source multi delivery natural gas transmission pipeline network. *Chemical Product and Process Modelling*, 13(3).
- 59) Arya, A. K., & Honwad, S. (2018). multi-source optimization of a gas pipeline network: an ant colony approach. *Petroleum Exploration and Production Technology*, 8(4), 1389-1400.
- 60) Kioupis, N., Kouloumbi, N., & Batis, G. (2013). Simulation of cathodically protected pipeline with capacitive AC mitigation devices for interpretation of misleading instant Eoff readings. *Corrosion engineering, science and technology*, 48(3), 166-172.
- 61) Hansen, M. E., & Dursteler, E. (2017). Pipelines Rails and Trucks: Economic environmental and safety impacts of transporting oil and gas in the US. *Corrosion*.

- 62) Poberezhny, L., Hrytsanchuk, A., Okipnyi, I., Poberezhna, L., Stanetsky, A. and Fedchyshyn, N. (2019). Minimizing losses during natural gas transportation. *Journal of Mechanical Engineering*, 69(1): 97-108.
- 63) Günther, W. and Focke, J. (2014). *Strategic Analysis and Planning of Pipeline Assets—Methods and Tools*. In 9th Pipeline Technology Conference EITEP Institute.
- 64) Stalder, F., 1997. Pipeline failures. *Materials Science*.
- 65) Bera, K. (2019). *Electrical Interference-Emerging Threat to Pipeline*. SPE Oil and Gas India Conference and Exhibition.
- 66) Presse, A.F. (2018). Chinese Oil Giant Sinopec to pay big over pipeline blast that killed more than 60 people. *Business Insider Inc*.
- 67) Bortels, L., Parlongue, J., Fieltsch, W., & Segall, S. (2010). Manage pipeline integrity by predicting and mitigating HVAC interference. *Corrosion*.
- 68) Gummow, R. A., Wakelin, R. G., & Segall, S. M. (1996). *AC Corrosion: A New Threat to Pipeline Integrity*. International Pipeline Conference, American Society of Mechanical Engineers.
- 69) Borteles, L., & Purcar, M. (2009). Manage pipeline integrity by predicting and mitigating high voltage AC interference. *Annals of the University of Oradea. Fascicle of energetics*, 15, 189-195.
- 70) Singh, G., Gharibi, A., Perez, B. M., & Almandoz, R. (2017). *Enhancing Pipeline Integrity Management by Integrating Advanced Geoprocessing Models*. ASME India Oil and Gas Pipeline Conference.
- 71) Khan, F., Yarveysy, R., & Abbassi, R. (2021). Risk-based pipeline integrity management: A road map for the resilient pipelines. *Journal of Pipeline Science and Engineering*, 1(1), 74-87.
- 72) Zarifi, M. H., Deif, S., & Daneshmand, M. (2017). Wireless passive RFID sensor for pipeline integrity monitoring. *Sensors and Actuators A: Physical*, 261, 24-29.
- 73) Al-Gabalawy, M. A., Mostafa, M. A., Hamza, A. S., & Hussien, S. A. (2020). Modelling of the KOH-Polarization cells for mitigating the induced AC voltage in the metallic pipelines. *Heliyon*, 6(3), e03417.
- 74) Babagayou, F., Zegnino, B., & Seghier, T. (2018). Study and Mitigation of AC Corrosion on Pipelines Nearby the HV Power Lines. *Revue des sciences et sciences de l'ingénieur*, 7(2), 10-17.
- 75) Hosein, S. M., Evans, B., & Morales, J. (2019). Effect of AC Mitigation System on Potential Surveys Correlation Potential Correction. *Corrosion*.
- 76) Dabkowski, J. (1996). A statistical approach to designing mitigation for induced AC voltages on pipelines. *Materials performance*, 35(8).

- 77) Du, Y., Jiang, Z., Lu, M., & Wang, L. (2013). Study on AC interference mitigation design methods for buried pipelines. *Corrosion*.
- 78) Djekidel, R., Bessedik, S. A., Spiteri, P., & Mahi, D. (2018). Passive mitigation for magnetic coupling between HV power line and aerial pipeline using PSO algorithms optimization. *Electric Power Systems Research*, 165, 18-26.
- 79) Dabkowski, J., Allen, R. F., & Perry, F. A. (2001). Mitigation design, installation and post commissioning measurements for a pipeline collocated with AC transmission lines. *Corrosion*.
- 80) Floyd, R. (2004). Testing and mitigation of AC corrosion on 8 line: a field study. *Corrosion*.
- 81) Frazier, M. (1984). Power line-induced ac potential on natural gas pipelines for complex rights-of-way configurations. Volume 4. Field verification of horizontal wire mitigation method. Final report (No. EPRI-EL-3106-Vol. 4). *Science Applications, Inc.*
- 82) Gummow, R. A., Segall, S. M., & Fieltch, W. (2010). Pipeline AC mitigation misconceptions. *Corrosion*.
- 83) Hilleary, J., & DeWitt, J. (2011). Continuous Verification Monitoring at AC Mitigation Stations. *Corrosion*.
- 84) Ismail, R., Hasibuan, A., Isa, M., Abdurrahman, F., & Islami, N. (2019). Mitigation of high voltage induction effect on ICCP system of gas pipelines: a field case study. *Telecommunication Computing Electronics and Control*, 17(6), 3226-3231.
- 85) Ibrahim, I., Meyer, M., Tribollet, B., Takenouti, H., Joiret, S., Fontaine, S., & Schoneich, H.G. (2008). *On the mechanism of AC assisted corrosion of buried pipelines and its CP mitigation*. International Pipeline Conference, 48586: 601-625.
- 86) Jiang, Z., Lu, M., Du, Y., & Dong, L. (2012). Study on factors influencing the mitigation of AC interference. *Corrosion*.
- 87) Kondamgire, R. V. (2015). *AC interference effect on NG pipeline and its mitigation techniques*. ASME India Oil and Gas Pipeline Conference.
- 88) Kolawole, F. O., Kolawole, S. K., Agunsoye, J. O., Adebisi, J. A., Bello, S. A., & Hassan, S. B. (2018). Mitigation of corrosion problems in API 5L steel pipeline-a review. *J. Mater. Environ. Sci*, 9(8), 2397-2410.
- 89) Kirkpatrick, E. L. (2003). Retrofit Induced AC Mitigation. *Corrosion*.
- 90) N., Kouloumbi, N., Batis, G. and Asteridis, P. (2003). *Study of the effect of AC-Interference and AC-Mitigation on the Cathodic Protection of a Gas Pipeline*. Conference: 6th CeoCor International Congress.

- 91) Kumleh, B. P., Varahram, M. H., & Kumleh, S. P. (2003). *Mitigation of AC Voltage Occurring in Pipeline Located Closed to Electric Transmission Lines with Design of Joint Right of Way*. IFAC Proceedings Volumes.
- 92) Li, Y., Dawalibi, F. P., Southey, R., & Ruan, W. (2005). Increasing the Cost Effectiveness of AC Interference Mitigation Designs with Integrated Electromagnetic Field Modelling. *Corrosion*.
- 93) Li, X., Liang, Y., Du, Y., Tang, D., Xing, L., & Che, Z. (2017). Case Study of AC Interference on an Urban Gas Pipeline: Field Test, AC Mitigation Design and Assessment. *Corrosion*.
- 94) Liang, Y., Du, Y., & Chen, L. (2021). Case Study of AC-Induced Corrosion on Buried Pipeline: Field Test and Mitigation Design. *Corrosion*.
- 95) Lindemuth, D., Hernandez, H., Creel, J., & Neeley, M. (2010). AC mitigation and cathodic protection for a long-regulated pipeline. *Corrosion*.
- 96) Lu, D., Liu, C., Qi, L. and Yuan, H. (2012). *Mitigation of electromagnetic influence on the buried metal pipeline near overhead AC transmission line*. In Sixth International Conference on Electromagnetic Field Problems and Applications.
- 97) Metwally, I. A., & Heidler, F. (2005). Mitigation of the produced voltages in AC overhead power-lines/pipelines parallelism during power frequency and lightning conditions. *European transactions on electrical power*, 15(4), 351-369.
- 98) Mostafa, M. A., Al-Gabalawy, M., Shaalan, E. M., & Hamza, A. S. (2022). Mitigation of the AC corrosion of the metallic pipelines using the hydroxide and solid-state polarization cells; A comparative study. *Electric Power Systems Research*, 202, 107585.
- 99) Mahmoudian, A., Niasati, M., & Karam, F. (2020). A comprehensive review: Evaluation of AC Induced Voltage on Buried Pipeline Near Overhead Transmission Lines and Mitigation Techniques Comparison. *International Journal of Electrical Engineering and Applied Sciences (IJEEAS)*, 3(1), 53-60.
- 100) Keener, B. (2012). *Hazardous liquids accident data with emphasis on crude oil and internal corrosion*. Washington, DC: Transportation Research Board.
- 101) da Cunha, S. B. (2016). A review of quantitative risk assessment of onshore pipelines. *Journal of Loss Prevention in the Process Industries*, 44, 282-298.
- 102) Du, Y., Liang, Y., Tang, D., & Xie, S. (2021). Discussion on AC Corrosion Rate Assessment and Mechanism for Cathodically Protected Pipelines. *Corrosion*, 77(6), 600-617.
- 103) Cheng, Y. F. (2015). Pipeline corrosion. *Corrosion Engineering, Science and Technology*, 50(3), 161-162.

- 104) Kirkpatrick, E. L. (1997). Induced AC voltages on pipelines may present a serious hazard. *Pipeline and Gas Journal*, 224(10).
- 105) Orazem, M. (2014). Underground pipeline corrosion, *Elsevier*.
- 106) Frazier, M., Thomas, P., Robertson, H., Dunlap, J., & Morgan, T. (1986). Transmission line, railroad and pipeline common corridor study. *IEEE transactions on power delivery*, 1(3), 294-300.
- 107) Leidheiser Jr, H. (1979). Electrical and electrochemical measurements as predictors of corrosion at the metal-organic coating interface. *Progress in Organic Coatings*, 7(1), 79-104.
- 108) Leidheiser, H., & Granata, R. D. (1988). Ion transport through protective polymeric coatings exposed to an aqueous phase. *IBM journal of research and development*, 32(5), 582-590.
- 109) Chen, X., Li, X. G., Du, C. W., & Cheng, Y. F. (2009). Effect of cathodic protection on corrosion of pipeline steel under disbanded coating. *Corrosion Science*, 51(9), 2242-2245.
- 110) Kuang, D., & Cheng, Y. F. (2015). AC corrosion at coating defect on pipelines. *Corrosion*, 71(3), 267-276.
- 111) Kuang, D., & Cheng, Y. F. (2015). Study of cathodic protection shielding under coating disbondment on pipelines. *Corrosion Science*, 99, 249-257.
- 112) Neal, D. (2000). Pipeline coating failure-not always what you think it is. *Corrosion*.
- 113) Cosham, A., P. Hopkins, and K. A. Macdonald, K. A. (2007). Best practice for the assessment of defects in pipelines–Corrosion. *Engineering Failure Analysis*, 14(7): 1245-1265.
- 114) Kamar, A.R., Abd-Elhady, A.M., Sabiha, N.A. and Izzularab, M.A. (2018). Location estimation of coating defects and mitigation of induced AC voltages along buried gas pipeline. *IET Science, Measurement & Technology*, 12(2): 209-217.
- 115) Xu, L.Y. and Cheng, Y.F. (2014). Experimental and numerical studies of effectiveness of cathodic protection at corrosion defects on pipelines. *Corrosion Science*, 78: 162-171.
- 116) Kulman, F. E. (1961). Effects of alternating currents in causing corrosion. *Corrosion*, 17(3), 34-35.
- 117) Al-Badi, A. H., & Metwally, I. A. (2006). Induced voltages on pipelines installed in corridors of AC power lines. *Electric Power Components and Systems*, 34(6), 671-679.
- 118) Metwally, I. A., Al-Mandhari, H. M., Gastli, A., & Nadir, Z. (2007). Factors affecting cathodic-protection interference. *Engineering Analysis with Boundary Elements*, 31(6), 485-493.

- 119) Moran, A., & Lillard, R. S. (2019). AC corrosion evaluation of cathodically protected pipeline steel. *Corrosion*, 75(2), 144-146.
- 120) Cui, G., Li, Z. L., Yang, C., & Wang, M. (2016). The influence of DC stray current on pipeline corrosion. *Petroleum Science*, 13(1), 135-145.
- 121) Song, H. S., Kho, Y. T., Kim, Y. G., Lee, S. M., & Park, Y. S. (2002). Competition of AC and DC current in AC corrosion under cathodic protection. *Corrosion*.
- 122) Kim, D. K., Ha, T. H., Ha, Y. C., Bae, J. H., Lee, H. G., Gopi, D., & Scantlebury, J. D. (2004). Alternating current induced corrosion. *Corrosion engineering, science and technology*, 39(2), 117-123.
- 123) Kim, H. S., Min, H. Y., Chase, J. G., & Kim, C. H. (2021). Analysis of Induced Voltage on Pipeline Located Close to Parallel Distribution System. *Energies*, 14(24), 8536.
- 124) Junker, A., Heinrich, C., Nielsen, L.V. and Møller, P. (2018). *Laboratory and field investigation of the effect of the chemical environment on AC corrosion*. NACE International Corrosion Conference Proceedings.
- 125) Ibrahim, I., Tribollet, B., Takenouti, H. and Meyer, M. (2015). AC-induced corrosion of underground steel pipelines. Faradaic rectification under cathodic protection: I. Theoretical approach with negligible electrolyte resistance. *Journal of the Brazilian Chemical Society*, 26: 196-208.
- 126) Lazzari, L., Goidanich, S., Marco Ormellese, M.O. and Pedferri, M. (2005). Influence of AC on corrosion kinetics for carbon steel, zinc and copper. *Corrosion*.
- 127) Li, H., Wan, H., Wang, S., Du, C., & Zhang, D. (2020). The influence of half-cycle rectified sinusoidal alternating current (AC) on corrosion of X80 pipeline steel in an acid bicarbonate solution. *Anti-Corrosion Methods and Materials*.
- 128) Cui, Z. Y., Wang, L. W., Liu, Z. Y., Du, C. W., & Li, X. G. (2015). Influence of alternating voltages on passivation and corrosion properties of X80 pipeline steel in high pH 0.5 mol L⁻¹ NaHCO₃+ 0.25 mol L⁻¹ Na₂CO₃ solution. *Corrosion Engineering, Science and Technology*, 50(3), 248-255.
- 129) Kioupis, N., Kouloumbi, N. and Greece, G. B. N. (2013). Simulation of a cathodically protected pipeline with capacitive ac-mitigation devices for the interpretation of the falsification of instant-off pipe-to-soil potential measurements, *Ceocor*.
- 130) Saied, M. M. (2004). The capacitive coupling between EHV lines and nearby pipelines. *IEEE Transactions on Power Delivery*, 19(3), 1225-1231.

- 131) Frazier, M., Thomas, P., Robertson, H., Dunlap, J., & Morgan, T. (1986). Transmission line, railroad and pipeline common corridor study. *IEEE transactions on power delivery*, 1(3), 294-300.
- 132) Abdel-Gawad, N. M., Shaalan, E. M., Darwish, M. M. F., & Basuny, M. A. (2019). *Influence of fault locations on the pipeline induced voltages near to power transmission lines*. 21st International Middle East Power Systems Conference.
- 133) AlShahri, A. S. (2021). *Assessment of Induced Potential on Metallic Pipeline Located Nearby to EHV AC OHTL*. IEEE 2nd International Conference on Signal, Control and Communication.
- 134) Al-Badi, A. H., & Al-Rizzo, H. M. (2005). Simulation of electromagnetic coupling on pipelines close to overhead transmission lines: A parametric study. *Journal of Communications Software and Systems*, 1(2), 116-125.
- 135) Hanson, H. R., & Smart, J. (2004). AC corrosion on a pipeline located in a HVAC utility corridor. *Corrosion*.
- 136) Markovic, D., Smith, V., Perera, S., & Elphich, S. (2004). *Modelling of the interaction between gas pipelines and power transmission lines in shared corridors*. Australasian Universities Power Engineering Conference, Brisbane.
- 137) Popoli, A., Sandrolini, L., & Cristofolini, A. (2020). Inductive coupling on metallic pipelines: Effects of a nonuniform soil resistivity along a pipeline-power line corridor. *Electric Power Systems Research*, 189, 106621.
- 138) Popoli, A., Cristofolini, A., Sandrolini, L., Abe, B.T., Jimoh, A.A., Popoli, A., Cristofolini, A. and Sandrolini, L. (2017). *The State of Art in the Field of AC Interference caused by Transmission Power-Lines affecting buried Metallic Pipelines*. Proceedings of the World Congress on Engineering and Computer Science
- 139) Shwehdi, M. H., Alaqil, M. A., & Mohamed, S. R. (2019). EMF Analysis for a 380kV Transmission OHL in the Vicinity of Buried Pipelines. *IEEE Access*, 8, 3710-3717.
- 140) Hosokawa, Y., Kajiyama, F., & Fukuoka, T. (2003). AC Interference Arising from AC Powered Rail Transit Systems on Cathodically Protected Buried Steel Pipelines and its Measures. *Zairyo-to-Kankyo*, 52(4), 218-222.
- 141) AKM Sydul Haque PhD, P. E., & Smith, M. (2019). *The importance of IAC studies during route selection*. NACE International Corrosion Conference Proceedings.
- 142) Ding, H., Zhang, Y., Gole, A. M., Woodford, D. A., Han, M. X., & Xiao, X. N. (2010). Analysis of coupling effects on overhead VSC-HVDC

- transmission lines from AC lines with shared right of way. *IEEE Transactions on Power Delivery*, 25(4), 2976-2986.
- 143) Racasan, A., Munteanu, C., Topa, V., Pop, I.T. and Merdan, E. (2011). *3D electromagnetic field model for numerical analysis of the electromagnetic interferences between overhead power lines and pipelines*. 11th International Conference on Electrical Power Quality and Utilisation:1-6.
 - 144) AKM Sydul Maque PhD, P. E., & Smith, M. (2019). *Design considerations when constrained by a fixed route*. NACE International Corrosion Conference Proceedings.
 - 145) Wagner, D. (2017). *Identification and Prioritization of Potential HVAC Interference Locations on a 6,000 Mile Crude and Product Transmission Pipeline System*. NACE International Corrosion Conference Proceedings.
 - 146) Christoforidis, G. C., Dokopoulos, P. S., & Psannis, K. E. (2001). *Induced voltages and currents on gas pipelines with imperfect coatings due to faults in a nearby transmission line*. In IEEE Porto Power Tech Proceedings.
 - 147) Nazemi, M., Dommerque, R. and Hennig, T. (2020). *An Analytical Approach for Evaluating the Effectiveness of Compensation Lines to Reduce the Inductive Coupling Interface between High Voltage Transmission Lines and Buried Pipelines*. International Symposium on Electromagnetic Compatibility.
 - 148) Jayasinghe, K., Marcollo, H., Potts, A.E., Dillon-Gibbons, C., Kurts, P. & Pezet, P. (2018). *Mitigation of Pipeline Free Span Fatigue due to Vortex Induced Vibration Using Longitudinally Grooved Suppression*. In International Conference on Offshore Mechanics and Arctic Engineering. *Corrosion*.
 - 149) Al-Badi, A., Ellithy, K. and Al-Alawi, S. (2007). *Prediction of voltages on mitigated pipelines paralleling electric transmission lines using an artificial neural network*. *The Journal of Corrosion Science and Engineering*, 10: 24-28.
 - 150) Hayden, J. L. R. (1907). *Alternating-current electrolysis*. Proceedings of the American Institute of Electrical Engineers, 26(2), 103-131.
 - 151) Williams, J. F. (1966). *Corrosion of metals under the influence of alternating current*. *Mater Prot Performance*, 5(2): 52.
 - 152) Pookote, S. R., & Chin, D. A. (1978). *Effect of alternating current on the underground corrosion of steels*. *Materials Performance (MP)*, 17(3).
 - 153) Galvele, J. R. (1976). *Transport processes and the mechanism of pitting of metals*. *Journal of the Electrochemical Society*, 123(4), 464.

- 154) Fernandes, S. Z., Mehendale, S. G., & Venkatachalam, S. (1980). Influence of frequency of alternating current on the electrochemical dissolution of mild steel and nickel. *Journal of applied electrochemistry*, 10(5), 649-654.
- 155) Gellings, P. J. (1962). The influence of alternating potential or current polarization on the corrosion rates of metals. *Electrochimica Acta*, 7(1), 19-24.
- 156) Bertocci, U. (1979). AC induced corrosion. The effect of an alternating voltage on electrodes under charge-transfer control. *Corrosion*, 35(5), 211-215.
- 157) Denison, I. A., & Darnielle, R. B. (1939). Observations on the behaviour of steel corroding under cathodic control in soils. *Transactions of the Electrochemical Society*, 76(1), 199.
- 158) Rossum, J. R. (1969). Prediction of pitting rates in ferrous metals from soil parameters. *Journal-American Water Works Association*, 61(6), 305-310.
- 159) Campbell, G. S. (1974). A simple method for determining unsaturated conductivity from moisture retention data. *Soil science*, 117(6), 311-314.
- 160) Chin, D. T., & Venkatesh, S. (1979). A study of alternating voltage modulation on the polarization of mild steel. *Journal of the Electrochemical Society*, 126(11), 1908-1913.
- 161) Dabkowski, J.I.R.I. and Taflove, A. (1978). Mutual design considerations for overhead ac transmission lines and gas transmission pipelines. Volume 1. Engineering analysis. *Final report (No. EPRI-EL-904 (Vol. 1))*. IIT Research Inst., Chicago, IL (USA).
- 162) Dabkowski, J. (1980). Calculations and Mitigation of Induced Voltages on Buried Pipelines. *Corrosion*.
- 163) Chin, D. T., & Sabde, G. M. (1999). Current distribution and electrochemical environment in a cathodically protected crevice. *Corrosion*, 55(03).
- 164) Chin, D. T., & Sachdev, P. (1983). Corrosion by alternating current: polarization of mild steel in neutral electrolytes. *Journal of the Electrochemical Society*, 130(8), 1714.
- 165) Taflove, A. and Genge, M., 1979. Mitigation of buried pipeline voltages due to 60 Hz AC inductive coupling Part I-Design of joint rights-of-way. *IEEE Transactions on Power Apparatus and Systems*, (5): 1806-1813.
- 166) Frazier, M. J., Dunlap, J., Klumb, F. R., & Nose, B. T. (1993). Mitigation of AC-Induced Pipeline Voltage. *Corrosion*.
- 167) Ruedisueli, R. L., Hager, H. E., & Sandwith, C. J. (1987). An application of a state-of-the-art corrosion measurement system to a study of the effects of alternating current on corrosion. *Corrosion*, 43(6), 331-338.

- 168) Ellis, R. (2001). *AC induced corrosion on onshore pipelines, a case history*. UKOPA publication, UKOPA-United Kingdom Onshore Pipeline Operators' Association.
- 169) Fieltsch, W., & Wakelin, R. (2017). The AC Close Interval Survey and Other Common AC Measurement Errors. *Corrosion*.
- 170) Wakelin, R. G., & Sheldon, C. (2004). Investigation and mitigation of AC corrosion on a 300 MM natural gas pipeline. *Corrosion*.
- 171) Pourbaix, A. (2000). Detection and assessment of alternating current corrosion. *Materials performance*, 39(3): 34-37.
- 172) Li, X., Liang, Y., Du, Y., Tang, D., Xing, L., & Che, Z. (2017). Case Study of AC Interference on an Urban Gas Pipeline: Field Test, AC Mitigation Design and Assessment. *Corrosion*.
- 173) Fu, A. Q., & Cheng, Y. F. (2009). Characterization of corrosion of X65 pipeline steel under disbonded coating by scanning Kelvin probe. *Corrosion Science*, 51(4), 914-920.
- 174) Yan, M., Sun, C., Xu, J., Wu, T., Yang, S., & Ke, W. (2015). Stress corrosion of pipeline steel under occluded coating disbondment in a red soil environment. *Corrosion Science*, 93, 27-38.
- 175) Southey, R., & Dawalibi, F. P. (1998). Computer Modelling of AC Interference Problems for the Most Cost Effective Solutions. *Corrosion*.
- 176) Satsios, K. J., Labridis, D. P., & Dokopoulos, P. S. (1998). Currents and voltages induced during earth faults in a system consisting of a transmission line and a parallel pipeline. *European transactions on electrical power*, 8(3), 193-199.
- 177) Collet, E., Delores, B., Gabillard, M., & Ragault, I. (2001). Corrosion due to AC influence of very high voltage power lines on polyethylene-coated steel pipelines: evaluation of risks—preventive measures. *Anti-Corrosion Methods and Materials*.
- 178) Ragault, I. (1998). AC corrosion induced by VHV electrical lines on polyethylene coated steel gas pipelines. *Corrosion*.
- 179) Buchler, M., Voute, C. H., Shoneich, H. G., Stalder, F. (2003). *Characteristics of potential measurements in the field of AC Corrosion*. International Conference Ceocorr.
- 180) Bosch, R. W., & Bogaerts, W. F. (1998). A theoretical study of AC-induced corrosion considering diffusion phenomena. *Corrosion Science*, 40(2-3), 323-336.
- 181) Kuang, D., & Cheng, Y. F. (2014). Understand the AC induced pitting corrosion on pipelines in both high pH and neutral pH carbonate/bicarbonate solutions. *Corrosion Science*, 85, 304-310.

- 182) Kuang, D., & Cheng, Y. F. (2017). Effects of alternating current interference on cathodic protection potential and its effectiveness for corrosion protection of pipelines. *Corrosion Engineering, Science and Technology*, 52(1), 22-28.
- 183) Moran, A. J. (2020). *An Assessment of the Susceptibility to Corrosion from Alternating Current of Cathodically Protected Steel Pipelines in Soils* (Doctoral dissertation, The University of Akron).
- 184) Wang, L., Cheng, L., Li, J., Zhu, Z., Bai, S., & Cui, Z. (2018). Combined effect of alternating current interference and cathodic protection on pitting corrosion and stress corrosion cracking behaviour of X70 pipeline steel in near-neutral pH environment. *Materials*, 11(4), 465.
- 185) Wang, Y., Wang, X., Zhu, Z., Zeng, L., & Yong, J. (2022). Effects of harmonic induction on metallic pipeline caused by overhead power lines. *International Journal of Electrical Power & Energy Systems*, 137, 107758.
- 186) Zhu, Q., Cao, A., Zaifend, W., Song, J., & Shengli, C. (2011). Stray current corrosion in buried pipeline. *Anti-Corrosion Methods and Materials*.
- 187) Zhu, M., Du, C., Li, X., Liu, Z., Li, H., & Zhang, D. (2014). Effect of AC on stress corrosion cracking behaviour and mechanism of X80 pipeline steel in carbonate/bicarbonate solution. *Corrosion Science*, 87, 224-232.
- 188) Lalvani, S. B., & Lin, X. A. (1994). A theoretical approach for predicting AC-induced corrosion. *Corrosion Science*, 36(6), 1039-1046.
- 189) Lalvani, S. B., & Zhang, G. (1995). The corrosion of carbon steel in a chloride environment due to periodic voltage modulation: Part I. *Corrosion Science*, 37(10), 1567-1582.
- 190) Pagano, M. A., & Lalvani, S. B. (1994). Corrosion of mild steel subjected to alternating voltages in seawater. *Corrosion Science*, 36(1), 127-140.
- 191) Qiu, W. W., Pagano, M., Zhang, G., & Lalvani, S. B. (1995). A periodic voltage modulation effect on the corrosion of Cu-Ni alloy. *Corrosion Science*, 37(1), 97-110.
- 192) Lalvani, S. B., & Lin, X. (1996). A revised model for predicting corrosion of materials induced by alternating voltages. *Corrosion Science*, 38(10), 1709-1719.
- 193) Lalvani, S. B., & Zhang, G. (1995). The corrosion of carbon steel in a chloride environment due to periodic voltage modulation: Part II. *Corrosion Science*, 37(10), 1583-1598.
- 194) Mateo, M. L., Otero, T. F., & Schiffrin, D. J. (1990). Mechanism of enhancement of the corrosion of steel by alternating currents and electrocatalytic properties of cycled steel surfaces. *Journal of applied electrochemistry*, 20(1), 26-31.

- 195) Brichau, F. R. A. N. K., & Deconinck, J. (1994). A numerical model for cathodic protection of buried pipes. *Corrosion*, 50(01).
- 196) Brichau, F. R. A. N. K., Deconinck, J., & Driesens, T. (1996). Modelling of underground cathodic protection stray currents. *Corrosion*, 52(06).
- 197) Aghay Kaboli, S. H., Al Hinai, A., Al-Badi, A. H., Charabi, Y., & Al Saifi, A. (2019). Prediction of metallic conductor voltage owing to electromagnetic coupling via a hybrid ANFIS and backtracking search algorithm. *Energies*, 12(19), 3651.
- 198) Li, Y., Dawalibi, F. P., & Ma, J. (2000). *Electromagnetic interference caused by a power system network on a neighboring pipeline*. Proceedings of the American Power Conference.
- 199) Li, Y., & Dawalibi, F. P. (2004). Effects of current unbalance and transmission line configuration on the interference levels induced on nearby pipelines. *Corrosion*.
- 200) Li, Z.L. and Yang, Y., 2011. Mechanism, influence factors and risk evaluation of metal alternating current corrosion. *CIESC J*, 62(7):1790-1799.
- 201) Munteanu, C., Mates, G., Purcar, M., Topa, V., Pop, I.T., Grindei, L. and Racasan, A. (2012). Electromagnetic field model for the numerical computation of voltages induced on buried pipelines by high voltage overhead power lines. *The European Physical Journal-Applied Physics*, 58(3).
- 202) Moraes, C. M., Martins-Britto, A. G., & Lopes, F. V. (2020). *Electromagnetic Interferences Between Power Lines and Pipelines Using EMTP Techniques*. Workshop on Communication Networks and Power Systems.
- 203) Munteanu, C., Topa, V., Mates, G., Purcar, M., Racasan, A. and Pop, I.T. (2012). *Analysis of the electromagnetic interferences between overhead power lines and buried pipelines*. International Symposium on Electromagnetic Compatibility-EMC.
- 204) Martins-Britto, A.G., Moraes, C.M. and Lopes, F.V. (2021). Transient electromagnetic interferences between a power line and a pipeline due to a lightning discharge: An EMTP-based approach. *Electric Power Systems Research*, 197: 107321.
- 205) Alexandru, M., Czumbil, L., Micu, D.D. and Papadopoulos, T. (2020). *Analysis of electromagnetic interferences between AC high voltage power lines and metallic pipeline using two different approaches based on circuit theory and electromagnetic field theory*. International Conference and Exposition on Electrical and Power Engineering (EPE).
- 206) Chrysostomou, D., Dimitriou, A., Kokkinos, N. D., & Charalambous, C. A. (2020). Short-term electromagnetic interference on a buried gas pipeline

- caused by critical fault events of a wind park: A realistic case study. *IEEE Transactions on Industry Applications*, 56(2), 1162-1170.
- 207) Christoforidis, G.C., Papadopoulos, T.A., Parisses, C. and Mantzaras, G.E. (2013). Photovoltaic power plants as a source of electromagnetic interference to metallic agricultural pipelines. *Procedia Technology*, 8: 192-199.
- 208) Dushimimana, G. (2019). *Influence of Electromagnetic Field Generated by HVAC Transmission Lines on Nearby Underground Metal Pipelines* (Doctoral dissertation, North China Electric Power University).
- 209) Ellithy, K.A. and Al-Badi, A.H. (2002). *Determining the electromagnetic interference effects on pipelines built in power transmission lines right-of-way*. International Conference on Electrical Engineering.
- 210) Elgayar, A., Abdul-Malek, Z., Othman, R., Elshami, I. F., Elbreki, A. M., Ibrahim, V. M., & Wooi, C. L. (2019). Power transmission lines electromagnetic pollution with consideration of soil resistivity. *Telecommunication Computing Electronics and Control*, 17(4), 1985-1991.
- 211) Shwehdi, M. H., & Johar, U. M. (2003). *Transmission line EMF interference with buried pipeline: Essential and cautions*. Proceedings of international conference on non-ionizing.
- 212) Shwehdi, M. H. (2004). *A practical study of electromagnetic interference (EMI) problem from Saudi Arabia*. Large Engineering Systems Conference on Power Engineering.
- 213) Xiaolin, W. A. N. G., Maocheng, Y. A. N., Yun, S. H. U., Cheng, S. U. N., & Wei, K. E. (2017). AC interference corrosion of pipeline steel beneath delaminated coating with holiday. *Journal of Chinese Society for Corrosion and protection*, 37(4), 341-346.
- 214) Wei, L. I., Yanxia, D. U., & Zitao JIANG, M. L. (2016). Research Progress on AC Interference of Electrified Railway on Buried Pipeline. *Journal of Chinese Society for Corrosion and protection*, 36(5), 381-388.
- 215) Qin, Q., Wei, B., Bai, Y., Fu, Q., Xu, J., Sun, C., & Wang, Z. (2021). Effect of alternating current frequency on corrosion behaviour of X80 pipeline steel in coastal saline soil. *Engineering Failure Analysis*, 120, 105065.
- 216) Wei, L. I., Yanxia, D. U., & Zitao JIANG, M. L. (2016). Research Progress on AC Interference of Electrified Railway on Buried Pipeline. *Journal of Chinese Society for Corrosion and protection*, 36(5), 381-388.
- 217) McCollum, B., & Ahlborn, G. H. (1916). The influence of frequency of alternating or infrequently reversed current on electrolytic corrosion. *Transactions of the American Institute of Electrical Engineers*, 35(1), 301-345.

- 218) Hosokawa, Y., & Kajiyama, F. (2005). External corrosion risk management for aged steel pipelines buried in high consequence areas. *Corrosion*.
- 219) Hosokawa, Y., Koga, R., & Ametani, A. (2008). Studies on the Prediction Method of an Induced AC Level on Buried Steel Pipelines Using Magnetic Field Sensors. *Corrosion Engineering*, 57(11), 647.
- 220) Kajiyama, F. and Nakamura, Y. (2010). Development of an advanced instrumentation for assessing the AC corrosion risk of buried pipelines. *Corrosion*.
- 221) Kajiyama, F. (2011). *Strategy for eliminating risks of corrosion and overprotection for buried modern pipelines*. International gas union research conference.
- 222) Hosokawa, Y., & Kajiyama, F. (2004). New Cp Maintenance Concept for Buried Steel Pipelines-Current Density-based CP Criteria, and On-line Surveillance System for CP Rectifiers. *Corrosion*.
- 223) Trichtchenko, L. (2004). Modelling electromagnetic induction in pipelines. *Corrosion*.
- 224) Ibrahim, I., Takenouti, H., Tribollet, B., Campaignolle, X., Fontaine, S., France, P. and Schoeneich, H.G. (2007). Harmonic analysis study of the AC corrosion of buried pipelines under cathodic protection. *Corrosion*.
- 225) Frazier, M. J., Dunlap, J., Klumb, F. R., & Nose, B. T. (1993). Mitigation of AC-Induced Pipeline Voltage. *Corrosion*.
- 226) Pikas, J. (2018). Looking Back and Understanding a Case History of Ac Corrosion. *Corrosion*.
- 227) Bae, J. H., Ha, Y. C., Ha, T. H., Lee, H. G., Kim, D. K., & Lee, J. D. (2004). *Data logger apparatus for stray current measurement of subway and power line*. 30th Annual Conference of IEEE Industrial Electronics Society.
- 228) Daratt, J. P. (1954). Insulating Joints in Long Pipelines—Electrical Effects on Underground Pipelines. *Gas*, 30(9), 124-126.
- 229) Dabkowski, J., Allen, R. F., & Perry, F. A. (2001). Mitigation design, installation and post commissioning measurements for a pipeline collocated with AC transmission lines. *Corrosion*.
- 230) Dawalibi, F. P., Ma, J., & Li, Y. (1999). Mechanisms of electromagnetic interference between electrical networks and neighboring metallic utilities. *Corrosion*.
- 231) Galimberti, C. E. (1964). Corrosion of Lead By Alternating Current. *Corrosion*, 20(5), 150t-157t.
- 232) Hoar T. P. (1967). The production and breakdown of the passivity of metals. *Corrosion Science*, 7: 341-365.

- 233) Lan, Zhigang, Xiutong Wang, Baorong Hou, Zaifeng Wang, Jiwen Song, and Shengli Chen. (2012). Simulation of sacrificial anode protection for steel platform using boundary element method. *Engineering Analysis with Boundary Elements*, 36(5). 903-906.
- 234) Fu, A., Yuan, J., Li, L., Long, Y., Song, C., Bai, Z., & Lin, K. (2016). Influence of Stray Alternating Current on Corrosion Behavior of Pipeline Steel in Near-Neutral pH Carbonate/Bicarbonate Solution. *International Journal of Simulation. Systems, Science & Technology*, 17(20).
- 235) Wan, H., Song, D., Liu, Z., Du, C., Zeng, Z., Yang, X., & Li, X. (2017). Effect of alternating current on stress corrosion cracking behaviour and mechanism of X80 pipeline steel in near-neutral solution. *Journal of Natural Gas Science and Engineering*, 38, 458-465.
- 236) Song, H. S., Kho, Y. T., Kim, Y. G., Lee, S. M., & Park, Y. S. (2002). Competition of AC and DC current in AC corrosion under cathodic protection. *Corrosion*.
- 237) Song, F. M., & Sridhar, N. J. C. S. (2008). Modelling pipeline crevice corrosion under a disbonded coating with or without cathodic protection under transient and steady state conditions. *Corrosion Science*, 50(1), 70-83.
- 238) Wan, H., Song, D., Liu, Z., Du, C., Zeng, Z., Wang, Z., & Li, X. (2017). Effect of negative half-wave alternating current on stress corrosion cracking behaviour and mechanism of X80 pipeline steel in near-neutral solution. *Construction and Building Materials*, 154, 580-589.
- 239) Kioupis, N. & Maroulis, K. (2006). *AC-corrosion detection on electrical resistance probes connected to a natural gas transmission pipeline*. Proc. 8th International Conference Pipeline Rehabilitation and Maintenance.
- 240) Bolzoni, Fabio Maria, Sara Goidanich, Luciano Lazzari, and Marco Ormellese, (2003). Laboratory test results of AC interference on polarised steel. *Corrosion*.
- 241) Brenna, Andrea, Silvia Beretta, Fabio Bolzoni, MariaPia Peddeferri, and Marco Ormellese (2017). Effects of AC-interference on chloride-induced corrosion of reinforced concrete. *Construction and Building Materials*, 137, 76-84.
- 242) Wang, C., Liang, X., & Freschi, F. (2019). *Factors affecting induced voltages on underground pipelines due to inductive coupling with nearby transmission lines*. IEEE Industry Applications Society Annual Meeting.
- 243) Wu, X., Zhang, H., & Karady, G. G. (2017). Transient analysis of inductive induced voltage between power line and nearby pipeline. *International Journal of Electrical Power & Energy Systems*, 84, 47-54.

- 244) Wrobel, L. C., & Miltiadou, P. (2004). Genetic algorithms for inverse cathodic protection problems. *Engineering analysis with boundary elements*, 28(3), 267-277.
- 245) Yunovich, M., & Thompson, N. G. (2004). *AC corrosion: mechanism and proposed model*. International Pipeline Conference.
- 246) Goidanich, S., Lazzari, L., & Ormellese, M. (2010). AC corrosion—Part 1: Effects on overpotentials of anodic and cathodic processes. *Corrosion Science*, 52(2), 491-497.
- 247) Markovic, D. (2005). Induced currents in gas pipelines due to nearby power lines. *Corrosion*.
- 248) Markovic, D., Smith, V., & Perera, S. (2005). Evaluation of gradient control wire and insulating joints as methods of mitigating induced voltages in gas pipelines. *Corrosion*.
- 249) Kim, Dae-Kyeong, Srinivasan Muralidharan, Tae-Hyun Ha, Jeong-Hyo Bae, Yoon-Cheol Ha, Hyun-Goo Lee, and J. D. Scantlebury. (2006). Electrochemical studies on the alternating current corrosion of mild steel under cathodic protection conditions in marine environments. *Electrochimica Acta*, 51(25), 5259-5267.
- 250) Purcar, M., Munteanu, C., Bortels, L. and Baeté, C. (2014). *AC interference assessment and impact on personnel safety*. International Conference and Exposition on Electrical and Power Engineering.
- 251) De Lacerda, Luiz Alkimin, José Maurílio Da Silva, and José Lázaris. Dual boundary element formulation for half-space cathodic protection analysis. (2007). *Engineering analysis with boundary elements*, 31(6), 559-567.
- 252) Machczyński, W. (2007). *AC-induced corrosion effects on cathodically protected pipelines*. International Corrosion Engineering Conference.
- 253) Bueno, V., Luciano Lazzari, Marco Ormellese, and P. Spinelli. (2008). *Interaction between alternating current and cathodic protection over nano-sized/structured surface metals*. Nanotech 2008-Nsti Nanotechnology Conference and Trade Show.
- 254) Meng, G. Z., Zhang, C., & Cheng, Y. F. (2008). Effects of corrosion product deposit on the subsequent cathodic and anodic reactions of X-70 steel in near-neutral pH solution. *Corrosion Science*, 50(11), 3116-3122.
- 255) Guo, Y., Tan, H., Wang, D., & Meng, T. (2017). Effects of alternating stray current on the corrosion behaviours of buried Q235 steel pipelines. *Anti-Corrosion Methods and Materials*.
- 256) Youwen, J., Wuxi, B., Kaizhi, C., Meng, L., & Jun, Z. (2018). Mitigating Pipeline AC Interference Using Numerical Modelling and Continuous AC Voltage Monitoring. *Corrosion*.

- 257) Guo, Yanbao, Tao Meng, Deguo Wang, Hai Tan, and Renyang He. (2017). Experimental research on the corrosion of X series pipeline steels under alternating current interference. *Engineering Failure Analysis*, 78, 87-98.
- 258) Guo, Y., Tan, H., Wang, D., & Meng, T. (2017). Effects of alternating stray current on the corrosion behaviours of buried Q235 steel pipelines. *Anti-Corrosion Methods and Materials*.
- 259) Xiao, H., & Lalvani, S. B. (2007). A linear model of alternating voltage-induced corrosion. *Journal of the Electrochemical Society*, 155(2), C69.
- 260) Zhang, R., Vairavanathan, P. R., & Lalvani, S. B. (2008). Perturbation method analysis of AC-induced corrosion. *Corrosion Science*, 50(6), 1664-1671.
- 261) Abootalebi, O., Kermanpur, A., Shishesaz, M. R., & Golozar, M. A. (2010). Optimizing the electrode position in sacrificial anode cathodic protection systems using boundary element method. *Corrosion Science*, 52(3), 678-687.
- 262) Chengyuan, L.I., Xu, C.H.E.N., Chuan, H.E., Hongjin, L.I. and Xin, P.A.N. (2021). Alternating Current Induced Corrosion of Buried Metal Pipeline: A Review. *Journal of Chinese Society for Corrosion and protection*, 41(2): 139-150.
- 263) Fu, A. Q., & Cheng, Y. F. (2010). Effects of alternating current on corrosion of a coated pipeline steel in a chloride-containing carbonate/bicarbonate solution. *Corrosion Science*, 52(2), 612-619.
- 264) Xu, L. Y., Su, X., Yin, Z. X., Tang, Y. H., & Cheng, Y. F. (2012). Development of a real-time AC/DC data acquisition technique for studies of AC corrosion of pipelines. *Corrosion Science*, 61, 215-223.
- 265) Xu, L., & Cheng, Y. F. (2013). A Real-Time AC/DC Measurement Technique for Investigation of AC Corrosion of Pipelines and Its Effect on the Cathodic Protection Effectiveness. *Corrosion*.
- 266) Xu, L. Y., and Y. F. Cheng. (2013). Development of a finite element model for simulation and prediction of mechano electrochemical effect of pipeline corrosion. *Corrosion Science*, 73, 150-160.
- 267) Xu, L. Y., Su, X., & Cheng, Y. F. (2013). Effect of alternating current on cathodic protection on pipelines. *Corrosion Science*, 66, 263-268.
- 268) Yi Liang, Yanxia Du, Le Chen, Nianpei Tian, Lei Zhang, Lijie Qiao. (2022). AC corrosion behaviour and the effect of stone-hard-soil on corrosion process in the earth alkaline rich environment. *Engineering Failure Analysis*, 135.
- 269) Zhu, Min, Cuiwei Du, Xiaogang Li, Zhiyong Liu, Shengrong Wang, Jiankuan Li, and Dawei Zhang (2014). Effect of AC density on stress corrosion cracking behaviour of X80 pipeline steel in high pH carbonate/bicarbonate solution. *Electrochimica Acta*, 117, 351-359.

- 270) Zhu, M., & Du, C. W. (2017). A new understanding on AC corrosion of pipeline steel in alkaline environment. *Journal of Materials Engineering and Performance*, 26(1), 221-228.
- 271) Zhu, M., Yang, J. L., Chen, Y. B., Yuan, Y. F., & Guo, S. Y. (2020). Effect of alternating current on passive film and corrosion behaviour of pipeline steel with different microstructures in carbonate/bicarbonate solution. *Journal of Materials Engineering and Performance*, 29(1), 423-433.
- 272) Zhang, H., Karady, G. G., & Hunt, J. (2011). *Effect of various parameters on the inductive induced voltage and current on pipelines*. IEEE Power and Energy Society General Meeting.
- 273) Ormellese, M., Lazzari, L., Goidanich, S., & Sesia, V. (2008). CP criteria assessment in the presence of AC interference. *Corrosion*.
- 274) Ormellese, M., Lazzari, L., Brenna, A., & Trombetta, A. (2010). Proposal of CP criterion in the presence of AC-interference. *Corrosion*.
- 275) Ormellese, M., Lazzari, L., & Brenna, A. (2010). AC-induced corrosion on passive metals. *Corrosion*.
- 276) Ormellese, M., Brenna, A., & Lazzari, L. (2015). AC corrosion of cathodically protected buried pipelines: Critical interference values and protection criteria. *Corrosion*.
- 277) Wei, B., Qin, Q., Bai, Y., Yu, C., Xu, J., Sun, C., & Ke, W. (2019). Short-period corrosion of X80 pipeline steel induced by AC current in acidic red soil. *Engineering Failure Analysis*, 105, 156-175.
- 278) Wen, C., Li, J., Wang, S., & Yang, Y. (2015). Experimental study on stray current corrosion of coated pipeline steel. *Journal of Natural Gas Science and Engineering*, 27, 1555-1561.
- 279) Wang, L. W., Wang, X. H., Cui, Z. Y., Liu, Z. Y., Du, C. W., & Li, X. G. (2014). Effect of alternating voltage on corrosion of X80 and X100 steels in a chloride containing solution—Investigated by AC voltammetry technique. *Corrosion Science*, 86, 213-222.
- 280) Simon, P. D., Lopez-Garrity, M., Wagner, D., & Garrity, K. (2017). Identification & Prioritisation of potential HVAC interference locations on a 6000-mile crude and product transmission pipeline system. *Corrosion*.
- 281) Thakur, A. K., Arya, A. K., & Sharma, P. (2022). Analysis of cathodically protected steel pipeline corrosion under the influence of alternating current. *Materials Today: Proceedings*, 50, 789-796.
- 282) Strandheim, Espen Oldeide. (2012). *AC induced corrosion of carbon steel in 3.5 wt% NaCl electrolyte*. Master's thesis, Institutt for materialteknologi.

- 283) Shabangu, Thabane Hendry, Purva Shrivastava, Bolanle Tolulope Abe, and Peter A. Olubambi (2018). Stability assessment of pipeline cathodic protection potentials under the influence of AC interference. *Progress In Electromagnetics Research*, 66, 19-28.
- 284) Shabangu, Thabane H., Purva Shrivastava, Bolanle Tolulope Abe, Kazeem B. Adedeji, and Peter A. Olubambi, (2017). *Influence of AC interference on the cathodic protection potentials of pipelines: Towards a comprehensive picture*. Africon.
- 285) Shaalan, E.M., Mostafa, M.A., Hamza, A.S. and Al-Gabalawy, M. (2022). Cathodic Protection Performance Improvement of Metallic Pipelines based on Different DC Compensation Methods. *Electric Power Systems Research*, 210: 108064.
- 286) Wang, C., Liang, X., & Radons, R. (2019). Minimum separation distance between transmission lines and underground pipelines for inductive interference mitigation. *IEEE Transactions on Power Delivery*, 35(3), 1299-1309.
- 287) Shabangu, T. H., Shrivastava, P., Abe, B. T., Adedeji, K. B., & Olubambi, P. A. (2017). *Influence of AC interference on the cathodic protection potentials of pipelines: Towards a comprehensive picture*. Africon.
- 288) Olesen, A. J. (2021). AC Corrosion of Cathodically Protected Pipelines—A Summary. *Corrosion*.
- 289) Zhang, H., Du, Y., Li, W., & Lu, M. (2017). Investigation on AC-induced corrosion behaviour and product film of X70 steel in aqueous environment with various ions. *Acta Metall Sin*, 53(8), 975-982.
- 290) Yanhu, M., Guoyu, L., Wei, M., Zhengmin, S., Zhiwei, Z., & Wang, F. (2020). Rapid permafrost thaw induced by heat loss from a buried warm-oil pipeline and a new mitigation measure combining seasonal air-cooled embankment and pipe insulation. *Energy*, 203, 117919.
- 291) Tang, D., Yang, X., Yong, J., & Xu, W. (2019). Active method for mitigation of induced voltage in integrated energy systems. *Applied Energy*, 235, 553-563.
- 292) Ouadah, M. H., Touhami, O., Ibtouen, R., & Bouzida, A. (2019). *Diagnoses and Mitigation of the Corrosion due to the Electromagnetic Coupling Between the HVPTL and Buried Pipeline*. Algerian Large Electrical Network Conference.
- 293) Ouadah, M., Touhami, O., Ibtouen, R., Benlamnouar, M.F. and Zergoug, M., 2017. Corrosive effects of the electromagnetic induction caused by the high voltage power lines on buried X70 steel pipelines. *International Journal of Electrical Power & Energy Systems*, 91: 34-41.

- 294) Ouadah, M. H., Touhami, O., Ibtouen, R., & Zergoug, M. (2017). Method for diagnosis of the effect of AC on the X70 pipeline due to an inductive coupling caused by HVPL. *IET Science, Measurement & Technology*, 11(6), 766-772.
- 295) Olesen, A. J., Nielsen, L. V., & Møller, P. (2019). Investigation of high pH corrosion under alternating current interference. *Corrosion*, 75(8), 982-989.
- 296) Garcia, Alfonso, Len J. Krissa, and Jerry DeWitt. (2017). Effect of Transmission Pipeline properties on alternated induced voltage. *Corrosion*.
- 297) Smart, I. I. I., Smart, J., & van Oostendorp, D. L. (1999). Induced AC creates problems for pipelines in utility corridors. *Pipe Line & Gas Industry*, 82(6), 25-32.
- 298) Qi, L., Yuan, H., Wu, Y., & Cui, X. (2013). Calculation of overvoltage on nearby underground metal pipeline due to the lightning strike on UHV AC transmission line tower. *Electric Power Systems Research*, 94, 54-63.
- 299) Dushimimana, G., Simiyu, P., Ndayishimiye, V., Niringiyimana, E. and Bikorimana, S (2019). *Induced electromagnetic field on underground metal pipelines running parallel to nearby high voltage AC power lines*. E3S Web of Conferences.
- 300) Dezhi, T. A. N. G., Yanxia, D. U., Minxu, L. U., Liang, D. O. N. G., & Zitao, J. I. A. N. G. (2013). Progress in the mutual effects between AC interference and the cathodic protection of buried pipelines. *Journal of Chinese Society for Corrosion and protection*, 33(5), 351-356.
- 301) Wang, X., Wang, Y., Sun, T., Yang, X., Yang, L. and Qi, Y. (2023). Study of transmission line AC interference with steel-buried pipelines under lightning strikes. *Electric Power Systems Research*, 218, 109226.
- 302) Gouda, O. E., & Al-Gabalawy, M. A. (2021). Screening of the high voltage overhead transmission lines impacts on the neighboring metallic gas pipelines based on the distributed KOH-PCs. *Egyptian Journal of Petroleum*, 30(2), 45-53.
- 303) Elgayar, A. I., & Abdul-Malek, Z. (2016). Induced voltages on a gas pipeline due to lightning strikes on nearby overhead transmission line. *International Journal of Electrical and Computer Engineering*, 6(2), 495.
- 304) Gouda, O. E., & Al-Gabalawy, M. A. (2021). Overhead transmission lines impact on neighboring buried metallic gas pipelines. *Electrical Engineering*, 103(6), 3119-3137.
- 305) George, J. (2018). Alternating current interference on cathodically protected pipeline from railway electrification systems. *Corrosion*.
- 306) Papavinasam, S. (2013). Corrosion control in the oil and gas industry. *Elsevier*.

- 307) Babaghayou, F., Zegnini, B., & Seghier, T. (2017). Effect of Alternating Current Interference Corrosion on Neighbouring Pipelines. *Electrotehnica, Electronica, Automatica*, 65(4).
- 308) Babaghayou, F., Zegnini, B. and Seghier, T. (2018). Experimental and Numerical Investigations of the effect of Alternating Current Interference Corrosion on Neighboring Pipelines. *Transactions on Electrical and Electronic Materials*, 19(2): 134-145.
- 309) Quang, K. V., Brindel, F., Laslaz, G, Buttoudin, R. (1983). Pitting Mechanism of Aluminium under Hydrochloric acid under Alternating current. *Electrochemical Society*, 130: 124-252.
- 310) Al Shahri, A. S., & Nair, N. K. C. (2015). *AC potential on pipelines nearby EHV power lines due to Low Frequency Induction*. Australasian Universities Power Engineering Conference.
- 311) Cotton, I., Kopsidas, K., & Zhang, Y. (2007). Comparison of transient and power frequency-induced voltages on a pipeline parallel to an overhead transmission line. *IEEE transactions on power delivery*, 22(3), 1706-1714.
- 312) Min, Z.H.U., Cuiwei, D.U., Xiaogang, L.I., Zhiyong, L.I.U. and Liye, W.A.N.G. (2014). Effects of alternating current (AC) frequency on corrosion behaviour of X80 pipeline steel in a simulated acid soil solution. *Journal of Chinese Society for Corrosion and protection*, 34(3): 225-230.
- 313) Thompson, I., & Saithala, J. R. (2013). Review of pipe line coating systems from an operators perspective. *Corrosion*.
- 314) Taflove, A. and Dabkowski, J. (1979). Prediction method for buried pipeline voltages due to 60 Hz AC inductive coupling part I-analysis. *IEEE Transactions on Power Apparatus and Systems*, (3): 780-787.
- 315) Stet, D., Micu, D.D., Czumbil, L. and Manea, B. (2014). *Case studies on electromagnetic interference between HVPL and buried pipelines*. International Conference and Exposition on Electrical and Power Engineering.
- 316) Finneran, S., & Krebs, B. (2014). Advances in HVAC transmission industry and its effects on pipeline induced AC corrosion. *Corrosion*.
- 317) Jiang, Z., Lu, M., Tang, D., Du, Y., & Dong, L. (2013). Case Study of AC Interference on 20 km Buried Pipeline: Field Test and Mitigation Design. *Corrosion*.
- 318) Zhu, M., Yuan, Y., Yin, S., & Guo, S. (2018). Corrosion Behavior of X65 and X80 Pipeline Steels under AC Interference Condition in High pH Solution. *Int. J. Electrochem. Sci*, 13, 10669-10678.

- 319) Cui, Y., Shen, T., & Ding, Q. (2019). Study on the Influence of AC Stray Current on X80 Steel under Stripped Coating by Electrochemical Method. *International Journal of Corrosion*.
- 320) Xu, J., Bai, Y., Wu, T., Yan, M., Yu, C., & Sun, C. (2019). Effect of elastic stress and alternating current on corrosion of X80 pipeline steel in simulated soil solution. *Engineering Failure Analysis*, 100, 192-205.
- 321) Wang, H., Du, C., Liu, Z., Wang, L., & Ding, D. (2017). Effect of alternating current on the cathodic protection and interface structure of X80 steel. *Materials*, 10(8), 851.
- 322) Wang, Xinhua, Xinghua Tang, Liwei Wang, Cui Wang, and Zhenzhen Guo. (2014). Corrosion behaviour of X80 pipeline steel under coupling effect of stress and stray current. *Int J Electrochem Sci*, 9 (8), 4574-4588.
- 323) Guo, Y. B., Liu, C., Wang, D. G., & Liu, S. H. (2015). Effects of alternating current interference on corrosion of X60 pipeline steel. *Petroleum Science*, 12(2), 316-324.
- 324) Kajiyama, F. (2011). *Strategy for eliminating risks of corrosion and overprotection for buried modern pipelines*. International gas union research conference.
- 325) Hosokawa, Y., Kajiyama, F., & Nakamura, Y. (2002). New CP criteria for elimination of the risks of AC corrosion and overprotection on cathodically protected pipelines. *Corrosion*.
- 326) Tang, D., Lu, M., Du, Y., Gao, J., & Wu, G. (2015). Electrochemical studies on the performance of zinc used for alternating current mitigation. *Corrosion*, 71(6), 795-806.
- 327) Bortels, L., Dorochenko, A., Van den Bossche, B., Weyns, G., and Deconinck, J. (2007). Three-dimensional boundary element method and finite element method simulations applied to stray current interference problems. A unique coupling mechanism that takes the best of both methods. *Corrosion*, 63(6): 561-576.
- 328) Osborne, T. C., & Summerland, A. J. (2003). Computer Modelling to Predict the Magnitude of AC Voltages on Buried and Well-Coated Pipelines. *Corrosion*.
- 329) Racasan, A., Munteanu, C., Topa, V., Purcar, M. and Grindei, L. (2011). Computation of the potential induced on the fluid transport pipelines by overhead high voltage lines. *Environmental engineering & management Journal*, 10(4).
- 330) Dan D. M., Levente Z., Andrei C., Denisa S. (2012). Evaluation of Induced AC Voltage in underground metallic Pipeline. *Int. J. Computation & Mathematics in Electrical & Electronic Engineering*, 31: 1133-1143.

- 331) Micu, D. D., Czumbil, L., Christoforidis, G. C., Ceclan, A., & Şteţ, D. (2012). Evaluation of induced AC voltages in underground metallic pipeline. *COMPEL-The international journal for computation and mathematics in electrical and electronic engineering*.
- 332) Charalambous, C.A., Demetriou, A., Lazari, A.L. and Nikolaidis, A. (2018). Effects of electromagnetic interference on underground pipelines caused by the operation of high voltage AC traction systems: The impact of harmonics. *IEEE Transactions on Power Delivery*, 33(6): 2664-2672.
- 333) Christoforidis, G. C., Labridis, D. P., & Dokopoulos, P. S. (2005). Inductive interference on pipelines buried in multilayer soil due to magnetic fields from nearby faulted power lines. *IEEE Transactions on Electromagnetic Compatibility*, 47(2), 254-262.
- 334) Coelho, L., Sotelo, G., & Lima, A. C. (2022). Detailed versus simplified representation of a pipeline for assessment of inductive and conductive couplings to an overhead transmission line during steady-state and fault conditions. *International Journal of Electrical Power & Energy Systems*, 142, 108350.
- 335) Djekidel, R., Bentouati, B., Javaid, M.S., Bouchekara, H.R.E.H., Bayoumi, A.S. and El-Sehiemy, R.A. (2021). Mitigating the effects of magnetic coupling between HV transmission line and metallic pipeline using slime mould algorithm. *Journal of Magnetism and Magnetic Materials*, 529, 167865.
- 336) Martins-Britto, A.G., Rondineau, S.R.M.J. and Lopes, F.V. (2019). *Power Line Transient Interferences on a Nearby Pipeline Due to a Lightning Discharge*. Proceedings of the International Conference on Power Systems Transients (IPST 2019), Perpignan, France, 16-20.
- 337) Popoli, A. P., Cristofolini, A. C., & Sandrolini, L. S. (2018). Numerical Modelling of Interference from AC Power Lines on Buried Metallic Pipelines in Presence of Mitigation Wires. *Corrosion*.
- 338) Popoli, A., Sandrolini, L. and Cristofolini, A (2019). *Finite element analysis of mitigation measures for ac interference on buried pipelines*. International Conference on Environment and Electrical Engineering and 2019 IEEE Industrial and Commercial Power Systems Europe.
- 339) Popoli, A., Sandrolini, L., & Cristofolini, A. (2021). Comparison of screening configurations for the mitigation of voltages and currents induced on pipelines by HVAC power lines. *Energies*, 14(13), 3855.
- 340) Popoli, A., Cristofolini, A. and Sandrolini, L. (2021). A numerical model for the calculation of electromagnetic interference from power lines on

- nonparallel underground pipelines. *Mathematics and Computers in Simulation*, 183, 221-233.
- 341) Haynes, G. J., Manning, T., Baeté, C., & Barton, L. (2019). Variances in Pipeline AC Interference Computational Modelling. *Corrosion*.
- 342) Cole, I. S., & Marney, D. J. C. S. (2012). The science of pipe corrosion: A review of the literature on the corrosion of ferrous metals in soils. *Corrosion Science*, 56, 5-16.
- 343) Chen, X., Wu, Z., Chen, W., Kang, R., He, X., & Miao, Y. (2019). Selection of key indicators for reputation loss in oil and gas pipeline failure event. *Engineering failure analysis*, 99, 69-84.
- 344) Chapman, C. (2021). AC Power Interactions with Pipelines—The Usual Suspect, The Ugly Geology, and, Finally, The Weird: Faulty AC Power Conditioning Capacitors Interacting with Well-Coated Pipeline. *Corrosion*.
- 345) Hosokawa, Y., Kajiyama, F., & Nakamura, Y. (2004). New cathodic protection criteria based on direct and alternating current densities measured using coupons and their application to modern steel pipelines. *Corrosion*, 60(3), 304-312.
- 346) Ibrahim, I., Meyer, M., Takenouti, H. and Tribollet, B. (2016). AC Induced Corrosion of Underground Steel Pipelines. Faradaic Rectification under Cathodic Protection: II. Theoretical Approach with Electrolyte Resistance and Double Layer Capacitance for Bi-Tafelian Corrosion Mechanism. *Journal of the Brazilian Chemical Society*, 27(3), 605-615.
- 347) Jiang, Z., Du, Y., Lu, M., Zhang, Y., Tang, D., & Dong, L. (2014). New findings on the factors accelerating AC corrosion of buried pipeline. *Corrosion Science*, 81, 1-10.
- 348) Lillard, R.S., Cong, H. and Wagner, D. (2020). Understanding and Mitigating the Threat of AC Induced Corrosion on Buried Pipelines. *Corrosion*.
- 349) Liu, G. C., Sun, W., Wang, L., & Li, Y. (2013). Modelling cathodic shielding of sacrificial anode cathodic protection systems in seawater. *Materials and Corrosion*, 64(6), 472-477.
- 350) Lucca, G. (2021). AC interference from faulty power cables on buried pipelines: A two-step approach. *IET Science, Measurement & Technology*, 15(1), 25-34.
- 351) Martins-Britto, A.G., Moraes, C.M. and Lopes, F.V. (2021). Inductive interferences between a 500 kV power line and a pipeline with a complex approximation layout and multi-layered soil. *Electric Power Systems Research*, 196: 107265.

- 352) Chen, M., Liu, S., Zhu, J., Xie, C., Tian, H., & Li, J. (2018). Effects and characteristics of AC interference on parallel underground pipelines caused by an AC electrified railway. *Energies*, 11(9), 2255.
- 353) Wang, X., Wang, Y., Sun, T., Yang, X., Yang, L. and Qi, Y. (2023). Study of the coupling interference of high-voltage transmission lines on adjacent buried steel pipelines based on CDEGS. *Electric Power Systems Research*, 217, 109125.
- 354) Platt, K. (2021). An Operator's Experience with AC-Induced Corrosion. *Corrosion*.
- 355) Wu, W., Pan, Y., Liu, Z., Du, C., & Li, X. (2018). Electrochemical and stress corrosion mechanism of submarine pipeline in simulated seawater in presence of different alternating current densities. *Materials*, 11(7), 1074.
- 356) Olesen, A. J., Dideriksen, K., Nielsen, L. V., & Møller, P. (2019). Corrosion Rate Measurement and Oxide Investigation of AC Corrosion at Varying AC/DC Current Densities. *Corrosion*, 75(9), 1026-1033.
- 357) Sheldon, C., Teall, C., & Tidwell, S. (2020). Cathodic protection of a long-distance, multi-material water pipeline. *Pipelines*.
- 358) Fieltsch, W., & Silva, D. (2016). AC interference risk ranking: case study. *Corrosion*.
- 359) Zhang, S., Yan, J., Zheng, L., Sun, J., & Gao, J. (2023). Effect of alternating current and Cl-ions on corrosion behaviour of X70 steel in NaCl solution. *International Journal of Electrochemical Science*, 18(2), 49-58.
- 360) Yazdi, M., Khan, F. and Abbassi, R. (2023). A dynamic model for microbiologically influenced corrosion (MIC) integrity risk management of subsea pipelines. *Ocean Engineering*, 269, 113515.

APPENDIX A

LIST OF PUBLICATIONS

1. Thakur, A. K., Arya, A. K., & Sharma, P. (2020). The science of alternating current-induced corrosion: A literature review on pipeline corrosion induced due to high-voltage alternating current transmission pipelines. *Corrosion Reviews*, 38(6), 463-472.
2. Thakur, A. K., Arya, A. K., & Sharma, P. (2021). Corrosion of pipe steels under alternating currents. *Int J Electrochem Sci*, 16(11).
3. Thakur, A. K., Arya, A. K., & Sharma, P. (2022). Analysis of cathodically protected steel pipeline corrosion under the influence of alternating current. *Materials Today: Proceedings*, 50, 789-796.
4. Thakur, A. K., Arya, A. K., & Sharma, P. (2022). Prediction and mitigation of AC interference on the pipeline system. *Corrosion Reviews*, 40(2), 149-157.

Unlicensed Published by De Gruyter October 26, 2020

The science of alternating current-induced corrosion: a review of literature on pipeline corrosion induced due to high-voltage alternating current transmission pipelines

Ajit Kumar Thakur , Adarsh Kumar Arya and Pushpa Sharma


From the journal [Corrosion Reviews](#)

<https://doi.org/10.1515/corrrev-2020-0044>

Cite this



6

 You currently have no access to view or download this content. Please log in with your institutional or personal account if you should have access to this content through either of these. Showing a limited preview of this publication:

Abstract

The state of art in alternating current (AC)-induced corrosion in pipelines is reviewed. Growing pipeline networks and their co-location with high-voltage (HV) transmission networks have brought into focus the issue of induced AC corrosion on the pipeline networks. Induced AC corrosion may quickly and severely affect the integrity of pipeline networks, especially considering that a number of such pipelines are transporting huge quantities of hazardous fluids. Any breach in pipeline integrity due to AC corrosion may result in disastrous consequences. In the last 30 years, it

has been established that the induced AC corrosion can affect the buried pipeline integrity severely. During operations, the resistive as well as inductive coupling with transmission lines pose a significant risk of pipeline corrosion. The literature is reviewed to put together various issues and factors responsible for AC-induced corrosion in pipelines. The various publications on induced AC corrosion are reviewed to identify characteristics of AC-induced corrosion and major factors that determine the severity and impact of AC-induced corrosion. The areas have been identified wherein scope exists for additional studies on AC corrosion.

Keywords: [AC corrosion](#); [AC corrosion dimensions](#); [AC interference](#); [pipeline](#)

Corresponding author: Ajit Kumar Thakur, Indian Oil Corporation Ltd., A-1, Sec-1, Noida 201301, India; and Department of Chemical Engineering, School of Engineering, UPES, Bidholi, Dehradun, India, E-mail: ajitsumedha@gmail.com

Author contribution: All the authors have accepted responsibility for the entire content of this submitted manuscript and approved submission.

Research funding: None declared.

Conflict of interest statement: The authors declare no conflicts of interest regarding this article.

References

Adedeji, K.B., Ponnle, A.A., Abe, B.T., Jomih, A.A., Abu-Mahfouz, A.M., and Hamam, Y.A. (2018). A review of the effect of AC/DC interference on corrosion and cathodic protection potentials of pipelines. *Rev. Electr. Eng.*

13: 495–508, <https://doi.org/10.15866/iree.v13i6.15766>.

[Search in Google Scholar](#)

Arya, A.K. and Honwad, S. (2016). Modeling, simulation, and optimization of a high-pressure cross-country natural gas pipeline: application of an ant colony optimization technique. *Pipeline Sys. Eng. Pract.* 7: 1–8, [https://doi.org/10.1061/\(ASCE\)PS.1949-1204.0000206](https://doi.org/10.1061/(ASCE)PS.1949-1204.0000206).

[Search in Google Scholar](#)

Arya, A.K. and Honwad, S. (2018). Optimal operation of a multi source multi delivery natural gas transmission pipeline network. *Chem. Prod. Process Model.* 13: 1–17, <https://doi.org/10.1515/cppm-2017-0046>.

[Search in Google Scholar](#)

Bertocci, U. (1979). AC Induced corrosion – the effect of an alternating voltage on electrodes under charge transfer control. In: *NACE International Conference Corrosion*. Atlanta, Georgia.

[10.5006/0010-9312-35.5.211](https://doi.org/10.5006/0010-9312-35.5.211)

[Search in Google Scholar](#)

Bosch, R.W. and Bogaerts, W.F. (1997). A theoretical study of AC-induced corrosion considering diffusion phenomenon. *Corros. Sci.* 40: 323–336.

[10.1016/S0010-938X\(97\)00139-X](https://doi.org/10.1016/S0010-938X(97)00139-X)

[Search in Google Scholar](#)

Brenna, A. (2011). *A proposal of AC corrosion mechanism of carbon steel in cathodic protection condition*, Ph. D. thesis. Milano: Politecnico de.

[Search in Google Scholar](#)

Brenna, A., Lazzari, L., Pedferri, M., and Ormellese, M. (2014). Cathodic protection condition in the presence of ac interference. *La Metallurgia Italiana* 6: 29–34.

[Search in Google Scholar](#)

Buchler, M., Voute, C. H., Shoneich, H. G., and Stalder, F. (2003). Characteristics of potential measurements in the field of AC Corrosion. In: *International Conference Ceocorr*. Sicily, Brussels.

[Search in Google Scholar](#)

Chin, D.T. and Sachdev, P. (1983). Corrosion by Alternating Current : polarisation of mild steel in neutral electrolytes. *Electrochem. Sci. Technol.* 130: 1714–1718 <https://doi.org/10.1149/1.2120068>.

[Search in Google Scholar](#)

Chin, D.T. and Sachdev, P. (1979). A study of Alternating Voltage modulation on the polarisation of mild steel. *Electrochem. Sci. Technol.* 126: 1908–1913, <https://doi.org/10.1149/1.2128825>.

[Search in Google Scholar](#)

Cole, I.S. and Marney, D. (2012). The science of pipe corrosion : a review of the literature on the corrosion of ferrous metals in soils. *Corros. Sci.* 56: 5–16 <https://doi.org/10.1016/j.corosci.2011.12.001>.

[Search in Google Scholar](#)

Collet, E., Delores, B., Gabillard, M., and Ragault, I. (2001). Reviewed articles Corrosion due to AC influence of very high voltage power lines on steel pipelines : evaluation of risks - preventive measures. *Anti Corros. Method Mater.* 48: 221–226, <https://doi.org/10.1108/eum0000000005629>.

[Search in Google Scholar](#)

Cosham, A., Hopkins, P., and Macdonald, K.A. (2007). Best practice for the assessment of defects in pipelines. *Eng. Fail. Anal.* 14: 1245–1265, <https://doi.org/10.1016/j.engfailanal.2007.05.001>.

[Search in Google Scholar](#)

Kuangg, D. (2016). *Pipeline corrosion and coating failure under*

alternating current interference, Ph. D. thesis: University of Calgary.

[Search in Google Scholar](#)

Dan, D.M., Levente, Z., Andrei, C., and Denisa, S. (2012). Evaluation of induced AC voltage in underground metallic pipeline. *Comput & Math Electr Electron Eng* 31: 1133–1143.

[10.1108/03321641211227375](https://doi.org/10.1108/03321641211227375)

[Search in Google Scholar](#)

Denison, I. A. and Darneielle, R. B. (1939). Observations on the behaviour of steel corroding under cathodic control in soils. In: *ESCDL 76th General Meeting*. New York City, New York.

[Search in Google Scholar](#)

Finneran, S. and Krebs, B. (2014). Advances in HVAC transmission industry and its effects on pipeline induced AC corrosion. In: *NACE International Conference Corrosion*. San Antonio, Texas.

[Search in Google Scholar](#)

Floyd, R. (2004). Testing & mitigation of AC corrosion on 8” line: a field study. In: *NACE International Conference Corrosion*. New Orleans, Louisiana.

[Search in Google Scholar](#)

Frazier, N., Robertson, H., Dunlap, J., Thomas, P., and Morgan, T. (1986 In this issue). Transmission line, Railroad and Pipeline Corridor study. *IEEE Transaction on Power Delivery* 3: 294–300.

[10.1109/TPWRD.1986.4308006](https://doi.org/10.1109/TPWRD.1986.4308006)

[Search in Google Scholar](#)

Fu, A.Q. and Cheng, Y.F. (2012). Effect of alternating current on corrosion and effectiveness of cathodic protection of pipelines. *Can. Metall. Quart.* 51: 81–90, <https://doi.org/10.1179/1879139511y.0000000021>.

[Search in Google Scholar](#)

Garcia, A., Krissa, L.J., and Dewitt, J. (2017). Effect of Transmission Pipeline properties on alternated induced voltage. In: *NACE International Conference Corrosion*. New Orleans, Louisiana.

[Search in Google Scholar](#)

Gellings, P.J. (1962). The influence of alternating potential or current polarisation on the corrosion rates of metals. *Electrochim. Acta* 7: 19–24, [https://doi.org/10.1016/0013-4686\(62\)80013-9](https://doi.org/10.1016/0013-4686(62)80013-9).

[Search in Google Scholar](#)

Goidanich, S., Lazzari, L., and Ormellese, M. (2010a). AC corrosion. Part 1: effects of overpotentials of anodic and cathodic processes. *Petrol. Sci.* 12: 316–324.

[10.1016/j.corsci.2009.10.005](https://doi.org/10.1016/j.corsci.2009.10.005)

[Search in Google Scholar](#)

Goidanich, S., Lazzari, L., and Ormellese, M. (2010b). AC corrosion. Part 2: parameters influencing corrosion rate. *Corros. Sci.* 52: 916–922, <https://doi.org/10.1016/j.corsci.2010.05.015>

[Search in Google Scholar](#)

Guo, Y., Liu, C., Wang, D., and Liu, S. (2015). Effect of alternating current interference on corrosion of X60 pipeline steel. *Petrol. Sci.* 12: 316–324, <https://doi.org/10.1007/s12182-015-0022-0>.

[Search in Google Scholar](#)

Hanson, H.R., and Smart, J. (2004). AC Corrosion in a pipeline located in a HVAC corridor. In: *NACE International Conference Corrosion*. New Orleans, Louisiana.

[Search in Google Scholar](#)

Jiang, Z., Du, Y., Lu, M., Zhang, Y., Tang, D., and Dong, L. (2013). New

findings on the factors accelerating AC corrosion of buried pipeline.

Corros. Sci. 52: 491–497.

[10.1016/j.corosci.2013.09.005](https://doi.org/10.1016/j.corosci.2013.09.005)

[Search in Google Scholar](#)

Kim, D.K., Hai, T.H., Bae, J.H., Lee, G.H., Gopi, D., and Scantlebury, J. D. (2004). Alternating current induced corrosion. *Corros. Eng. Sci. Technol.* 39: 117–123, <https://doi.org/10.1179/147842204225016930>.

[Search in Google Scholar](#)

Kuang, D. and Cheng, Y.F. (2016). Effects of alternating current interference on cathodic protection potential and its effectiveness for corrosion protection of pipelines. *Corros. Eng. Sci. Technol.* 52: 22–28, <https://doi.org/10.1179/1478422016YFS00001>.

[Search in Google Scholar](#)

Lalvani, S.B. and Lin, X.A. (1994). A Theoretical approach for predicting AC-induced corrosion. *Corros. Sci.* 36: 1039–1046, [https://doi.org/10.1016/0010-938x\(94\)90202-x](https://doi.org/10.1016/0010-938x(94)90202-x).

[Search in Google Scholar](#)

Li, Y., Dawalibi, F.P., and Ma, J. (2000). Electromagnetic Interference caused by a power system network on a neighbouring pipeline. In: *Proceedings of the 62nd Annual Meeting of the American power Conference*. Chicago, Illinois.

[Search in Google Scholar](#)

Li, Y., Xu, C., Zhang, R., Liu, Q., Wang, X., and Chen, Y. (2017). Effects of stray AC interference on corrosion behaviour of X70 pipeline steel in a simulated marine soil solution. *Electrochem. Sci.* 12: 1829–1845, <https://doi.org/10.1039/C6EE02433A>.

[Search in Google Scholar](#)

Mccollum, B. and Ahlborn, G.H. (1916). The influence of frequency of

alternating or infrequently reversed current on electrolytic corrosion. In: *Presented at 319th meeting of American Institute of Electrical Engineers*, pp. 301–327, <https://doi.org/10.1109/t-aiee.1916.4765386>.

[Search in Google Scholar](#)

Metwally, I.A., Al-Mandhari, H.M., Gastli, A., and Nadir, Z. (2007). Factors affecting cathodic-protection interference. *Eng. Anal. Bound. Elem.* 31: 485–493, <https://doi.org/10.1016/j.enganabound.2006.11.003>.

[Search in Google Scholar](#)

Milano, P., Chimica, D., Chimica, I., and Natta, G. (2003). Laboratory test results of AC interference on polarised steel. In: *NACE International Conference Corrosion*. San Diego, California.

[Search in Google Scholar](#)

NACE International Publication 35110 (2010). *AC corrosion state-of-the-art: corrosion rate, mechanism and mitigation requirements*, Available at: www.nace.org.

[Search in Google Scholar](#)

Ormellese, M., Lazzari, L., and Brenna, A. (2010). AC induced corrosion on passive metals. In: *NACE International Conference Corrosion*. San Antonio, Texas.

[Search in Google Scholar](#)

Pagano, M.A., and Lalvani, S.B. (1994). Corrosion of mild steel subjected to alternating voltages in sea water. *Corros. Sci.* 36: 127–140, [https://doi.org/10.1016/0010-938x\(94\)90114-7](https://doi.org/10.1016/0010-938x(94)90114-7).

[Search in Google Scholar](#)

Pookote, S.R., and Chin, D.T. (1978). Effect of alternating current on

underground corrosion of steels. *Mater. Perform.* 17: 9–15.

[Search in Google Scholar](#)

Qi, L., Yuan, H., Wu, Y., and Cui, X. (2013). Calculation of overvoltage on nearby underground metal pipeline due to the lightning strike on UHV AC transmission line tower. *Elec. Power Syst. Res.* 94: 54–63, <https://doi.org/10.1016/j.epsr.2012.12.010>.

[Search in Google Scholar](#)

Quang, K.V., Brindel, F., Laslaz, G, and Buttoudin, R. (1983). Pitting mechanism of aluminium under hydrochloric acid under alternating current. *Electrochem. Soc.* 130: 124–252.

[Search in Google Scholar](#)

Rossum, J. R (1969). Prediction of pitting rates in ferrous metals from soil parameters. *Am. Water Work Assoc.* 61: 305–310, <https://doi.org/10.1002/j.1551-8833.1969.tb03761.x>.

[Search in Google Scholar](#)

Saied, M.M. (2004). The capacitive coupling between EHV lines and nearby pipelines. *IEEE Trans. Power Deliv.* 19: 1225–1231, <https://doi.org/10.1109/tpw.2004.1345888>.

[Search in Google Scholar](#)

Sankara, P. (2013). *Corrosion control in the oil and gas industry*. London: Elsevier.

[Search in Google Scholar](#)

Smart, J.S., Smart, J., and Oostendorp, V. D.L. (1999). Induced AC creates problems for pipelines in utility corridors. *Corros. Technol.* 82: 1–12.

[Search in Google Scholar](#)

Song, H., Kim, Y., Lee, S., Kho, Y., and Park, Y. (2002). Competition of AC and DC current in AC corrosion under cathodic protection. In: *NACE International Conference Corrosion*. Denver, Colorado.

International Conference Corrosion. Denver, Colorado.

[Search in Google Scholar](#)

Taflove, A. and Dabkowski, J. (1979). Prediction method for buried pipeline voltages due to 60 Hz Inductive coupling. *IEEE Trans. Power App. Syst.* 98: 780–787, <https://doi.org/10.1109/tpas.1979.319290>.

[Search in Google Scholar](#)

Tang, D.Z., Du, Y.X., Lu, M.X., Jiang, Z.T., Dong, L., and Wang, J.J. (2013). Effect of AC current on corrosion behaviour of cathodically protected Q235 steel. *Mater. Corros.* 66: 278–285, <https://doi.org/10.1002/maco.201307234>.

[Search in Google Scholar](#)

Thompson, I. and Saithala, J.R. (2016). Review of pipeline coating systems from an operator's perspective. *Corros. Eng. Sci. Technol.* 51: 118–135, <https://doi.org/10.1002/cet.201600011>.

[Search in Google Scholar](#)

Wakelin, R.G., Gummow, R.A., and Segall, S.M. (1998). AC Corrosion – case histories, test procedures & mitigation. In: *NACE International Conference Corrosion*. Houston, Texas.

[Search in Google Scholar](#)

Wang, H, Cuiwei, Du, Zhiyong, Liu, Wang, Lunao, and Ding, De (2017). Effect of Alternating current on the Cathodic Protection & Interface Structure of X80 Steel. *Materials* 10: 1–21.

[10.3390/ma10080851](https://doi.org/10.3390/ma10080851)

[Search in Google Scholar](#)

[PubMed](#)

[PubMed Central](#)

Williams, J.F. (1966). Corrosion of metals under the influence of alternating current. *Mater. Prot. Perform.* 5: 52–54.

[Search in Google Scholar](#)

Xu, L.Y., Su, X., and Cheng, Y.F. (2013). Effect of alternating current on cathodic protection of pipelines. *Corros. Sci.* 66: 263–268, <https://doi.org/10.1016/j.corsci.2013.05.010>.
[Search in Google Scholar](#)

Yunovich, M. and Thomson, N. G. (2004). AC Corrosion : mechanism and proposed model. In: *ASME International Pipeline Conference*. Calgary, Alberta, <https://doi.org/10.1115/ipc2004-0574>.
[Search in Google Scholar](#)

Zhu, M. and Du, C.W. (2017). A new understanding on AC corrosion of pipeline steel in alkaline environment. *Mater. Eng. Perform.* 26: 221–228, <https://doi.org/10.1007/s11665-016-2416-6>.
[Search in Google Scholar](#)

Zhu, Q., Cao, A., Zaifend, W., Song, F., and Shengli, C. (2011). Stray Current corrosion in buried pipeline. *Anti-corros. Method Mater.* 58: 234–237, <https://doi.org/10.1007/s11665-011-0234-7>.
[Search in Google Scholar](#)

Received: 2020-05-09

Accepted: 2020-08-27

Published Online: 2020-10-26

Published in Print: 2020-11-18

© 2020 Walter de Gruyter GmbH, Berlin/Boston



Access through your institution

— or —

PDF 30,00 €

[Buy Article](#)

From the journal



Corrosion Reviews

Volume 38 Issue 6

Journal and Issue



This issue All issues

Articles in the same Issue

Frontmatter

[The science of alternating current-induced corrosion: a review of literature on pipeline corrosion induced due to high-voltage alternating current transmission pipelines](#)

[Stress corrosion cracking and precipitation strengthening mechanism in TWIP steels: progress and prospects](#)

[Effect of pH on the degradation kinetics of a Mg-0.8Ca alloy for orthopedic implants](#)

[Enhancement of barrier and anti-corrosive performance of zinc-rich epoxy coatings using nano-](#)

[Nonlinear trending of corrosion of high nickel alloys in extended marine and atmospheric exposures](#)

[Effect of small amounts of chalcogen alloying elements on the oxidation resistance of copper](#)

Subjects

Architecture and Design

Arts

Asian and Pacific Studies
Business and Economics
Chemistry
Classical and Ancient Near Eastern Studies
Computer Sciences
Cultural Studies
Engineering
General Interest
Geosciences
History
Industrial Chemistry
Islamic and Middle Eastern Studies
Jewish Studies
Law
Library and Information Science, Book Studies
Life Sciences
Linguistics and Semiotics
Literary Studies
Materials Sciences
Mathematics
Medicine
Music
Pharmacy
Philosophy
Physics
Social Sciences
Sports and Recreation
Theology and Religion

Services

For journal authors

For book authors

For librarians

Rights & Permissions

Publications

Publication types

Open Access

About

Contact

Career

About De Gruyter

Partnerships

Press

New website FAQs



Winner of the OpenAthens
Best Publisher UX Award 2022

[Help/FAQ](#)

[Privacy policy](#)

[Cookie Policy](#)

[Accessibility](#)

[Terms & Conditions](#)

[Legal Notice](#)

© Walter de Gruyter GmbH 2022



Corrosion of pipe steels under alternating currents

Ajit Kumar Thakur¹, Adarsh Kumar Arya^{1*}, Pushpa Sharma²

¹ Department of Chemical Engineering, UPES, Dehradun, INDIA

² Department of Petroleum and Energy Studies, UPES, Dehradun, INDIA

*E-mail: akarya@ddn.upes.ac.in

Received: 5 August 2021 / Accepted: 30 September 2021 / Published: 10 November 2021

The present paper aims to analyze and compare AC interference on pipeline steel grades in soil simulating solutions. DC current density (J_{DC}) and protection potential (PP) are measured to determine AC interference. The study presents the corrosion resistance of several grades of steel. The paper describes experimental studies involving potentiostatic and galvanostatic measurements. The experimental arrangement has been set up for AC and DC couplings to measure DC current density (J_{DC}), protection potential (PP), and AC current density (J_{AC}). The paper presents findings on the AC corrosion behavior of different pipeline steels based on variation in AC current density. The study shows the comparative performance of varying pipe steels. Experimental studies have been conducted on pipe steel in soil simulating solutions under controlled conditions using a specially designed experimental setup. Special care in the experimental setup prevents errors in measurements due to IR drop. The behavior in the field may be influenced by other factors also. The results may be helpful to the pipeline industry in making informed selections of pipe steels subjected to AC interference.

Keywords: Cathodic protection, Pipeline corrosion, X grade pipeline, Protection Potential, Alternating current density

1. INTRODUCTION

The need for transporting massive amounts of oil and gas has prompted an interest in developing an efficient method of transportation. Pipelines have been considered a sound way to transport oil and gas since the beginning of modern civilization. [1-2; 38-39]. The pipelines ensure the safe and environmentally responsible transportation of hazardous substances. Experts recommend monitoring the pipeline networks continuously to ensure their integrity. The health of the pipeline system affects people's health and the environment. An accident involving a pipeline would have disastrous consequences for the ecosystem.

Corrosion monitoring and protection is a critical component of pipeline integrity maintenance. Corrosion [3] related failures are the leading cause of pipeline integrity failures (65 percent in oil and 34

percent in gas service). The application of an appropriate coating to the steel pipeline serves as the principal corrosion prevention system. A secondary corrosion prevention system typically contains a cathodic protection (CP) system to ensure the pipeline system's long-term integrity. The CP system improves the effectiveness of primary coatings in preventing corrosion [4, 5]. Cathodic protection systems provide direct current circulation between the cathode (pipeline) and anode (ground) via electrolytic processes, including oxidation and reduction, preventing pipe corrosion in the soil. CP system polarizes and forms a passive film on the surface of pipe steel. The commonly accepted conditions [6, 7] for pipeline corrosion prevention include polarising pipelines in the negative direction by more than (-) 850 mV. Polarisation of more than (-) 850 mV is insufficient to defend against corrosion.

Voltage transfer may occur from power lines to pipelines when they are situated close to each other. Such voltages can increase exponentially in the presence of a power line fault condition. When a pipeline is adjacent to a high-voltage transmission line, it may carry voltage. Other than the high risk of injury to service workers, it may also reduce the steel quality in the pipe. Alternating current interference renders the parameters listed here inadequate for corrosion protection.

Experiments [8] on carbon steel pipe samples exposed to varying AC current densities under CP demonstrated that the (-) 850 mV threshold is inadequate. With induced AC, the negative polarization potential of (-) 850 mV may not be sufficient to defend against corrosion [9]. The application of the coating on a prolonged basis is harmful if it is above (-) 1200 mV in the negative direction.

For pipeline networks, cathodic protection techniques consider the pipe-to-soil potential (PSP), the ratio of AC/DC current density, and the AC current density (J_{AC}). AC corrosion factors such as the AC/DC current density ratio, the AC current density (J_{AC}), and the alternating voltage (AV) are crucial. Corrosion is possible at AC current densities of between 30 and 100 A/m², and damage from AC corrosion is likely at densities of more than 100 A/m² [24]. Conventional CP procedures are unsuccessful at protecting pipelines from corrosion caused by AC interference [10-12]. A touch potential of 15 V or greater caused by induced AC [13] poses a severe concern for worker safety.

Electromagnetic induction causes interference with pipelines due to closeness to transmission lines, creating resistive, capacitive, and inductive coupling [14, 15]. Corrosion problems linked with AC interference have developed dramatically in proximity to buried pipelines [16, 17]. Different experiments and studies have attempted to quantify and assess AC interference [18-23].

In the presence of AC, avoid excessive protection should since it results in severe corrosion [8]. A 2020 study [25] shows that the effect of variable AC corrosion with increasing interference time is similar to that of steady-state AC corrosion. Increased AC/DC current density suggests an increased risk of decay. A reduced current density ratio implies a lower probability of corrosion but does not assure corrosion prevention. AC moderation techniques, such as pipeline grounding, are required to reduce the amplitude of coating stress voltage and hence the likelihood of AC corrosion [26, 27]. Algorithms for assessing induced current and voltage are increasingly being explored [27]. The passive film is mainly unaffected by lower AC densities, resulting in minor polarization potential changes. Pipeline steel is subjected to extensive localized corrosion attack at higher AC densities, whereas uniform corrosion occurs at lower AC densities [28, 29]. Corrosion is also affected by the characteristics of coating pores [30]. The shift in potential for polarisation caused by AC is due to the increased corrosion current caused

by passive film breakdown [5]. AC forms a thin passive film and increases the chances of it collapsing [31–33].

The applied coating on the metal surface and soil resistivity influence the demand of CP current density (Table 1) to achieve cathodic protection of bare metal surface within a short span.

The present study aims to ascertain how alternating current interference affects the steel in underground pipelines. Additional mitigating procedures are necessary to mitigate the effect of AC interference on pipelines. AC corrosion tests under similar circumstances are essential to evaluate the relative performance of different pipe steel types. This study bridges the gap by evaluating and assessing the corrosion resistance of many other pipeline plates of steel. Investigations include performing potentiostatic and galvanostatic tests in soil mimicking solutions to assess pipe steels' resistance to AC corrosion.

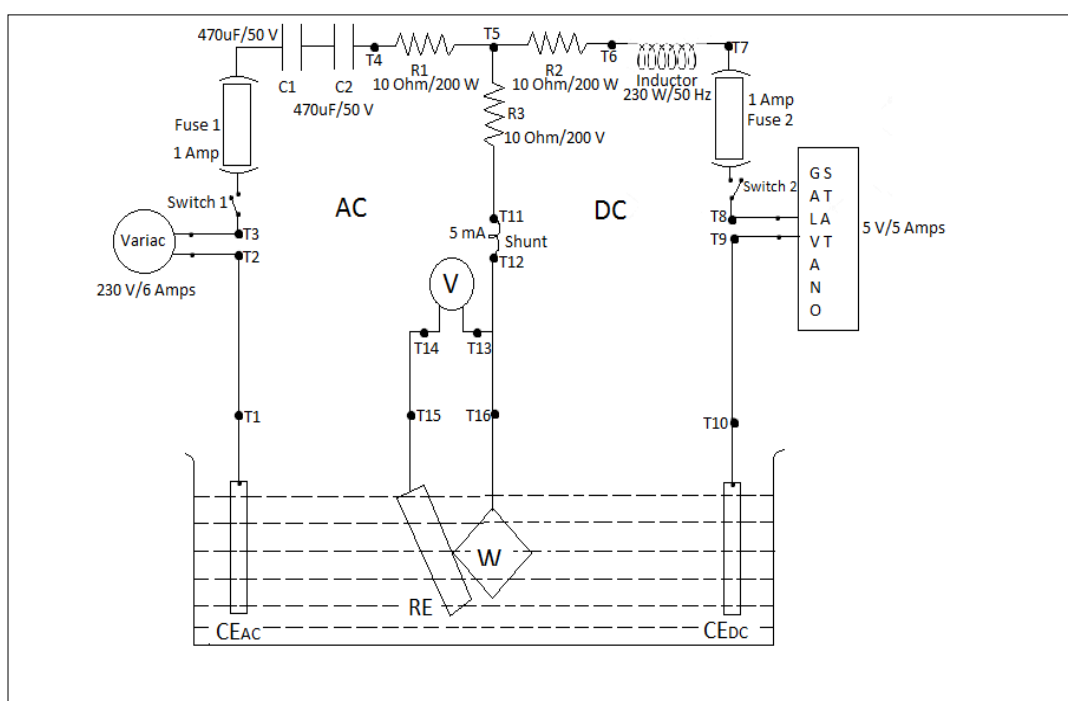


Figure 1. Experimental Circuitry with AC and DC circuits coupled using Capacitors and Inductors. Shunts enable the measurement of DC current density (J_{DC}) and AC current density (J_{AC}). The potential of the specimen is measured using the Cu-CuSO₄ Reference electrode.

2. EXPERIMENTAL

The present section details the methodology used to ascertain the impact of alternating current on pipe steel.

2.1. AC and DC Electrical Circuits

The specially designed suitably coupled AC and DC circuits (Figure 1) prevented interference between the two circuits. The coupling leveraged the fundamental features of inductors and capacitors.

In a direct current circuit, an inductor inhibits the circulation of alternating current, while a capacitor blocks the circulation of direct current in an alternating current circuit [34]. Through the pipe specimen, the variable autotransformer provided the necessary alternating current. A galvanostat injected the required DC into the pipe specimen. While AC flow provided the required current for AC interference, DC flow maintained the pipe specimen's corrosion-free state. Shunts measured current flow, and counter electrodes completed necessary circuits. The specimen's potential was determined using the Cu-CuSo₄ reference electrode.

2.2. Preparation of Steel Specimen and Solution for Simulating Soil

The wide use of pipe grades (API 5L) in oil and gas pipelines is due to their appropriateness for sour service, prolonged duration of service, and opposition to crack spreading. API 5L steels are resistant to corrosion and have a high tensile and yield strength. These pipes' composition and microstructure can vary significantly depending on the carbon, manganese, sulfur, and phosphorous concentration limits. Steel specimen of the respective grade measured 6 mm in thickness and 100 mm in diameter.

Each specimen, after washing, is inserted into a cylindrical PVC tube with an internal diameter of 10 mm with a length of 40 mm. Welding a copper cable (6 mm²) to one of the specimen's faces provides an electrical connection. A bare surface is available on the opposite facet of the sample. The PVC tube is then filled with epoxy to provide an airtight seal and prevent moisture ingress. The simulating soil solution contained 200 mg chlorides and 500 mg sulfates per liter of clean water at room temperature. The test solution used purified water and analytic-grade reagents. Tests performed involving novel solution each time and the previous solution discarded after the test. The soil solution is a popular NS4 solution that is close to neutral.

2.3. Measuring the protection potential (PP) with different AC current density (J_{AC})

Each specimen is dipped in a solution simulating soil to measure the protection potential at different AC densities. It is essential to examine the alternating current's effect on the protection potential by varying the DC with a galvanostat. Different alternating current densities in steps interfere with the DC current densities and monitor the protection potential. After applying a DC current density (J_{DC}) of 0.01 A/m² for 24 hours without AC, measured the protection potential. Subsequently, administered 30 minutes of alternating current density (J_{AC}) in steps of 10, 30, 50, 100, and 200 A/m². For each stage, measured the sample potential at an interval of 5 minutes.

2.4. Measurement of DC current density (J_{DC})

Alternating current is deployed in potentiostatic tests to measure DC current density (J_{DC}) variation by changing the protection potential in steps at various AC current densities. Conducted the potentiostatic test to determine the effect of alternating current on the DC current density (J_{DC}) by applying a protection potential of (-) 0.850 V for 24 hours without AC. Subsequently, administered 30 minutes of alternating current density (J_{AC}) in 10, 30, 50, 100, and 200 A/m² steps. For each stage, measured the DC current density (J_{DC}) every 5 minutes.

Table 1. Soil resistivity, Coating Type, and Design current density

S. No.	Soil resistivity (Ωm)	Design current density ($\mu\text{A}/\text{m}^2$)		
		Fusion Bonded Epoxy coating	Three Layer Polyethylene coating	Coal tar Enamel coating
1	<10	70	50	150
2	10-100	50	25	125
3	>100	25	15	75

3. RESULTS AND DISCUSSION

3.1. AC Interference Analysis

3.1.1. X46 Steel

The DC current density (J_{DC}) increased from $0.020 \text{ A}/\text{m}^2$ to $0.054 \text{ A}/\text{m}^2$, at a potential of (-) 850 mV, with a variation in AC current density (J_{AC}) in steps from $10 \text{ A}/\text{m}^2$ to $200 \text{ A}/\text{m}^2$, indicating an increase (Figure 2) of 179% in DC current density (J_{DC}).

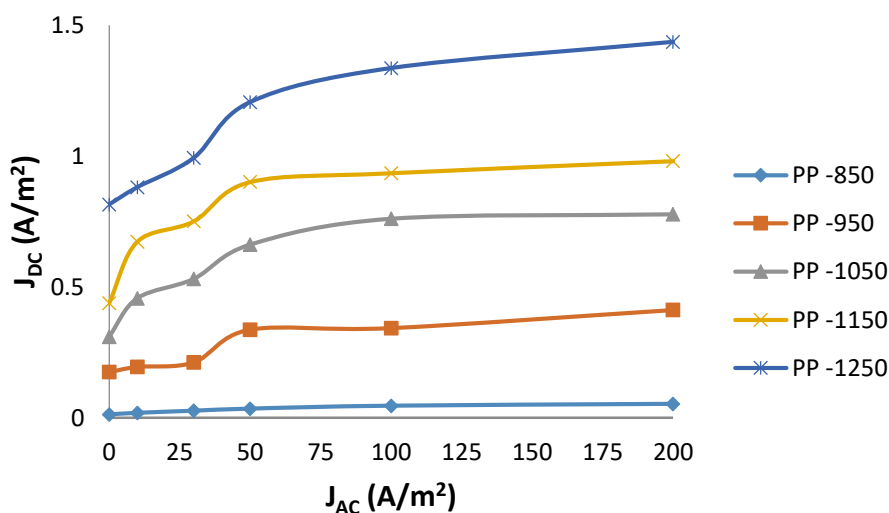


Figure 2. DC current density (J_{DC}) variation with AC current density (J_{AC}) at protection potentials ((-) 850, (-) 950, (-)1050, (-) 1150, and (-) 1250 mV) for X46 steel in soil simulating solution.

With a potential of (-) 950 mV, the protection density increased from $0.196 \text{ A}/\text{m}^2$ to $0.413 \text{ A}/\text{m}^2$ with variation in AC current density (J_{AC}) from $10 \text{ A}/\text{m}^2$ to $200 \text{ A}/\text{m}^2$, indicating an increase of 111% in DC current density (J_{DC}). The percentage change in DC current density (J_{DC}) is low for protection potential variation from (-) 1050 mV to (-) 1250 mV. The results align with earlier investigations [35] which concluded that the CP protection levels influence AC interference, and DC current density (J_{DC})

higher than 5 A/m² may result in AC corrosion. For X46 steel, specimens remain protected at a DC current density (J_{DC}) of 0.1 A/m² without AC interference at a protection potential of (-) 1069 mV.

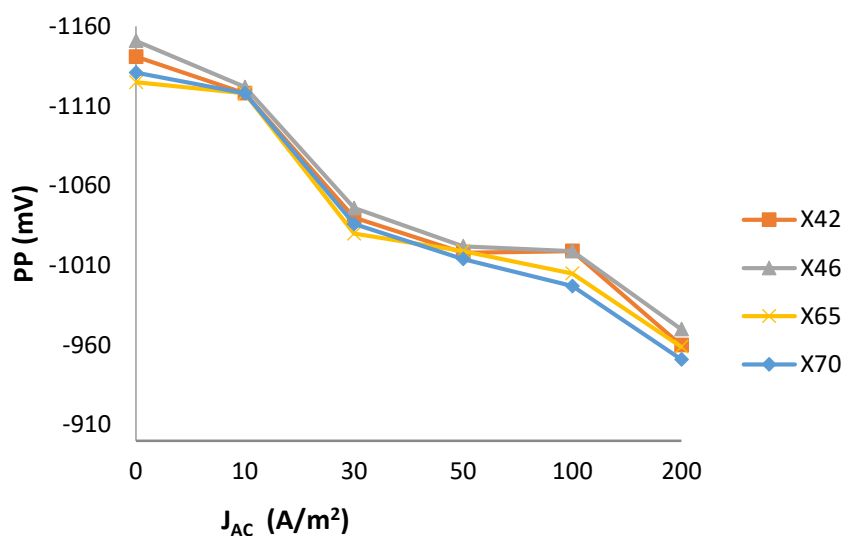


Figure 3. Protection potential (PP) with AC current density (J_{AC}) at a DC current density (J_{DC}) of 0.3 A/m² for X42, X46, X65, and X70 steels in soil simulating solution.

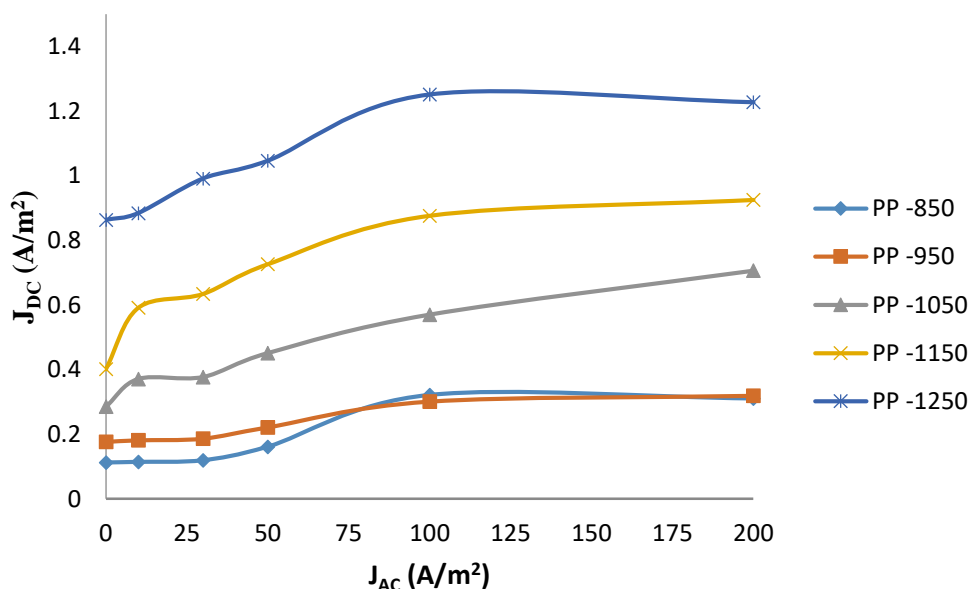


Figure 4. DC current density (J_{DC}) variation with AC current density (J_{AC}) at protection potentials ((-) 850, (-) 950, (-)1050, (-) 1150, and (-) 1250 mV) for X42 steel in soil simulating solution.

The increase in DC current density (J_{DC}) from 0.1 A/m² to 10 A/m² made the potential more hostile, improving corrosion prevention. At a DC current density (J_{DC}) of 0.3 A/m², the protection potential of X46 steel samples varied from (-) 1151 mV to (-) 970 mV, with an AC current density (J_{AC}) change from 0 A/m² to 200 A/m² (Figure 3). Published research [36] has observed the AC corrosion rate at an AC current density of 10 A/m² to be twice the corrosion rate without AC. It is evident here that the

AC corrosion rate at a particular AC current density may vary depending upon the level of steel polarization. The observation is in close agreement with a published study that concluded that the direction of potential shifting depends upon applied CP [33]. At the protection potential (PP) of (-) 1150 mV, the DC current density (J_{DC}) is almost constant for X46 pipe, with variation in AC current density (J_{AC}) from 50 A/m² to 100 A/m², indicating better corrosion performance of X46 steel to other steels. High pitting corrosion due to specific AC current density is likely at higher DC current densities in line with available literature [11, 12].

3.1.2. X42, X65, and X70 Steel

For X42 steel, the DC current density (J_{DC}) increased (Figure 4) from 0.114 A/m² to 0.31 A/m² at a protection potential of (-) 850 mV, with a change in AC current density (J_{AC}) in steps from 10 A/m² to 200 A/m², indicating a 176% jump in DC current density (J_{DC}).

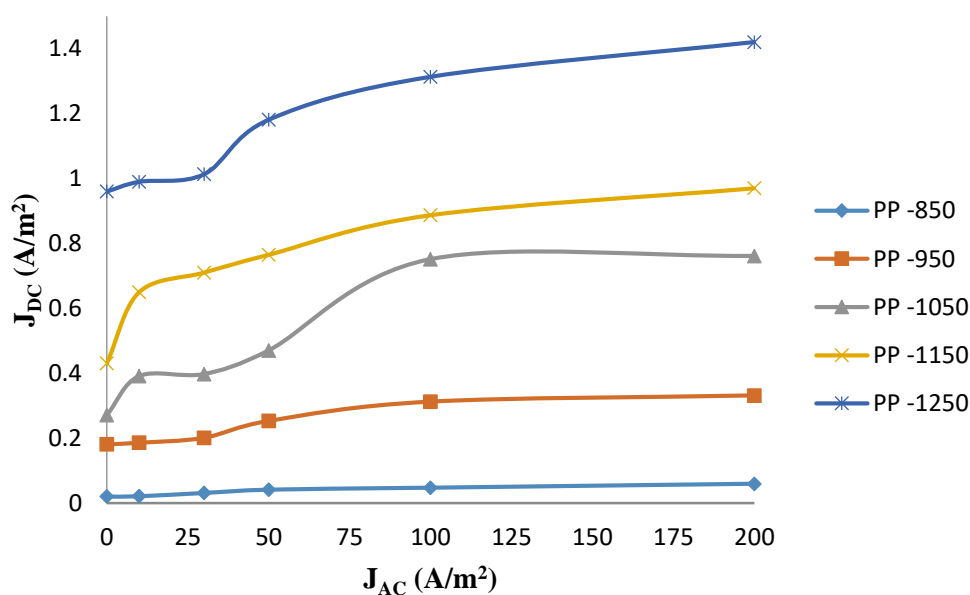


Figure 5. DC current density (J_{DC}) variation with AC current density (J_{AC}) at protection potentials ((-) 850, (-) 950, (-)1050, (-) 1150, and (-) 1250 mV) for X65 steel in soil simulating solution.

With a potential of (-) 850 mV for X65 steel, the DC current density (J_{DC}) changed from 0.022 A/m² to 0.060 A/m² with a variation in AC current density (J_{AC}) from 10 A/m² to 200 A/m², indicating a 181% jump (Figure 5) in DC current density (J_{DC}). For X70, observed a 167% jump in DC current density (J_{DC}). The different percentage increases are attributable to the pipe steel's unique microcrystalline structure. The Gibbs free energy change, resulting in a negative shift in corrosion potential, explains the tendency of enhanced corrosion [29] and agrees well with the results obtained.

For X65 steel, samples are protected at a DC current density (J_{DC}) of 0.1 A/m² with a potential of (-) 1061 mV with no AC. The protection potential shifted negatively with the increase in DC current density (J_{DC}), indicating better corrosion prevention. With a DC current density (J_{DC}) beyond 0.5 A/m²,

the protection potential exceeds (-) 1200 mV. Overprotection conditions after some time may lead to coating damage. At a DC current density (J_{DC}) of 1 A/m², the protection potential of X65 steel samples changed from (-) 1241 mV to (-) 1065 mV, with a variation in AC current density (J_{AC}) from 0 A/m² to 200 A/m². The severe damage to passive film at AC current densities ranging from 50 to 200 A/m² leading to enhanced corrosion (Figure 6). Up to an AC current density (J_{AC}) of 10 A/m², X65 exhibits comparable corrosion resistance. The passive film quickly deteriorates, at higher AC current densities, allowing the protection potential to shift positively.

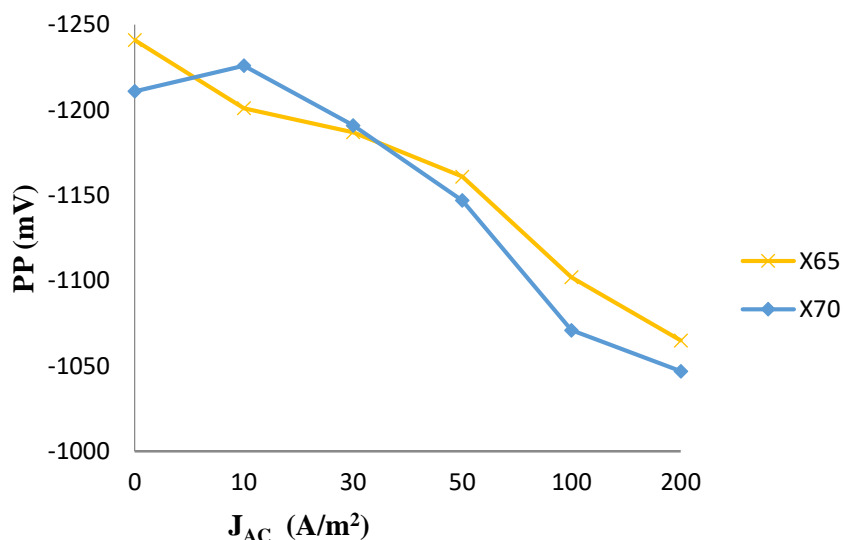


Figure 6. Protection potential (PP) of X65 and X70 steels with change in AC current density (J_{AC}), at a DC current density (J_{DC}) of 1 A/m² in soil simulating solution

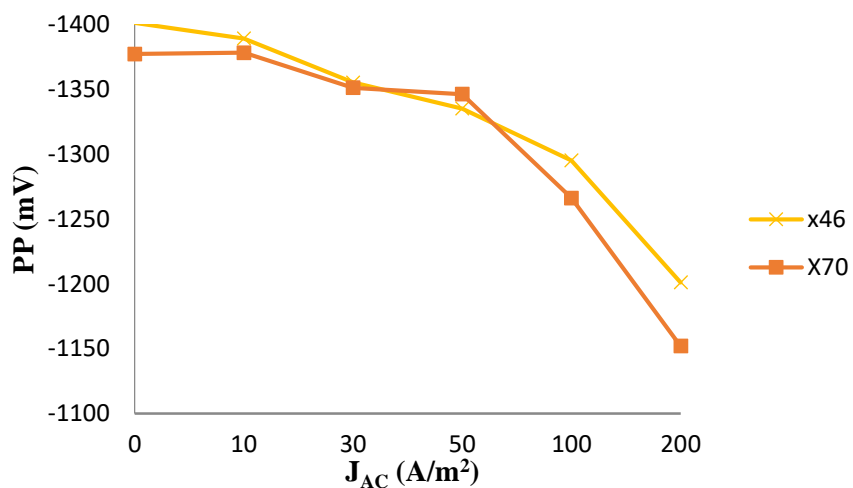


Figure 7. Protection potential (PP) of X46 and X70 steels with AC current density (J_{AC}) at a DC current density (J_{DC}) of 10 A/m² in soil simulating solution.

At a DC current density (J_{DC}) of 0.3 A/m², the protection potential of X70 grade steel samples shifted to (-) 959 mV from (-) 1125 mV with variation in AC current density (J_{AC}) in steps from 0 A/m² to 200 A/m². AC corrosion occurs at lower AC densities with a positive potential change in the X65 and X70 samples. The protection potential for the X70 pipe shifted to (-) 839 mV from (-) 1061 mV due to a change in AC current densities (Figure 7). With an AC current density (J_{AC}) of 200 A/m² at a DC current density (J_{DC}) of 0.1 A/m², X70 steel could not satisfy the (-) 850 mV protection criterion, which may result in accelerated corrosion. Protection current cannot prevent corrosion at larger AC densities, which agrees with the available publication [37].

4. CONCLUSION

The DC protection current density (J_{DC}) increases initially with a variation in AC current density (J_{AC}) from 0 A/m² to 30 A/m² for all pipe steels. The passive film on the metal surface is intact at lesser AC current densities, thereby resisting AC corrosion. However, observed no significant change in DC current density with AC current densities from 50 A/m² to 200 A/m². The inactive film at high AC densities is increasingly unstable, decreasing thickness and significant damage, leading to enhanced corrosion. For the X46 pipeline, the substantial percentage rise in DC current density illustrates the CP system's ability to provide adequate cathodic protection at lower potentials. However, at protection potentials more negative than (-) 1200 mV, overprotection may eventually lead to severe coating failure.

For X42 and X46 steels, protection potential shifted positively with variation in AC current density. Experimental data indicates that steel of the X42 and X46 grades exhibit a similar response to AC interference. The higher positive potential shift for X65 and X70 grades steels with increased AC current density to 100 A/m² indicates higher susceptibility to corrosion at a DC current density (J_{DC}) of 1 A/m². The X65 and X70 steels are likely to corrode more rapidly when exposed to AC interference, which could be because of the differences in the microstructure and morphology of steel. Factors like soil resistivity and pH may also affect the corrosion prevention response.

Corrosion protection of the steel sample is due to thick passive film on the sample surface. With no AC, pipe samples remain protected at a DC current density (J_{DC}) of 0.1 A/m². However, with the increasing density of protective currents, protection potential has become more negative. The steel of all grades shows a DC current density (J_{DC}) of 1 A/m², a protection potential higher than (-) 1200 mV in the negative direction, which may severely damage the coating over time and lead to localized corrosion.

Pipeline engineers to address AC corrosion behavior while selecting the suitable pipe steel for the necessary application. Additional modeling/optimization studies are required to determine appropriate measures for the mitigation of AC corrosion. Additionally, design mitigation methodologies to minimize deterioration due to AC interference.

ACKNOWLEDGMENT

Any specific public, commercial, or not-for-profit funding agencies did not support this research.

NOMENCLATURE:

AC	Alternating Current
DC	Direct Current
API	American Petroleum Institute
CP	Cathodic Protection
pH	Power of Hydrogen, a measure of acidity or alkalinity of a solution

References

1. A. K. Arya, and S. Honwad, *J. Pet. Explor. Prod. Technol.*, 8 (2018) 1389.
2. A. K. Arya, and S. Honwad, *J. Pipeline Syst. Eng. Pract.*, 1 (2016) 04015008.
3. Z. M. Hossein, S. Deif, and M. Daneshmand, *Sens. Actuators, A*, 261 (2017) 24.
4. D. H. Kroon, and M. Urbas, *Mater. Perform.*, 33 (1994) 26.
5. S. Goidanich, L. Lazzari, and M. Ormellese, *Corros. Sci.*, 52 (2010) 491.
6. D. Z. Tang, Y. X. Du, M. X. Lu, Y. Liang, Z. T. Jiang, and L. Dong, *Mater. Corros.*, 12 (2015) 1467.
7. M. Büchler, *Corrosion*, 76 (2020) 451.
8. A. Brenna, L. Luciano, P. Mariapia, and M. Ormellese, *Metall. Ital.*, 6 (2014) 29.
9. D. Kuang, and Y. F. Cheng, *Corros. Eng., Sci. Technol.*, 52 (2017) 22.
10. Y. B. Guo, C. Liu, D. G. Wang, and S. H. Liu, *Pet. Sci.*, 12 (2015) 316.
11. S. B. Lalvani, and X. A. Lin, *Corros. Sci.*, 36 (1994) 1039.
12. S. B. Lalvani, and G. Zhang, *Corros. Sci.*, 37 (1995) 1567.
13. J. Mystkowska, K. Niemirowicz-Laskowska, D. Lysik, G. Tokajuk, J. R. Dabrowski, and R. Bucki, *Int. J. Mol. Sci.*, 19 (2018) 743.
14. M. Zhu, C. Du, X. Li, Z. Liu, S. Wang, J. Li., and D. Zhang, *Electrochim. Acta*, 117 (2014) 351.
15. B. P. Kumleh, H. V. Mohammad, and S. P. Kumleh, *IFAC Proceedings Volumes* 36 (2003) 1151.
16. A. K. Thakur, A. K. Arya, and P. Sharma, *Corros. Rev.* 38 (2020) 463.
17. I. S. Cole, and D. Marney, *Corros. Sci.*, 56 (2012) 5.
18. M. Zhu, Y. Yuan, S. Yin, and S. Guo, *Int. J. Electrochem. Sci.*, 13 (2018) 10669.
19. D. Kuang, and Y. F. Cheng, *Corrosion*, 71 (2015) 267.
20. M. A. Azam, S. Sukarti, and M. Ziami, *Eng. Fail. Anal.*, 115 (2020) 104654.
21. D. Kuang, and Y. F. Cheng, *Corros. Sci.* 85 (2014) 304.
22. D. Kuang, and Y. F. Cheng, *Corros. Sci.* 99 (2015) 249.
23. F. E. Kulman, *Corrosion*, 17 (1961) 34.
24. S. Goidanich, L. Luciano and M. Ormellese, *Corros. Sci.*, 52 (2010) 916.
25. L. Chen, D. Yanxia, Y. Liang and L. Jianjun, *Corros. Eng., Sci. Technol.*, 56 (2021) 219.
26. C. Wen, J. Li, S. Wang, and Y. Yang, *J. Nat. Gas Sci. Eng.*, 27 (2015) 1555.
27. G. Lucca, *IET Sci., Meas. Technol.*, 15 (2021) 25.
28. A. Q. Fu, and Y. F. Cheng, *Corros. Sci.* 52 (2010) 612.
29. Y. Li, C. Xu, R. H. Zhang, Q. Liu, X. H. Wang, and Y. C. Chen, *Int. J. Electrochem. Sci.*, 12 (2017) 1829.
30. Z. Jiang, Y. du, M. Lu, Y. Zhang, D. Tang, and L. Dong, *Corros. Sci.*, 81 (2014) 1.
31. M. Zhu, and C. W. Du, *J. Mater. Eng. Perform.*, 26 (2017) 221.
32. M. Zhu, J. L. Yang, Y. B. Chen, Y. F. Yuan, and S. Y. Guo., *Mater. Eng. Perform.*, 29 (2020) 423.

33. H. Wang, C. Du, Z. Liu, L. Wang, and D. Ding, *Materials*, 10 (2017) 851.
34. A. K. Thakur, A. K. Arya, and P. Sharma. *Mater. Today. Proc.*, (2021) 1.
35. L. Chen, Y. Du, Y. Liang, and J. Li, *Corros. Eng., Sci. Technol.*, 56 (2021) 219.
36. D. K. Kim, T. H. Ha, Y. C. Ha, J. H. Bae, H. G. Lee, D. Gopi, and J. D. Scantlebury, *Corros. Eng., Sci. Technol.*, 39 (2004) 117.
37. H. Qin, Y. Du, M. Lu, X. Sun, and Y. Zhang, *Mater. Corros.*, 71 (2020) 1856.
38. A.K. Arya, and S. Honwad, *Chem. Prod. Process Model.*, 13 (2018) 1.
39. A. K. Arya, *J. Pet. Explor. Prod. Technol.*, (2021) 1.

© 2021 The Authors. Published by ESG (www.electrochemsci.org). This article is an open access article distributed under the terms and conditions of the Creative Commons Attribution license (<http://creativecommons.org/licenses/by/4.0/>).



Contents lists available at ScienceDirect

Materials Today: Proceedings

journal homepage: www.elsevier.com/locate/matpr

Analysis of cathodically protected steel pipeline corrosion under the influence of alternating current

Ajit Kumar Thakur ^{a,b,*}, Adarsh Kumar Arya ^b, Pushpa Sharma ^c

^a Indian Oil Corporation Ltd, Paradip, Orissa, India

^b Department of Chemical Engineering, School of Engineering, UPES, Bidholi, Dehradun, India

^c Department of Petroleum Engineering, School of Engineering, UPES, Bidholi, Dehradun, India

ARTICLE INFO

Article history:

Received 30 April 2021

Received in revised form 22 May 2021

Accepted 25 May 2021

Available online xxxx

Keywords:

Pipeline steel

Protection Potential

Pipe Grade

AC Corrosion

Potentiostatic

Galvanostatic

ABSTRACT

The study analyzes alternating current interference by potentiostatic and galvanostatic measurements on coated pipeline steels in simulated soil solutions. The polarization potential and protection current density of pipe samples of various grades is measured. The effect of alternating current on each pipe grade at various polarisation potentials and protection current densities are measured. Different pipe grades' relative performance is measured to determine the pipe grades exhibiting better alternating current corrosion performance under cathodic protection. The experimental study uniquely compares alternating current corrosion performance of different pipeline steel grades, which helps the pipeline operators carefully select the API grades of pipes for long-term trouble-free operation.

© 2021 Elsevier Ltd. All rights reserved.

Selection and peer-review under responsibility of the scientific committee of the 2nd International Conference on Functional Material, Manufacturing and Performances.

1. Introduction

For transporting oil and gas, pipelines are considered the best mode [1–3]. When run parallel to a high voltage power line for a significant distance, these pipelines can be transferred to the pipeline under regular power line operating conditions and short-circuit conditions on the power line. These voltages can result in electrical shock hazards for maintenance personnel and be detrimental to the integrity of cathodic protection (CP) equipment, the pipeline coating, and the pipeline steel, particularly during short-circuit conditions.

The challenge is to identify the extent of alternating current (AC) interference on underground pipelines and mitigate these effects to protect pipelines.

Many corrosion problems attributable to AC interference have been observed with the exponential growth of high voltage transmission lines near the buried pipelines [4]. The traditional cathodic protection measures have been ineffective in protecting pipelines from corrosion in the presence of induced AC corrosion [4]. American Petroleum Institute (API) 5L Grade pipes are extensively used for oil/gas service because of their long service life, suitability to sour service, and resistance to cracks propagation. API 5L Grade

pipes comply with mechanical parameters, such as toughness, tensile strength, and yield strength. The microstructure and composition of these pipes may vary significantly, as per maximum limits of the composition of manganese, carbon, phosphorous, and Sulphur [4].

2. Literature review

Literature reviews [5–7] indicate that several studies and experiments have been conducted in the field of AC interference. Studies have investigated the induced AC corrosion affects the life of steel pipelines. Previous studies [8] have concluded that overprotection is the most dangerous condition in the presence of AC interference due to enhanced corrosion. A recent study [9] in the year 2020 concluded that the extent of dynamic AC corrosion with higher interference time is similar to steady-state AC corrosion. However, comparative experimental studies, considering AC corrosion of various pipeline steels under similar conditions, are not available.

This work attempts to bridge the gap to determine and compare various pipeline steels' corrosion performance. The experiments are performed, in soil simulating solution, through potentiostatic and galvanostatic tests. AC corrosion-resistant behavior of various pipeline steels is then analyzed systematically. The following section first reviews the fundamentals of cathodic protection applied on steel pipelines to avoid corrosion.

* Corresponding author.

<https://doi.org/10.1016/j.matpr.2021.05.548>

2214-7853/© 2021 Elsevier Ltd. All rights reserved.

Selection and peer-review under responsibility of the scientific committee of the 2nd International Conference on Functional Material, Manufacturing and Performances.

3. Cathodic protection

In an electrochemical process, the formation of oxide layers at the metal surface limits oxygen diffusion to the metal surface [10]. The oxide layer thereby prevents/inhibits further corrosion. Cathodic protection is one such electrochemical process for secondary corrosion protection of underground pipeline assets. Cathodic protection thereby supports the primary protection provided by coatings to underground assets [11]. Circulation of direct current (DC) under cathodic protection between pipeline (cathode) and anode through soil helps to minimize the pipe corrosion through a combination of oxidation and reduction reactions:



The commonly accepted criteria [12] for corrosion protection under cathodic protection of pipelines are briefed below:

- Pipeline steel shall be polarized to (–) 850 mV under cathodic protection. Polarised potential shall be measured using a reference electrode with saturated copper/copper sulfate electrolyte. Positive side polarization from (–) 850 mV shall be inadequate for corrosion protection—polarization towards the negative side from (–) 1200 mV results in coating disbandment.
- (–) 950 mV polarisation is considered in acid environments, dissimilar metals, presence of sulfides, anaerobic bacteria, etc.
- Polarisation potential on a coated pipeline is measured between pipe and earth. Measurement is recorded immediately upon interrupting the current output from all cathodic protection sources affecting that portion of the pipeline simultaneously.

The required corrosion protection is achieved by maintaining polarisation potential in pipelines not under AC currents' influence. The typical protective current density required to maintain polarisation potential depends upon soil resistivity and coating type, as summarized in Table 1. However, the polarized potential of (–) 850 mV does not consider corrosion protection in the presence of AC interference [13].

4. Cathodic protection under AC interference

Optimum protection is not achieved fully by cathodic protection under the influence of AC interference [14]. Corrosion protection methodologies for pipelines under AC interference consider determining the pipe-to-earth potential, AC density, DC density, and AC/DC density ratio. Previous studies have revealed that the AC density should not exceed a time-weighted average of 30 Am^{-2} if DC density exceeds 1 Am^{-2} and shall not exceed 100 Am^{-2} if DC density is less than 1 Am^{-2} . The enhanced corrosion at AC density of 30 Am^{-2} is very high [15].

AC mitigation technologies and suitable grounding are implemented to minimize AC voltage induced on a pipeline for minimal AC corrosion possibilities [16]. Steady-state touch potential of 15 V

or more due to induced AC [17] is a personnel safety hazard and shall be mitigated.

AC interference is experienced on pipelines due to AC transmission lines through Resistive, Capacitive, and Inductive coupling [18]. Algorithms are under development to assess the induced voltage and current on pipelines [19]. The critical AC Corrosion parameters include alternating voltage (AV), AC density, and AC/DC density ratio.

Weight loss experiments [8] on cathodically protected carbon steel pipe samples under the influence of AC densities (10 Am^{-2} to 500 Am^{-2}) have established that (–) 0.850 V CSE criterion is not adequate. AC/DC density ratio of more than 3 indicates high corrosion risk. A lower AC/DC density ratio indicates lower risk but is not risk-free. However, an AC/DC density ratio of 10 or more [20] indicates risk certainty.

5. Methodology

The following section discusses the methodology adopted to measure AC's effect on steel pipes.

5.1. Preparation of pipeline steel specimen

Experimental tests are conducted on pipeline steel specimens with the grade, chemical composition, and yield strength as per Table 2. Steel specimen (6 mm thick, 100 mm diameter) are prepared from respective pipes. After a thorough cleaning, each specimen is placed in a PVC cylindrical tube of 10 mm internal diameter and 40 mm length (Fig. 1). One side of the specimen was welded with attachment to secure a 6 mm² copper cable for electrical connection. The other side of the specimen ensured the availability of a 10 mm diameter bare surface. The cylindrical tube is then filled with epoxy for an airtight arrangement to avoid water ingress (Fig. 2).

5.2. Preparation of soil simulating solution

Experiments were conducted on the specimen, dipped in soil simulating solution, having 500 mg/L Sulphates, 200 mg/L Chlorides, and silica sand. The electrical resistivity of the soil simulating solution is measured. A new solution is utilized for each specimen testing, and after testing, the existing solution is discarded.

5.3. Electrical circuit

Experiments are conducted using an AC Circuit and a DC circuit suitably coupled (Figs. 3 and 4) to avoid interference between the two using Capacitors and Inductors' basic properties. Capacitor blocked circulation of DC in AC Circuit, and Inductor prevented AC circulation in the DC circuit.

Variac provided requisite AC, which was forced through pipeline specimen (W). Requisite DC was injected using Galvanostat through the pipeline specimen. While the flow of DC provided cathodic protection to the pipeline specimen, AC provided the necessary current for AC interference.

Requisite circuits were completed through counter electrodes, and a shunt was provided to measure the current flow. A Cu-

Table 1
Typical Protective Current Density.

S. No.	Soil Resistivity (Ωm)	3 LPE Coated Pipe (μAm^{-2})	FBE Coated Pipe (μAm^{-2})	Coal Tar Enamel Coated Pipe (μAm^{-2})
1	10–100	25	50	125
2	<10	50	70	150
3	>100	15	25	75

Table 2
Pipeline Steel Specimens.

Pipe Grade API 5L	Chemical Composition (%)						Yield Strength psi
	C	Mn	P	S	Ti		
X46	0.28	1.40	0.030	0.030	0.04	46,000	
X52	0.28	1.40	0.030	0.030	0.04	52,000	
X80	0.24	1.40	0.025	0.015	0.06	80,000	

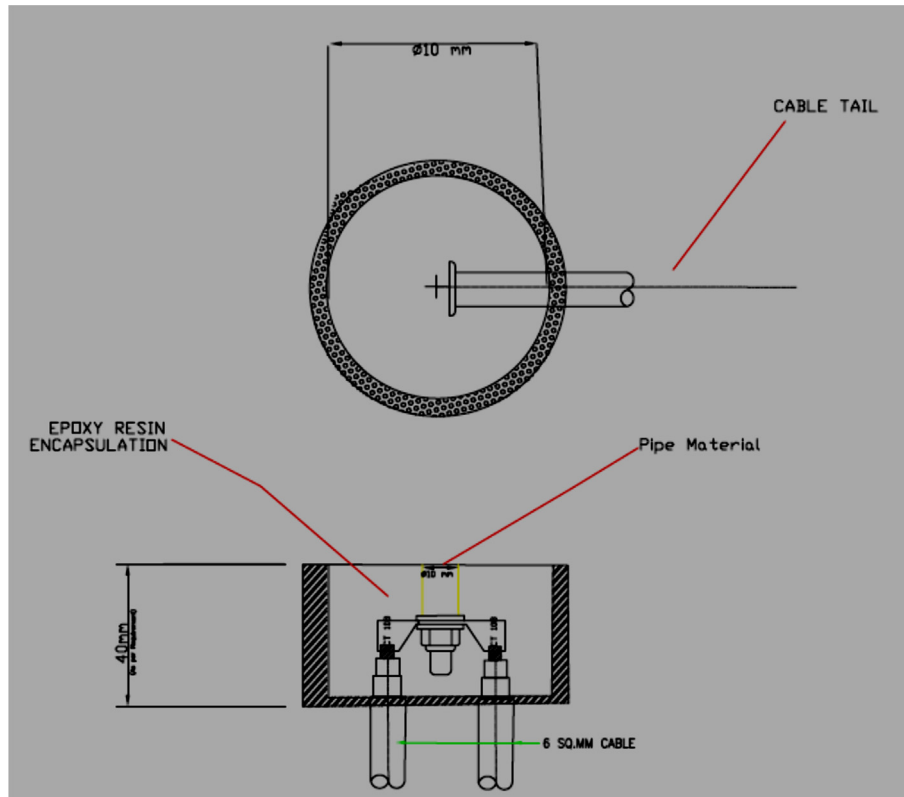


Fig. 1. Typical Pipeline steel specimen.



Fig. 2. Pipeline steel specimen.

CuSo₄ reference electrode (RE) was provided to measure the DC potential of the specimen.

5.4. Galvanostatic tests

Galvanostatic tests are conducted on pipeline specimens at various AC densities. Each prepared specimen in a cylindrical tube is cleaned and immersed in soil simulating solution. Fresh soil simulating solution is used for each set of tests on the specimen.

Galvanostatic tests included studying the effect of Alternating current on protection potential. Various alternating current densities were applied (Table 3) in steps as interference to the applied protection densities, and the resultant protection potential was measured. Initially, the protection current was applied at 0.01 Am^{-2} for 24 h without AC. Protection potential was then measured. AC is then applied in 30 min from 10 Am^{-2} to 200 Am^{-2} . During each step, protection potential is measured using a reference electrode every 5 min.

5.5. Potentiostatic tests

Potentiostatic tests included studying the effect of Alternating current on protection density. Tests included applying various current densities in steps as interference to the applied protection potential, and resultant protection current density was measured.

Potentiostatic tests included studying the effect of Alternating current on protection current density. Various alternating current

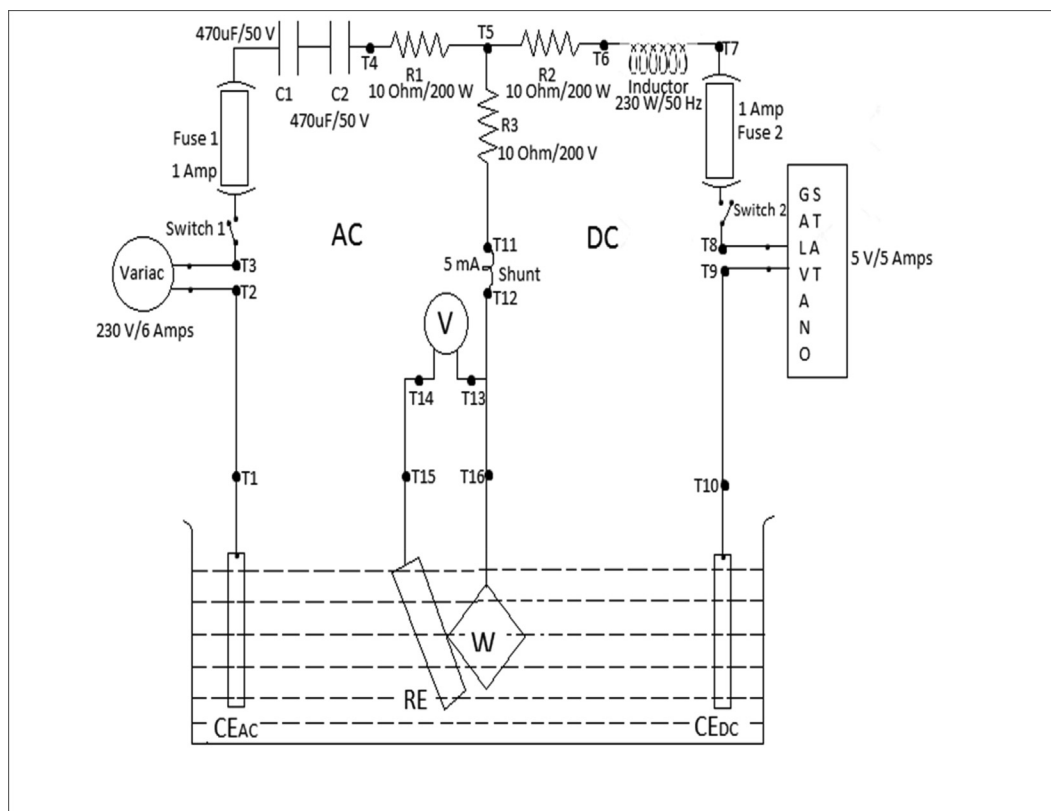


Fig. 3. Schematics for Experimental Setup.



Fig. 4. Experimental setup.

Table 3
Experimental conditions - Galvanostatic test.

Protection Current Density (Am^{-2})	AC Current Density (Am^{-2})
0.1	10, 30, 50, 100, 200
0.3	10, 30, 50, 100, 200
0.5	10, 30, 50, 100, 200
1.0	10, 30, 50, 100, 200
2.0	10, 30, 50, 100, 200
10.0	10, 30, 50, 100, 200

densities were applied (Table 4) in steps as interference to the applied protection potential, and the resultant protection current

Table 4
Experimental conditions - Potentiostatic test.

Protection Potential (mV)	AC Current Density (A/m^2)
-850	10, 30, 50, 100, 200
-950	10, 30, 50, 100, 200
-1050	10, 30, 50, 100, 200
-1150	10, 30, 50, 100, 200
-1250	10, 30, 50, 100, 200
-1350	10, 30, 50, 100, 200

density was measured. Initially, protection potential was applied at (-) 0.850 V for 24 h without AC. Protection current density was then measured. AC is then applied in 30 min from 10 Am^{-2} to 200 Am^{-2} . During each step, the current protection density is measured every 5 min.

6. Results and discussions

6.1. Protection potential with no AC interference

For X46 pipe, in the absence of AC interference, in the simulated soil solution, samples were cathodically protected with the protection potential near (-) 1069 mV at a DC density of 0.01 Am^{-2} . Protection potential became more cathodic (from (-) 1070 to (-) 1401 mV) with an increase in DC density (from 0.01 Am^{-2} to 10 Am^{-2}), indicating improved corrosion protection. The pipe sample is protected from corrosion due to passive film formation at the metal surface. However, with a DC density of more than 1 Am^{-2} , protection potential is more negative than -1200 mV, resulting in coating disbandment over a while.

The variation in protection potential with an increase of DC Current density is summarized in (Table 5) without AC interference.

Table 5
Polarisation Potential with DC density without AC interference.

DC Current Density (Am^{-2})	Protection Potential (mV)		
	X46	X52	X80
0.1	-1070	-1065	-1066
0.3	-1151	-1143	-1135
0.5	-1201	-1196	-1181
1.0	-1250	-1241	-1215
2.0	-1280	-1278	-1256
10.0	-1401	-1387	-1383

Without any AC interference, the pipe sample undercurrent protection density is polarised due to passive film formation. This helps protect the X46 sample from corrosion. The polarised potential is positively shifted (Fig. 5) with an increase of AC density. Protection potential is observed near (-) 1200 mV at the current protection density of 0.5 Am^{-2} . A similar observation is made for X52 and X80 pipes when protection potential is observed more negatively than (-) 1200 mV at 1.0 Am^{-2} or higher DC density (Figs. 6 and 7). For mitigating the coating disbandment of the pipes, current protection density shall be maintained up to 0.5 Am^{-2} or below in the absence of AC.

6.2. Shift in protection potential under AC interference

Under AC interference at protection current density of 0.1 Am^{-2} , the protection potential positively shifted for all three pipe grades with AC density change from 0 to 200 Am^{-2} . For API 46 Grade Pipe samples (Fig. 8), the protection potential became more positive from (-) 1070 mV to (-) 865 mV with an increase in AC density from 0 to 200 Am^{-2} .

The positive shift in polarization potential upon AC application is attributable to the progressive thinning of the passive film and its breakdown, resulting in enhanced corrosion current flow [21]. At lower AC densities, the polarised potential is affected marginally as the passive film is minimally affected.

Pipeline steel corrosion is uniform at low AC density, whereas extensive localized pitting corrosion occurs at higher AC densities [4,22,23]. The size of coating holidays also affects corrosion [24].

The passive film gets damaged substantially at higher current densities of $30\text{--}100 \text{ Am}^{-2}$, resulting in enhanced corrosion.

Similar corrosion performance is observed in X52 up to a low AC density of 10 Am^{-2} . The passive film rapidly breaks for the polarised potential to shift positively at the higher AC density. At AC density of 200 Am^{-2} , the polarised potential is just (-) 856 mV. Similarly, similar AC corrosion of the X80 sample is evident at lower AC densities and the positive shift of polarised poten-

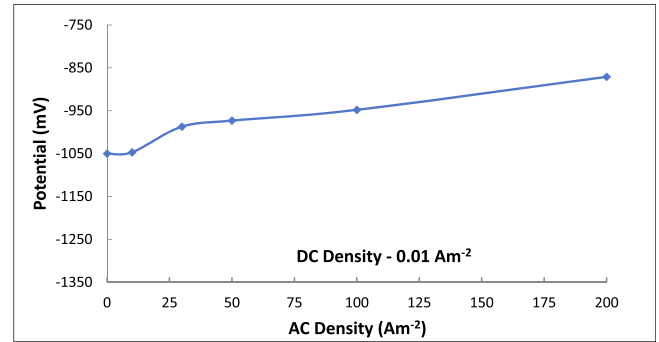


Fig. 6. Polarised Potential X52.

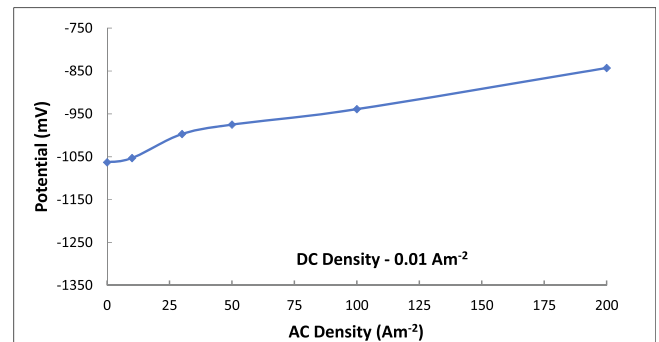


Fig. 7. Polarised Potential X80.

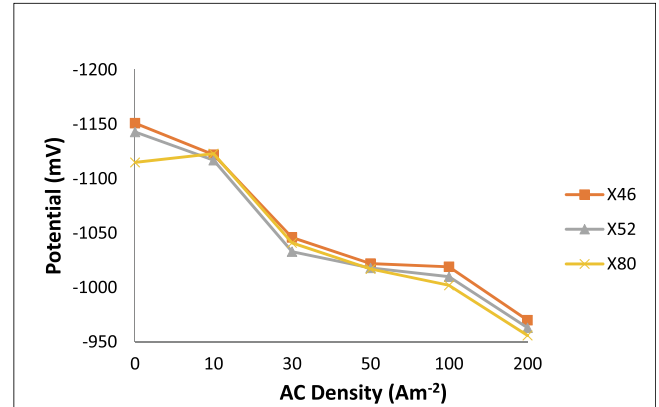


Fig. 8. Polarised potential @ Protection current density 0.3 Am^{-2} .

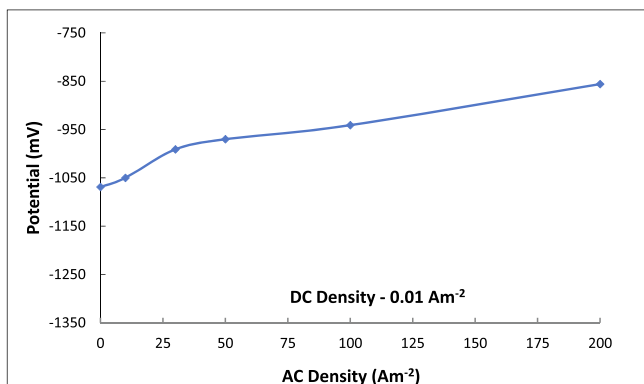


Fig. 5. Polarised Potential X46.

tial. At higher AC densities, the passive film is ruptured, resulting in increased corrosion.

AC reduces the uniformity of the passive film, decreases film thickness, and increases the possibility of its breakdown [25–28].

The protection potential changed from (-) 1065 mV to (-) 873 mV for X52 pipe and from (-) 1066 mV to -844 mV for X80 Grade pipe for a corresponding change in AC densities. It is seen that the X46 and X52 pipes remained protected with protection potential more negative than (-) 850 mV with DC density for all AC densities up to 200 Am^{-2} . However, X80 pipes could not meet the protection criteria of (-)850 mV with a current protection density of 0.1 Am^{-2} at AC density of 200 Am^{-2} , resulting in severe corrosion in alkaline soil conditions [29]. The protection potential has shifted positively with the increase of AC for all three grades (Figs. 8, 9, and 10). At the current protection density of 0.1 Am^{-2} , polarised potential remained within the range from (-) 1200 mV

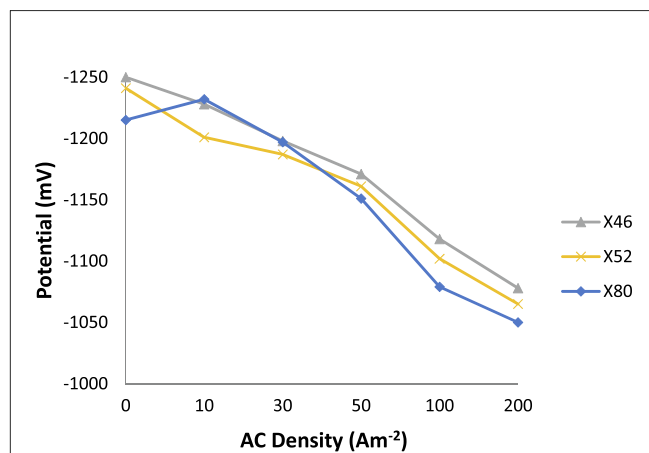


Fig. 9. Polarised potential @ Protection current density 1 Am⁻².

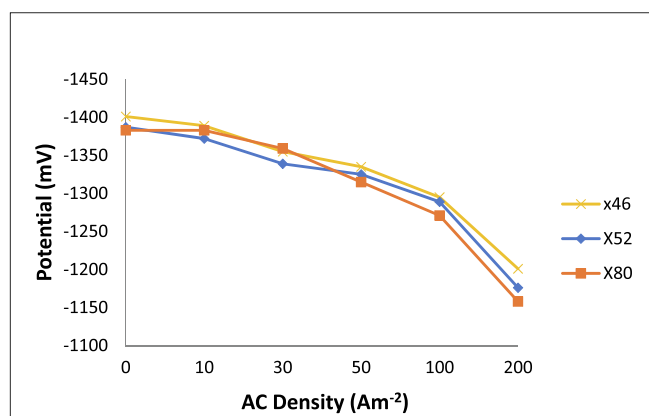


Fig. 10. Polarised potential @ Protection current density 10 Am⁻².

to (-) 850 mV. At the current protection density of 1 Am⁻², the polarised potential remained within a range of (-) 1250 mV to (-) 1050 mV. At the current protection density of 10 Am⁻², the polarised potential is found within (-) 1400 mV to (-) 1150 mV.

At higher protection current densities, the condition of overprotection may prevail, leading to cathodic disbandment coupled with severe AC corrosion.

The protection potential shift with a change in AC density, at protection current density of 0.1 Am⁻² and 1 Am⁻² is summarized in Table 6 and Table 7. The protection potential shift with a change in AC density from 30 to 50 Am⁻² and from 50 to 100 Am⁻² is more pronounced for X80 pipe samples (at protection current density of 1 Am⁻²), indicating higher susceptibility to AC corrosion.

Table 6
Potential shift at Protection current density of 0.1 Am⁻².

AC Density increase (Am ⁻²)	Protection Potential Shift (mV)		
	X46	X52	X80
0-10	19	18	10
10-30	56	56	58
30-50	20	11	22
50-100	28	29	35
100-200	82	78	97

Table 7
Potential shift at Protection current density 1 Am⁻².

AC Density increase (Am ⁻²)	Protection Potential Shift (mV)		
	X46	X52	X80
0-10	22	40	17
10-30	30	14	35
30-50	27	26	46
50-100	53	59	72
100-200	40	37	29

6.3. Effect on protection current density

With an increase in protection potential from (-)850 mV to (-) 1350 mV, the protection current density increased from 0.013 to 1.29 Am⁻² with no AC interference for X46 pipes (Fig. 11). Under AC interference of 30 Am⁻², the current protection density increases from 0.027 to 1.985 Am⁻².

Without any AC interference, with an increase in protection potential from (-)850 mV to (-)1350 mV, the current protection densities increased from 0.02 to 1.33 Am⁻² for X52 pipes (Fig. 12) and from 0.18 to 1.211 Am⁻² for X80 pipes (Fig. 13).

Also, under AC interference of 30 Am⁻², with an increase in protection potential from (-)850 mV to (-)1350 mV, the protection current density increased from 0.031 to 1.792 Am⁻² for X52 pipes and from 0.189 to 1.663 Am⁻² for X80 pipes.

For X46 pipe, protection current density change is minimal with a change in AC density at protection potential of (-) 850 mV. However, at a protection potential of (-)1350 mV, the maximum protection current density of 3.5 Am⁻² is required at an AC density of 200 Am⁻². For X52 and X80 pipes at the protection potential of -1350 mV, the maximum protection current density is required at 100 Am⁻².

The rate of change of protection density (Table 8) for X80 pipes under AC interference is lesser than X46 or X52 pipes, indicating a lesser tendency for corrosion protection under AC interference.

7. Conclusions

In the absence of AC interference, the pipeline samples of all three grades were found to remain protected in the presence of protection current density of 0.1 Am⁻². However, an increase in protection current density increased protection potential. With the protection density of 1 Am⁻², all the pipe grades were subjected to protection potential more negative to (-) 1200 mV. Any further increase in protection current density results in coating disbandment over a while.

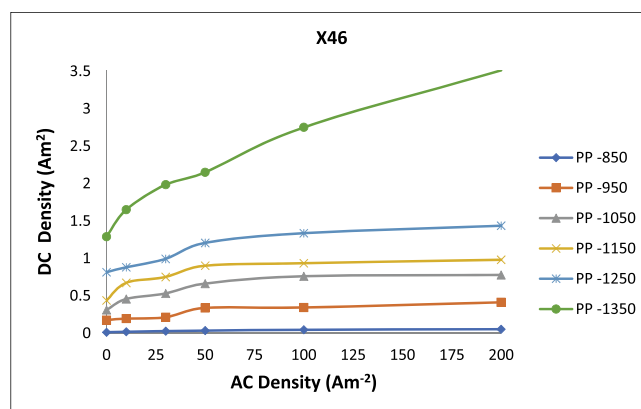


Fig. 11. Protection current density change with AC density: X46.

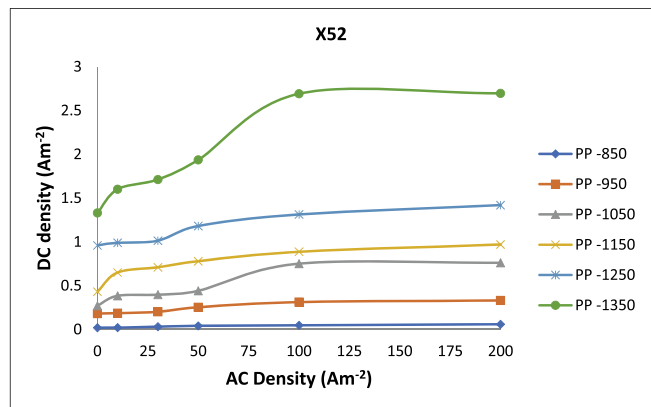


Fig. 12. Protection current density change with AC density: X52.

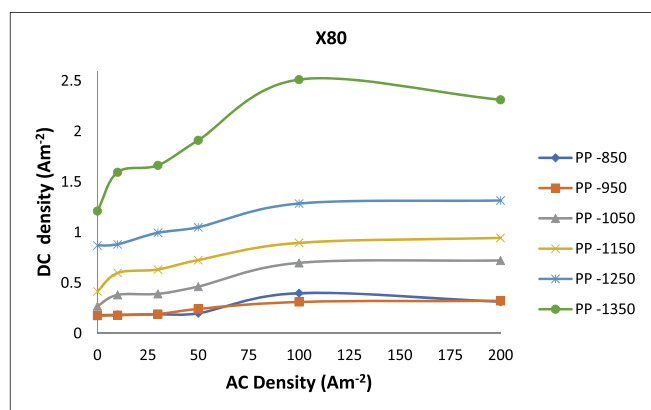


Fig. 13. Protection current density change with AC density: X80.

Table 8
Protection Current Density Shift with polarisation potential.

AC Current Density (Am ⁻²)	Change in protection density (Am ⁻²)		
	X46	X52	X80
0	1.474	1.130	1.031
30	1.958	1.761	1.474

The higher positive potential shift for X80 grade pipes with a change in AC density from 30 to 100 Am⁻² indicates enhanced corrosion at protection current density of 1 Am⁻². X46 and X52 grade pipes also have positive potential shifts, but the intensity is less than X80. It is evident from experimental data that X46 and X52 grade pipes exhibit a similar response to AC interference. However, X80 grade pipes are likely to corrode more rapidly under AC interference. This should be due to differences in the microcrystalline structure of the corresponding pipe grades. Corrosion prevention response may also be influenced by other factors such as soil resistivity, pH, etc.

While selecting the pipe grades for the respective application, considerations for AC corrosion shall be considered suitably. Further appropriate modeling/optimization studies need to be carried out to incorporate suitable mitigation measures for AC corrosion.

It is also necessary to investigate the possibility of AC interference, evaluate the magnitude of the interference, design and install mitigation facilities as necessary, and monitor the performance of the mitigation system and the cathodic protection system.

CRediT authorship contribution statement

Ajit Kumar Thakur: Conceptualization, Methodology, Writing - original draft. **Adarsh Kumar Arya:** Supervision, Writing - review and editing. **Pushpa Sharma:** Supervision.

Declaration of Competing Interest

The authors declare that they have no known competing financial interests or personal relationships that could have appeared to influence the work reported in this paper.

Acknowledgment

This research has not received any specific grant from funding agencies in public, commercial, or not-for-profit sectors.

References

- [1] A.K. Arya, S. Honwad, Modeling, simulation, and optimization of a high-pressure cross-country natural gas pipeline: application of an ant colony optimization technique, *J. Pipeline Syst. Eng. Pract.* 7 (1) (2016) 04015008, [https://doi.org/10.1061/\(ASCE\)PS.1949-1204.0000206](https://doi.org/10.1061/(ASCE)PS.1949-1204.0000206).
- [2] A.K. Arya, S. Honwad, Multiobjective optimization of a gas pipeline network: an ant colony approach, *J. Pet. Explor. Prod. Technol.* 8 (4) (2018) 1389–1400.
- [3] A.K. Arya, S. Honwad, Optimal operation of a multi-source multi-delivery natural gas transmission pipeline network, *Chem. Prod. Process Model.* 13 (3) (2018).
- [4] Y.-B. Guo, C. Liu, D.-G. Wang, S.-H. Liu, Effects of alternating current interference on corrosion of X60 pipeline steel, *Pet. Sci.* 12 (2) (2015) 316–324.
- [5] D.-K. Kim, T.-H. Ha, Y.-C. Ha, J.-H. Bae, H.-G. Lee, D. Gopi, J.D. Scantlebury, Alternating current induced corrosion, *Corros. Eng., Sci. Technol.* 39 (2) (2004) 117–123.
- [6] Adedeji, Kazeem B., Akinlolu A. Ponnle, Bolanle T. Abe, Adisa A. Jimoh, Adnan MI Abu-Mahfouz, and Yskandar Hamam. "A review of the effect of AC/DC interference on corrosion and cathodic protection potentials of pipelines." (2018).
- [7] A.K. Thakur, A.K. Arya, P. Sharma, The science of alternating current-induced corrosion: a review of literature on pipeline corrosion-induced due to high-voltage alternating current transmission pipelines, *Corros. Rev.* 38 (6) (2020) 463–472.
- [8] Brenna, Andrea, Luciano Lazzari, Mariapia Pedeferra, and Marco Ormellese. "Cathodic protection condition in the presence of AC interference." *La Metallurgia Italiana* (2014).
- [9] L.e. Chen, D.u. Yanxia, Y.i. Liang, J. Li, Research on corrosion behavior of X65 pipeline steel under dynamic AC interference, *Corros. Eng., Sci. Technol.* (2020) 1–11.
- [10] I.S. Cole, D. Marney, The science of pipe corrosion: a review of the literature on the corrosion of ferrous metals in soils, *Corros. Sci.* 56 (2012) 5–16.
- [11] Thakur, Ajit Kumar. "Corrosion Control for Above Ground Crude Oil Storage Tanks." In *NACE International Corrosion Conference Proceedings*, pp. 1-11. NACE International, 2017.
- [12] M. Büchler, On the mechanism of cathodic protection and its implications on criteria including AC and DC interference conditions, *Corrosion* 76 (5) (2020) 451–463.
- [13] D. Kuang, Y.F. Cheng, Effects of alternating current interference on cathodic protection potential and its effectiveness for corrosion protection of pipelines, *Corros. Eng., Sci. Technol.* 52 (1) (2017) 22–28.
- [14] T.H. Shabangu, P. Shrivastava, B.T. Abe, P.A. Olubambi, Stability assessment of pipeline cathodic protection potentials under the influence of AC interference, *Prog. Electromagn. Res.* 66 (2018) 19–28.
- [15] S. Goidanich, L. Lazzari, M. Ormellese, AC corrosion. Part 2: Parameters influencing corrosion rate, *Corros. Sci.* 52 (3) (2010) 916–922.
- [16] Adedeji, K. B., B. T. Abe, Y. Hamam, Adnan MI Abu-Mahfouz, T. H. Shabangu, and A. A. Jimoh. "Pipeline grounding condition: A control of pipe-to-soil potential for ac interference induced corrosion reduction." (2017).
- [17] Dabkowski, John, Robert F. Allen, and Frank A. Perry. "Mitigation design, installation and post commissioning measurements for a pipeline collocated with AC transmission lines." In *CORROSION 2001*. OnePetro, 2001.
- [18] Di Biase, L. "Interaction and stray-current corrosion." (2010): 2833-2838.
- [19] G. Lucca, AC interference from faulty power cables on buried pipelines: a two-step approach, *IET Sci. Meas. Technol.* 15 (1) (2021) 25–34.
- [20] E. Collet, B. Delores, M. Gabillard, I. Ragault, Corrosion due to AC influence of very high voltage power lines on polyethylene-coated steel pipelines: evaluation of risks—preventive measures, *Anti-Corros. Methods Mater.* 48 (4) (2001) 221–227.
- [21] M. Büchler, H.-G. Schöneich, Investigation of alternating current corrosion of cathodically protected pipelines: development of a detection method, mitigation measures, and a model for the mechanism, *Corrosion* 65 (9) (2009) 578–586.

- [22] A.Q. Fu, Y.F. Cheng, Effects of alternating current on corrosion of a coated pipeline steel in a chloride-containing carbonate/bicarbonate solution, *Corros. Sci.* 52 (2) (2010) 612–619.
- [23] Li, Yingchao, Cheng Xu, R. H. Zhang, Qiang Liu, Xinhua Wang, and Yingchun Chen. "Effects of stray AC interference on corrosion behavior of X70 pipeline steel in a simulated marine soil solution." *Int. J. Electrochem. Sci* 12, no. 3 (2017): 1829–1845.
- [24] Z. Jiang, Y. Du, M. Lu, Y. Zhang, D. Tang, L. Dong, New findings on the factors accelerating AC corrosion of buried pipeline, *Corros. Sci.* 81 (2014) 1–10.
- [25] Ormellese, Marco, Luciano Lazzari, and Andrea Brenna. "AC-induced corrosion on passive metals." National Association of Corrosion Engineers, P. O. Box 218340 Houston TX 77084 USA.[np]. 14–18 Mar (2010).
- [26] D.-Z. Tang, Y.-X. Du, M.-X. Lu, Y. Liang, Z.-T. Jiang, L. Dong, Effect of pH value on corrosion of carbon steel under an applied alternating current, *Mater. Corros.* 66 (12) (2015) 1467–1479.
- [27] M. Zhu, C.W. Du, A new understanding on AC corrosion of pipeline steel in alkaline environment, *J. Mater. Eng. Perform.* 26 (1) (2017) 221–228.
- [28] M. Zhu, J.L. Yang, Y.B. Chen, Y.F. Yuan, S.Y. Guo, Effect of alternating current on passive film and corrosion behavior of pipeline steel with different microstructures in carbonate/bicarbonate solution, *J. Mater. Eng. Perform.* 29 (1) (2020) 423–433.
- [29] H. Wang, D.u. Cuiwei, Z. Liu, L. Wang, D.e. Ding, Effect of alternating current on the cathodic protection and interface structure of X80 steel, *Materials* 10 (8) (2017) 851.



 Unlicensed Published by [De Gruyter](#) February 1, 2022


Prediction and mitigation of AC interference on the pipeline system

Ajit Kumar Thakur , *Adarsh Kumar Arya* and *Pushpa Sharma*

From the journal [Corrosion Reviews](#)

<https://doi.org/10.1515/corrrev-2021-0061>

[Cite this](#)

 You currently have no access to view or download this content. Please log in with your institutional or personal account if you should have access to this content through either of these. Showing a limited preview of this publication:

Abstract

The purpose of this paper is to predict and mitigate AC interference on buried pipeline systems due to transmission lines. Modeling and field verification of AC interference is done. The article also presents the issue of optimizing the mitigation measures. The paper uses the field data on soil resistivity, transmission line, and pipeline details to develop a model using current distribution electromagnetic interference grounding and soil structure analysis (CDEGS) software to predict the AC interference on the pipeline system. The model is validated with field measurements, and post-mitigation measures are considered. Mitigation measures are optimized to develop an economical mitigation plan. The case demonstrates the use of modeling techniques to predict and mitigate AC

interference on pipelines. The field validation of modeling results helps improve the modeling results and plan optimized mitigation measures. The study requires providing comprehensive field data relevant to the pipeline system under consideration. The accuracy of the field data may have a bearing on the outcome of the study. The study enables designing and optimizing mitigation measures using modeling. Comparisons with field measurements help achieve desired pipeline system integrity against AC corrosion.

Keywords: [coating stress voltage](#); [leakage current density](#); [modelling](#); [prediction](#); [simulation](#)

Corresponding author: **Adarsh Kumar Arya**, Department of Chemical Engineering, School of Engineering, UPES, Bidholi, Dehradun, Uttarakhand 248007, India, E-mail: akarya@ddn.upes.ac.in

Author contributions: All authors have accepted responsibility for the entire content of this submitted manuscript and approved submission.

Research funding: None.

Conflict of interest statement: The authors declare no conflicts of interest regarding this article.

Data availability: All relevant data are in the article.

References

Adedeji, K.B., Ponnle, A.A., Abe, B.T., Jimoh, A.A., Abu-Mahfouz, A.M., and Hamam, Y. (2018). A review of the effect of AC/DC interference on corrosion and cathodic protection potentials of pipelines. *Int. Rev. Electr. Eng.* 13: 495, <https://doi.org/10.15866/iree.v13i6.15766>.

[Search in Google Scholar](#)

Brenna, A., Lazzari, L., Pedferri, M., and Ormellese, M. (2014). Cathodic protection condition in the presence of AC interference. *La Metall. Ital.* 106: 29–34.

[Search in Google Scholar](#)

Büchler, M. (2020). On the mechanism of cathodic protection and its implications on criteria including AC and DC interference conditions. *Corrosion* 76: 451–463, <https://doi.org/10.5006/3379>.

[Search in Google Scholar](#)

Carson, J.R. (1926). Wave propagation in overhead wires with ground return. *Bell Syst. Tech. J.* 5: 539–554, <https://doi.org/10.1002/j.1538-7305.192>

[Search in Google Scholar](#)

Charalambous, C.A., Demetriou, A., Lazari, A.L., and Nikolaidis, A.I. (2018). Effects of electromagnetic interference on underground pipelines caused by the operation of high voltage AC traction systems: the impact of harmonics. *IEEE Trans. Power Deliv.* 33: 2664–2672, <https://doi.org/10.1109/>

[Search in Google Scholar](#)

Chen, L., Du, Y., Liang, Y., and Li, J. (2021). Research on corrosion behavior of X65 pipeline steel under dynamic AC interference. *Corrosion Eng. Sci. Technol.* 56: 219–229, <https://doi.org/10.1080/1478422x.2020.1843819>.

[Search in Google Scholar](#)

Chen, M., Liu, S., Zhu, J., Xie, C., Tian, H., and Li, J. (2018). Effects and characteristics of AC interference on parallel underground pipelines caused by an AC electrified railway. *Energies* 11: 2255, <https://doi.org/10.3390>

[Search in Google Scholar](#)

Christoforidis, G.C., Labridis, D.P., and Dokopoulos, P.S. (2005). A hybrid method for calculating the inductive interference caused by faulted power

lines to nearby buried pipelines. *IEEE Trans. Power Deliv.* 20: 1465–1473, [http://doi.org/10.1109/TPWRD.2005.2582222](#)
[Search in Google Scholar](#)

Cole, I.S. and Marney, D. (2012). The science of pipe corrosion: a review of the literature on the corrosion of ferrous metals in soils. *Corrosion Sci.* 56: 5–16, <https://doi.org/10.1016/j.corsci.2011.12.001>.

[Search in Google Scholar](#)

Cristofolini, A., Popoli, A., and Sandrolini, L. (2018). Numerical modelling of interference from ac power lines on buried metallic pipelines in presence of mitigation wires. 2018 IEEE international conference on environment and electrical engineering and 2018 IEEE industrial and commercial power systems Europe (EEEIC/I&CPS Europe). IEEE, pp. 1–6.

[10.1109/EEEIC.2018.8493677](https://doi.org/10.1109/EEEIC.2018.8493677)

[Search in Google Scholar](#)

Dabkowski, J. and Taflove, A. (1979). Mitigation of buried pipeline voltages due to 60 Hz AC inductive coupling part II: pipeline grounding methods. *IEEE Trans. Power Apparatus Syst.* 5: 1814–1823, <https://doi.org/10.1109/tpas.1979.1041702>

[Search in Google Scholar](#)

De Lacerda, L.A., Da Silva, J.M., and Lázaris, J. (2007). Dual boundary element formulation for half-space cathodic protection analysis. *Eng. Anal. Bound. Elem.* 31: 559–567, <https://doi.org/10.1016/j.enganabound.2006.11.001>

[Search in Google Scholar](#)

Goidanich, S., Lazzari, L., and Ormellese, M. (2010). AC corrosion. Part 2: parameters influencing corrosion rate. *Corrosion Sci.* 52: 916–922, <https://doi.org/10.1016/j.corsci.2010.05.021>

[Search in Google Scholar](#)

Guo, Y.B., Liu, C., Wang, D.G., and Liu, S.H. (2015). Effects of alternating current interference on corrosion of X60 pipeline steel. *Petrol. Sci.* 12: 1–10, <https://doi.org/10.1016/j.petrol.2015.06.001>

316–324, <https://doi.org/10.1007/s12182-015-0022-0>.

[Search in Google Scholar](#)

Jacquet, B. (1995). Guide on the influence of high voltage AC power systems on metallic pipelines. *CIGRE WG 36*: 1–56, <https://doi.org/10.3917/at>

[Search in Google Scholar](#)

Kim, D.K., Ha, T.H., Ho, Y.C., Bae, J.H., Lee, H.G., Gopi, D., and Scantlebury, J.D. (2004). The alternating current induced corrosion. *Corrosion Eng. Sci. Technol.* 39: 117–123, <https://doi.org/10.1179/147842204225016930>.

[Search in Google Scholar](#)

Kuang, D. (2016). Pipeline corrosion and coating failure under alternating current interference.

[Search in Google Scholar](#)

Kuang, D. and Cheng, Y.F. (2014). Understand the AC-induced pitting corrosion on pipelines in both high pH and neutral pH carbonate/bicarbonate solutions. *Corrosion Sci.* 85: 304–310, <https://doi.org/>

[Search in Google Scholar](#)

Kuang, D. and Cheng, Y.F. (2015a). AC corrosion at coating defect on pipelines. *Corrosion* 71: 267–276, <https://doi.org/10.5006/1377>.

[Search in Google Scholar](#)

Kuang, D. and Cheng, Y.F. (2015b). Study of cathodic protection shielding undercoating disbandment on pipelines. *Corrosion Sci.* 99: 249–257, <https://>

[Search in Google Scholar](#)

Kuang, D. and Cheng, Y.F. (2017). Effects of alternating current interference on cathodic protection potential and its effectiveness for

corrosion protection of pipelines. *Corrosion Eng. Sci. Technol.* 52: 22–28, [http://dx.doi.org/10.1016/j.ces.2017.09.002](#), [Search in Google Scholar](#)

Lalvani, S.B. and Lin, X.A. (1994). A theoretical approach for predicting AC-induced corrosion. *Corrosion Sci.* 36: 1039–1046, [https://doi.org/10.1016/0010-938x\(94\)90202-x](https://doi.org/10.1016/0010-938x(94)90202-x).

[Search in Google Scholar](#)

Lucca, G. (2018). Different approaches in calculating AC inductive interference from power lines on pipelines. *IET Sci. Meas. Technol.* 12: 802–806, <https://doi.org/10.1049/iet-smt.2018.0086>.

[Search in Google Scholar](#)

Markovic, D., Smith, V., and Perera, S. (2005). Evaluation of gradient control wire and insulating joints as methods of mitigating induced voltages in gas pipelines.

[Search in Google Scholar](#)

M'ziou, N. (2020). Electromagnetic compatibility problems of indirect lightning stroke on overhead power lines. *Math. Comput. Simulat.* 167: 429–442.

[10.1016/j.matcom.2018.04.007](https://doi.org/10.1016/j.matcom.2018.04.007)

[Search in Google Scholar](#)

Popoli, A., Cristofolini, A., and Sandrolini, L. (2021). A numerical model for the calculation of electromagnetic interference from power lines on nonparallel underground pipelines. *Math. Comput. Simulat.* 183: 221–233, [http://dx.doi.org/10.1016/j.matcom.2021.04.007](#)

[Search in Google Scholar](#)

Popoli, A., Sandrolini, L., and Cristofolini, A. (2019). Finite element analysis of mitigation measures for ac interference on buried pipelines. 2019 IEEE international conference on environment and electrical

engineering and 2019 IEEE industrial and commercial power systems Europe (EEEIC/I&CPS Europe). IEEE, pp. 1–5.

[10.1109/EEEIC.2019.8783843](https://doi.org/10.1109/EEEIC.2019.8783843)

[Search in Google Scholar](#)

Samouëlian, A., Cousin, I., Tabbagh, A., Bruand, A., and Richard, G. (2005). Electrical resistivity survey in soil science: a review. *Soil Tillage Res.* 83: 173–193, <https://doi.org/10.1016/j.still.2004.10.004>.

[Search in Google Scholar](#)

Shabangu, T.H., Shrivastava, P., Abe, B.T., and Olubambi, P.A. (2018). Stability assessment of pipeline cathodic protection potentials under the influence of AC interference. *Prog. Electromagn. Res. M* 66: 19–28, <https://doi.org/10.1109/PTM.2018.8401004>.

[Search in Google Scholar](#)

Thakur, A.K. (2017). Corrosion control for above ground crude oil storage tanks. In: *CORROSION 2017. OnePetro*.

[Search in Google Scholar](#)

Thakur, A.K., Arya, A.K., and Sharma, P. (2020). The science of alternating current-induced corrosion: a literature review on pipeline corrosion-induced due to high-voltage alternating current transmission pipelines. *Corrosion Rev.* 38: 463–472, <https://doi.org/10.1515/corrrev-2020-0044>.

[Search in Google Scholar](#)

Thakur, A.K., Arya, A.K., and Sharma, P. (2021). Analysis of cathodically protected steel pipeline corrosion under the influence of alternating current. *Mater. Today Proc.*, <https://doi.org/10.1016/j.matpr.2021.05.548>.

[Search in Google Scholar](#)

Tiegna, H., Amara, Y., and Barakat, G. (2013). Overview of analytical models of permanent magnet electrical machines for analysis and design

purposes. *Math. Comput. Simulat.* 90: 162–177, <https://doi.org/10.1016/j.matc>

[Search in Google Scholar](#)

Zhu, M., Du, C., Li, X., Liu, Z., Wang, S., Li, J., and Zhang, D. (2014). AC density on stress corrosion cracking behavior of X80 pipeline steel in high pH carbonate/bicarbonate solution. *Electrochim. Acta* 117: 351–359, <https://doi.org/10.1016/j.electacta.2014.05.011>

[Search in Google Scholar](#)

Received: 2021-08-09

Accepted: 2022-01-06

Published Online: 2022-02-01

Published in Print: 2022-04-26

© 2022 Walter de Gruyter GmbH, Berlin/Boston



Access through your institution

— or —

PDF **30,00 €**

[Buy Article](#)

From the journal



Corrosion Reviews

Volume 40 Issue 2

Journal and Issue



This issue All issues

Articles in the same Issue

Frontmatter

[An overview of microbiologically influenced corrosion: mechanisms and its control by microbes](#)

[Sulfamic acid is an environment-friendly alternative electrolyte for industrial acid cleaning and corrosion inhibition: a mini review](#)

[Ideal corrosion inhibitors: a review of plant extracts as corrosion inhibitors for metal surfaces](#)

[Improved corrosion inhibition by heterocyclic compounds on mild steel in acid medium](#)

[Prediction and mitigation of AC interference on the pipeline system](#)

[Kinetics and mechanistic reaction pathway of carbon steel dissolution in simulated CO₂-H₂S medium in the presence of formic acid](#)

[Corrosion behavior of low carbon steels and other non-ferrous metals exposed to a real calcareous soil environment](#)

[Retraction of: Resistance to chemical attack of cement composites impregnated with a special polymer sulfur composite](#)

Subjects

Architecture and Design

Arts

Asian and Pacific Studies

Business and Economics

Chemistry

Classical and Ancient Near Eastern Studies

Computer Sciences

Cultural Studies

Engineering
General Interest
Geosciences
History
Industrial Chemistry
Islamic and Middle Eastern Studies
Jewish Studies
Law
Library and Information Science, Book Studies
Life Sciences
Linguistics and Semiotics
Literary Studies
Materials Sciences
Mathematics
Medicine
Music
Pharmacy
Philosophy
Physics
Social Sciences
Sports and Recreation
Theology and Religion

Services

For journal authors
For book authors
For librarians
Rights & Permissions

Publications

Publication types
Open Access

About

[Contact](#)

[Career](#)

[About De Gruyter](#)

[Partnerships](#)

[Press](#)

[New website FAQs](#)



Winner of the OpenAthens
Best Publisher UX Award 2022

[Help/FAQ](#)

[Privacy policy](#)

[Cookie Policy](#)

[Accessibility](#)

[Terms & Conditions](#)

[Legal Notice](#)

© Walter de Gruyter GmbH 2022



Ajit Kumar Thakur

B.E (Elec), MBA, FIE, CPM(NUS), CPM-C(IPMA), SMP



Permanent Address: 482A, Sector 61A, Chandigarh – 160061, India

Contact details : +919971744599; ajitsumedha@gmail.com;
ajit.thakur@iggl.co.in

Brief Resume

As Chief Executive Officer, spearheading implementation of 1656 km long North East Gas Grid. Handling energy projects spanning 30 years and expertise in managing complex projects and high energy-intensive facilities. Experience in managing projects, designing, execution, commission, and facilities operation for hydrocarbon installations. Specialize in dealing with permissions, project liaisons, and acquisition, crucial for achieving project completion in a timely manner. Expertise of comprehensive monitoring and large infrastructure implementation.

Work experience includes managing a variety of jobs and tasks for a Fortune 500 energy company, which provided an opportunity to work in a cross-cultural setting with a special emphasis on the core values of Care, Innovation, Passion, and Trust.

Currently implementing flagship North East Gas Grid to usher in Gas based economy in North Eastern States.

Working with the Institution of Engineers and the National Association of Corrosion Engineers to provide voluntary services.

Educational Details

- B.E. (Electrical) from Punjab Engineering College, Chandigarh (1989-1993)
- M. B. A (HR & Systems) from Institute of Management Technology, Ghaziabad (2007)
- Certificate in Project Management from U21global, NUS, Singapore
- Certified Project Manager (Level C) from IPMA, Switzerland
- Certificate in Project Management (CIPM # Level D) from PMA, India
- FIE, Institution of Engineers (India)
- Flagship Senior Management Program of Indian Oil (Oct 2019)
- Member (NACE Customer Number: 123829) AMPP(NACE), USA since 2007

PLAGIARISM CERTIFICATE

1. We Dr Adarsh kr Arya (Internal Guide), Dr. Pushpa Sharma (Co Guide/
External Guide) certify that the Thesis titled
Prediction & Mitigation of AC Induced Pipeline
Corrosion under Cathodic Protection
submitted by Scholar Mr/ Ms Ajit Kumar Thakur having SAP ID
50056543 has been run through a Plagiarism Check Software and the Plagiarism
Percentage is reported to be 9 %.
2. Plagiarism Report generated by the Plagiarism Software is attached.

A.K. Arya 10/04/2023
Signature of the Internal Guide

Pushpa Sharma 21/04/2023
Signature of External Guide/Co Guide

Ajit 5/4/23
Signature of the Scholar

DRAFT THREE

ORIGINALITY REPORT

9%

SIMILARITY INDEX

6%

INTERNET SOURCES

6%

PUBLICATIONS

1%

STUDENT PAPERS

PRIMARY SOURCES

1	Ajit Kumar Thakur. "Corrosion of pipe steels under alternating currents", International Journal of Electrochemical Science, 2021 Publication	1%
2	enresi.com Internet Source	1%
3	coek.info Internet Source	1%
4	theses.ucalgary.ca Internet Source	<1%
5	www.politesi.polimi.it Internet Source	<1%
6	link.springer.com Internet Source	<1%
7	es.scribd.com Internet Source	<1%
8	backend.orbit.dtu.dk Internet Source	<1%
